Studies Utilising a Transgenic Mouse Model to Investigate the Pathogenesis of HTLV-I *tax*

By

A. Peter Hall

A thesis submitted for the degree of Doctor of Philosophy
In the Faculty of Veterinary Medicine,
The University of Glasgow

Department of Veterinary Pathology
September 1999

Abstract

In order to investigate the contribution that the HTLV-I (Human T-cell Leukaemia Virus Type I) *tax* oncogene contributes to the transformed phenotype we generated transgenic mice that expressed the HTLV-I *tax* transgene under the regulatory influence of the CD3-ε promoter-enhancer elements. These mice developed a variety of different types of pathology, the most pertinent of which were tumours (overall incidence 28/57 (49%)). The principal tumours were mesenchymal tumours which developed at sites of wounding (ear and tail tips) (overall incidence 18/31 (58%); average latency 202.5 days), and salivary and mammary adenomas (overall incidence 10/26 (38%); average latency 399 days). Immunocytochemical analysis of these tumours revealed that subpopulations of tumour cells expressed high levels of Tax protein as well as Myc, Fos, Jun and p53 proteins. Analysis of these tumours using the TUNEL (Terminal dUTP Nick End Labelling) technique revealed a similar pattern of apoptosis. Dual immunofluorescent localisation of Tax expressing cells with cells undergoing apoptosis revealed a remarkable degree of coincidence between these processes indicating that Tax expression and apoptosis are intimately linked *in vivo*. When CD3-*tax* transgenic mice were bred onto a p53 null or hemizygous background the resultant tumours which emerged at ear and tail tips were identical to the original cohort of tumours indicating a lack of co-operation between *tax* and p53 (average latency for mesenchymal tumours emerging on a p53 wild type background: 277d (9.2months) and 128d (4.3 months) cf $p53^{+/-}$ background: 233d (7.8 months) and 156d (5.2 months)).

A Tax expression system was also developed *in vitro* using a pBabe retroviral vector which transcribed a Tax-MER (Tax-modified oestrogen receptor) fusion product. This fusion protein was dependent upon functional activity by induction with 4-hydroxy tamoxifen. The results of these experiments using a CREB/ATF responsive reporter gene indicated that this system produced a functional fusion protein that was well regulated by 4-hydroxy tamoxifen. Functional mutants of Tax were made (M1, M47 and C23S) based on published data (Smith and Greene, 1990; Semmes and Jeang, 1992) which were designed to segregate the functional domains of Tax. Analysis of these mutants indicated

that M47 least efficiently induced apoptosis *in vitro*. In our hands this protein also least efficiently transactivated the CREB/ATF pathway (although transactivation of the NFκB pathway was difficult to determine in this assay system). These results may indicate the general importance of the CREB/ATF pathway for apoptotic induction. Similarly these results, together with the transgenic mouse experiments, may also indicate that low levels of Tax expression does not induce apoptosis.

Contents

Chapter 1: Overview of HTLV-I and mechanisms of viral transformation

List of Abbreviations

AEC	3-amino-9-ethylcarbazole (AEC)
ALV	avian leukosis virus.
AMP	adenosine monophosphate
AP-1	activator protein 1
ATF	activating transcription factor
ATL	adult T-cell leukaemia
ATP	adenosine triphosphate
b-GAL	beta-galactosidase
BHK	baby hamster kidney cells
BLV	bovine leukaemia virus
bZIP	basic region leucine zipper
C23S	mutant C23S
cAMP	cyclic AMP
CAT	chloramphenicol acetyl transferase
CDK	cyclin dependent kinase
CIP	cdk inhibitor protein
CNS	central nervous system
CRE	creb responsive element
CREB	creb responsive element binding protein
CREM	creb responsive element modulator protein
CTL	cytotoxic T-lymphocyte
DAB	3,3'-diaminobenzidine (DAB)
dd	double distilled
DNA	deoxyribonucleic acid
DRE	direct repeat element
dUTP	deoxyuridine triphosphate
EBV	Epstein Barr Virus
ELISA	enzyme linked immunosorbent assay
ENV	envelope
ETS	Ets responsive element
FCS	foetal calf serum
FeLV	feline leukaemia virus
GAG	group antigen
Gla WT	Glasgow wild type
GM-CSF	granulocyte monotcye-colony stimulating factor
H+E	haematoxylin and eosin
HBV	hepatitis B virus
HCV	hepatitis C virus
HIV	Human Immunodeficiency Virus
HPV	human papilloma virus
HTLV-1	Human T-cell Leukaemia Virus Type 1
Ig	immunoglobulin
IkB	inhibitor kappa B protein

IL	interleukin
IL2R	interleukin 2 receptor
INK	inhibitor kinase
Jak-STAT	Janus kinase-signal transducers and activators of transcription
kb	kilobase
LTR	long terminal repeat
M1	mutant 1
M47	mutant 47
MAP	multiple antigenic peptide
M-CSF	monocyte-colony stimulating factor
MER	modified oestrogen receptor
MF	mycosis fungoides
MuLV	murine leukaemia virus
NF	neurofibromatosis
NF-KB	nuclear factor kappa B
NLR	nuclear localisation region
o/n	overnight
ORF	open reading frame
p/t	p53/tax line of mice/tumours
p/t 50	p53+/-/tax 50 tumour/cell line
p/t 50-1/2/3	p53+/-/tax 50-1/2/3 cell line
p/t 54	p53+/-/tax 54 tumour/cell line
p53	p53 tumour suppressor gene
PBMC	peripheral blood mononuclear cells
PBS	phosphate buffered saline
PCR	polymerase chain reaction
PKC	protein kinase C
POL	polymerase
Pr	promoter
PTHrP	parathyroid hormone releasing peptide
R	repeat region
REF	rat embryo fibroblasts
REX	regulator of transcription
RNA	ribonucleic acid
RT	room temperature
RT-PCR	reverse transcriiptase PCR
RxRE	Rex responsive element
SD	standard deviation
SIE	transactivator of transcription
SIE	v-sis conditioned medium inducible element
SRE	serum response element
SRE	serum response element
SRF	serum response factor
SRF	serum response factor
SS	Sezary syndrome

ST Dev	standard deviation
STLV	Simian T-lymphotrophic virus
SV40	Simian Virus 40
T1	p53+/+/tax tumour/cell line
TAX	transactivator of transcription
TBP	TATA binding protein
TCR	T-cell receptor
TDT	terminal deoxytransferase
TFIIA	transcription factor II A
TNF	tumour necrosis factor
TRE	tax responsive element
TSP/HAM	tropical spastic paraparesis/HTLV-1 associated myelopathy
TUNEL	terminal dUtp nick end labeling
U3/5	unique region 3/5 prime

C23S	Mutant C23S
C23S-MER	Mutant C23S -modified oestrogen receptor
IEX-Tax	IEX-Tax (wild type Tax from external source)
LTR^{HIV-I} /pBabe	HIV-I LTR (NF-κB responsive)-pBabe
LTR^{HTLV-I}/pBabe	HTLV-I LTR (CREB/ATF responsive)-pBabe
M1	Mutant M1
M1-MER	Mutant M1-modified oestrogen receptor
M47	Mutant M47
M47-MER	Mutant M47-modified oestrogen receptor
MER-Tax	Modified oestrogen receptor-Tax (wild type from Glasgow)
MER-Tax-MER	MER -Tax (wild type) - MER
$Tax^{Gla\ WT}$	Tax (wild type from Glasgow)
$Tax^{Gla\ WT}$-MER	Tax (wild type from Glasgow) - MER
Tax-MER	Tax (wild type from Glasgow) - MER
Tax^{Tumour}	Tax (wild type from a transgenic mouse tumour)

List of Tables

List of figures

All photomicrographs are in colour in the original copies of this thesis.

List of Graphs

Declarations

I hereby declare that the work presented in this thesis is original and was conducted by the author under supervision except where stated.

I certify that no part of this thesis has been submitted previously for the award of a degree to any University but has been reproduced in parts in the following paper: -

Tumours derived from HTLV-I Tax transgenic mice are characterised by enhanced levels of apoptosis and oncogene expression.

A.P. Hall, J. Irvine, K. Blyth, E.R. Cameron, D.E. Onions, M.E.M. Campbell

J Pathology **186** (2): 209-214 1998

Acknowledgements

These studies were carried out in the Department of Veterinary Pathology with the support of the Wellcome Trust. I would like to acknowledge my supervisor Dr Campbell who provided continual support and encouragement throughout the duration of my studies. I would also like to thank Karen Blyth and the animal house staff for their help with the transgenic mouse experiments and Ms J Irvine and Mr I McMillon who provided technical help at various stage in the production of the histology slides. I would also like to thank Professor Onions for the use of laboratory space. Finally I would like to thank the very many people who made my studies in the department a thoroughly enjoyable and fulfilling experience.

Chapter 1

Overview of HTLV-I and mechanisms of viral transformation

Overview of HTLV-I and mechanisms of viral transformation

1.1 Introduction

"In 1775, Percival Pott, a London physician, described the alarmingly high rate of scrotal cancer in men who worked as chimney sweeps during childhood. In the mid-nineteenth century, pitchblende miners in eastern Germany were observed to die at extremely high rates from lung cancer. By the latter part of the century, snuff and cigar smoking were thought by some medical practitioners to be closely linked to the development of oral cancers." It was these and other early observations that helped to develop the concept that cancers arose from exogenous sources and so dispel the widely held dogma that cancer was a breakdown of the body's internal machinery uninfluenced by the outside world (Varmus and Weinberg, 1993).

While most scientific studies focused upon chemical and physical agents as the possible causes of human cancer, a fundamental paradigm shift occurred in 1911 when Peyton Rous showed that a cell free filterable agent derived from a chicken cancer (Rous sarcoma virus) could transmit a chicken sarcoma. Although the work was not recognised at the time, it went some way to substantiate the infectious theory of human malignancy. By 1965, a polyoma virus and Simian Virus 40 (SV40) had been found to induce tumours when injected into rodents, one year before Rous and his coworkers were awarded a much-deserved Nobel Prize.

It is now clear that a number of viruses act as inciting factors or cofactors in human cancer, namely: Epstein-Barr Virus (EBV), Hepatitis B (HBV) and Hepatitis C Viruses (HCV), Human Papilloma Viruses (HPV), and Human T-cell Leukaemia Virus Type I (HTLV-I). The recent cloning of a γ-herpesvirus from Karposi's sarcoma (Chang et al, 1994) has added another potential oncogenic virus to the list.

Table 1.1: Human oncogenic viruses

Virus	Family	Malignancy
HBV	Hepadnaviridae	Hepatocellular carcinoma
HCV	Flaviviridae	Hepatocellular carcinoma
HTLV-I	Retroviridae	Adult T-cell Leukaemia
EBV	Herpesviridae	Burkitt's lymphoma
		Undifferentiated nasopharyngeal carcinoma
		Hodgkin's disease
		B-lymphomas in immunosuppressed individuals
HPV-16,18 (31,33,35,39, 45,51,52,56, 58,59,61)	Papovaviridae	Cervical cancer

Table 1.1 summarising the most important human oncoviruses and the types of malignancy they induce

It was not until the discovery in 1976 of a growth factor for mature T-cells, interleukin-2 (IL-2) (Morgan et al, 1976) that the necessary tools were available for the growth of T-lymphocytes *in vitro*. This led to the discovery in the early 1980's by two independent laboratories of type C retrovirus particles isolated from patients retrospectively diagnosed with Adult T-cell Leukaemia (ATL). The first isolate was derived from an American patient suffering from cutaneous T-cell Lymphoma (Poiesz et al, 1980; Poiesz et al, 1981; Popovic et al, 1983) and the second from a Japanese patient suffering from ATL (Yoshida et al, 1982). These isolates were very soon recognised to be identical, or very nearly so, and were designated Human T-cell Leukaemia Virus (Wong-Staal et al, 1983).

Soon-after, two new sub-types were discovered. Both of these viruses were isolated from atypical malignancies, the first designated HTLV-II-Mo from a patient suffering from atypical hairy cell leukaemia (Kalyanaraman et al, 1982). The second, designated HTLV-II-NRA (Rosenblatt et al, 1986), was isolated from a patient suffering from two malignancies: a B-cell malignancy that did not contain HTLV-II, consistent with atypical hairy cell leukaemia, and a $CD8^+$ lymphoproliferative syndrome with oligoclonally integrated HTLV-II (Rosenblatt et al, 1988).

Meanwhile, an Italian isolate, HTLV-V was derived from a continuous cell line originating from the peripheral lymphocytes of a patient suffering from a $CD4^+$ Tac^- (IL2Rα chain) cutaneous T-cell lymphoma/leukaemia and subsequently identified in seven other patients from Italy with the same disease (Manzari et al, 1987).

1.2 Phylogeny and classification

The complete nucleotide sequence of HTLV-I was provided by Seiki and co-workers in 1983 and was found to have a genomic organisation substantially different to the simple retroviruses. HTLV-I can be grouped based on nucleotide sequence homology with Simian T-lymphotropic virus (STLV) (90-95% homology) and Bovine Leukaemia Virus (BLV) (Ina and Gojobori, 1990). These viruses form part of a group known as the complex retroviruses, which are characterised by their greater genomic complexity making them distinct from the simple retroviruses typified by Feline Leukaemia Virus (FeLV), Avian Leukosis Virus (ALV), and Murine Leukaemia Virus (MuLV).

It is now clear that there are at least five major molecular subtypes of HTLV-I, namely the widespread cosmopolitan subtype, the Japanese, West African, Central African, and Melanesian subtypes (Vidal et al, 1994). These isolates show only low genetic variability which is linked to geographical location rather than pathogenicity (Malik et al, 1988; Komurian et al, 1991; Miura et al, 1994; Renjifo et al, 1995; Mahieux et al, 1995). The geographical restriction and the relatedness of HTLV subtypes to their STLV counterparts,

recently illustrated by the close sequence identity between a new HTLV-I subtype D and chimpanzee STLV-I (>98% nucleotide sequence identity) (Mahieux et al, 1997) reinforces the hypothesis of interspecies transmission between humans and monkeys.

The complete nucleotide sequence of an infectious clone of HTLV-II was reported in 1985, and shown to have approximately 60% sequence homology with HTLV-I (Shimotohno et al, 1985). There are now known to be at least three major molecular subtypes of HTLV-II which again show only minor sequence variations from the prototypic subtype HTLV-II_{Mo}. These have been designated HTLV-IIb (Dube et al, 1993) and HTLV-IIc (Eiraku et al, 1996).

1.3 Transmission and Epidemiology of HTLV

Transmission of HTLV occurs by transfer of infected lymphocytes during breast feeding, blood transfusion, sexual intercourse, and intravenous drug abuse. Transmission through the non-cellular fraction of blood apparently does not occur (Yamamoto et al, 1982). Mother-to-child transmission of the virus poses the most serious public health concern since horizontal transmission between spouses only very rarely leads to ATL (Sanada et al, 1989). Vertical transmission of HTLV-I through breast milk has been well documented (Hino et al, 1989, Ichimaru et al, 1991) and the importance of this mode of transmission was underscored by an intervention study carried out in Nagasaki which showed that refraining from breast feeding by carrier mothers reduced the incidence of maternal transmission of HTLV-I by at least 80% (Hino et al, 1994).

Blood products contaminated with HTLV appear to be a very efficient mode of transmission (Osame et al, 1990; Manns et al, 1992). Blood transfusion has been associated with the very rapid development of TSP/HAM, often within a few months from initial date of transfusion (Gout et al 1990). In these cases it is likely that the sudden exposure to a high viral challenge coupled with usually some degree of immunosuppression represent

important factors contributing to the development of TSP/HAM (Nowak and Bangham, 1996).

Other modes of vertical transmission have not yet been clearly demonstrated. Intrauterine transmission of HTLV-I does occur when a human T-cell line (MT-2) producing HTLV-I is injected into pregnant rats (Hori et al, 1995). However, transplacental infection by HTLV-I in humans has not been demonstrated and at least one report suggests that the placental trophoblast may represent a barrier to infection protecting the foetal compartment from exposure to the virus (Liu et al, 1996).

Sexual transmission of HTLV-I poses a higher risk for male-to-female transmission (Murphey et al, 1989) and interestingly may be a risk factor for the development of TSP/HAM. In a retrospective study carried out in Jamaica two risk factors were identified as contributors to the development of TSP/HAM but not ATL: early initial age of sexual intercourse and high sexual promiscuity (Kramer et al, 1995).

In common with other oncogenic viruses, only a subset of infected individuals develop disease with more than 95% of HTLV-I infected individuals leading an unremarkable lifelong infection. In these individuals a symptomless balance ensues between host immune surveillance and uncontrolled viral proliferation. It appears that viral load in carriers attains a certain level in a relatively short period of time after infection and then shows little or no change afterwards (Shinzato et al, 1993). It is thought that it is the breakdown of this virus-host relationship which marks the turning point leading to disease. This manifests as either a chronic inflammatory immune response typified by TSP/HAM, or as a malignant out-growth of a T-cell clone (ATL).

1.4 HTLV-I Associated Diseases

The cumulative life-time risk of ATL for those individuals infected before the age of 20 years is estimated to be 4.0% for males and 4.2% for females (Murphy et al, 1989b). ATL normally occurs in the latter decades of life (average age: 58 years (Japan), 43 years (Caribbean and Africa) [Yamaguchi and Takatsuki, 1993]) which mirrors the disease incidence of many multi-step, time-dependent models of tumour development, such as the prototypic adenomatous polyposis coli (familial colon cancer). In this disease, just as in ATL, it is thought that several rare genetic events combine before the emergence of the malignant phenotype. Indeed, the multistep nature of ATL was modelled by Okamoto et al, (1990) who suggested that nearly 5 independent somatic mutations were required before the onset of malignancy.

HTLV-I is now considered to be the aetiological agent of both Adult T-cell Leukaemia (Hinuma et al, 1981; Yoshida et al, 1982) and Tropical Spastic Paraparesis (TSP)/HTLV-I associated Myelopathy (HAM) (Jacobson et al, 1988, Reddy et al, 1988). However HTLV-I has been linked less substantially with a number of chronic inflammatory conditions summarised in Table 1.2.

The central question of whether ATL or TSP/HAM is associated with a specific strain of HTLV-I has not been conclusively answered (Gessain et al, 1995 and references therein). To date no HTLV isolate has been consistently associated with pathogenicity - it appears that the low genetic variability of HTLV-I depends more upon the geographic origin of the patients than the diagnosis of the infected individuals (Schirabe et al, 1990; Komurian et al, 1991; Schulz et al, 1991).

On the other hand HTLV-II has no clear association with any form of disease or lymphoproliferative disorder (Hjelle et al, 1991) despite its early isolation from atypical hairy cell leukaemia and other rare forms of leukaemia (Rosenblatt et al, 1987; Lion et al, 1988; Loughran et al, 1992; Loughran et al, 1994). Recently HTLV-II has been isolated

from HTLV-I negative chronic neurodegenerative conditions (Hjelle et al, 1992; Jacobson et al, 1993) although its causal role remains uncertain.

Table 1.2: Clinical outcome of HTLV-I infection

- **Asymptomatic Carrier state:**

  This is the usual outcome after infection

- **Neoplastic disease:**

  Adult T-cell Leukaemia

  Cutaneous T-cell Lymphoma/Leukaemia

  (Sezary syndrome/ mycosis fungoides) — Hall et al, 1991; Pancake et al, 1995

- **Chronic Inflammatory diseases:**

  TSP/HAM (discussed later)

  HTLV-1 associated arthropathy — Nishioka et al, 1989, Sato et al, 1991, Kitajima et al, 1991

  HTLV-1 associated uveitis — Mochizuli et al 1992a, 1992b Yamaguchi et al, 1992, and Taguchi et al, 1993

  HTLV-1 associated alveolitis/pneumonitis — Sugimoto et al, 1993, Mita et al, 1993

  HTLV-1 associated polymyositis — Wiley et al, 1989

  Infective dermatitis in Jamaican children — LaGrenade et al, 1990

- **HTLV-I induced immunosuppression**

HTLV-I is associated with a number of opportunistic diseases due partly to the immunodeficiency induced by HTLV-I infection:

HTLV-I associated lymphadenitis	Ohishima et al, 1992
chronic renal failure	Lee et al, 1987
strongyloidiasis	Nakada et al, 1987
monoclonal gammopathy	Matsuzaki et al, 1985
cancer of other organs	Strickler et al, 1995

Table 1.2 summarising the various clinical outcomes following HTLV-I infection.

1.5 Adult T-cell Leukaemia

ATL was first described as a distinct clinical entity in 1977 by Takatsuki and co-workers (Uchiyama et al, 1977) as a malignancy endemic to Southern Japan. Since that time HTLV-I (and consequently ATL) has been found to be endemic to a number of regions throughout the world including the Caribbean basin, north-eastern S. America, Central America and equatorial Africa. Many of the ATL patients studied in the USA, the UK, France and the Netherlands originated from the Caribbean area (Yamaguchi and Takatsuki, 1993).

Phenotypically, ATL usually presents as a $CD3^+$, $CD4^+$, $CD8^-$, $CD25^+$ (Tac antigen/IL2-R_α) malignancy of mature T-cells, although occasionally, $CD4^-$/ $CD8^+$, $CD4^+$/ $CD8^+$, and $CD4^-$ /$CD8^-$ isolates occur (Kamihira et al, 1992).

ATL can be classified into four sub-types according to clinical symptoms and course of disease: **smouldering**, **chronic**, **lymphoma** and **acute** (Takatsuki et al, 1985, Kawano et al, 1985; Yamaguchi and Takatsuki et al, 1993) with acute being the prototypic form. Clinically the disease often evolves through a number of intermediate steps before progressing to fulminant end-stage ATL. Infection usually gives rise to a symptomless carrier state characterised usually by the presence of antibodies to HTLV-I but with only a low viral burden, polyclonally integrated, and undetectable by conventional Southern blotting techniques. This condition may then progress to an intermediate state (Yamaguchi

et al, 1988) distinguished by polyclonal integration but with a higher proviral burden before developing into smouldering ATL. Smouldering ATL typically presents with a monoclonal or oligoclonal proviral integration which is readily detected by conventional molecular techniques.

Acute ATL is characterised by a highly malignant T-cell leukaemia/lymphoma which is usually unresponsive, or poorly responsive to aggressive combination chemotherapy. Mean survival time for typical ATL ($CD4^+$ phenotype) is 10.2 months, with an even poorer prognosis for the rarer atypical presentations, ranging between 4.9 and 7.8 months (Kamihira et al, 1992).

The more indolent pre-leukaemic or **smouldering** form of ATL and the **chronic** form of ATL represent less severe phenotypes which often progress to full-blown full ATL (often termed **crisis** ATL) after a protracted latency period. In both conditions abnormal circulating leukaemic cells within the peripheral circulation can be detected. These cells resemble Sezary cells having indented or lobulated nuclei (so-called flower cells) (Takatsuki et al, 1985; Kawano et al, 1985).

Lymphoma-type ATL represents a cutaneous manifestation of ATL with few circulating abnormal leukaemic cells within the peripheral circulation. Speculation as to whether this sub-type of ATL belongs to a wider spectrum of disease has recently come under scrutiny. Several viruses have been implicated in the pathogenesis of cutaneous T-cell lymphomas (Chan et al, 1993; Zucker Franklin 1992) of which Sezary syndrome (SS) and Mycosis Fungoides (MF) are particularly strongly implicated, specifically with HTLV (Wantzin et al, 1986; Detmar et al, 1991; Zucker-Franklin et al, 1991). It has long been suspected that MF and SS are caused by HTLV since deleted HTLV-I provirus can be detected by polymerase chain amplification (PCR) from blood and cutaneous lesions of patients with MF/SS (Hall et al, 1991; Pancake et al, 1995), and MF/SS cells are readily immortalised *in vitro* to yield HTLV like particles on electron microscopy (Zucker-Franklin et al, 1991). However few patients exhibit HTLV-I/II antibodies, and detection by S. hybridisation or pcr has not been

met with success by all authors (Capesius et al, 1991; Lisby et al, 1992; Fujihara et al, 1997; Wood et al, 1997). This raises the intriguing possibility that large deletions in structural regions of the HTLV genome or a closely related variant virus could limit replication and subsequent detection by either the immune system or standard molecular techniques. Preferential retention of the transforming pX region including *tax* and loss of *gag*, *pol* and *env* genes, has been noted, hand-in-hand with limited sero-prevalence to the Tax protein (Pancake et al, 1995).

1.6 Tropical Spastic Paraparesis/HTLV-I Associated Myelopathy

TSP is a chronic inflammatory condition of the central nervous system (CNS) resulting over a protracted period of time in a demyelinating myelopathy. Approximately one out of 2,000 individuals infected with HTLV-I go on to develop TSP/HAM (Osame et al, 1990). Clinically patients present with a progressive spasticity and weakness, particularly of the lower limbs, which usually results in paralysis of the legs and urinary dysfunction. Sensory loses are not a prominent feature of the disease.

Histologically the initial pathology within the CNS is characterised by diffuse inflammation in both the white and grey matter of the spinal cord. No particular cell type appears to be the focus of an (auto)-immune response. Inflammatory infiltrates are initially dominated by $CD4^+/CD45RO^+$ (memory) T-cells (Iwasaki et al, 1992). The balance between immune clearance of infected $CD4^+/CD45RO^+$ cells by CTL induced apoptosis and enhanced T-cell survival due to elevated *bcl-2* expression may reflect important determinants of disease pathogenesis (Umehara et al, 1994). More advanced lesions are composed of a predominantly $CD8^+$ CTL infiltrate (Akizuki et al, 1987, Moore et al, 1989) superimposed upon a mixed picture of demyelination/remyelination and axonal loss with secondary tract degeneration.

The aetiopathogenesis of TSP/HAM is still very poorly understood. Empirically TSP/HAM could develop due to one of four principal mechanisms namely poor immune responsiveness

by the host to HTLV-I infection, infection with a neurotropic strain of HTLV-I, autoimmune destruction of a cross-reactive antigen within the CNS or immune destruction of HTLV-I infected CNS cells.

Several lines of evidence supports poor immune responsiveness resulting in 'bystander damage' to the CNS. Neurotropic strains of HTLV-I have not been identified (Yoshida et al, 1987) despite Renjifo and colleges reporting a candidate mutant virus. These authors demonstrated that infection with an HTLV-I isolate carrying a *tax* mutation at nucleotide 7959 exhibited enhanced transactivation of the HTLV-I U3 promoter and conferred an increased risk of developing TSP/HAM (Renjifo et al, 1995). However Gessain et al (1995 and references therein) remarked that the same mutation is found in the consensus *tax* sequence of the Cosmopolitan strain of HTLV-I which infects many healthy seropositive individuals as well as patients with ATL.

The pathology of TSP/HAM does not support autoimmune mediated destruction of the spinal cord since the CTL response is characterised by a diffuse inflammation without targeting a specific cell type. Immune mediated destruction of the CNS would pre-suppose infection of the CNS by HTLV-I - this has not been conclusively demonstrated or linked with CNS pathology. Kira et al (1991 and 1992) suggested that constituent cells within the CNS might harbour the HTLV-I genome since they were able to clone pX region sequences from whole thoracic cord or cerebral tissue samples derived from TSP/HAM patients. However this method was unable to differentiate between invading lymphocytes and resident CNS cells. Nevertheless, expression of viral proteins within the CNS of transgenic mice which have the viral LTR cloned from a HTLV-I provirus isolated from a case of TSP/HAM has been demonstrated (Gonzalez-Dunia et al, 1992). Moreover an *in situ* hybridisation study demonstrated the presence of *tax* expression within isolated and infrequent resident CNS cells, but was unable to spatially correlate the presence of proviral RNA with infiltration of lymphocytes (Lehky et al, 1995).

Recently a coherent framework has been developed by Bangham and colleges which postulates that bystander damage by CTL cells to susceptible tissues results in HTLV-I associated inflammatory disease (reviewed by Daenke and Bangham, 1994). They propose that the main determinant of disease is the chronically activated CTL response to the HTLV-I Tax protein. Since the virus spreads mainly by cell to cell syncytium formation and cell division it is likely that there is very little cell free virus. Consequently the humoral immune response is not considered to be a critical determinant contributing to disease pathogenesis.

It is now clear that both healthy seropositives as well as patients with TSP mount vigorous anti-HTLV-1-specific cytotoxic T-lymphocyte responses (Parker et al, 1992; Daenke et al, 1996) and humoral immune responses (Shinzato et al, 1993). The immunodominant anti-viral CTL response is directed against the viral Tax protein (Jacobson et al, 1990, Parker et al 1992; Pique et al, 1996). Sequencing of several HTLV-I quasispecies has revealed that the intraisolate sequence variability is much greater than the variability between isolates. Furthermore, the naturally occurring nucleotide sequence variation within the *tax* open reading frame appears to be more variable within healthy carriers than within either TSP patients or ATL patients (Niewiesk et al, 1994). This suggests that healthy seropositives mount a stronger anti-Tax immune response driving *tax* sequence variability, and the production of 'escape' sequences that evade immune recognition (Phillips et al, 1991). Naturally occurring amino-acid substitutions in Tax both abolish recognition by CTL of the appropriate Tax peptide, and moderately or severely reduce the ability of Tax to transactivate various promoters (HTLV-I LTR, *c-fos* promoter, IL2-R_{α} chain promoter) (Niewiesk et al, 1995). Thus a vigorous anti-Tax CTL response drives the generation of Tax-escape mutants, but at the functional cost of impaired Tax activity. An elegant mathematical model proposed by Nowak and Bangham (1996) suggests that because the ratio of non-synonymous (coding) to synonymous (non-coding) codon changes (Nei and Gojobori, 1986) is significantly higher in healthy HTLV-I carriers (Niewiesk et al, 1996) these patients generate a higher selection pressure for immunologically driven amino-acid change in Tax. Since both healthy seropositives and TSP/HAM patients have an equally

vigorous CTL response, the resolution of the paradox lies in the fact that TSP/HAM patients have between 10-100-fold higher proviral load within PBMC (Yoshida et al, 1989; Gessain et al, 1990; Kira et al, 1991). Consequently, low CTL responders have a higher proviral burden resulting in higher antibody titres (Shinzato et al, 1993) and widespread activation of T-cells. Extravasation of T-cells leads to a focus of inflammation, the site of inflammation possibly determined by adhesion molecules displayed by proliferating lymphocytes (reviewed by Butcher and Picker 1996). Foci of chronically active inflammation would manifest symptoms particularly in sensitive tissues such as the spinal cord, which has little or no powers of regeneration. Hence genetic factors such as HLA haplotype (Usuku et al, 1988 and 1990) and the effectiveness of immune response genes which determine the efficiency of peptide processing and presentation may be the crucial factors in the development of these diseases.

1.7 Genomic Organisation of HTLV-I

The HTLV-I genome is organised into essentially two regions (Figure 1.1). A 3' region which is homologous to the simple retroviruses containing gag, pol, and env flanked by long terminal repeats (LTR) plus an additional 3' region (termed as the pX, x, or x-lor region) unique to the complex retroviruses. This region is now known to be alternatively spliced to increase the genetic diversity of what would otherwise be a relatively limited genomic repertoire. This region contains (at least) four overlapping open reading frames (orf) generating six extra proteins. The first of these to be discovered were Tax, Rex, and a C-terminally truncated Rex homologue, $p21^{rex}$ (Miwa et al, 1984; Kiyokawa et al, 1984; Kiyokawa et al, 1985). RT-pcr (reverse transcriptase-polymerase chain reaction) further revealed the presence of another three messenger RNA species which code for putative proteins, $p12^{I}$, $p13^{II}$ and $p30^{II}$ (Ciminale et al, 1992; Berneman et al, 1992; Koralnik et al, 1992).

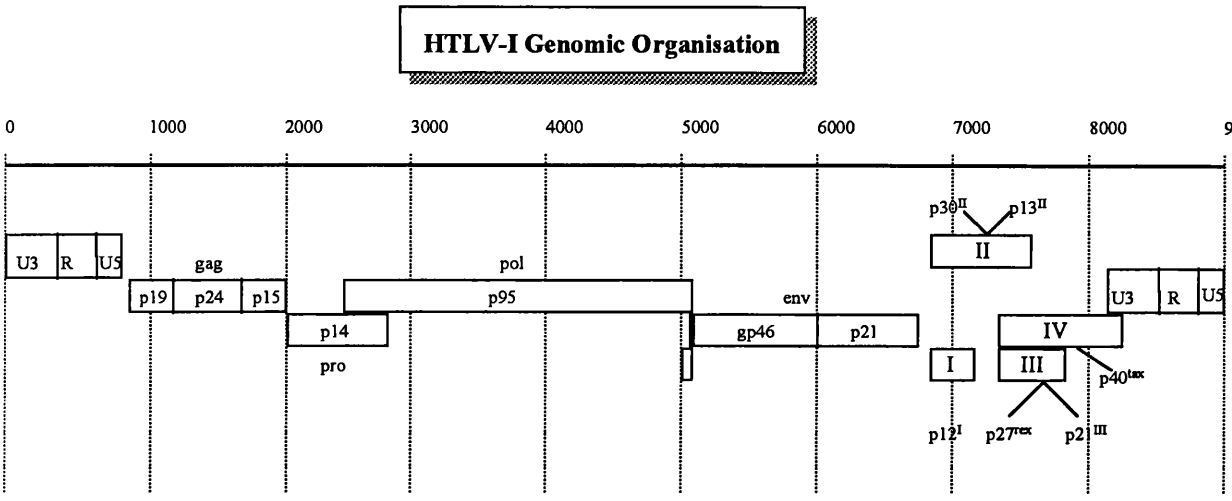

protein	orf	location	function
$p40^{tax}$	IV	nucleus	viral transactivator
$p27^{rex}$	III	nucleolus	post-transcriptional regulator
p21	III	cytoplasm	?
p12	I	perinuclear endombranes	binds IL-2Rβ/γ and 16kDa subunit og H^+-ATPase
p13	II	nucleus	?
p30	II	nucleolus	?

Figure 1.1: Schematic diagram illustrating the genomic organisation of HTLV-I

Complex retroviruses such as HTLV, BLV and HIV are composed of a 5' simple region analogous to the simple retroviridae such as MuLV or FeLV containing the late structural genes *gag*, *pol* and *env* and a more complex 3' region. This region contains multiple overlapping orfs, which are alternatively spliced to generate a number of extra proteins. These proteins (shown in the box above) represent the principal genes transcribed in the early phase of infection by HTLV-I before the switch to the unspliced/singly spliced messages mediated by $p27^{rex}$. [Compiled from Franchini [1995].)

1.7.1 Long Terminal Repeats

The long terminal repeats (Figure 1.2) located at the flanking 5' and 3' ends of the viral genome are non-coding *cis*-acting elements which serve to regulate viral transcription, latency, and genomic replication. They consist of three highly conserved regions designated U3 region (353bp), the R region (221bp), and the U5 region (120bp) (Seiki et al, 1983; Josephs et al, 1984). The 5' U3 region contains several important regulatory elements, which modulate viral gene expression. The first of these regions to be characterised were designated the Tax-responsive elements 1 (TRE 1) and 2 (TRE 2) and the Ets responsive region 1 (ERR 1) and 2 (ERR 2) (Bosselut et al, 1990 and 1991).

The viral LTR also contains other over-lapping *cis*-acting sequences which allow the interaction of a variety of host transcription factors. Factors such as YB-1 (Kasanchi et al, 1994), Myb, (Bosselut et al, 1992; Dasgupta et al, 1992) Ets1/Sp-1, (Gitlin et al, 1991; Gegonne et al, 1993), Elf-1 (Clark et al, 1993) and AP-1, the Fos-Jun heterodimer, (Jeang et al, 1991; Fujii et al, 1995) can transactivate the viral LTR in the absence of Tax. This raises the intriguing possibility that host factors play key roles in the initiation of viral transcription following infection, and maintenance of basal viral transcription during latency. The switch from latency to active viral gene expression may fall under the control, at least in part, of the cAMP Responsive Element Binding (CREB) transcription factor (Brauweiler et al, 1995). The CREB factor forms a heterodimer with phosphorylated Activating Transcription Factor 2 (ATF-2) (Xu et al, 1996) which when it binds to the R region suppresses Tax expression from cell lines derived from LTR-Tax/LTR-βGal double transgenic mouse fibroblast tumours (Xu et al, 1994). Re-activation of HTLV-I may be signalled by phosphorylation of CREB and recruitment of the co-activator CREB binding protein (CBP) (Kwok et al, 1996).

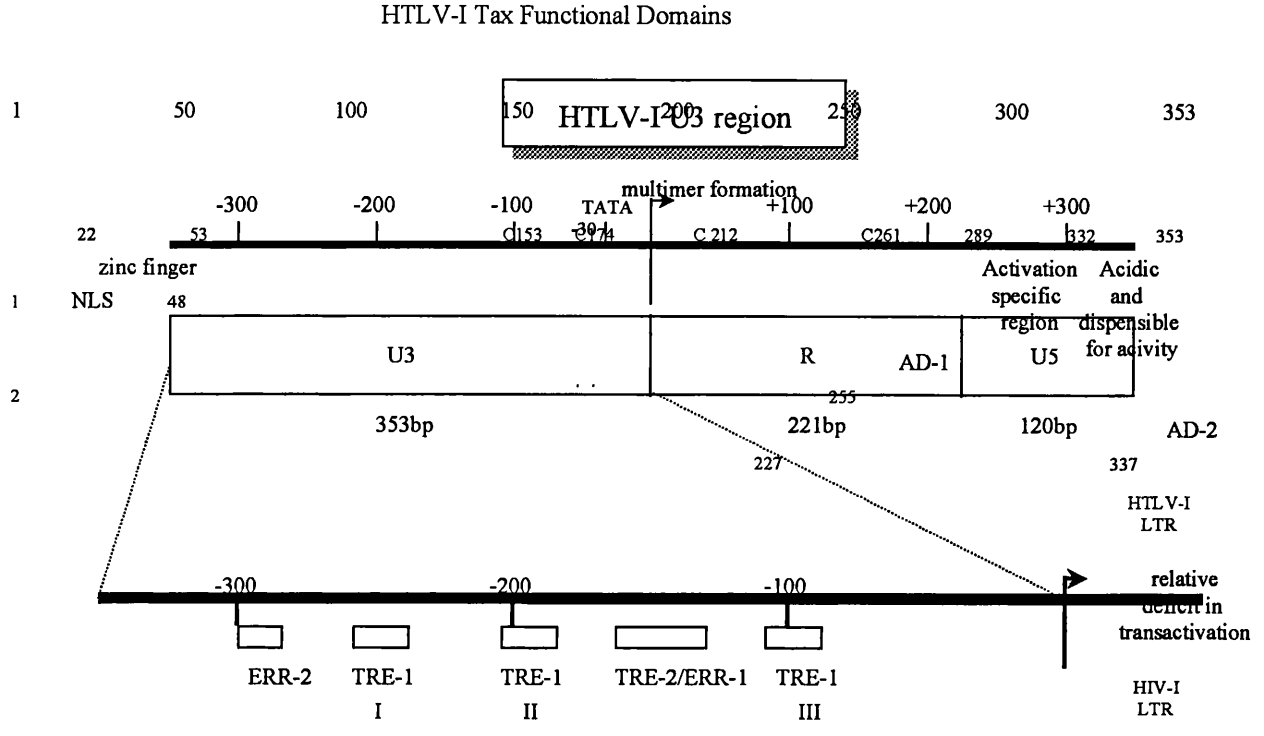

TRE-I I 5'-TAGGCGTTGACGACAACCCCT-3'

TRE-I II 5'-TAGGCCCTGACGTGTCCCCCT-3'

TRE-I III 5'-AAGGCTCTGACGTCTCCCCCC-3'

Figure 1.2: Schematic diagram illustrating the *cis*-acting sequences located within the HTLV-I LTR

The viral LTR contain multiple *cis*-acting sequences which are organised into a number of functional regions – the Tax Responsive Elements (TRE) 1 and 2 and the Ets Responsive Region (ERR) 1 and 2. These elements together with binding sites for other host transcription factors constitute the viral promoter-enhancer regions. The viral promoter-enhancer is crucial for viral life cycle controlling responsiveness to the viral transcriptional regulator *tax*, as well as other host factors, which may modulate viral gene expression and latency. [Compiled from Goren et al, 1995; Semmes and Jeang, 1992; 1995; Gitlin et al, 1991; Tsuchiya et al, 1994.]

1.7.2 The TRE-I Region

The TRE-1 region consists of three imperfectly repeated 21bp elements which are highly conserved between HTLV-I and HTLV-II (Sodroski et al, 1984). They act as viral enhancers conferring Tax responsiveness in a position and orientation-independent manner (Felber et al, 1985; Shimotohno et al, 1986; and Paskalis et al, 1986). Each repeat element contains three domains designated 5' to 3' as A, B, and C. Domain B contains a <TGACGT> motif that is homologous to the cAMP-responsive element (CRE) consensus sequence and is crucial for *tax* transactivation (Montagne et al, 1990). Tax transactivates viral gene expression through these repetitive elements by stimulating complex formation between several members of the CREB/ATF family of transcription factors (Xu et al, 1990; Montagne et al, 1990; Yoshimura et al, 1990; Jeang et al, 1991; Zhao and Giam, 1992; Suzuki et al, 1993a). These proteins form a family of transcription factors that contain a homologous basic region-leucine zipper (bZIP) DNA binding domain (reviewed by Watson et al, 1992). bZIP domains are composed of a leucine repeated every seven residues arranged upon a coiled-coil which forms a hydrophobic interface for dimerisation (the leucine zipper) and a basic region which forms two arms to specifically contact DNA. Tax homodimers (Tie et al, 1996; Jin et al, 1997) stimulate binding of bZIP proteins by enhancing their dimerisation which in turn facilitates their specific binding to DNA (Wagner and Green, 1993). Apparently Tax recognises the basic region of bZIP proteins (rather than the coiled-coil region) and in so doing alters the affinity of the transcription factor for its cognate sequence (Perini et al, 1995; Baranger et al, 1995). The Tax_2-$bZIP_2$-DNA interaction results in a stable ternary complex which specifically enhances transcription from CRE motifs, especially those with 5' G-rich and/or 3' C-rich flanking regions. CREB, ATF-1, and possibly CREM appear to be the most important bZIP family members which interact with Tax (Zhao and Giam, 1992; Suzuki et al, 1993a). In a *Saccharomyces cerevisiae* reporter system where β-gal was fused downstream from two HTLV-I 21bp repeats and a minimal yeast cytochrome c1 oxidase promoter, Tax in conjunction with either CREB or ATF-1 could stimulate expression of β-galactosidase in the absence of any other mammalian proteins (Shnyreva and Munder, 1996).

1.7.3 The TRE-2 region

A second Tax responsive region, designated TRE-2 (Marriott et al, 1989) is located between the two proximal TRE-1 elements. This region binds a number of nuclear factors [Sp-1, Nuclear Factor-1, Myb] (Nyborg et al, 1990; Bosselut et al, 1992; Dasgupta et al, 1992) including the product of the c-Ets-1 and c-Ets-2 proto-oncogene, Ets-1 and Ets-2 (Bosselut et al, 1990; Gitlin et al, 1991).

1.7.4 The ERR-1 and ERR-2

Two distinct Ets Responsive Regions have been defined, ERR-1 which is located within TRE-2 and ERR-2 which is located upstream from the most proximal TRE-1 (Gitlin et al, 1991). These regions bind Ets as well as the product of the c-myb proto-oncogene, Myb (Bosselut et al, 1992). Ets-1 is preferentially expressed in lymphoid tissue and can trans-activate the LTR in the absence of Tax. In the presence of Tax it co-operates to enhance transactivation above the combined individual effects (Gitlin et al, 1993).

1.8 Functions of the 3' pX region genes

1.8.1 The major HTLV-I regulatory genes: *tax*, *rex* and p21^{rex}

Tax, *rex*, and *p21^{rex}* represent the major RNA species both in HTLV-I infected cells and *ex vivo* samples. Tax and Rex are derived from a bicistronic mRNA molecule by the alternative use of AUG initiation codons located from within the second exon. The doubly spliced pX mRNA can support the synthesis of either a 27kDa (Rex) or a 40kDa (Tax) phosphoprotein.

1.8.2 Tax

The HTLV-I Tax protein is a 353 amino-acid phosphoprotein distributed predominantly within the nuclear compartment of infected cells (Goh et al, 1985; Beimling and Moelling, 1989). Tax acts as a transcriptional activator of its long terminal repeats (Cann et al, 1985; Felber et al, 1985) as well as modulating host gene transcription by usurping at least three different classes of transcription factors: CREB/ATF family, NF-κB family and the $p67^{SRF}$ (serum response factor) (Suzuki et al, 1993a; 1993b). However Tax does not bind DNA directly but rather acts indirectly by forming multi-protein complexes with these transcription factors (Fujisawa et al, 1991) which in turn bind DNA in a sequence specific fashion.

The amino-terminal residues of Tax (amino-acids 22-53) contain two overlapping zinc-finger motifs (Semmes and Jeang, 1992) which act as a novel nuclear localisation domain (Gitlin et al, 1991) [Figure 1.3]. Indeed, mutants which were unable to localise to the nucleus were unable to transactivate heterologous CREB/ATF or NF-κB promoters (Smith and Greene, 1990; Gitlin et al, 1991; Smith and Greene, 1992).

Mutational analysis of the Tax protein has allowed the functional segregation of the CREB/ATF and NK-κB transcription factor pathways of gene activation employed by Tax (Smith and Greene, 1990; Semmes and Jeang, 1992). Surprisingly, discrete functional domains have not been easily defined since point mutations throughout the Tax protein can affect one or other of these pathways with approximately 95% of these mutations being completely redundant (Semmes and Jeang, 1992). Interestingly, the carboxyl terminal 22 amino-acids (331-353) were completely dispensable for Tax transactivation (Smith and Greene, 1990). Mutation of a region of amino-acids located between 315-325 abrogated CREB-mediated Tax transactivation whereas three changes in amino-acids at serine 113, 160, and 258 were found to specifically affect NF-κB function (Semmes and Jeang, 1992).

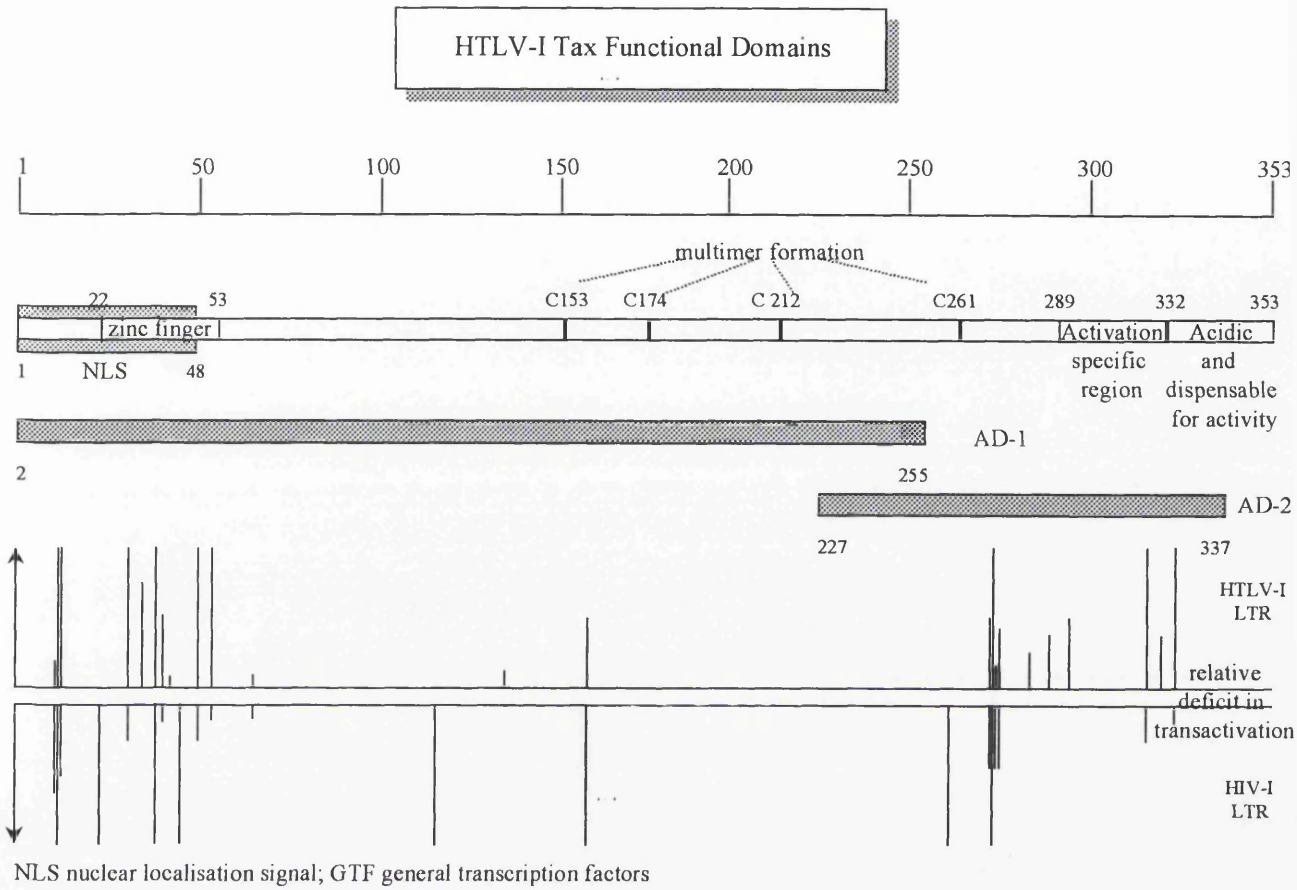

NLS nuclear localisation signal; GTF general transcription factors

Figure 1.3: Schematic diagram illustrating the various functional domains of HTLV-I Tax

The three figures illustrated from top to bottom represent:

1) (Top) The structural domains of the Tax protein: The 5' terminus contains the Nuclear Localisation Domain whereas the 3' terminus contains the acidic region which can be deleted without changes in the transcriptional activity of Tax. Acidic regions which define the activation domains of a large number of transcription factors have historically been associated with interaction with the basal transcriptional machinery being critical for transcriptional activity (Hope et al, 1988). Four cysteine residues (C153, C174, C212 and C261) have been suggested to mediate multimerisation.
2) (Central) The transcriptionally functional domains of Tax: Tsuchiya et al (1994) noted that Tax contained two independent domains (AD1 and AD2), which were largely

overlapping and inseparable. Semmes and Jeang (1995) however noted that an activation specific region could be defined as a discrete domain (amino acids 289-332) sufficient to confer a transcriptional activation function.

3) (Bottom) Mutational analysis of Tax: point mutations introduced into Tax generally have little effect on the transcriptional properties of Tax (Semmes and Jeang, 1992). However other authors have found that substitution of two amino acids drastically reduces the function of Tax causing conformational changes incompatible with nuclear localisation or transcriptional activity. The generation of these mutants has allowed the functional segregation of the NF-κB and CREB/ATF pathways which have each been found to be necessary for transformation of rodent fibroblasts.

[Compiled from Goren et al, 1995; Semmes and Jeang 1992 and 1995; Gitlin et al, 1991; and Tsuchiya et al, 1994.]

Recently, the Tax protein has been dissected using Tax-Gal4 chimeric proteins to reveal two modular domains encompassing amino-acids 2-255 and 227-337 both of which are required for a functional activation domain (Tsuchiya et al, 1994). Furthermore, using a similar assay, Semmes and Jeang (1995) showed that amino-acids 289-322 alone were sufficient to confer transactivation function when fused to a Gal4 DNA binding domain, and may represent a minimal activation domain contacting a transcription factor. Supporting this notion, Tax mutants with alterations within the amino-terminal portion of Tax were unable to interact with CREB suggesting that the carboxyl end of Tax is involved in communication with the basal transcriptional machinery (Adya and Giam, 1995; Goren et al, 1995). Evidence that Tax does indeed contact a host transcription factor mediating Tax transcriptional activity was quickly provided by Clemens et al (1996). They demonstrated that Tax interacts with the TFIIA transcription factor, a member of the basal transcriptional machinery, which forms part of the pre-initiation complex necessary for RNA polymerase II-directed transcription. Other members of the pre-initiation complex may also interact with Tax including TATA Binding protein (TBP) and TFIID (Caron et al, 1993; Duvall et al, 1995).

A substantial body of evidence now supports the role that Tax may be effecting transcriptional activation by acting as a bridging transcription factor. In brief, transcriptional activators facilitate interactions between upstream enhancer-promoter complexes and the basal transcriptional machinery resulting in enhanced transcription rates. They exhibit activation domain-dependent interactions with specific members of the basal transcriptional machinery and may function by increasing the number of pre-initiation complexes. Prominent examples of this type of transcription factor include the Adenoviral protein E1A, and Herpes Simplex VP16 (reviewed by Nevins et al, 1993 [E1A]; Hayward et al, 1993 [VP16]) the latter of which specifically interacts with TFIIA in an activation domain-dependent manner (Ozer et al, 1994).

1.8.3 Trans-regulation of viral gene expression by Rex ($p27^{rex}$)

The HTLV-I Rex protein is responsible for the trans-regulation of viral gene expression, positively controlling pol, env and gag protein expression, and inhibiting expression of protein pX genes (Hidaka et al, 1988). A highly basic amino terminal sequence, the nucleolar targeting sequence targets the Rex protein to the nucleolus (Siomi et al, 1988). Lack of this sequence abolishes the accumulation of unspliced pX mRNA species within the cytoplasm (Nosaka et al, 1989). This regulation of viral gene expression requires a cis-acting rex responsive element (RxRE) which consists of 255 nucleotides located within the 3'U3/5'R region of the 3'LTR (Toyoshima et al, 1990). A critical stem-loop region located within the RxRE is sufficient to mediate high affinity binding (Bogred et al, 1992; Grone et al, 1994) possibly through direct DNA-protein contacts between the RxRE and the Rex arginine-rich RNA binding domain (Baskerville, 1995). A recent report suggests that $p27^{rex}$ may promote the accumulation of unspliced mRNA within the cytoplasm of infected cells by increasing both the stability and nucleocytoplasmic transport of unspliced mRNA transcripts, as well as decreasing the rate of splicing by directing unspliced mRNA to the cytoplasm via a nuclear compartment which avoids intron excision and degradation (Grone et al, 1996). Interestingly, this effect is not limited to viral mRNA, since $p27^{rex}$ also stabilises the human IL-$2R_{\alpha}$ chain mRNA (Kanamori et al, 1990).

Two RxRE have been identified in HTLV-II, one in the 5' LTR (R/U5 region), the other in the 3' LTR (R/U3 region) (reviewed by Gitlin et al, 1993). In this virus it is the active phosphorylated form of Rex ($p26^{rex}$) which binds to the 5' RxRE (Green et al, 1992) and critically this RxRE requires an intact splice-donor site (Black et al, 1991b). Moreover, the HTLV-II 5' RxRE has been shown to contain cis-acting repressive elements (Black et al, 1991a) which bind host cell factors known to be involved in RNA splicing (Black et al, 1994; and 1995). HTLV-II Rex interacts with these elements to inhibit pre-mRNA splicing (Bakker et al, 1996) and so promote unspliced mRNA accumulation within the cytoplasm. Since all viral HTLV mRNAs contain the RxRE it is highly probable that the different

regulation of spliced versus unspliced mRNA must rely on other cis-acting elements within the viral genome, as well as host factors (Black et al, 1994 and 1995).

1.8.4 Viral mRNA polyadenylation

A second function of the RxRE is to mediate a novel form of mRNA polyadenylation. The 3' RxRE region forms a stable secondary stem loop structure (Toyoshima et al, 1990) which serves to spatially juxtapose the widely separated AAUAAA poly(A) signal with the poly(A) site (Ahmed et al, 1991). It is the close approximation of these two sites which facilitates efficient 3' processing and polyadenylation.

1.8.5 $p21^{rex}$

$p21^{rex}$ is a 21kd phosphoprotein of unknown function. It has been isolated constitutively from both cultured HTLV-I infected cells and *ex-vivo* samples supporting its role as a biologically relevant protein (Kiyokawa et al, 1985, Berneman et al, 1992; Orita et al, 1992). The protein lacks the $p27^{rex}$ N-terminal 78 amino-acids which contain the nucleolar targeting sequence therefore restricting its distribution to the cellular cytoplasm. $p21^{rex}$ may serve to potentiate the biological effects of $p27^{rex}$ by modulating the nucleocytoplasmic shuttling of $p27^{rex}$ and thus repress its nuclear export (Kubota et al, 1996).

1.8.6 The minor mRNA species: $p12^{I}$, $p13^{II}$, and $p30^{II}$

The minor RNA species represented by $p12^{I}$, $p13^{II}$, and $p30^{II}$ have not yet been well characterised, and indeed, direct protein expression of any of these proteins has not been shown. RT-pcr reveals that these rare mRNA species are only detected in a minority of *ex vivo* samples (Koralnik et al, 1992, Berneman et al, 1992). None of these proteins are required for $p27^{rex}$, *tax*, or *env* expression (Roithmann et al, 1994). Furthermore, the gene encoding $p13^{II}$, and $p30^{II}$ is frequently mutated within leukaemic cells, leading to premature

termination codons, suggesting it is not required either for outgrowth of leukaemic clones *in vivo* (Chou et al, 1995) or for *in vitro* replication (Berneman et al, 1992b).

1.8.7 $p13^{II}$ and $p30^{II}$

$p13^{II}$, and $p30^{II}$ are derived by alternatively splicing an ORF II mRNA which generates two potential proteins of 13kDa ($p13^{II}$) and 30kDa ($p30^{II}$). Transient transfection of $p13^{II}$ and $p30^{II}$ epitope tagged proteins into rodent fibroblast cell lines revealed that they localise to the nucleus and nucleolus respectively (Koralnik et al, 1993). The nucleolar localisation region (NLR) of $p30^{II}$ has been mapped to a region between amino acids 71 and 98 (Ciminale et al, 1997) and can functionally replace that of $p27^{rex}$ mediating activation of RxRE containing mRNAs (Ciminale et al, 1997).

1.8.8 $p12^{I}$

$p12^{I}$ is a highly hydrophobic 12kDa protein which contains two potential transmembrane domains separated by a proline rich turn. Scattered throughout $p12^{I}$ are highly conserved LLFL motifs (the significance of which are unknown) and four putative SH3 (PXXP) binding motifs (Franchini et al, 1993). Attention has focused upon the $p12^{I}$ protein due to its known homology to the bovine papilloma virus type I (BPV-I) transforming oncoprotein E5. Both proteins are very hydrophobic, contain a critical glutamine residue located within the middle of a potential transmembrane region, bind growth-factor receptors as well as the 16kDa subunit of the vacuolar H^{+}-ATPase [via the proline rich turn of $p12^{I}$ and molecular determinants located between the second and third transmembrane region of 16K (Koralnik et al, 1995)] and localise to similar sub-cellular compartments (perinuclear endomembranes [$p12^{I}$]; golgi apparatus and endoplasmic reticulum membrane [E5]) (Franchini et al, 1993). The functional extent of this homology was revealed by experiments in which E5 and $p12^{I}$ encoding cDNA were cotransfected into rodent fibroblast cell lines. Although $p12^{I}$ alone could not induce focus formation it could significantly potentiate the transforming ability of

E5 (Franchini et al, 1993). The mechanism of this co-operation however remains unclear although it does not directly correlate with $p12^I$ binding the 16kDa subunit (Koralnik et al, 1995) - the presumed cellular target of both $p12^I$ and E5 within the rodent fibroblast system.

The extent of the functional homology between $p12^I$ and E5 is remarkable - $p12^I$ also binds (and down regulates) a growth factor receptor, in this case the immature forms of the interleukin 2 receptor (IL2-R) β and γ_c chains in the pre-golgi compartment (Mulloy et al, 1996). These binding results have been somewhat substantiated in an *in vitro* transcription/translation system in which $p12^I$ was found to bind the IL2R β chain but not the γ_c (Da Costa personal communication). The IL2R is a pivotal component of the immune response. It is composed of at least three chains designated α, β, and γ (for a recent review see Theze et al, 1996). The γ chain is now denoted as the common γ chain (γ_c) since it is also a functional component of the IL-4, IL-7, IL-9, and IL-15 receptors. The β chain also forms a functional component of the IL15 receptor (Giri et al, 1994). Inheritance of a defective γ_c chain gene gives rise to X-linked severe combined immunodeficiency in humans (Noguchi et al, 1993). The importance of the interaction between $p12^I$ and the IL2-R are not fully understood although they may contribute to the mild immunosuppression observed in HTLV-I infected patients (Broder 1986; Yamaguchi and Takatsuki, 1993). Furthermore, the $p12^I$ protein binds the IL2-Rβ chain at its acidic region and may therefore interfere with the normal functioning of the lymphocyte specific protein tyrosine kinase ($p56^{lck}$). This tyrosine kinase also binds the acidic region of the IL2 receptor β chain and serves to couple recognition of IL2 binding at the cell surface to the downstream signal transduction network (Hatakeyama et al, 1991). Therefore $p12^I$ may contribute to the switch from IL2 dependent to IL2 independent cell growth observed in HTLV-I transformed T cell lines (discussed later).

1.9 Phenotype of cells infected with HTLV-I

Primary cultures of T-cells from HTLV-I infected individuals, or HTLV-I infection of primary T-cells, most often leads to the outgrowth of an activated IL-2 dependent (immortalised) cell line (Popovic et al, 1983) which upon co-culture with PBMC or cord blood eventually leads to the generation of an IL-2 independent (transformed) T-cell line. Typically HTLV-I infected cultures are at first immortalised and express high levels of IL2-Rα chain, (Franchini et al, 1984; Chlichlia et al, 1995) *egr-1*, and *c-fos* (Akagi et al, 1995) but clonal selection occurs with time and generally T-cells become ligand independent and do not express IL2 mRNA (Arya et al, 1984; Tendler et al, 1990). In common with HTLV transformed cell lines, leukaemic cells from ATL patients express neither IL2 nor IL4 (Mori et al, 1994) although they continuously express IL2-Rα chain. The transition from IL2 dependent to IL2 independent growth correlates with the acquisition of a constitutively activated Jak-STAT pathway (Migone et al, 1995) as well as elevated levels of *lyn* (B cell specific kinase) and decreased expression of CD3 and $p56^{lck}$ (Akagi et al, 1995). The Jak-STAT pathway is an important signal transduction pathway which networks signals received at the cell surface after binding of the IL2R ligand with the activation of cellular transcription factors in the nucleus (reviewed by Ihle et al, 1995). In brief, ligand induced association of the IL2R β and γ_c chains brings the Janus kinases, Jak 1 and Jak 3 together which in turn phosphorylate signalling proteins recruited to the receptor complex. The primary substrates of Jak 1 and Jak 3 appear to be the signal transducers and activators of transcription (STAT 3 and STAT 5). Phosphorylation of these proteins induces dimerisation, nuclear translocation and transcriptional activity which is associated with the functional rather than mitogenic responses to cytokines. The factors however which govern the transition from IL2 dependent to IL2 independent growth are largely unknown but may represent contributions from other HTLV-I pX gene products since *tax* immortalised T-cells cannot be fully transformed even after 3 years in culture (Akagi et al, 1995). Thus a weight of evidence confirms that the minimal effect of Tax is to act as a mitogen to induce initially a ligand (IL2) dependent autocrine or paracrine proliferative response (Marriott et al, 1991) which in HTLV infected lymphocytes becomes ligand independent (transformed).

1.10 Mechanisms of Transformation by HTLV-I

Two paradigms of retroviral oncogenesis have been developed over the past 20 years or so. The acutely transforming retroviruses discovered by Rous and co-workers in 1911 represent one class of transforming agents. Stehelin et al (1976) demonstrated that these viruses had transduced a host proto-oncogene - in the case of the Rous sarcoma virus this was the *c-src* proto-oncogene. Capture of the *c-src* gene resulted in highly elevated levels of the Src protein. Additionally, the error prone mechanism of reverse transcription resulted in mutation of the *c-src* gene such that the *v-src* gene resulted in a much more oncogenic protein (Varmus and Weinberg, 1993). This mechanism of transformation has since been widely accepted and represents an important mode of leukaemogenesis by the feline leukaemia virus (FeLV) in which it is estimated that one third of naturally occurring T-cell lymphomas in cats contain an FeLV transduced *c-myc* gene (Neil et al, 1984).

The second paradigm of retroviral transformation is illustrated by the chronically transforming class of retroviruses. This mechanism of oncogenesis probably represents the more common mode of tumour induction within the naturally infected host. In this scenario, proto-oncogene subversion is achieved by promoter-enhancer insertional mutagenesis (reviewed by Kung et al, 1991). In brief, neoplasia arises from promotion or enhancement of proto-oncogene expression by nearby integration of the viral LTR promoter-enhancer cis-acting sequences. In this case retroviral infection causes derangement of normal host control of proto-oncogene expression. As before this initiates the cell and spontaneous secondary collaborating lesions serve to progress the cell to the fully transformed phenotype. Examples of this type are provided by the Avian Leukosis Virus (ALV) in which 80% of B-cell tumours induced by experimental infection were due to integration close to the *c-myc* gene (Hayward et al, 1981). These mechanisms of oncogenesis has since provided useful tools to identify hitherto unknown oncogenes through retroviral transduction or insertional mutagenesis (reviewed by Jones and Katy, 1996).

The discovery of the first human retrovirus in the early 1980s was therefore seen as an important step towards elucidating the underlying principals governing human oncogenesis. Contrary to expected opinion at the time HTLV does not transform through either of the aforementioned retroviral mechanisms since it does not contain a transduced cellular proto-oncogene and integration within the genome is essentially random with the site varying from patient to patient (Seiki et al, 1984). Furthermore, infection with HTLV-I leads to the development of ATL in only a small proportion of individuals after a prolonged latency typically of the order of several decades. Clearly transformation represents the accretion of multiple genetic aberrations combined possibly with epigenetic factors such as immunosuppression or mitogenic stimuli (e.g. Strongyloidiasis infection [Nakada et al, 1987]).

However deregulation of host proto-oncogenes is still thought to be a central and perhaps critical mechanism through which HTLV-I transforms cells. Relevant to this hypothesis is the observation by a number of authors that Tax selectively up-regulates expression of various genes involved in T-cell growth and activation [e.g. *c-myc*, *c-fos*, *c-jun*, IL2, IL2-Rα, GM-CSF (see Table 1.3)]. Stabilisation of IL2-Rα chain mRNA by Rex (Kanamori et al, 1990) and binding of the IL2-Rβ and γ_c chains by $p12^I$ (Mulloy et al, 1996) demonstrates that HTLV-I has targeted this cytokine network as a possible mechanism to induce at least an initial phase of autocrine polyclonal T-cell proliferation necessary for efficient viral integration and replication. Paracrine mechanisms have also been suggested since Tax is present in the supernatant of HTLV-I infected cells which can induce proliferation when internalised by human PBMC (Lindholm et al, 1990 and 1992; Marriott et al, 1991 and 1992). Transrepression of host genes involved in the maintenance of genomic integrity probably also contributes to transformation - Tax has been shown to repress the DNA repair enzyme β-polymerase (Jeang et al, 1989) as well as the anti-oncogene Neurofibromatosis Type I (Feigenbaum et al, 1996) (see Table 1.3).

1.11 Tax transactivation of host genes

1.11.1 CREB/ATF

Tax has been shown to act as a promiscuous transactivator of cellular genes and appears to achieve this effect by interacting with two classes of transcription factors (NF-κB and $p67^{SRF}$) in addition to the CREB/ATF family (described previously). Indeed, host genes containing CRE elements are largely unresponsive to Tax (Yin et al, 1995). It now appears likely that Tax forms a quaternary complex which specifically enhances the binding of CREB to both the viral and consensus cellular CRE by recruiting the transcriptional co-activator CREB binding protein (CBP). The differential activation of viral versus cellular CRE elements critically depended upon the phosphorylation status of CREB (Kwok et al, 1996). Tax may bypass the need for phosphorylated CREB to stimulate the viral LTR under basal conditions but activate cellular CRE-containing genes under conditions that lead to CREB phosphorylation.

1.11.2 NF-κB

The NF-κB family of transcription factors (NF-κB1 (p50), NF-κB2 (p52), RelA (p65), c-Rel, and RelB) are a family of dimer forming proteins that bind to the consensus sequence <GGGANNYYCC> (reviewed by Hiscott et al, 1995). A conserved amino-terminal Rel homology domain acts as an interface allowing dimerisation and interaction with another family of inhibitory molecules known as IκB. IκB retains these proteins as inactive complex within the cytoplasm. The IκB proteins (IκBα, IκBβ, IκBγ, bcl-3, p100, and p105 [p105=NF-κB p50 precursor]) are characterised by a carboxyl terminal domain containing five to seven repeats of an ankrin motif. The ankrin motif specifically binds and masks the nuclear localisation signal located within the Rel homology domain. Signals for cellular proliferation and differentiation activate NF-κB responsive genes through rapid phosphorylation, ubiquitination and proteasome mediated degradation of I-κB. This allows transcriptionally active NF-κB homo- and heterodimers to dissociate and translocate to the nucleus (Baeuerle and Baltimore, 1988; Ghosh and Baltimore, 1990).

Tax has been shown to interact with several members of the NF-κB family including p50 (Suzuki et al 1993) p52 (Murakami et al, 1995; Lanoix et al, 1994; Beraud et al 1994), p65 (Suzuki et al, 1994) and c-Rel (Suzuki et al 1994) as well as members of the I-κB family (IκBα Suzuki et al, 1995) IκBγ (Hirai et al, 1994) p105 (Hirai et al, 1992) and p100 (Murakami et al, 1995; Lanoix et al, 1994; Beraud et al 1994) probably through their Rel homology domain (reviewed by Beraud and Greene, 1996) rather than their conserved ankrin motif (Hirai et al, 1994). However Beraud and Green (1996) point out that not all these interactions may be specific suggesting that Tax interacts specifically with only p100, p52 and p65. The general *modus operandi* purports that Tax binds various members of the IκB family within the cytoplasm and targets them for proteasomal degradation. Tax has been shown to induce rapid phosphorylation of IκBα (Sun et al, 1994; Lacoste et al, 1995) and IκBβ (Good and Sun, 1996). Proteasomal mediated degradation of IκBα has been reported (Maggirwar et al, 1995) which may occur through promotion of protein kinase C membrane translocation thereby triggering the PKC cascade (Lindholm et al, 1996). Phosphorylation by Tax may also account for Tax targeted activation of p105 (the precursor of NF-κB p50) via partially processing the p105 inhibitor to yield the active p50 subunit (reviewed by Palombella et al, 1994). However differential effects of Tax on the p100 and p105 molecules have been achieved (Munoz et al, 1995; Murakami et al, 1995) with Watanabe et al (1994) suggesting that Tax only inhibits the p105 IκB molecule and not the p100 molecule.

Tax may also act to induce the constitutive nuclear expression of various biologically active members of the NF-κB/Rel family of enhancer-binding proteins (Arima et al, 1991; Li et al, 1993) through transcriptional upregulation. Binding of Tax to the p50 precursor p105 (Hirai et al, 1992) and p50 (Suzuki et al, 1993b) may serve to indirectly associate Tax with NF-κB responsive promoters and thereby transcriptionally activate these genes.

1.11.3 The serum response factor, $p67^{SRF}$

HTLV-I infected cells constitutively express a high proportion of immediate-early serum responsive genes as a result of enhanced transcription [AP-1: Fos, Fra-1, Jun, JunB, and JunD, and egr-1, egr-2] (Fujii et al, 1991; 1992; Kelly et al, 1992). Several of these immediate-early response genes [*c-fos, egr-1, egr-2*] are transactivated via a common mechanism whereby Tax complexes with and activates the $p67^{SRF}$ resulting in transactivation of its cognate recognition sequence [the CArG box] (Fujii et al, 1992; 1995; Suzuki et al, 1993). Tax binds the serum response factor, $p67^{SRF}$ at its C-terminal domain (Suzuki et al, 1993b; Fujii et al, 1995) which in turn not only acts as an intermediary tethering Tax to the CArG box but supplies an essential component to the transcriptional activation machinery (Fujii et al, 1994).

Table 1.3: Literature survey demonstrating the wide array of cellular genes whose expression is modulated by Tax/HTLV-I expression

Activation

Gene	**Tax responsive promoter /enhancer element**	**reference**
Act-2 cytokine		Napolitano et al, 1991
Egr-1 and Egr-2	$p67^{SRF}$ through CArG box	Fujii et al, 1991,1992
c-fos	$p67^{SRF}$ through CArG box	Fujii et al ,1988, 1991, 1992
	direct repeat element	Alexandre and Verrier, 1991
	cAMP response element	Nagata et al, 1989
	v-sis conditioned medium element	
Fra-1		Fujii et al, 1991
human β/ε globin genes	pentanucleotide CTGAC element	Fox et al, 1989

gp34		Miura et al, 1991
human GM-CSF	CREB/ATF and NF-κB	Himes et al, 1993
human G-CSF	NF-κB	Himes et al, 1993
murine GM-CSF	GC rich stretch and lymphokine element 1	Miyatake et al, 1988
HIV-1^{LTR}	NF-κB	Siekevitz et al, 1987 Zimmermann et al, 1991
HCMV I-E enhancer	18 and 19-bp repetitve sequence motif	Moch et al, 1992 Lal and Rudolph, 1991
IL2	NF-κB	Maruyama et al, 1987 Hoyos et al, 1989
IL2-Receptor α chain	NF-κB	Inoue et al, 1986 Leung and Nabel, 1988; Ruben et al, 1988 Hoyos et al, 1989
IL-3	GC-rich region	Nishida et al, 1991 Marriott et al, 1992
IL-4		Miyatake et al, 1988 Arai et al, 1989
IL-6	NF-κB	Muraoka et al, 1993 Yamashita et al, 1994
c-jun		Hooper et al, 1991 Fujii et al, 1991
junD		Fujii et al, 1991
Krox 20/Krox 24	Serum response element and cAMP responsive element	Alexandre et al, 1991
MHC class 1		Sawada et al, 1990
murine/human *c-myc*	NF-κB	Duyao et al, 1992a, 1992b
Nerve growth factor	AGGGTGTGACGA (92%	Green et al, 1991

	homology with 21bp repeat)	
$p56^{lyn}$		Yamanashi et al ,1989
PTHrP	P2 promoter via Ets-1/	Watanabe et al, 1990
	Ets-I binding site	Dittmer et al, 1993
proenkephalin gene	partly through cAMP-	Joshi and Dave, 1992
	responsive elements	
c-sis		Pantazis et al, 1987
		Ratner et al, 1989
TIMP-1(or erythroid	AP-1	Uchijima et al, 1994
-potentiating activity)		
murine TGF-β		Kim et al, 1991
murine TNF α (cachetin)	NF-κB2	Albrecht et al, 1992
		Lal and Rudolph, 1991
murine TNF-β (lymphotoxin)	NF-κB	Tschachler et al,1993
Transferrin receptor		Vidal et al, 1988
vimentin	NF-κB	Lilienbaum et al, 1990
		Salvetti et al, 1993
zinc-finger gene		Wright et al, 1990

Repressed

β-polymerase		Jeang et al, 1989
CD3 (T-cell recepetor)		De Waal Malefyt, 1990
$p56^{lck}$	E-box	Lemasson, 1997
Neurofibromatosis type 1 gene		Feigenbaum et al, 1996

Table 1.3 summarising the various domains which Tax up/down regulates to modulate gene transcription.

1.12 Oncogenicity of Tax

Several lines of evidence have now established that Tax is indeed an oncogene. Screening of tumours has shown that each tumour cell contains one or a few copies of the HTLV-I provirus monoclonally integrated into the host genome (Franchini et al, 1984). PCR analysis of proviral genomes demonstrate that a high proportion (56%) of patients carry deleted viral genomes, and that the pX region of the HTLV-I genome encoding the regulatory proteins Tax and Rex are preferentially retained (Korber et al, 1991; Tamiya et al, 1996). *In situ* hybridisation (Setoyama et al 1994), reverse transcriptase (RT)-pcr (Ciminale et al, 1992, Berneman et al, 1992, Koralnik et al, 1992) and the persistence of anti-Tax antibodies supports the notion that Tax expression occurs constitutively in PBMC of ATL patients but at very low levels.

Tax immortalises primary human $CD4^+$ cord blood lymphocytes in the context of a Herpes saimiri vector to yield T-cell lines with the same phenotype ($CD4^+$, $CD5^+$, HLA class I^+, IL2-Rα^+) as lymphocytes transformed by co-culture with HTLV-I (Grassman et al, 1989 and 1992). Tax transforms rodent fibroblast *in vitro* in NIH 3T3, Rat 1 and Rat 2 cells (Tanaka et al, 1990) which requires constitutive expression of Tax to maintain the transformed phenotype (Yamaoka et al, 1992). Tax also co-operates with the *ras* oncogene to transform early passage rat embryo cells (Pozzatti et al, 1990). A single amino acid substitution (58Pro→Ser) results in loss of Ras co-operative focus formation but does not affect other *tax* functions such as growth in soft agar, focus formation in Rat-1 cells, immortalisation of REF and transcriptional activation through the CREB/ATF or NF-κB pathways (Matsumoto et al, 1994).

1.13 Oncogenicity of Tax in transgenic mice

The expression of Tax in transgenic mice lends further support to the notion that Tax is a *bone fide* oncogene. HTLV-I Tax transgenic mice develop a number of interesting pathologies including several different types of tumours (as shown in Table 1.4). The cause

of the variance in phenotypic expression is unknown but it may be partly explained by the use of different promoter/enhancer elements and the different level of transgene expression. The most common and consistent phenotype is the development of mesenchymal tumours (Nerenberg et al, 1987) which have also been reported as neurofibromas (Hinrichs et al, 1987). These tumours occur in conjunction with adrenal medullary tumours and iris proliferation (Green et al, 1992) consistent with human neurofibromatosis, although the analysis of neurofibromas from Japan and the United States did not associate HTLV-I infection with neurofibromatosis (Nerenberg et al, 1991). Other phenotypes include inflammatory polyarthritis which resembles Rheumatoid arthritis (Iwakura et al, 1991; Yamamoto et al, 1993), an exocrinopathy resembling Sjogrens syndrome (Green et al, 1989), thymic atrophy (Furata et al, 1989), oxidative muscle degeneration (Nerenberg et al, 1989) and large granular lymphocytic (LGL) leukaemia (Grossman et al, 1995). Interestingly, leukaemic cells derived from these tumours could not be propagated *in vitro*, and did not display typical T-cell surface antigens (CD4, CD8, TCRα/β or TCRγ/δ). Other attempts to transform thymocytes have proven unsuccessful. A Thy-1 based vector which expressed high levels of Tax in the thymus of transgenic mice was unable to transform this compartment (Nerneberg et al, 1991) but instead produced mesenchymal tumours infrequently, and after a long latency.

LTR^{HTLV-I} *c-myc*/$IgG^{promoter}$-*tax* bigenic mice develop a mixed phenotype: 30% of tumours are $CD4^+$ $CD8^-$ T-cell lymphomas, and the remaining 70% are brain tumours derived from a neuronal lineage that resemble neuroblastomas (Benvenisty et al, 1992). Monogenic LTR $^{HTLV-I}$I *c-myc* mice develop $CD4^+$ $CD8^+$ T-cell lymphomas at a lower frequency whereas $IgG^{promoter}$-*tax* mice develop no pathology. This raises the interesting possibility that *c-myc* may co-operate with Tax to induce T-cell lymphomas since *c-myc* transgenic mice usually develop B-cell lymphomas. Alternatively, the enhanced expression of *c-myc* observed in these mice due to Tax transactivation of the LTR^{HTLV-I} *c-myc* promoter may also account for the development of these tumours.

Table 1.4: Phenotypes of various Tax transgenic mice

LTR^{HTLV-I}-*tax*	Mesenchymal tumours/ Neurofibromas
Thy-1-*tax*	Low frequency, long latency fibroblastic tumours
LTR^{HTLV-I}-*tax*	Oxidative muscle fibre degeneration
LTR^{HTLV-I}-*tax*	Adrenal medullary tumours and iris proliferation
LTR^{HTLV-I}-*tax*	Exocrinopathy resembling Sjogren's syndrome
LTR-env-pX	Inflammatory polyarthritis resembling Rheumatoid arthritis
LTR^{HTLV-I}-*tax*	Thymic atrophy
IgH^{enhancer}/SV40^{promoter}-*tax*	Thymic atrophy
LTR^{MMTV}-*tax*	Thymic atrophy
Granzyme B^{promoter}-*tax*	Large granular lymphocytic leukaemia

Table 1.4 summarising the phenotypes and transgene constructs used to generate various HTLV-I transgenic mice

1.14 Mechanisms of transformation by Tax

The use of Tax mutants has demonstrated that transformation of immortalised rat fibroblasts requires constitutive activation of the CREB/ATF pathway (Smith and Greene 1991). However these results are diametrically opposed to those of Yamaoka et al (1996) who demonstrated that the NF-κB pathway is necessary and sufficient for transformation of immortalised rat fibroblasts. The importance of this pathway was further underscored by the observation that HTLV-I *tax*-transformed tumours transplanted into mice were ablated by treatment with antisense NF-κB oligodeoxynucleotides (Kitajima et al, 1992). Activation of NF-κB has also been shown to mitigate the effects of tumour necrosis factor (TNF), ionising radiation, and anti-cancer drugs by specifically inhibiting apoptosis in cells treated with these agents (Beg et al, 1996; Wang et al, 1996; Van Antwerp et al, 1996; and Liu et al, 1996). These results argue strongly for the general importance of NF-κB in

tumourigenesis. In the light of these observations it is difficult to reconcile the discordance between CREB/ATF and NF-κB without invoking a hitherto undiscovered interaction critical for mediating the transforming potential of *tax* in rodent fibroblasts.

A third potential mechanism contributing to the transforming ability of *tax* is the physical interaction between Tax and members of the cell cycle apparatus. Low et al, (1997) and Suzuki et al, (1996) demonstrated that Tax functionally interacts with the cyclin-dependent kinase inhibitor $p16^{INK4A}$ which releases cells from $p16^{INK4A}$ induced G1 growth arrest (functionally equivalent to retinoblastoma inactivation). Cell lines infected with HTLV-I or immortalised by *tax* also demonstrated low levels of another cdk inhibitor, $p18^{INK4C}$ (Akagi et al, 1996).

Tax has also been shown to interfere with p53 function. Cell lines transformed by HTLV-I show a diminished p53-mediated response to ionising radiation (Cereseto et al, 1996). This could conceivably be due to direct transrepression of the p53 promoter (Uittenbogaard et al, 1995) or more directly via enhanced stabilisation of the p53 protein (Reid et al, 1993). However since Tax is not known to either transactivate or bind the p53 protein the mechanism of this interaction is uncertain. Furthermore the significance of these results *in vivo* are less convincing since only a minority of ATL patients exhibit mutations in the evolutionary conserved domain of p53 (Nagai et al, 1991; Yamato al, 1993). [Although where this does occur, p53 mutation is usually accompanied by loss of heterozygocity (Cesarman et al, 1992)]. Unexpectedly, these cell lines also demonstrated elevated expression of the p53 inducible gene, $p21^{waf1/cip1}$ (another cdk inhibitor) which is mediated either by direct transactivation of the $p21^{waf1/cip1}$ promoter (Ceserman et al, 1996) or by p53 independent mechanisms (Parker et al, 1995).

The central importance of these proteins is well recognised. p53, retinoblastoma, and the $p16^{INK4A}$ play important roles in the normal regulation of the cell cycle and the induction of growth arrest in senescent cells. They act as critical tumour suppressor proteins whose functional inactivation contributes to the genesis of a wide variety of human cancers

(Nobori et al, 1994; Kamb et al, 1994; Hollstein et al, 1991 and 1994; Hirama and Koeffler, 1995; Weinberg, 1992a and 1992b). The presence of a biological clock preventing indefinite proliferation and their high frequency of inactivation within human neoplasia suggests that their functional loss maybe pre-requisite for tumour emergence. Their crucial importance to the induction of malignancy is further highlighted by the evolutionary convergence of the DNA tumour viruses (Adenovirus, Human Papilloma Virus (HPV), SV40) and HTLV-I. Each virus has evolved to inactivate the p53 and retinoblastoma or $p16^{INK4a}$ tumour suppressor genes. In the case of Adenovirus and SV40 the E1B 55 kDa protein, and the large T antigen each bind to and stabilise the p53 protein to inactivate its transcriptional activity (Linzer and Levine, 1979; Sarnow et al, 1982) whereas HPV-16 and HPV-18 E6 proteins bind to p53 (Werness et al, 1990) and target it for proteolytic degradation *in vitro* (Scheffner et al, 1990). Furthermore Adenovirus E1A, SV40 large T antigen, and HPV E7 each bind and functionally inactivate the hypophosphorylated (active) form of the retinoblastoma protein (DeCaprio et al, 1988; Whyte et al, 1988; and Dyson et al, 1989). The retinoblastoma gene acts as another negative regulator of the cell cycle and radiation induced apoptosis (Haas-Kogan et al, 1995; Haupt et al, 1995). Inactivation of retinoblastoma results in release of the E2F transcription factor (Bagchi et al, 1991; Chellappan et al, 1991 and 1992; Nevins et al, 1992; Shirodkar et al, 1992) stimulating quiescent cells into G1 cycle progression. This represents a final common pathway for these types of viruses necessary for efficient replication and dissemination. Likewise HTLV-I *tax* functionally inactivates the retinoblastoma (p105, p107 and p130) family of proteins through inhibition of $p16^{INK4A}$. The $p16^{INK4A}$ cdk inhibitor (plus other family members: $p16^{INK4A}$, $p15^{INK4b}$, $p18^{INK4c}$, and $p19^{INK4D}$) inhibit the active cyclin D-cdk 4/6 complex (Hunter and Pines, 1994; Grana and Reddy, 1995; Sherr and Roberts, 1995) which are critical negative upstream regulators of retinoblastoma phosphorylation (Akiyama et al, 1992; Dowdy et al, 1993; Ewen et al, 1993). Retinoblastoma functional activity is tightly regulated by phosphorylation at each stage in the cell cycle (DeCaprio et al, 1989; Buchkovich et al, 1989; Chen et al, 1989). In this context, hyperphosphorylated retinoblastoma is functionally equivalent to inactivation via E1A, E7 or large T antigen.

1.15 Cellular responses to oncogenic stimuli

Cells respond to oncogenic stimuli via two principal mechanisms which appear to represent hard-wired default pathways serving to delete initiated cells from the body. Introduction of oncogenic *ras* into immortalised rodent fibroblasts rapidly transforms them whereas introduction of the same oncogene into normal primary rat embryo fibroblasts results in growth arrest at confluency (Newbold and Overell, 1983). Phenotypically these cells are characterised by accumulation of p53 and $p16^{INK4a}$ causing G1 growth arrest, which is indistinguishable from cellular senescence (Serrano et al, 1997). Complete transformation of normal cells (primary REF) requires the co-operation of oncogenic *ras* with a second oncogene, typically loss of a tumour suppressor gene (for example p53 or $p16^{INK4a}$) or over-expression of *c-myc*, Adenovirus E1a, SV40 large T antigen, HPV E7 (reviewed by Weinberg, 1997). Similarly HTLV-I *tax* immortalises primary REF and fully transforms them in co-operation with mutant ras (Pozzatti et al, 1990). This property of *tax* can be functionally segregated from activation of either the CREB/ATF or the NF-κB pathways (Matsumoto et al, 1994). Thus functional inactivation of $p16^{INK4A}$ or the retinoblastoma protein by HTLV-I and the DNA tumour viruses may circumvent the cellular response to proliferative lesions induced by ras or cellular ageing.

Cells respond to other oncogenic stimuli via induction of programmed cell death or apoptosis. Apoptosis appears to be an evolutionarily conserved 'suicide' programme present in all metazoan cells. It is distinguished morphologically by the rapid onset of cytoplasmic blebbing, nuclear and cellular fragmentation, and the surface expression of novel determinants that trigger phagocytosis (Ucker et al, 1991; Arends and Wyllie, 1991). Deregulated expression of *c-myc* in rodent fibroblasts acts as a powerful mitogen under idealised conditions but results in overwhelming apoptosis upon serum withdrawal (Evan et al, 1992). Addition of specific cytokines (survival factors) can inhibit this effect (Harington et al, 1992). These observations have been extended to the Adenoviral protein E1A (White et al, 1991; Mymyk et al, 1994; Rao et al, 1992; Debbas et al, 1993), and *c-fos* (Preston et al, 1996) both of which are known to be mitogenic. Unsurprisingly Tax which also acts as a

potent mitogen very efficiently induces apoptosis in rodent fibroblasts (Yamada et al, 1994) and T-cells (Chlichlia et al, 1995) and can be rescued by concomitant expression of *bcl-2* (Yamada et al, 1994) in parallel to that observed for E1A (Rao et al, 1992; Chiou et al, 1994). In contrast Bovine Leukaemia Virus (BLV) induced lymphocytosis in sheep is associated with a reduction in spontaneous B-cell apoptosis (SchwartzCornil et al, 1997). The mechanism by which Tax induces apoptosis is unknown. Induction of apoptosis in *tax* transformed cell lines differs in sensitivity to that observed for Myc and Fos transformed cell lines (Fujita and Shiku, 1995) suggesting that transcriptional activation of these proteins is not necessary to mediate the apoptotic response. Expression of TNF (Brady et al, 1992) and DNA damage in Molt-3 cells (Saggioro et al, 1994) both of which are induced by *tax* could trigger apoptosis directly. However the intimate linkage of *tax* with the cell cycle suggests that induction of apoptosis may be due to enforced inappropriate proliferation in the absence of specific survival factors in an analogous manner to that observed for *c-myc* (Evan et al, 1992).

1.16 Development and Progression of ATL

The inactivation of the host response to oncogenic stimuli dictates that tumourigenesis is multistep requiring the functional complementation of co-operating oncogenes. *C-myc* co-operates with H-ras to transform primary REF, in the same way that crossing MMTV-H-ras transgenic mice with MMTV-myc transgenic mice dramatically accelerates tumour development (Sinn et al, 1987). Similar co-operation is observed for *c-myc* transgenic mice crossed with *bcl-2* transgenic or p53 knock-out mice (McDonnell and Koremeyer, 1991; Blyth et al, 1995). The development of acute ATL clearly requires the accumulation of several tumourigenic lesions. The Tax protein most likely provides the initiator. Inactivation of p53 (Cereseto et al, 1996) and $p16^{INK4a}$ function (Low et al, 1997; Suzuki et al, 1996), DNA damage induced by *tax* (Saggioro et al, 1994), as well as trans-repression of β-polymerase (Jeang et al, 1989) [a host DNA repair enzyme] and PCNA [a polymerase δ cofactor involved in DNA replication and repair] undoubtedly creates genetic instability. Loss of p53 function predisposes to gene amplification and aneuploidy (Livingstone et al,

1992) [although it does not affect the rate of spontaneous point mutation or small deletions (Sands et al, 1995)]. Consistent with these notions is the observed rate of proviral deletion and chromosomal anomalies within ATL cells. Upto 56% of individuals with ATL have defective proviruses monoclonally integrated within their leukaemic cells (Tamiya et al, 1996) with preferential retention of the transforming pX region. Additionally karyotypic instability has been frequently reported in leukaemic cells from ATL patients as well as from other forms of leukaemia/lymphoma associated with a T_{helper} phenotype (reviewed by Pandolfi et al, 1992). Sadamori and colleges (1986) showed that six out of eight patients with acute ATL had a 14q11 anomaly which consisted either of inversions or small deletions. A follow up study involving 107 cases of ATL demonstrated that 103 cases showed karyotypic anomalies (96%) and that the most frequent structural chromosomal anomalies in ATL cells were translocations involving 14q32 (28%) or 14q11 (14%) and 6q deletions (23%) (Kamada et al, 1992). Moreover, the presence and extent of aneuploidy and structural chromosomal abnormalities correlated with clinical ATL subtype and therefore the degree of tumour aggressiveness. Interestingly, inversion of chromosome 14 is also frequently observed in HTLV-I negative chronic lymphocytic leukaemias (Zech et al, 1984). The significance of these chromosomal breakpoints in ATL progression is still unknown although the TCRα chain locus has been located at 14q11.2 (Croce et al, 1985) and translocations involving this region may juxtapose the TCRα locus and the *c-myc* locus in certain T-cell leukaemias (Mathieu et al, 1985; Mckiethan et al, 1986).

1.17 Concluding Remarks

The full implications of the complexity woven by the interactions between oncoviruses and host cells are only now becoming apparent. Cellular metabolism is complex and seemingly chaotic – large biochemical networks co-exist in dynamic equilibrium favouring biochemical diversity and functional redundancy. The induction of cancers in multi-cellular organisms is therefore correspondingly complex and non-intuitive reflecting the multi-step range of genetic aberrations required to subvert the cellular machinery which exists to control normal replication and programmed cell death (or apoptosis). Viruses have co-evolved with these

control mechanisms and selectively disrupted them so as to favour replication and survival of infected cells and so enhance the production and dissemination of the virus. In rare circumstances these processes go awry and lead to malignancy. The simple retroviruses and the DNA tumour forming viruses represent two classes of viruses which have solved this problem in seemingly very different ways. However both strategies lead to a final common pathway which ultimately impinge upon and deregulate the central control of the cell cycle - the simple retroviruses by promoting the unusual contextual expression of cellular proto-oncogenes and the DNA tumour forming viruses by functionally inactivating the checkpoint control anti-oncogenes. HTLV-I appears to have adopted a hybrid strategy. Convergent evolution perhaps has generated a molecule, Tax, that can transcriptionally activate a wide repertoire of host oncogenes as well as directly interfering with members of the cell cycle machinery. In parallel to this multi-cellular organisms have evolved to carefully couple cell replication with programmed cell death or enforced growth arrest which serves to functionally delete rogue cells from the body before genetic damage can become stably integrated and propagated within the genome.

Chapter 2

Materials and Methods

Materials and Methods

2.1 Transgenic Mouse stocks

The *tax* gene (a gift from Dr G. Franchini, NCI, Bethseda, Maryland) was derived from a cDNA of the pX region which was transcribed from an HTLV-I provirus. An EcoRI fragment containing the *tax* gene was subcloned and the SphI site which contained the *rex* initiation site was deleted. The chloramphenicol acetyl transferase (CAT) gene from CD3-ε p/CAT/1-9 was then replaced by a Bam HI/XbaI fragment containing *tax* (Clevers et al, 1989) thus placing *tax* under the regulatory control of the CD3-ε promoter-enhancer.

The generation of the CD3-*tax* transgenic mice was carried out by Dr. E. Cameron and Dr. K. Blyth. The CD3-*tax* transgenic founder mice were made by microinjecting the linearised DNA into fertilised mouse ova to generate C57xCBA F1 hybrids according to previously published protocols (Palmiter et al, 1982). The resultant offspring were then back-crossed onto littermate controls to develop 4 lines of transgenic mice.

The $p53^{-/-}$ knock-out mice were a gift from Donehower (Donehower et al, 1992). The p53/tax mice (denoted p/t) were created by crossing $p53^{+/-}$ mice onto the 1300 and 1400 series of CD-3 *tax* mice.

22 Mouse Genotyping by Southern Blot Analysis

22.1 Buffers

All chemicals were purchased from Sigma Chemical Co. unless otherwise stated.

Lysis buffer.
100mM TrisHCL pH 8.5
5mM EDTA pH 8.0
02% SDS

200 mM sodium chloride.

24 x SSC (5 litre)

sodium chloride	1kg
citric acid.	500g

Alkali Buffer (5 litre).

sodium chloride	438.3g
sodium hydroxide	100g

Neutralising Buffer (5 litre).

Tris base	303.5g
sodium chloride	438.3g
hydrochloric acid	165 ml

Reaction Mixture 1.

5µl reaction buffer 3 (Gibco BRL)

3µl E*co*R 1 restriction enzyme (Gibco BRL)

3µl Bg1 11 restriction enzyme (Gibco BRL)

1µl Rnase

1µl spermidine

7µl ultra pure water.

10 x TBE Buffer (2 litre).

Tris base	216g
boric acid	110g
0.5m EDTA pH8.0	80 ml

5x TBE Loading Dye.

50% glycerol

50% 10x TBE

bromophenol blue

TE buffer pH8.0
10 mM Tris-HCL pH8.0
1mM EDTA pH8.0

2.2.2 Genomic DNA extraction.

High molecular weight DNA was extracted from mouse tails using a Nucleon II Kit (Scotlab) according to the manufacturers protocol. A small section of tail (1-2 cm) was placed in a 1.5 ml reaction tube with 500µl lysis buffer and 25µl proteinase k (10mg/ml) (Sigma Chemical Co.) and incubated overnight at 55°C on a rocking platform. 125µl of 5M sodium perchlorate was added and rotary mixed for 15 minutes at room temperature. Samples were then incubated in a shaking water bath at 65°C for 25 minutes. DNA was extracted by adding 500µl of cold chloroform (BDH Ltd), rotary mixed for 10 minutes at room temperature and then microcentrifuged at 3,000 r.p.m. for 1 min. 75µl of Nucleon silica suspension was added and the sample was microcentrifuged at 4,000 r.p.m. for 3 minutes. The DNA phase above the nucleon silica suspension layer was transferred to a fresh tube. Two volumes of 4°C 100% ethanol was added and the tube inverted gently to precipitate the DNA. The DNA was recovered by lifting the precipitate from the solution and dissolved in 100µl ultra pure water. The DNA was left overnight at room temperature to allow complete dissolution. The concentration of DNA was determined by measuring the absorbency at 260nm.

2.2.3 Restriction digestion of DNA for detection of the *tax* transgene

A Bam HI/Eco RI fragment digest was carried out on tail genomic DNA in CD3-*tax* mice to release a *tax* fragment of 1.0kb. Each digestion required 10 µg of DNA made up to 30µl of water and 20µl of reaction mixture 1 and was incubated overnight at 37°C. The samples were removed from the water bath and 5µl of TBE loading dye was added.

2.2.4 Separation by gel electrophoresis

The DNA samples were run on an 0.8% agarose gel at 28 volts overnight in 1x TBE buffer containing a 1/20 dilution of stock ethidium bromide (0.5μg/ml, Sigma Chemical Co.). The gel was photographed under UV transillumination.

2.2.5 Southern blot

The gel was washed in alkali buffer for 45 minutes, followed by washing in neutralising buffer (45 minutes) and finally in 10x SSC buffer for 15-30 minutes. The DNA was transferred overnight onto Hybond membrane (Amersham Ltd) by an upward capillary transfer. The DNA on the membrane was immobilised by UV crosslinking for 8s at 1200μ joules × 100 using a UV stratalinker 1800 (Stratagene).

2.2.6 Radioactive labelled probes

Detection of the CD3-*tax* transgene was carried out using a 1.0kb Bam H1/Eco R1 *tax* fragment derived from the original p30 vector. DNA fragments were labelled using a multi-prime labelling kit (Amersham Ltd) with α 32 P dCTP (3000 Ci/mMole, Amersham Ltd) to specific activities of > 0.5×10^{8} cpm/μg. 50-100 ng/μl of DNA fragment was added to 23μl water and boiled for 5 minutes, then chilled on ice. 5μl primer, 10μl labelling buffer and 2μl Klenow enzyme were added and mixed gently. To this 8μl of α 32 P dCTP was added and left overnight at room temperature. The labelled DNA fragment was then separated from unincorporated nucleotides by column chromatography and the fragment was eluted through a sephedex (G-50, DNA grade, Pharmacia) column using TE buffer pH 8.0. The labelled DNA moved down the column quicker than the unincorporated nucleotides creating 'two peaks' which were detected using a hand held minimoniter. The first peak contained the labelled DNA probe which was collected in a reaction tube and stored at -20°C until required.

2.2.7 Hybridisation using dsDNA radioactive probes

DNA blots were prehybridised with 10-15ml Quikhyb (Stratagene) at 68°C for 15 minutes. 500µl of denatured gene bloc (5mg/ml) (Immunogen Ltd) and 100µl of denatured *tax* probe was added and incubated at 65°C for three hours. The blots were then washed twice in 2x SSC, 0.1% SDS for 15 minutes, followed by 2 x 15 minutes in 0.2% SSC, 0.1%SDS and a final wash in 0.1% SSC, 0.1% SDS for 15 minutes. The blot was then dried and wrapped in Saran wrap, placed in a hypercassette (Amersham Ltd) with autoradiograph hyperfilm-MP (Amersham Ltd) overnight in -70°C freezer prior to development.

2.3 Histopathology Techniques

2.3.1 Preparation of tissues

The mice were examined three times per week and sacrificed according to the home office guidelines. Each mouse was autopsied and samples immediately taken for histopathological examination and RNA analysis. Tissue samples for histology were fixed in 10% neutral buffered formalin, post-fixed in mercuric chloride, and embedded in paraffin wax. Sections (2-3µm) for immunocytochemistry were mounted on 3-aminopropyltriethoxysilane (Sigma Chemical Co.) coated glass slides and routinely stained with haematoxylin and eosin (H+E). Age-matched control samples were taken from normal C57/CBA mice and stained in parallel to tumour samples.

2.3.2 Generation of Tax Antibody

Synthetic four branch multiple antigenic peptides (MAPs) were made by Fmoc solid phase polyamide synthesis (Jackwood et al, 1995; Tam et al, 1988; Posnett et al, 1988) using amino-acid (aa) sequences corresponding to two distinct regions of the Tax molecule (aa 109-121 NH2-MRKYSPFRNGYME (Tax-14) and aa 338-353 NH_2-GGLEPPSEKHFRETEV (Tax-16)). New Zealand White rabbits were immunised by a subcutaneous injection of 100µg of the MAPs dissolved in non-ulcerative Freund's

adjuvent (Guildhay Ltd., UK.) every 6-8wks. The primary immunisation was administered complete with BCG vaccine (John Bell + Croyden, UK) - all other immunisations were incomplete. Blood from the rabbits was collected aseptically 1-2 weeks after each immunisation until a high titre was achieved. After each collection the blood was allowed to clot, the serum was harvested and stored at -20^0C or at 4^0C with the addition of 0.01% sodium azide (Sigma Chemical Co.).

2.3.3 Analysis of the anti-peptide Tax serum

Serum from the rabbits, designated Tax-14 and Tax-16 (denoting antibody generation from Tax peptide 14 or 16 respectively) was tested for antibody production by indirect ELISA using the Pierce ELISA kit (Pierce & Warriner UK, Ltd.). The system was optimised according to the manufacturer's protocols.

1μg of MAP was immobilised directly onto 96 well microtitre plates, incubated for 1 hour at room temperature, washed, and blocked using manufacturer's washing and blocking solutions. Both primary and secondary antibodies were titrated out by serial 1:2 dilutions according to the manufacturer's standard two-dimensional ELISA protocol. Primary antibody was first serially diluted vertically, incubated for 1 hour at room temperature, rinsed and washed. Secondary labelled sheep anti-rabbit antibody was serially diluted horizontally, incubated for 1 hour at room temperature, rinsed and washed. The alkaline phosphatase chromagen was then added, incubated for half an hour at room temperature, and the absorption measured at 405nm.

Serial dilutions of serum were then analysed for antibody titre using a fixed dilution of secondary antibody (1:1000).

2.3.4 Immunocytochemical Analysis

Fos (SC-052), Myc (N-262) (both from Santa Cruz Biotechnology Inc.), and Jun (PC-07) (Calbiochem-Novabiochem, UK) polyclonal antibodies were titrated and optimised on

known positive samples and used at the appropriate dilution (Fos 1:250; Myc 1:500; Jun 1:500) together with 0.1% bovine serum albumin/0.01% sodium azide in PBS (Sigma Chemical Co.).

Tax-14 and Tax-16 serum was also optimised using the above method by serial dilution on control sections which were known to express *tax* by Northern analysis. Control sections were either untreated, pre-incubated with 0.1% trypsin, 0.1% $CaCl_2$ in PBS (120 mM NaCl, 11.5 mM NaH_2PO_4, 31.3 mM KH_2PO_4, pH 7.6) (Sigma Chemical Co.) or heat treated by microwaving in 0.01M sodium citrate (Sigma Chemical Co) for optimum antigen retrieval. The optimum dilution of Tax antibody (1:100 on untreated sections) was then used for all subsequent immunocytochemical staining.

Immunopositive cells were detected using the ABC method: tissues fixed in formalin were deparaffinized, rehydrated, and washed in Lugol's iodine to remove mercuric chloride. Incubating in 0.5% hydrogen peroxide in methanol for 30 minutes inactivated endogenous peroxidases. Sections, where appropriate, were incubated in saponin (Sigma Chemical Co.) according to the recommendations of the suppliers of the primary antibody, washed and then pre-blocked in 1.5% normal rabbit serum for 30 min at room temperature (RT). (Blocking antibody concentration was varied between 1.5 – 20% to reduce background staining. 1.5 % was chosen as the optimum concentration of blocking antibody).

Primary antibodies were incubated with the sections overnight at 4°C. The sections were then washed and a biotinylated swine anti-rabbit secondary antibody (Dako) was added for 30 minutes at RT, washed, and an avidin-biotin complex (Dako) containing horseradish peroxidase was added for 45 minutes at RT. The sections were washed again, stained using 3,3'-diaminobenzidine/hydrogen peroxide tablets (Sigma Chemical Co.) and counterstained with Mayer's/Gill's haematoxylin.

All washes were performed in triplicate for 5 min at RT in PBS. Incubations were performed in humidified chambers.

The same procedure was used for the p53 antibody (CM5) (Novacastra Laboratories Ltd.). However these sections were heat-treated to unmask antigens by pressure cooking for either one or two minutes in 0.01M sodium citrate, pH 6.0.

The same procedure was used for the MCA519 (rat anti-mouse macrophage antibody) except the sections were not deparaffinised.

2.3.5 DNA Nick End Labelling of Tissue Sections

Sections were deparaffinised and rehydrated as before. Slides were deproteinised with 20μg/mL proteinase K (Sigma Chemical Co.) for 15 minutes at RT, washed in PBS, and endogenous peroxidases were inactivated with 3% hydrogen peroxide in methanol for 5 min at RT. After washing in PBS, the slides were rinsed in terminal deoxytransferase (TDT) buffer (30mM Trizma base pH 7.2 + 140mM Na Cacodylate + 1mM $CoCl_2$) for 2 minutes at RT, and then incubated in a humid chamber for 1 hr at 37°C in TDT (Boehringer Mannheim) (0.25 units/μL) and biotinylated-16-dUTP (Boehringer Mannheim) made up in TDT buffer. The reaction was terminated by washing in TB buffer (300mM NaCl + 30mM sodium citrate) twice for 5 minutes at RT, washed in PBS and then incubated for 1hr at RT in horseradish peroxidase-streptavidin (Dako) diluted 1:200 in house detection diluent (100mM Trizma base, 50mM NaCl, 20mM $MgCl_2$, with 0.5μL/mL Tween 20, pH 8.5). Staining was performed either with 3-amino-9-ethylcarbazole (AEC) (Vector Laboratories, Peterborough, UK) or 3,3'-diaminobenzidine (DAB) (Sigma Chemical Co.) and counterstained with Mayer's/Gill's haematoxylin. As before all washes were performed in triplicate in PBS unless otherwise stated.

2.3.6 Immunofluorescent Co-localisation of Tax expression and Apoptosis

Sections were first nick-end labelled as before and then treated with the Tax antibody diluted 1:10. Fluorescent secondary antibodies were then incorporated, incubating with a Texas Red-streptavidin (Molecular Probes) (1:1000) and anti-rabbit IgG-FITC (Sigma Chemical Co.) (1:25) for 1 hour at RT. The Texas Red-streptavidin was allowed to bind to

the biotinylated dUTP nucleotides first before the addition of the anti-rabbit IgG-FITC. The sections were washed in PBS and directly visualised under UV illumination.

2.3.7 Analysis of apoptotic and mitotic indices

Mitotic and apoptotic indices were measured by counting the average number of cells for 5 random high power fields (x1000) using light microscopy. The numbers of metaphase/anaphase mitotic figures or the number of cells staining with PCNA (F051) (Santa Cruz Biotechnology Inc.) were counted as an estimate of mitotic index. Similarly the number of cells staining with the TUNEL technique were counted as an estimate of the apoptotic index.

2.4 Tissue Culture Techniques

All reagents were bought from Gibco BRL unless otherwise stated.

2.4.1 Media

Complete DMEM

Complete DMEM medium was prepared aseptically by supplementing DMEM (Gibco BRL) with 10% heat inactivated foetal calf serum (FCS), 100U/mL penicillin, 100μg/mL streptomycin, 2mM L-glutamine and 10mM HEPES buffer (all from Gibco BRL). For transfections 8% modified bovine serum (Stratagene mammalian MBS transfection kit) was substituted for FCS.

Cell Freeze Down Medium

Sterile 10% dimethyl sulphoxide (Sigma Chemical Co.) was added to 90% FCS under aseptic conditions.

Tamoxifen Stock solution

4-hydroxy-tamoxifen was dissolved in ethanol to a final concentration of 5mM and stored at –20°C.

2.4.2 Growth of cell lines

Tumour cell lines T1 (derived from a 1300 series mesenchymal tumour), p/t 50 and p/t 54 (derived from p/t 50 and p/t 54 transgenic mice) were generated by aseptically collecting tumour samples into complete DMEM medium and homogenising the tumour using a 100μM wire grill. The homogenate was grown in complete DMEM at 37°C and 5% CO_2. Tumour cell lines were serially passaged by splitting 1:4 twice per week into complete DMEM solution.

2.4.3 Transplantation of tumour cell lines

Tumour cell lines were washed in warm PBS (37°C), resuspended with 2mL trypsin-EDTA (Gibco BRL) and 10mL of warm PBS (37°C), and counted on a calibrated Coulter counter. $5x10^6$ cells were aliquoted into warm PBS (37°C), spun at 1500g for 2 minutes, and resuspended in 250μL of complete DMEM. The resuspended cells were then injected subcutaneously into nude mice. Each experiment was performed in triplicate.

2.4.4 Analysis of retroviral vector function

Functional integrity and inducibility of each expression construct was determined by analysis of the ability of each vector to transiently activate CAT expression from HTLV-I LTR-CAT, NF-κB-CAT and SRE-CAT reporter gene expression constructs. Each Tax-MER vector was transiently transfected into BHK cells (described later) together with HTLV-$I^{LTR-CAT}$, HIV-$I^{LTR-CAT}$ and c-fos-CAT reporter gene constructs. The HTLV-$I^{LTR-CAT}$, HIV-$I^{LTR-CAT}$ and c-fos-CAT reporter gene constructs each required functional activity of the Tax-MER protein CREB/ATF, NF-κB or SRF binding domains, and thereby tested

the function integrity of this domain. Induction of the Tax-MER protein was assayed by the addition of 250nm 4-hydroxy tamoxifen.

2.4.4.1 Transient Transfections

$8x10^4$ exponentially growing cells were aliquoted into 35mm dishes 24 hours prior to transfection. Transfections were carried out using the mammalian MBS transfection kit (Stratagene Ltd., Cambridge). 5μg of DNA was made up to a final vol. of 450μL with sterile water, and 50μL of 2.5M Ca_2Cl added. 500μL of 2xBBS (N,N-bis(2-hydroxyethyl)-2-aminoethanesulfonic acid and buffered saline) was added by drop-wise addition whilst shaking and allowed to stand at RT for 15-20 min. Cells were washed twice in PBS and 4mL of 8% MBS supplemented DMEM medium added. 400μL of transfection solution ($1/10^{th}$ vol.) was then added and the cells were incubated at 35°C, 3% CO_2 for three hours. Cells were then washed three times in PBS, 4mL of complete DMEM medium added and returned to 37°C, 5% CO_2. Induction of the Tax-MER construct was achieved by adding 250nm final concentration of tamoxifen.

2.4.4.2 Optimisation of transfections

Fixing solution (100mL)

5.41mL of 37% formaldehyde (2% final concentration)
2.00mL of 10% glutaraldehyde (0.2% final concentration)
10.00mL of 10xPBS (1xfinal concentration)
Sterile water to 100mL

Histochemical reaction mixture (250mL)

0.411g potassium ferricyanide (5mM final concentration)
0.53g of potassium ferrocyanide (5mM final concentration)
5mL of 100mM MgCl2 (2mM final concentration)

25mL of 10xPBS (1xfinal concentration)
Add X-gal just before use (40mg/mL in DMSO stock solution) to give a final concentration of 1mg/mL and make up to a final volume of 250mL with sterile water.
Optimisation was carried out according to the mammalian MBS transfection kit (Stratagene Ltd., Cambridge). BHK cells were aliquoted at approx. 20% confluency into 24 well plates 24 hours prior to transfection. A β-gal expression vector was used as a reporter construct. The transfection was carried out as described above except that a two–dimensional titration (DNA concentration versus MBS concentration) was performed. DNA was serially diluted from 0.5-5.0μg/mL (total amount of DNA per mL of transfection solution) in 1μg/mL increments. MBS was serially diluted from 2-8% MBS in 1% increments.

Cells were stained for expression at 6hr, 24 hours and 48 hours post transfection. This was done according to the Stratagene protocol: cells were washed twice in PBS, fixed for 5 minutes in fixing solution, washed once in PBS, and incubated in histochemical staining solution for 14-24 hrs at 37°C. Cells were then washed twice in PBS and viewed under a microscope.

Once the optimum concentration of DNA and MBS had been determined the optimum cell density (number of cells per dish) was determined. BHK cells were aliquoted at 37k, 48.1k, 74k, 99k, and 148k per well into 35mm diameter tissue culture dishes and transfected with $1/10^{th}$ volume of 5.0μg/mL transfection solution containing the β-gal reporter construct and 8% MBS as previously described.

2.4.4.3 Stable Transfections

Stable transfections were performed in the same way using the mammalian MBS transfection kit (Stratagene Ltd., Cambridge). However cells were split 1:10 and 1:20 after 24 hours incubation at $37^{O}C$ into medium supplemented with G418 (Gibco BRL) at 800μg/mL. Monoclonal colonies were picked using cloning rings once all control cells (untransfected cells) had died, typically at 7-14 days post transfection. Monoclonal

colonies were allowed to grow to confluence, maintained at 400μg/mL G418, and then frozen in freeze down medium and stored in liquid nitrogen.

2.4.4.4 CAT assays

CAT assays were performed using the Flash CAT non-radioactive CAT assay kit (Stratagene Ltd., Cambridge). 24hrs after transient transfection cells were washed in PBS, harvested using cell scrapers, pelleted, and resuspended in 100μL of reaction buffer. Cells were lysed by freeze thawing twice in a dry-ice/ethanol bath. 15μL of BODIPY 1-deoxyCAM substrate reagent and 10μL of 4mM acetyl CoA (Sigma Chemical Co.) were added to 55μL of cell extract and incubated at 37°C for 1/2hr – 3hr according to each reporter gene expression CAT construct. A positive control (1μL of chloramphenicol acetyl transferase (0.05IU/μL) was optionally included (Stratagene Ltd., Cambridge)) to validate the CAT reaction conditions as per the manufacturer's protocol. 5μL of reaction products were spotted onto a thin layer chromatography plate together with 5μL of acetylated 1-deoxy-CAM reference standard, separated by thin layer chromatography (87:13 ratio of chloroform:methanol), and photographed under UV transillumination. CAT assays were quantitated by scanning the photographed images into a digital format (Microtek Scanmaker) before analysing the image using a commercially available software programme (Phoretex Image analysis software). The results of each CAT assay were the average of 3 separate experiments performed on at least 2 separate days.

2.4.5 Cell Counting Experiments

Actively growing Rat 1 log phase cells were aliquoted into 24 well plates at $1x10^4$ cells per well and grown in complete DMEM medium at 37^oC and 5% CO_2 for up to 4 days. After 2 or 4 days incubation the supernatant was removed and the cells washed gently in warm PBS (37^oC) to remove non-adherent dead cells. The remaining adherent live cells were then removed from the wells by incubating with 0.1-0.5 mL of trypsin-EDTA (Gibco BRL) solution until retraction of the cells was evident under light microscopy. The cells

were then removed by agitation with 2mL of warm (37^{O}C) PBS and counted immediately using a calibrated Coulter counter.

The concentration of FCS was optimised by serial titration of the FCS from 0.1 to 0.5% concentration in 0.1% increments and the total live adherent Rat 1 cells were counted after 2 and 4 days incubation. Similarly the tamoxifen concentration was optimised by growth of Rat 1 cells in 100nm and 250nm tamoxifen solution and the total live adherent cells were counted after 2 and 4 days incubation.

Analysis of apoptosis was performed in the same way. Each of the Rat-1 stably transfected cell lines was assayed by growth of each cell line in complete DMEM medium at 37^{O}C, 5% CO_2 for 2-4 days containing 0.1% FCS with or without the addition of 250nm tamoxifen. After 2 or 4 days the number of live adherent cells was counted using a Coulter counter. Each experiment was performed 4 times on at least 2 separate days.

2.5 Molecular Biology Techniques

All reagents were purchased from Sigma Chemical Co. unless otherwise stated.

L-broth

1% (w/v) tryptone, 0.5% (w/v) yeast extract, 1% (w/v) sodium chloride in ddH2O, autoclaved and stored at RT. Ampicillin (final conc. 50μg/mL) or kanamycin (final conc. 50μg/mL) was added as needed.

STET solution

8% sucrose (w/v), 0.5% Triton X-100, 50mM EDTA, 10mM Tris

TE solution

10mM Tris.HCL, 1mM EDTA, pH as required.

TBE solution (x10)

0.9M Tris.HCL, 0.9M Boric Acid, 25mM EDTA pH 8.3.

X-gal

Stock solution at 40mg/mL dissolved in dimethylformamide.

10 x MOPS buffer

MOPS	41.8g
sodium acetate	6.8g
EDTA	3.7g
ultra pure water	made up to 1 litre.

pH was adjusted to 7.0 using 10 M sodium hydroxide and stored at room temperature in a dark bottle.

RNA loading buffer

formamide	50%
formaldehyde	2.2M
MOPS	1X

Stored at -20°C.

DEPC treated water

DEPC	2 %

ultra pure water

The mixture was shaken vigorously to dissolve the DEPC and left to stand overnight at room temperature, then autoclaved.

2.5.1 Preparation of oligonucleotides

Oligonucleotides were synthesised on an Applied Biosystems 3818A Automated DNA Synthesiser (operated by Mr McPherson, University of Glasgow, Dept. Veterinary Pathology). DNA was eluted from columns using 2.5mL of ammonia and deproteinised by incubating overnight (o/n) at 55°C. Ammonia was removed under vacuum and the resulting DNA pellet reconstituted in TE (pH 8.0). Yield and purity were estimated by measuring the absorbency at 260nm and 280nm on a GeneQuant II spectrophotometer (Pharmacia Biotech).

2.5.2 3' Terminal Tax primers: (amplifies the terminal 5' portion of tax, removes the stop codon and puts it in frame with a 3' MER fusion molecule).

The following primer pairs were used to facilitate cloning of the *tax* or modified oestrogen receptor cDNAs (a gift from Gerard Evan) into the pBabe retroviral vector to generate Tax-MER fusion proteins. PCR, restriction enzyme digestion, ligation, and sequencing methods are described later. Initially all pcr products were cloned into the TA cloning vector (pCRII) (Stratagene Ltd., Cambridge).

To generate the Tax-MER fusion protein the 3' XmaI/BamHI pcr *tax* fragment was cloned into pCRII (Stratagene Ltd., Cambridge). This fragment was then restriction enzyme digested (XmaI/BamHI), purified and ligated to the 5' BamHI/SmaI parental *tax* fragment derived from p30 (original pUC vector containing the *tax* fragment supplied by Dr Campbell). The full length purified BamHI/EcoRI MER fragment was then cloned directly into the BamHI/EcoRI retroviral vector multiple cloning site from the parental plasmid pBSk^{+}. Finally the modified full-length BamHI *tax* fragment was cloned into the pBabe-MER retroviral vector at the BamHI site which had been previously treated with alkaline phosphatase to prevent self-ligation. The *tax* cDNA was then orientated by restriction enzyme digestion.

27mer |--Sma I--|

Forward primer: 5'-CGG/CCC/GGG/GGC/TTA/GAG/CCG/CCC/AGT/GAA-3'

27mer |--Bam HI--|

Reverse primer: 3'-GC/CGG/ATC/CCA/GAC/TTC/TGT/TTC/GCG/GAA/A-5'

(stop→trp)

2.5.3 MER primers: amplifies the whole of MER, removes the stop codon, and puts it in frame with a 3' *tax* molecule

The MER-tax fusion molecule was derived in much the same as the Tax-MER molecule. In this case the parental *tax* molecule was cloned directly into the BamHI/EcoRI multiple cloning site of the pBabe retroviral vector directly from the parental plasmid p30. The whole MER molecule was pcr amplified and cloned into pCRII (Stratagene Ltd., Cambridge) and subsequently sub-cloned into the BamHI site of pBabe-*tax*. Orientation was performed as before by restriction enzyme digestion.

The double MER-Tax-MER molecule was derived by double ligating BamHI *tax* and MER molecules with the pBabe-MER molecule previously generated. Orientation was performed by restriction enzyme digestion as before.

All pcr products were sequenced using either the in house automated sequencer or by "Alta Biochem." (Birmingham).

|--Bam HI--|

Forward primer: 5'-CCC/GGA/TCC/ACG/AAA/TGA/AAT/GGG/TGC/TTC-3'

|--Bam HI--|

Reverse primer: 3'-AAA/ATG/GAT/CCA/GAT/CGT/GTT/GGG/GAA/GCC-5'

(stop→P)

2.5.4 Generation of mutant *tax* expression construct

Three mutant clones of *tax* based on published data (Smith and Greene, 1990; Semmes and Jeang, 1992; Yamaoka et al, 1996) were generated by Dr. M. Campbell. Point mutations were introduced into the primary amino acid sequence of Tax by mutating the pcr primer sequences to generate mutations in the parental *tax* sequence at positions 3 (M1), 23 (C23S) and 319 (M47) as previously described (Semmes and Jeang (1992) M1; Smith and Greene (1990); M47 Smith and Greene (1990). These were subcloned into the pBabe-Neo retroviral vector to generate C23S, M1, and M47 – MER fusion constructs.

2.5.5 Polymerase Chain Reaction (PCR) amplification of DNA molecules

PCR was performed using the thermostable Taq (*Thermus aquaticus*) DNA polymerase. The PCR reaction mixture was made up of 10μL of template DNA (usually 5ng/μL), 5μL of primers (1.25μM), 5μL of nucleotides (each nucleotide at 200μM), 5μL of buffer (10mM Tris.HCL pH8.3, 50mM KCl, 1.5mM $MgCl_2$, 0.001% w/v gelatin), 0.4μL of Taq enzyme and water to 50μL. Thermal cycling was carried out in a Perkin-Elmer 9600 GeneAmp thermocycler. A typical cycle reaction consisted of denaturation at 94°C for 1 minute, annealing at 50°C for 1 minute, and polymerisation at 72°C for 1 minute.

2.5.6 DNA purification from agarose gels

DNA was purified from agarose gel using the Qiaex I/II Gel Extraction kit (Qiagen Ltd, UK). After electrophoresis the DNA was excised from the agar gel under UV illumination. The gel was dissolved in buffer, incubated at 50^{O}C for 10 minutes, bound to 10μL of Qiaex beads, washed and pulse-centrifuged as per the manufacturer's recommendations. The resulting pellet was air-dried and the DNA eluted with 10μL of 10mM Tris-Cl, pH 8.5. 1μL of the final solution was electrophoresed against a known standard (5μL of 1kb ladder (Gibco BRL)) to determine fragment size and concentration.

2.5.7 Ligation of DNA molecules

Ligations of DNA molecules were carried out either using the TA cloning kit (Invitrogen BV, UK) for pcr products, the Rapid DNA Ligation kit (Boehringer Mannheim, UK) or T4 DNA ligase (Gibco BRL). Where appropriate vector DNA was pre-treated with 1U of calf intestinal alkaline phosphatase or 1U of shrimp alkaline phosphatase to prevent self-ligation. Approximately 50ng of vector DNA was ligated with a 3-10x excess of insert DNA. DNA ligase buffer was added (supplied with enzyme) to a final concentration of 1x and water to a final volume of 10 or 20μL. Optionally 1μL of 10mM ATP was added. Ligations were left o/n at 14°C.

2.5.8 Bacterial Transformation

1μL of ligation mixture (approx. 0.5-5ng DNA) together with 1μL of 2-mercaptoethanol was added to 50μL of DH5α™ competent cells (Gibco BRL) or '1 shot cells' (supplied with TA cloning kit (Stratagene Ltd., Cambridge)) and incubated on ice for 30 minutes. Cells were then heat shocked at 42°C for 45 seconds and returned to ice for 2 minutes. 450μL of SOC medium or L-broth was then added and incubated in a rotary shaker (220 rpm) for 1 hour at 37°C. Cells were then plated onto L-agar plates containing either ampicillin at 50μL/mL or kanamycin at 50μg/mL. Optionally agar plates were pre-treated with 25μL of a 40mg/mL stock solution of X-gal if colour selection was required. Plates were incubated o/n at 37°C and white recombinant colonies were picked.

2.5.9 Preparation of Plasmid DNA

2.5.9.1 Small scale Preparation

Colonies grown overnight were picked and inoculated into L-broth containing 50μg/mL of ampicillin or 50μg/mL of kanamycin. Cultures were grown o/n in a rotary shaker (220rpm) at 37°C. Plasmid DNA was purified using the boiling method. 1mL of culture

was pelleted at 6500 rpm for 2 min. The supernatant was discarded and 150μL of STET solution was added plus 10μL of freshly made lysozyme (10mg/mL) and vortexed. The tubes were boiled for 40 sec., cooled on ice for 2 min., and spun at 13000 rpm for 10 min. The large glutinous pellet was removed, 100μL of isopropanol added and stored at -20°C for at least 15 minutes to precipitate plasmid DNA. The DNA was then pelleted at 12000 rpm for 5 min., and 200μL of 70% ethanol added. After pelleting all ethanol was removed, allowed to dry and the DNA was dissolved in 50μL of ultra pure water. 1μL of RNAse A (10μg/mL) was added to any subsequent enzyme reactions to remove RNA contamination. 1μL of the final solution was electrophoresed against a known standard (5μL of 1kb ladder (Gibco BRL)) to determine fragment size and concentration.

2.5.9.2 Large Scale Preparation

Bulk scale preparations were prepared using the Wizard Maxi-Prep kit (Promega, UK). 500mL of colonies are grown overnight in L-broth containing 50μg/mL of ampicillin or 50μg/mL of kanamycin in a rotary shaker (220rpm) at 37°C. The DNA was extracted and allowed to bind to a 'Qiagen' tip as per the manufacturer's protocol. The DNA was washed with TBE, pH 8.0 and then eluted from the column with TE solution, pH 8.0. The DNA was then precipitated at room temperature using 70% ethanol, and centrifuged at 15,000 g for 10 minutes. The resulting pellet was air-dried for 10-15 minutes, and redissolved in 500μL of ultra-pure water. 1μL of the final solution was electrophoresed against a known standard (5μL of 1kb ladder (Gibco BRL)) to determine fragment size and concentration.

2.5.10 Restriction enzyme digestion

Restriction enzyme digestion was performed by adding 2μL of enzyme (Gibco BRL) with 2μL of enzyme buffer (Gibco BRL), 6μL of ultra-pure water and generally 0.5-1 μg of DNA (4μL) (total volume 10μL). The mixture was incubated for 1 hour at 37^{O}C and 1μL

electrophoresed on an agar gel to determine correct size and concentration of the fragment relative to a known DNA reference standard (5μL of 1kb ladder (Gibco BRL)).

2.5.11 Sequencing of PCR reaction products

Reaction products were sequenced either at Alta Biochem. (Birmingham) or on the Licor model 4000 DNA automated sequencer. Sequencing reactions were carried out using a cycle sequencing protocol based on the chain termination method of Sanger, which incorporates an infrared labelled nucleotide. A sequencing reaction mixture was made up using a long-read kit (Epicentre Technologies). This contained between 500ng and 1μg of plasmid DNA, 2pmol of an infrared labelled primer (M13 forward and reverse primers), 1.7μL of 10xsequencing buffer, 1μL of SequiTherm thermostable DNA polymerase, and water to 17μL. The reaction was denatured for 5 minutes at 95°C and then passed through 30 thermo-cycles (95°C denaturation, 30s. 60°C annealing, 30s., 70°C polymerisation 1min.). After cycling 4μL of stop solution was added before automated sequencing.

2.5.12 Extraction of RNA from samples

Total cellular RNA was prepared from mouse tissues and established cell lines using the RNazol B method (Biogenesis). Frozen tissue was ground with liquid nitrogen to a fine powder using a chilled mortar and pestle (BDH). The powder was resuspended in 2ml cold RNazol B liquid/per 100 mg of tissue. Cells were spun at 3,000 r.p.m. for 5 minutes to form a pellet and the tissue culture medium was removed. The pellet was washed with cold PBS buffer and resuspended in 200μl of cold RNazol B liquid. One tenth volume of cold chloroform was added and the homogenate was vortexed for 20 secs and chilled on ice for 5 minutes. Samples were then centrifuged at 1300 r.p.m. at 4°C for 15 minutes. The aqueous phase was then transferred to 1.5 ml eppendorf tubes and an equal volume of cold isopropanol was added. The samples were stored at 4°C for at least 15 minutes before centrifuging them at 1300 r.p.m. at 4°C for 15 minutes. A small white pellet is visible, the supernatant was moved and the RNA pellet washed with 500μl 70% ethanol and then

centrifuged again for 5 minutes at 1300 r.p.m. at 4°C. The ethanol was removed and the RNA pellet was dissolved in 40µl DEPC treated water. The RNA concentration was determined by measuring the optimal density of the sample at 260 nm. The RNA sample was stored in a -70 °C freezer until used.

2.5.13 Separation of RNA by gel electrophoresis.

10µg of RNA was dissolved in 10µl of DEPC treated water. To this, 17µl of RNA loading buffer was added. The samples were heated at 65 °C for 15 minutes and placed on ice for 5 minutes then 3µl of loading dye was added. The samples were then separated on a 1% agarose / formamide gel in 1 x MOPS overnight at 20 volts. The RNA gel was washed in several changes of deionised water for five hours, the gel was subsequently stained with 1/20 dilution of stock ethidium bromide (0.5µg/ml) for 30 minutes, followed by washing in water for a further 30 minutes. The gel was then photographed and washed in 10 x SSC for 30 minutes.

2.5.14 RNA Transfer.

The RNA was transferred overnight onto Hybond membrane (Amersham Ltd) by an upward capillary transfer in 10 x SSC. The RNA on the membrane was immobilised by UV crosslinking for 8 s at 1200 µ joules × 100 using a UV stratalinker 1800 (Stratagene). Probe labelling and hybridisation was carried out as for DNA probes.

Chapter 3

Investigation of the pathology of the HTLV-I *tax* transgenic mouse tumours

Investigation of the pathology of the HTLV-I *tax* transgenic mouse tumours

3.1 Introduction

The generation by several laboratories of HTLV-I *tax* transgenic mice using a variety of different promoters directing expression to the T-cell compartment has not given rise to $CD4^+$ T-cell tumours (see Chapter 1, Table 1.4). Moreover expression of *tax* within the lymphoid compartment appears to be associated with thymic atrophy (Furuta et al, 1989; Nerenberg et al, 1991) presumably due to the observed toxic effects of deregulated *tax* expression (Nerenberg et al, 1989; Chlichlia et al, 1995) causing apoptosis (Yamada et al, 1994; Chlichlia et al, 1995; Hall et al, 1998 [in press]). Thus although the advent of transgenic mouse technology has not provided a murine model for ATL *per se* the development of several types of tumours within these mice has provided a useful platform to investigate the mechanisms by which *tax* may transform primary cells *in vivo*.

HTLV-I *tax* transgenic mice develop a variety of spindle cell tumours, which were originally described as mesenchymal tumours (Nerenberg et al, 1987) or neurofibromas (Hinrichs et al 1987). Human neurofibromatosis can be divided into two anatomical divisions – the rarer central form (also known as bilateral acoustic neurofibromatosis) and the more common peripheral form (McGee et al, 1992). Both forms can occur spontaneously, presumably due to *de novo* somatic mutations, or as an inherited predisposition, known as von Recklinghausen's neurofibromatosis (Riccardi et al; 1981). Von Recklinghausen's disease is complicated by predisposition to other tumour types such as gliomas (including optic gliomas and diffuse glial tumours), astrocytomas, ependymomas, meningiomas, and phaeochromocytomas, as well as mental retardation, epilepsy, and spinal deformities. The central form occurs as an autosomal dominant disorder due to inactivation of the neurofibromatosis II (NF-II) gene (Seizinger et al, 1986) and is characterised by multiple intracranial and spinal tumours which are mainly Schwannomas and meningiomas. The NF-II gene encodes a membrane bound tumour suppressor protein called merlin/schwannomin (Rouleau et al, 1993; Trofatter et al, 1993). The mechanism of tumour suppression by merlin/schwannomin (Lutchman et al, 1995) is

unknown although it is thought to form part of a superfamily of proteins - the ezrin-moesin-radixin superfamily (Bellivue et al, 1995) – that associate with the cytoskeleton.

The peripheral form of neurofibromatosis, NF-I, is characterised by café-au-lait spots on the skin in childhood with neurofibromatosis developing in adults. This form occurs as an inherited autosomal dominant disorder due to inactivation of the neurofibromatosis I (NF-I) gene (Cawthon et al, 1990; Viskochil et al, 1990; Wallace et al, 1990) - a tumour suppressor gene which encodes a GTPase-activating protein named neurofibromin (Ballester et al, 1990; Martin et al, 1990; Xu et al, 1990). Significantly the HTLV-I *tax* gene has been shown to repress expression of the NF-I gene (Feigenbaum et al, 1996) and may therefore explain the development of neurofibromas in HTLV-I *tax* transgenic mice.

Neurofibromas are benign, solitary, or in the inherited form usually multiple proliferations of nerve sheath cells consisting of an admixture of Schwann cells, fibroblasts, and perineurial cells (Erlandson et al, 1991; Lassmann et al, 1977; Jurecka et al, 1987) together with scattered mast cells and phagocytic cells (Erlandson et al, 1982; Harkin et al, 1986). The true origin of the tumour cell is still unclear although recent reports favour the Schwann cell as the progenitor cell giving rise to all nerve sheath tumours (Sharma et al, 1990; Kharbanda et al, 1994).

HTLV-I *tax* transgenic mice express a phenotype, which resembles von Recklinghausen's neurofibromatosis due to the development of "peripheral neurofibromas", which occur principally at sites of wounding. Associated with these neurofibromas are adrenal medullary tumours and iris proliferations (Green et al, 1992) whose incidence parallel the development of adrenal medullary phaeochromocytomas and iris hamartomas which develop in certain forms of human type I neurofibromatosis (NF-I). However the validity of these pathological descriptions has recently been brought under close scrutiny. Both the adrenal medullary tumours and iris proliferations resemble the fibroblastic spindle cell tumours that occur at wound sites. Immunocytochemical analysis of these tumours reveals that they stain positively for vimentin, a cytoskeletal growth-regulated gene, expressed usually in cells derived from the embryonic mesoderm layer (Lazarides et al, 1980)

consistent with the notion of a perineurial or fibroblast derivation of neurofibromatosis. However the interpretation of this result is complicated by the observation that the HTLV-I *tax* gene trans-activates the vimentin promoter/enhancer (Lilienbaum et al, 1990) by relieving negative trans-repression of this gene (Salvetti et al, 1993) which normally serves to modulate expression of this protein. Furthermore, expression of the S-100 protein, a marker for Schwann cells which form a significant proportion of the neurofibroma cell population (Erlandson et al, 1985), could not be detected by most authors (Hinrichs et al, 1987) and only after trypsin pre-treatment by others (Nerenberg et al, 1991). The intense inflammatory infiltrate which accompanies these tumours (presumably due to transactivation of GM-CSF and G-CSF promoters [Himes et al, 1993]) does not resemble mast cell infiltrates present in human neurofibromas. It was not surprising therefore that further evaluation of these tumours led to an alternative pathological description of inflammatory malignant fibrous histiocytoma (Nerenberg et al, 1991) based upon the histopathological, immunocytochemical and ultrastructural features of these tumours. Furthermore, no association was found between the development of human type I Neurofibromatosis and HTLV-I infection (Nerenberg et al, 1991). Despite these obvious discrepancies within the literature, the spindle cell ear and tail tumours that develop at wound sites are still referred to as neurofibromas (Grossman et al, 1996).

HTLV-I *tax* transgenic mice develop other pathological abnormalities including an exocrinopathy, which resembles Sjogren's syndrome (SS) (Green et al, 1989) an inflammatory arthropathy resembling Rheumatoid arthritis (RA) (Iwakura et al, 1991; Yamamoto et al, 1993), and large granular lymphocytic leukaemia (LGL) (Grossman et al, 1995). Mice which develop SS are characterised by initial ductal proliferation followed by invasion with lymphocytes and plasma cells (Green et al, 1989). A late feature of the disease is extensive epithelial island enlargement with lymphocytic infiltration, leading to destruction of acinus architecture. However the aetiological role that HTLV-I plays in the development of SS is controversial (Rigby et al, 1996; Mariette et al, 1993 and 1995; Eguchi et al, 1995; Nakamura et al, 1997). These reports variously detect the presence or absence of HTLV-I antibodies (Mariette et al, 1995) or homologous HTLV pX gene sequences (Rigby et al, 1996; Mariette et al, 1993) in a proportion of patients with SS or

associate the high prevalence of SS in patients infected with HTLV-I (Nakamura et al, 1997; Eguchi et al, 1995). Other authors implicate the presence of HIV specific antigens (gag) (Yamano et al, 1997), novel exogenous retroviruses (Griffiths et al, 1997) or Human Endogenous Retroviruses (HERVs) (Urnovitz et al, 1996) as possible agents inducing SS and a range of other autoimmune, or inflammatory diseases including RA.

The involvement of retroviruses in destructive arthropathies is well documented (caprine arthritis encephalitis [Woodard et al, 1982] and ovine maedi-visna viruses [Dawson et al, 1983 and 1987]). In addition a substantial body of epidemiological evidence links HTLV as a risk factor for an inflammatory arthropathy similar to RA (Motokawa et al, 1996; Starkebaum et al, 1996; Eguchi et al, 1996; Pinheiro et al, 1995; Sato et al, 1991, Kitajima et al, 1991; Nishioka et al, 1989) - (although direct evidence linking exogenous retroviruses as causative agents of RA is still lacking [Nelson et al, 1994]). The first report of HTLV-I *tax* transgenic mice developing joint disease was therefore greeted with considerable interest (Iwakura et al, 1991). These mice developed an inflammatory arthropathy which resembled RA (Iwakura et al, 1991; Yamamoto et al, 1993; Iwakura et al, 1995, Saggioro et al, 1997) which was characterised by synovial and periarticular inflammation with articulator erosion caused by invasion with granulation tissue. Transgenic joints displayed an elevated profile of pro-inflammatory cytokine expression (IL-1α, IL-1β, IL-6, TNF-α, TGF-β1, IFN-γ, IL-2 [Iwakura et al, 1995]) which was thought to induce serum hyperactivity and autoimmunity.

The expression of *tax* within the lymphoid compartment has been met with only limited success (Furuta et al, 1989; Nerenberg et al, 1991). Transgenic mice which develop an exocrinopathy similar to SS also develop splenomegaly and lymphadenopathy (Peebles et al, 1995) composed primarily of B cells which display abnormal proliferative responses *in vitro*. Targeting of *tax* to the lymphoid compartment using the granzyme B promoter resulted in the development of leukaemia originating at wound sites after a prolonged incubation latency (Grossman et al, 1995).

We therefore decided to generate several lines of HTLV-I *tax* transgenic mice and characterise the various tumour pathologies especially with reference to tumour derivation using a variety of antibodies specific for cytoskeletal or neuronal proteins. As an adjunct to these studies we also wished to investigate the mechanism by which *tax* may transform primary cells *in vivo* and the role it plays in tumour development.

3.2 Results

3.2.1 Phenotype exhibited by HTLV-I transgenic mice

Dr Blyth and Dr Cameron generated four lines of HTLV-I *tax* transgenic mice in which expression from the *tax* transgene was regulated by the T-cell specific CD3 promoter/enhancer elements (Clevers et al, 1989) [Figure 3.1]. These mice, designated the 1000 series, 1200 series, 1300 series, and 1400 series, developed a variety of pathologies summarised in Table 3.1.

The CD3-*tax* transgenic mice developed three major tumour phenotypes, namely mesenchymal tumours that developed at sites of wounding (principally ear and tail tips), salivary and mammary adenomas, and histiocytic tumours. Expression of *tax* RNA was confirmed by N Blotting within both the mesenchymal tumours and adenomas (carried out by Ms J. McMillan). Expression of *tax* RNA was not detected within the histiocytic tumours or within normal tissues derived from *tax* transgenic mice.

Table 3.1: Phenotypes exhibited by each line of CD3-*tax* transgenic mice

Line	Phenotype	Average Latency (days)	Incidence
1000	thymic atrophy immunosuppression parasitic diseases	55	3/3 (100%)
1200	mammary adenomas	457	7/13 (54%)
	salivary adenomas	341	3/13 (23%)
1300	mesenchymal tumours	277	2/4 (50%)
	hind leg ataxia and paresis	229	5/26 (19%)
1400	mesenchymal tumours	128	16/27 (59%)
	histiocytic lymphadenopathy	336	sporadic (<5%)

Table summarising the phenotypes exhibited by the 1000, 1200, 1300, and 1400 lines of CD3-*tax* transgenic mice. The numbers refer to the line number, average time for the phenotype to emerge (in days), and total and percentage incidence.

Figure 3.1: Schematic representation of the CD3-*tax* expression construct

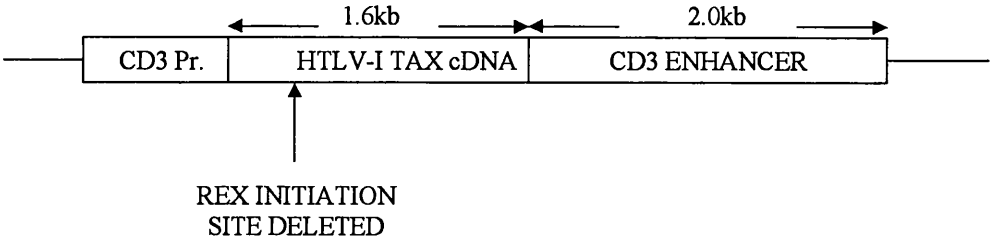

Pr.=PROMOTER
kb =KILOBASE

Figure 3.1: the schematic representation of the CD-3 *tax* promoter/enhancer region.

3.2.2 Mice from the 1300 and 1400 lines exhibit a variety of symptoms

The founders, F1 generation and a proportion of the F2 generation from the 1300 and 1400 lines developed mesenchymal tumours (Figure 3.2) (although this phenotype was not observed in subsequent F3 or F4 generations). These tumours developed at sites of wounding on the ear and tail tips and occasionally also at other sites prone to local trauma such as the face and palmar/plantar aspects of the limbs. Most tumours developed between 3 and 7 months of age. The tumours were composed of a background population of plump spindle cells with ovoid nuclei, and poorly defined eosinophilic cytoplasm set in a fine reticulin stroma with, invariably, a heavy accompanying infiltrate of polymorphs and macrophages (Figure 3.3). The tumours were locally aggressive and infiltrated along tissue planes and nerve fibres. These tumours appeared to be morphologically, and phenotypically identical to the neurofibromas reported by other authors (Nerenberg et al, 1987; Hinrichs et al, 1987). These mice also demonstrated systemic effects of *tax* expression such as ill-thrift and myeloid hyperplasia (within the spleen and red bone marrow).

A proportion of mice from the 1300 line exhibited other phenotypes such as wasting accompanied by thymic atrophy (although this was not as severe as that observed in the 1000 line), and hind leg paresis and ataxia. Four mice from the 1400 line also developed solitary lymphadenopathy characterised by trabecular thickening due to infiltration by large eosinophilic histiocyte like cells.

Figure 3.2: Photographs of CD3-*tax* transgenic mice bearing mesenchymal tumours at ear and tail tips.

Photographs showing the gross pathology of a CD3-*tax* mouse bearing a mesenchymal tumour. These tumours typically emerged at the ear and tail tips and other frequent sites of wounding (in this case ear notching for identification and tail tipping for genotyping).

Figure 3.2: Photographs of CD3-*tax* transgenic mice bearing mesenchymal tumours at ear and tail tips.

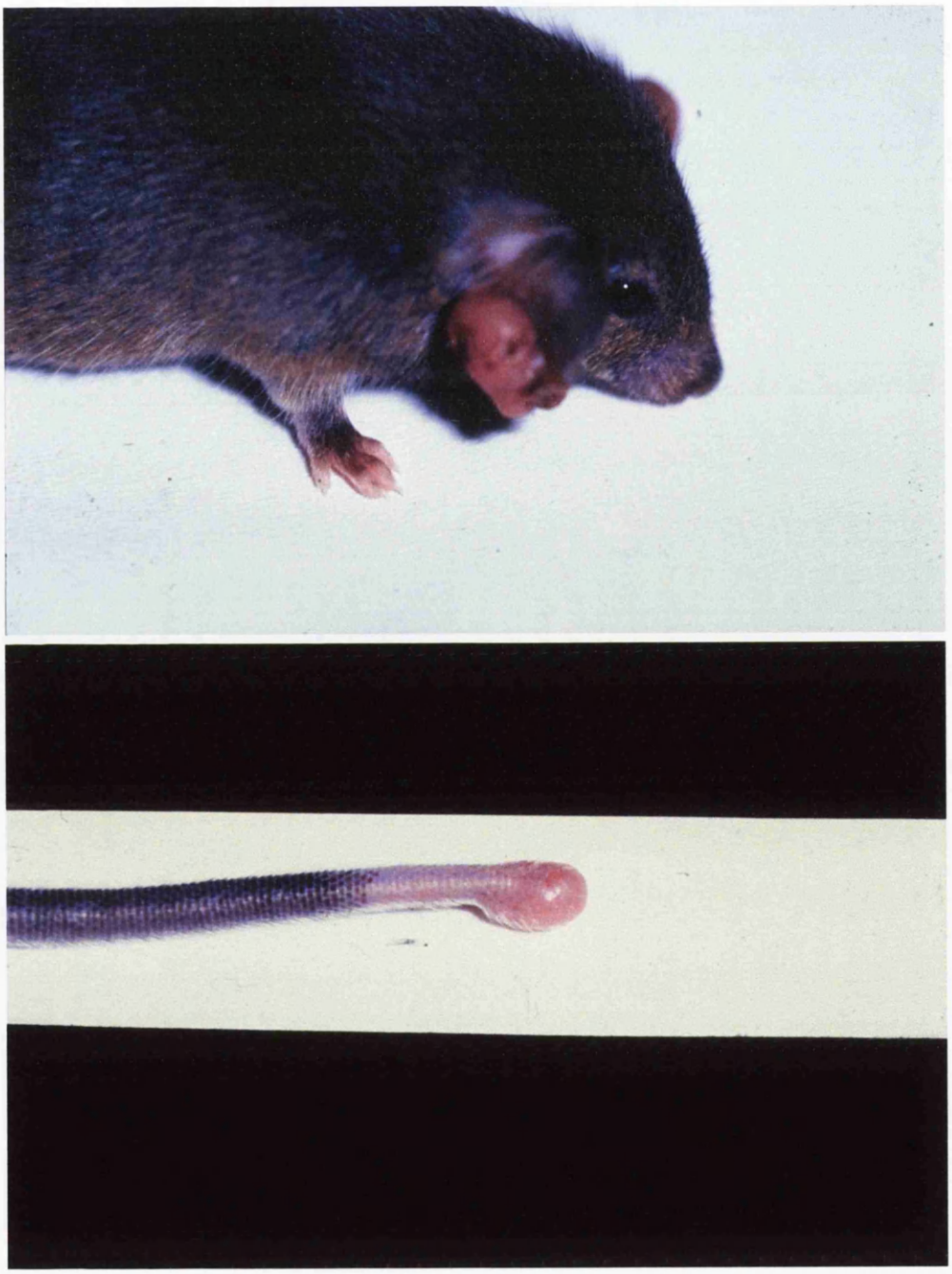

Figure 3.3: H+E photomicrographs of mesenchymal tumours

Photographs of a mesenchymal tumour stained with haematoxylin and eosin. The upper photograph (original magnification x4) and lower photograph (original magnification x1000) demonstrate the histological components of these tumours i.e. a spindle cell background population with a superimposed neutrophil and macrophage infiltrate. The oedematous nature of these tumours together with the neutrophil infiltrate indicates an active acute inflammatory process.

Figure 3.3: H+E photomicrographs of mesenchymal tumours

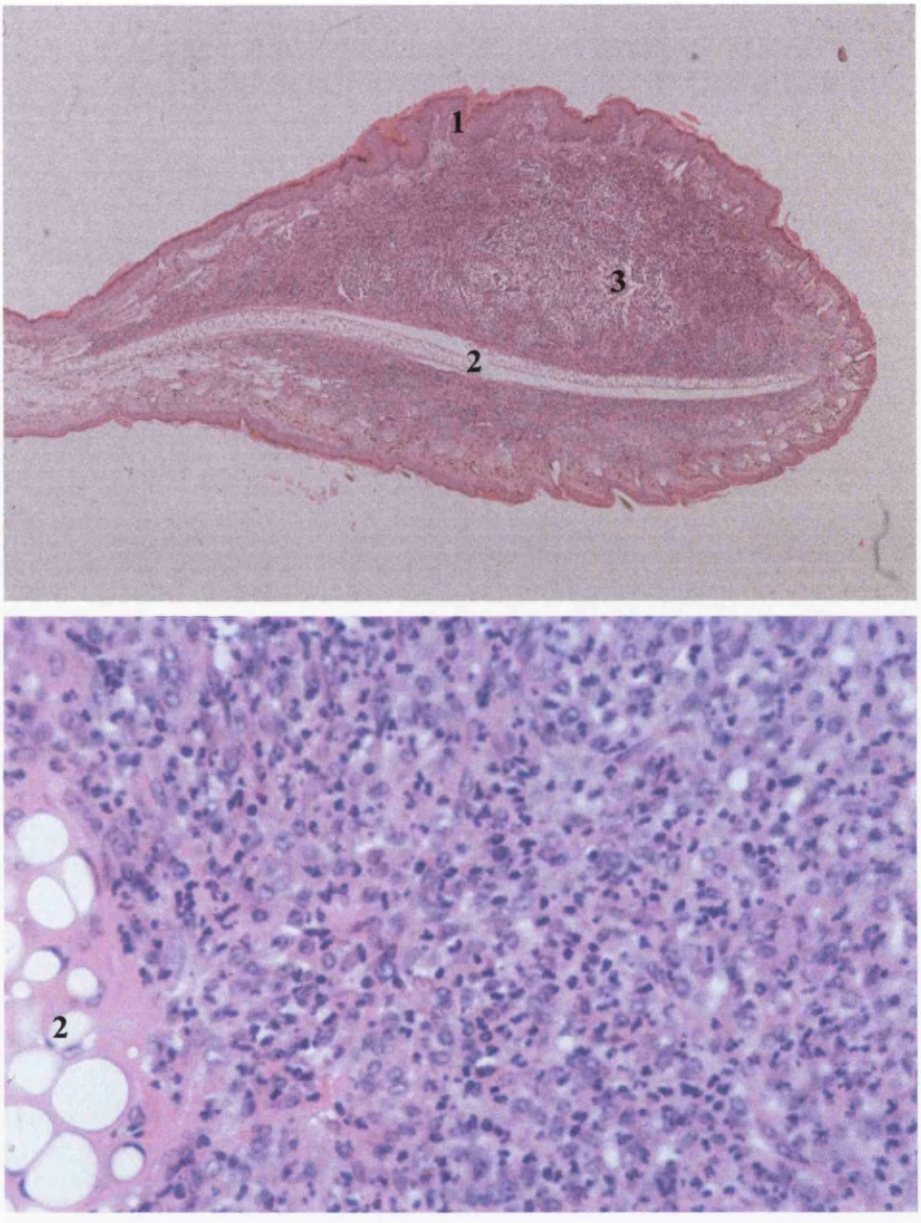

Top figure (original magnification x4) illustrates an oedematous spindle cell tumour developing within the ear of a CD3-*tax* transgenic mouse.
Lower figure (original magnification x1000) reveals more detail of the spindle cell background population with a superimposed macrophage and neutrophil inflammatory cell infiltrate.

1 hyperplastic epithelium; 2 central cartilaginous plate; 3 areas of oedema

3.2.3 Mice from the 1200 line develop salivary and mammary adenomas

Mammary and salivary adenomas were observed in the founder and 77% (54% mammary adenomas; 23% salivary adenomas) of the F1 generations occurring between 9 and 26 months of age. These adenomas were histologically identical, circumscribed but non-encapsulated, composed of closely packed ductules or tubules lined by a generally bilayered epithelium separated by solid trebeculae of epithelial cells (Figure 3.4). The luminal layer of the ductule lining comprised of closely packed cells with dark ovoid nuclei and scant cytoplasm while the outer layer had larger paler nuclei and moderate amounts of pale eosinophilic cytoplasm similar to cells in the more solid trebeculae. Mitoses were quite frequent. The bilayered pattern indicates origin from salivary or mammary duct and occasional cystic foci were present in larger lesions. The tumours had a fine vascular stroma and some had a scant polymorph infiltrate throughout.

Figure 3.4: H+E photomicrograph of a mammary adenoma.

Photograph of a mammary adenoma stained with haematoxylin and eosin (original magnification x4). The low power photograph broadly illustrates the histological nature of these lesions which consist of epithelial cells arranged into ductules and broad sheets of cells. The tumours are well circumscribed but not encapsulated.

Figure 3.4: H+E photomicrograph of a mammary adenoma

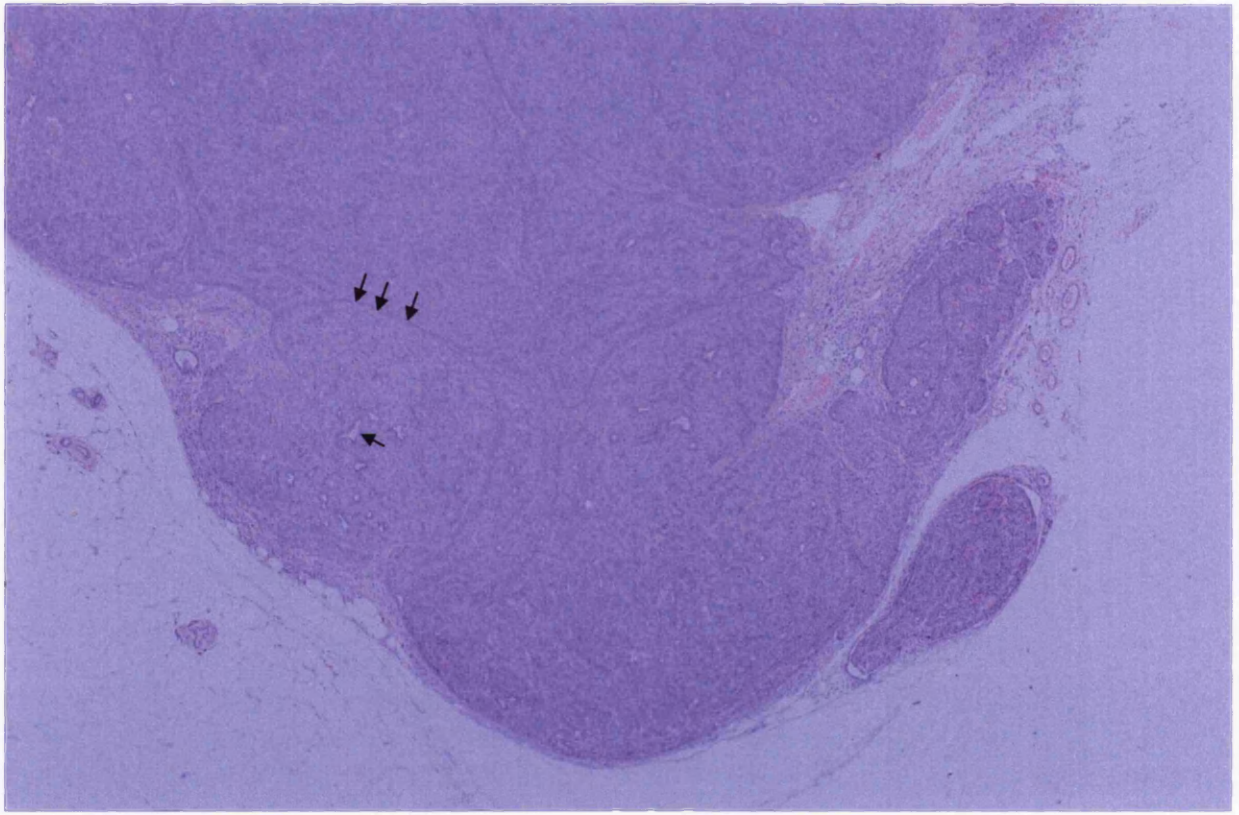

Low power (original magnification x4) of a mammary adenoma demonstrating a rather bland proliferation of mammary epithelium with obvious differentiation towards ductules (arrows).

3.2.4 Mice from the 1000 line develop thymic atrophy and immunosuppression

The 1000 line of mice developed early onset clinical signs of immunosuppression (parasitic and bacterial infections) and died generally after 8 weeks resulting in the loss of this line. Some mice showed signs of thymic atrophy in which the thymus was macroscopically reduced in size. These thymuses had normal cortical architecture but reduced size of the medulla. No lymphocytolysis or depletion was evident. Furthermore, no increase in the apoptotic index could be detected when these thymuses were stained with the TUNEL technique consistent with the observation that other mice from this line had histologically normal thymuses but displayed similar immunosuppression and died at 8 weeks old.

3.2.5 Several lines of mice develop hind leg paresis (HLP) and ataxia

Mice from the 1000 line (FO6), the 1300 line (F3, F4 [42%], and F5) and the $p53^{+/-}$xTax (P/T) lines of mice developed hind leg paresis and ataxia after a latency period of 6-12 months. Clinically mice presented with bilateral hind leg paresis and ataxia together with nervous signs such as twitching, trembling, and proprioceptive deficits when challenged. In contrast HLP and ataxia was only very rarely seen in other lines of mice (notably one case from an HTLV-I *rex* transgenic mouse). The spinal cord and brain from affected mice was fixed by perfusing the circulation with 10% neutral buffered formalin to preserve the delicate architecture of the CNS. Histological examination revealed extensive vacuolation extending from the brain stem to the caudal lumbar spinal cord. Vacuolation was restricted predominantly to the ventral fasiculi extending laterally and dorsally, and into the central grey. There was no evidence of lymphocytic meningomyelitis, lymphocytic infiltrate, or reactive astrogliosis within the substance of the spinal cord.

3.2.6 HTLV-I *tax* transgenic mouse tumours display an atypical immunostaining pattern

A thorough analysis of the pattern of cytoskeletal filament staining was not possible due to the limited availability of specific antibodies suitable for use in mouse tissues. However analysis of the mesenchymal and adenoma tumours with antibodies specific for proteins of neuronal lineage revealed that these tumours did not display an expression pattern normally associated with neurofibromas. Furthermore, immunocytochemical staining of the inflammatory infiltrate did not reveal a diffuse mast cell infiltrate typical of human neurofibromas, but a mixed inflammatory infiltrate normally associated with a wound response.

S-100 specifically stains cells displaying the S-100 A or S-100 B proteins. In the CNS it stains glial and ependymal cells as well as Schwann cells within the PNS. In the skin it stains melanocytes and Langerhans cells whereas in lymph nodes it stains interdigitating reticulum cells. The antibody also stains benign and malignant melanocytic tumours. S-100 staining of tumour samples revealed an unusual pattern. Mesenchymal and adenoma tumours were generally negative for this protein except distinct, variably sized foci of weakly staining immunopositive cells (within both tumour types) randomly distributed throughout the substance of the tumour (Figure 3.5). Trypsin pre-treatment had no effect upon the staining pattern or distribution of this protein.

Figure 3.5: H+E photomicrographs of S-100 staining of a mesenchymal tumour.

Photographs of a mesenchymal tumour stained immunocytochemically for S-100 protein and counterstained with haematoxylin (original magnification x1000). The upper photograph is a mesenchymal tumour demonstrating weak expression of S-100 occurring in isolated foci. The lower photograph is the epidermis from the same tumour illustrating weak expression of the s-100 protein in the upper epithelial layers (stratum granulosum).

Figure 3.5: H+E photomicrographs of S-100 staining of a mesenchymal tumour

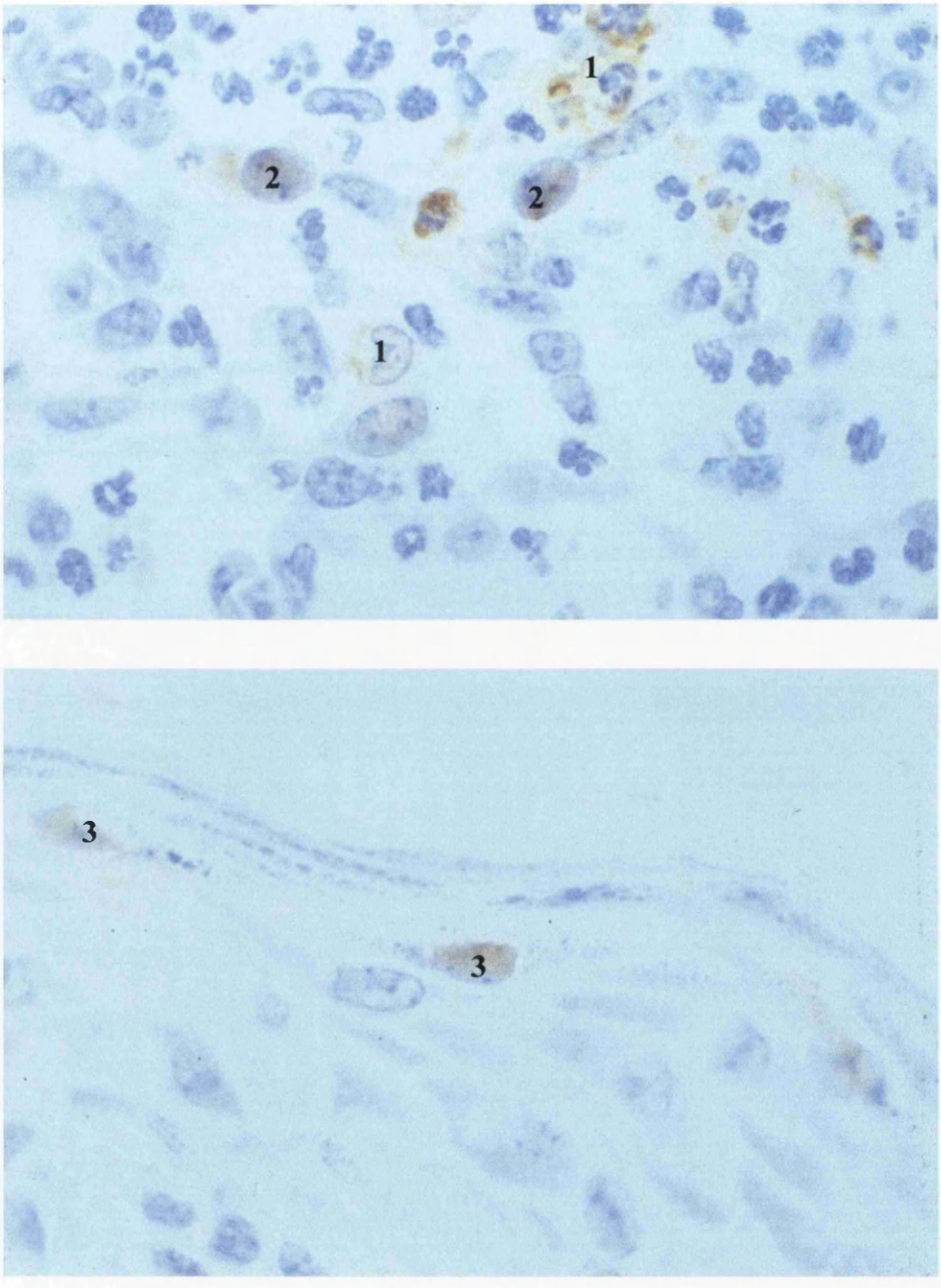

High power photomicrographs (original magnification x1000) demonstrating weak S-100 staining in the parenchyma (upper photo) and hyperplastic epithelium (lower photo) of a mesenchymal tumour.

1 inflammatory cell infiltrate with immunopositive staining cytoplasm; 2 occasional tumour cells expressing S-100 protein; 3 epithelial cells expressing S-100 protein

Glial Fibrillary Acidic Protein (GFAP) is a protein which specifically stains astrocytes and some groups of ependymal cells within the central nervous system (CNS) and Schwann cells, enteric glial cell and satellite cells within the peripheral nervous system (PNS). Weak staining of axons also occurs due to cross-reaction with a neurofilament protein (Dako specification sheet). Staining of mesenchymal and adenoma tumour samples demonstrated that mesenchymal tumours and salivary adenomas were uniformly negative. Mammary adenomas were generally negative although they exhibited very weak staining of isolated cells which were distributed as small foci within the expanded trabecular regions which were distinct from the ductular proliferations. This may indicate the presence of proliferating epithelial or myoepithelial cells (Viale et al, 1991).

MCA519 is a rat anti-mouse monoclonal antibody that specifically stains macrophages in cryostat sections. Staining of ear and tail lesions demonstrated that a not insubstantial proportion of the tumour mass (approx. ≤10% cells) consisted of infiltrating macrophages (Figure 3.6). Conversely very few macrophages were found within adenoma samples.

Figure 3.6 Photomicrographs illustrating macrophage staining within a mesenchymal tumour

Photographs of cryostat cut sections from a mesenchymal tumour stained with MCA519 (macrophage specific antibody) and counterstained with haematoxylin. The upper photograph (original magnification x100) and the lower photograph (original magnification x1000) demonstrate the strong cytoplasmic staining within the substance of the mesenchymal tumours.

Figure 3.6 Photomicrographs illustrating macrophage staining within a mesenchymal tumour

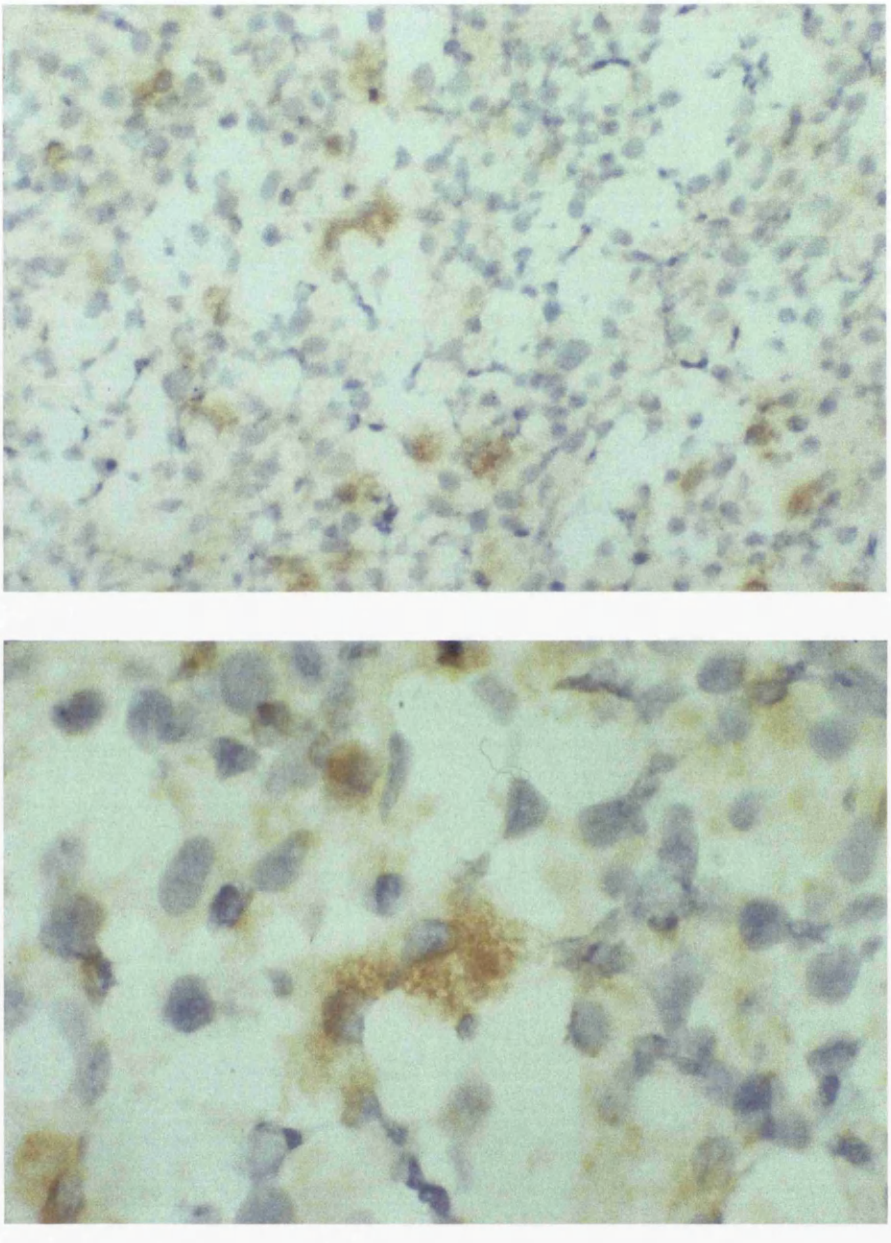

Low (original magnification x100) and high (original magnification x1000) power photomicrographs of a cryostat stained section demonstrating strong immunoreactivity with MCA519 (macrophage specific antibody) in a mesenchymal tumour.

3.3 Discussion

The CD3-*tax* transgenic mice exhibit a variety of pathologies ranging from proliferations of either epithelial or mesenchymal cells (resulting in tumour formation) to degenerative conditions (resulting in thymic atrophy, immunosuppression, or hind leg paresis). Expression of the *tax* transgene was demonstrated by N. blotting within both the mesenchymal tumours and adenomas. Weak expression was detected within the thymuses of those mice with thymic atrophy and immunosuppression whereas no *tax* mRNA was detected within normal tissues of *tax* transgenic mice or within the histiocytic tumours. Presumably under normal conditions the specificity of the CD3 promoter/enhancer prevented detectable expression within non-tumour tissue. "Switch-on" of the transgene (either stochastic or upregulation from a background low level expression) and tumour evolution most likely accounted for enhanced expression and detection of *tax* mRNA within tumours. Lack of *tax* expression associated with the histiocytic tumour phenotype may be due to either low level expression of the *tax* transgene which is sufficient to initiate tumours but below the level of sensitivity of detection by conventional N. blotting.

Loss of the *tax* phenotype in subsequent generations is unexplained but may be due to drift in the genetic background of the mice leading to an alteration in the susceptibility or permissiveness to transgene "switch on" through the CD3 promoter/enhancer in non-lymphoid tissues. Reports using p53 knock out mice have demonstrated that genetic background can influence tumour spectrum and latency (Purdie et al, 1994; Harvey et al, 1993; Donehower et al, 1992). Alternatively, methylation and genetic silencing of the transgene could reduce *tax* expression from the transgene (Turker et al, 1997). Methylation of the viral LTR in fresh ATL cells (Saggioro et al, 1990) inhibits *tax* directed transactivation from the viral promoter/enhancer regions of the LTR (Cassens et al, 1994; Saggioro et al, 1991) contributing to low level viral mRNA expression and viral latency.

Several lines of evidence indicate that the ear and tail lesion observed in several of the lines of mice are not neurofibromas. The intense inflammatory infiltrate consisting of polymorphs and macrophages does not resemble the scattered mast cell infiltrate noted in

human neurofibromas. Furthermore tumours are not consistently associated with nerve sheaths. Finally tumours fail to stain consistently with markers of neuronal lineage such as GFAP and S-100. An unusual pattern of expression of S-100 occurs in mesenchymal tumours, and adenomas, as well as being occasionally observed within the epithelium surrounding the ear and tail tumours. This turned out to be remarkably similar to the pattern of *tax* expression within these tumours raising the possibility that S-100 expression may be upregulated within *tax* expressing cells as a result of transactivation of the S-100 promoter by *tax* or a reflection of the profile of gene expression within apoptosing cells (discussed further in Chapter 4).

The adenoma tumours are most likely a proliferation of ductular epithelial cells as indicated by the bilayered ductular pattern observed within most of these tumours. A myoepithelial component may also be present giving rise to the weak GFAP staining occasionally encountered within some tumours. Light infiltrates of polymorphs or lymphocytes (the latter centred on ducts) were occasionally observed. However the secondary changes which occurred in the mice of Green et al, (1989) were not observed making this pathology distinct and unique to the CD3-*tax* mice.

The solitary histiocytic tumours that arose in four *tax* transgenic mice were unusual in that *tax* expression could not be detected by N. blotting. The reason for this is unknown but could be due to very low level expression of *tax* RNA beyond the sensitivity limit of conventional N blotting. Indeed, as little as 25pm exogenous Tax can stimulate proliferation of human lymphocytes (Marriott et al, 1991 and 1992) *in vitro*. However since this phenotype was only observed within one line of *tax* mouse it is also possible that the integration site of the transgene influenced tumourigenesis.

The clinical symptoms of hind leg paresis and ataxia accompanied by nervous disturbances (twitching and proprioceptive deficits) were interesting due to their similarity to patients with TSP/HAM. However the presence of vacuoles rather than a chronic demyelinating disease with lymphocytic infiltration (Iwasaki et al, 1990; Izumo et al, 1997) and the inability to associate *tax* expression with pathology did not favour an interpretation of

murine TSP/HAM. However this pathology did bear striking resemblance to a well-documented retroviral induced neurodegeneration (Saida et al, 1997; Stoica et al, 1993; Hoffman et al, 1992).

Finally, restricted expression of *tax* within the CD3 specific compartment was not consistently achieved. Similar to other groups (Furuta et al, 1989; Nerenberg et al, 1991) expression appears to be associated with deleterious effects which may be dependent upon the level of expression of the transgene (Saggioro et al, 1997). Low level expression may be tolerated within certain compartments (such as the solitary histiocytic tumours) but high level expression may induce apoptosis or degeneration (Nerenberg et al, 1989). These dichotomous effects of *tax* – proliferation versus apoptosis or degeneration - may therefore be dependent upon a number of complex and subtle interactions *in vivo*. Evidence for this is just emerging - whilst the association of *tax* expression with apoptosis is well established (Yamada et al, 1994; Chlichlia et al, 1995) recent reports suggest that under certain conditions *tax* may mitigate or even inhibit apoptotic induction (Brauweiler et al, 1997; Kishi et al, 1997; Schwartz-Cornil et al, 1997).

Chapter 4

Tumours derived from HTLV-I *tax* transgenic mice are characterised by enhanced levels of apoptosis and oncogene expression

Tumours derived from HTLV-I *tax* transgenic mice are characterised by enhanced levels of apoptosis and oncogene expression.

4.1 Introduction

Although the transforming potential of the HTLV-I *tax* oncogene is well established (Tanaka et al, 1990; Grassmann et al, 1989 and 1992; Ozden et al, 1996) the precise mechanism by which *tax* transforms cells is unknown. A consensus of opinion now purports that the transforming properties of *tax* reside, at least in part, in its ability to transactivate a wide number of cellular genes (Gazzolo et al, 1987) - especially those involved in T-cell activation and proliferation. However the significance and the contribution that each gene makes to the transformed phenotype *in vivo* is uncertain. Pertinent examples include the immediate early oncogenes *c-myc* (Duyao et al, 1992a and 1992b), *c-fos* (Fujii et al, 1988; Nagata et al, 1989; Alexandre et al, 1991; Iwakura et al, 1995), and *c-jun* (Iwakura et al, 1995; Hooper et al, 1991Fujii et al, 1991) as well as the T-cell growth factor IL2 (Inoue et al, 1986), and the IL2 α chain receptor (Leung et al, 1988).

Hand-in-hand with transformation and immortalisation is the third facet of tumour biology – apoptosis. Tax conforms to this basic framework of ideas since expression of *tax* in serum starved Rat 1 fibroblasts (Yamada et al, 1994) and human T-cells (Chlichia et al, 1995) causes apoptosis. This effect has also been observed with other oncogenes such as *c-fos* (Preston et al, 1996), *c-myc* (Evan et al, 1992) and the Adenoviral protein E1a (Rao et al, 1992). Although these effects are most clearly defined *in vitro*, it appears likely that *in vivo*, *tax* expression would be coupled to apoptosis. In order to test this hypothesis, we examined the pattern of Tax expression and apoptosis within the CD3-*tax* transgenic mouse tumours by generating specific anti-tax antibodies using the multiple antigenic peptide (MAP) system (Tam et al, 1988; Posnett et al, 1988).

The MAP system (Tam et al, 1988; Posnett et al, 1988) provides a direct method to generate high molecular weight synthetic peptides in which a core matrix made up of a tetravalent or octavalent poly-lysine nucleus provides the scaffolding to chemically link 4-

8 short immunogenic peptides. The high molecular weight (typically >10,000) of these MAPs precludes the need to chemically conjugate them to carrier proteins and therefore avoids the potential problem of an immune response to the carrier protein. The resultant peptides are highly immunogenic (Tam et al, 1988; Posnett et al, 1988; Wang et al, 1991), recognise both continuous and conformational determinants (Posnett et al, 1988) as well as frequently recognising the native protein (Tam et al, 1988; Posnett et al, 1988). This technology has now been advanced such that multivalent peptides can be developed allowing the simultaneous presentation of both B- and T-cell epitopes (Tam and Lu, 1989) without the need for a protein carrier (which normally provides the T-cell epitope help (Mitchinson et al, 1971; Benacerraf and McDevitt, 1972).

4.2 Results

4.2.1 Prediction of HTLV-I Tax Immunogenicity

A profile of the hydrophilicity (Hopp and Woods, 1981), surface probability (Emini et al, 1985), flexibility (Karplus and Shultz, 1985) and Jameson-Wolf (Jameson and Wolf, 1988; Wolf et al, 1988) antigenic index was generated based upon the HTLV-I Tax primary amino acid sequence using the Genetic Computer Group Sequence Analysis software package. This data was used in conjunction with a Chou-Fasman prediction (Chou and Fasman, 1978a and 1978b) of hydrophilicity/hydrophobicity and antigenic index to select two regions of the Tax molecule which combined regions of high hydrophilicity, high surface probability, and high flexibility (i.e. a high antigenic index). Based upon these criteria two likely immunogenic epitopes were selected corresponding to amino acids 109-121 and 338-353 (Table 4.1 and Figures 4.1-4.3).

Table 4.1: Primary amino acid sequence of peptide epitopes chosen for MAP production

Peptide identity	Single letter amino acid code	Epitope and MAP length
Tax Peptide (16)	MRKYSPFRNGYME	(aa 109-121 [13aa] MAP)
Tax Peptide (13)	GGLEPPSEKHFRRETEV	(aa 338-353 [17aa] MAP)

Table summarising the peptide epitopes (using the single amino acid code) used for the production of the multiple antigenic peptides. The figures 16 and 13 refer are arbitrary numbers used to identify each peptide epitope and subsequent antibodies produced from immunisation with that epitope. The figures 109-121 and 338-353 refer to the amino acid position in the primary Tax amino acid sequence used for MAP production. The figures in square brackets refer to the number of amino acids comprising each epitope.

Figure 4.1: HTLV-I Tax Plot structure: The curves are one-dimensional representations of the secondary structure of HTLV-I p40 Tax protein obtained using the programs "PeptideStructure" and "PlotStructure". Amino acid residues are numbered on the x-axis. Attributes to the sequences are shown as continuous curves. The top four panels indicate hydrophilicity (Hopp and Woods, 1981 [KD]), surface probability Emini et al, 1985), flexibility Karplus and Schulz, 1985), and antigenic index (Jameson and Wolf, 1988). The next three panels show the locations of turns, alpha helices and beta sheets as predicted by the algorithm of Chou and Fasman (1978a; 1978b) (CF). The bottom three panels show the predicted sites of tuns, alpha helices and beta sheets according to the algorithm of Garnier et al (1978) (GOR). The numbers 16 and 13 refer to the approximate amino acid regions chosen to generate MAPs 16 and 13 respectively.

PLOTSTRUCTURE of: Ht1tax.P2s;1 September 13, 1993 16:58

PEPTIDESTRUCTURE of: Ht1tax.Pep;1 Ck: 9025, 1 to: 353

TRANSLATE of: htlv1tax.seq check: 9964 from: 1 to: 1062

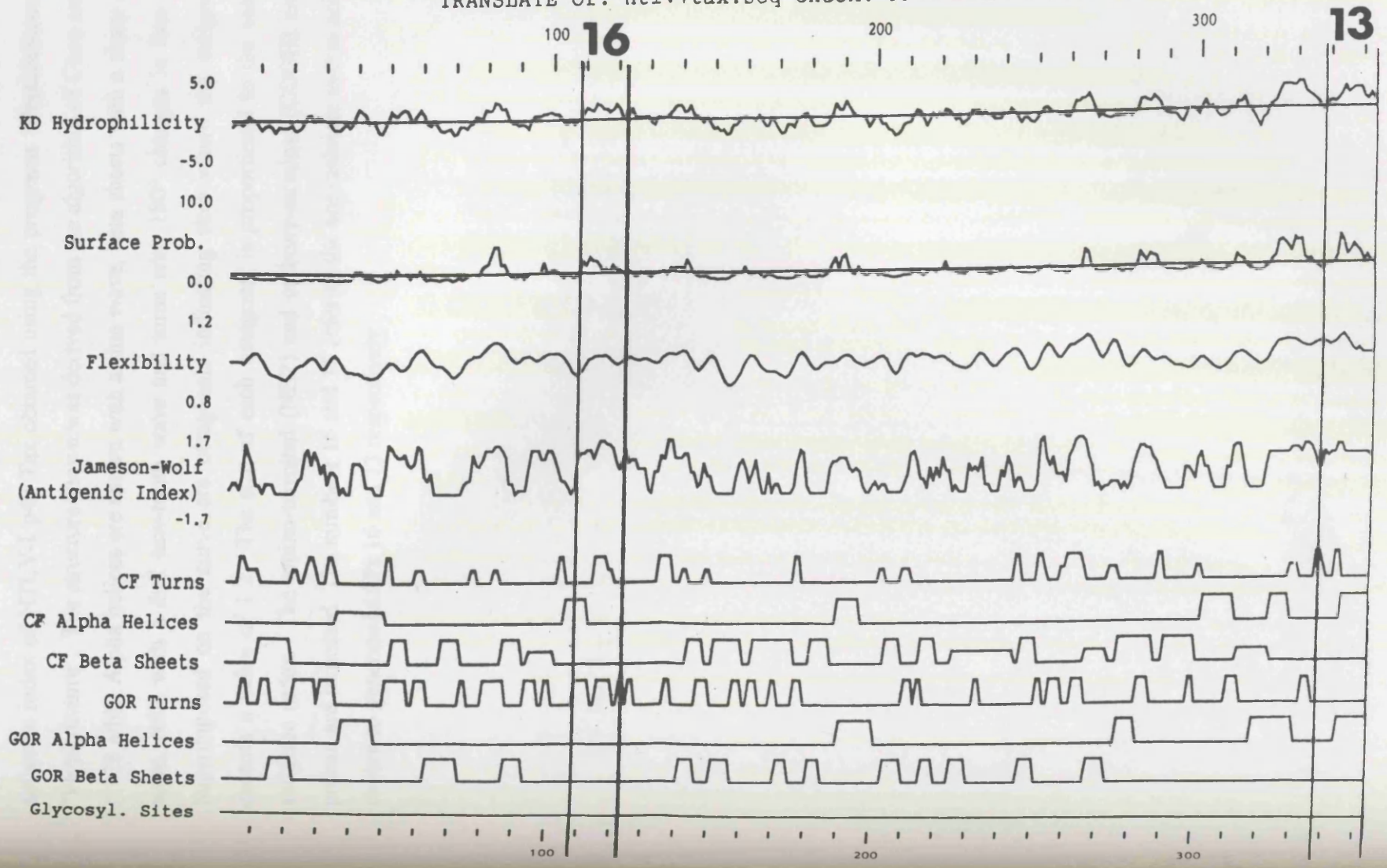

Figure 4.2: Chou-Fasman antigenic index: The predicted secondary structure and antigenic index of HTLV-I p40 Tax obtained using the programs "PeptideStructure" and "PlotStructure". The structure shown was derived from the algorithm of Chou and Fasman (1978 a/b). Alpha helices are shown with a sine wave, beta sheets with a sharp saw-tooth wave, coils with a dull saw-tooth wave and turns with 180° changes in line direction. Superimposed on the curve are octagonals indicating sites where the antigenic index exceeds a value of 1.2. The size of each octagonal is proportional to the value of the antigenic index. The amino-terminal (NH2) and carboxy-terminal (COOH) ends of the protein are indicated. The numbers 16 and 13 refer to the approximate amino acid regions chosen to generate MAPs 16 and 13 respectively.

PLOTSTRUCTURE of: Ht1tax.Pep;1 ck: 9025

TRANSLATE of: htlv1tax.seq check: 9964 from: 1 to: 1062

Chou-Fasman Prediction
September 13, 1993 16:58

0 Antigen.Index >= 1.2

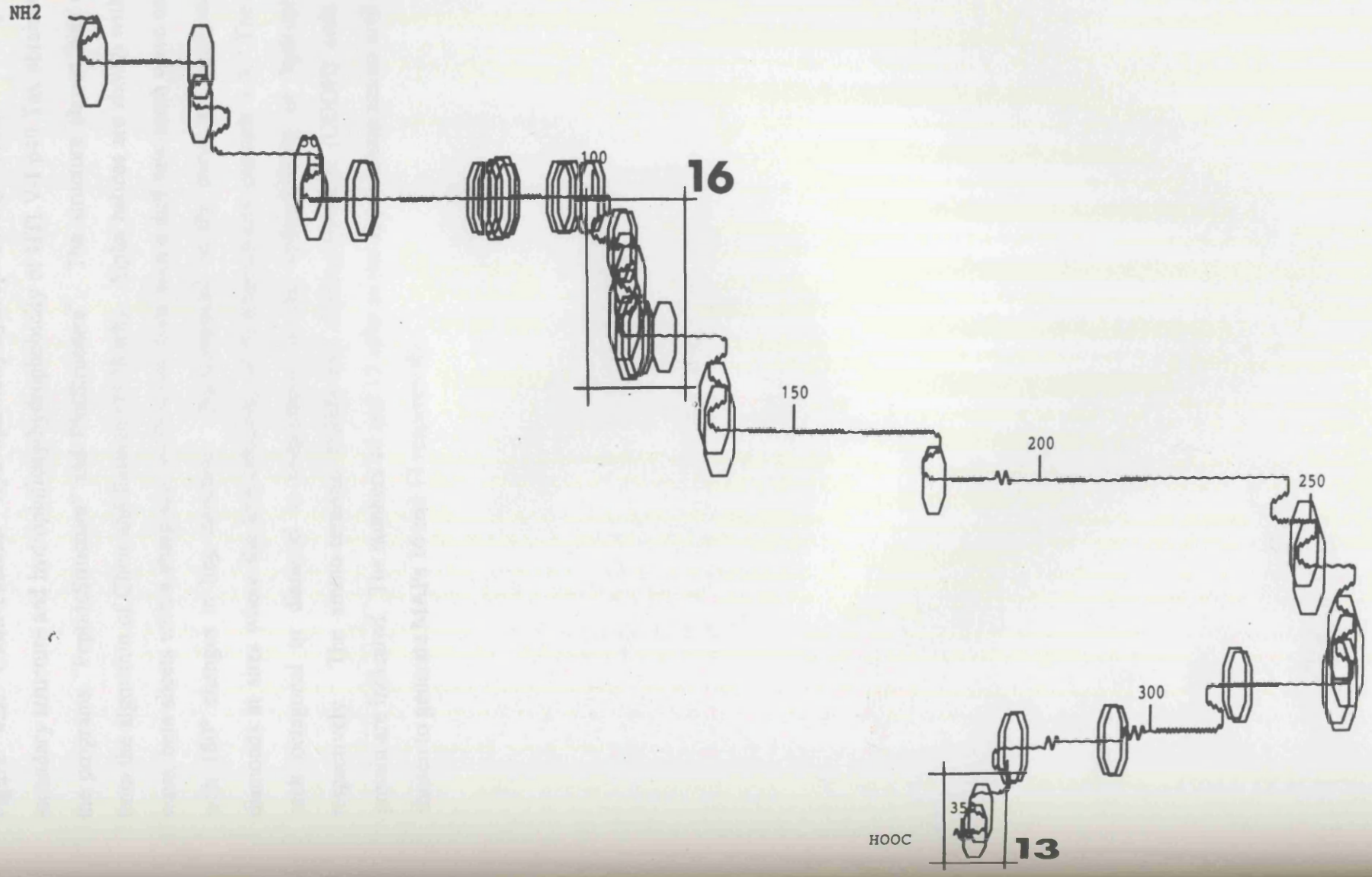

Figure 4.3: Chou-Fasman Hydrophilicity/hydrophobicity index: The predicted secondary structure and hydrophilicity/hydrophobicity of HTLV-I p40 Tax obtained using the programs "PeptideStructure" and PlotStructure". The structure shown was derived from the algorithm of Chou and Fasman (1978 a/b). Alpha helices are shown with a sine wave, beta sheets with a sharp saw-tooth wave, coils with a dull saw-tooth wave and turns with 180° changes in line direction. Superimposed on the curve are octagonals and diamonds at sites where the hydrophilicity or hydrophobicity exceeds 1.3. The size of each octagonal or diamond is proportional to the hydrophilicity or hydrophobicity respectively. The amino-terminal (NH2) and carboxy-terminal (COOH) ends of the protein are indicated. The numbers 16 and 13 refer to the approximate amino acid regions chosen to generate MAPs 16 and 13 respectively.

PLOTSTRUCTURE of: Ht1tax.Pep;1 ck: 9025

TRANSLATE of: htlvltax.seq check: 9964 from: 1 to: 1062

Chou-Fasman Prediction
September 13, 1993 16:58

KD Hydrophilicity >=1.3
KD Hydrophobicity >=1.3

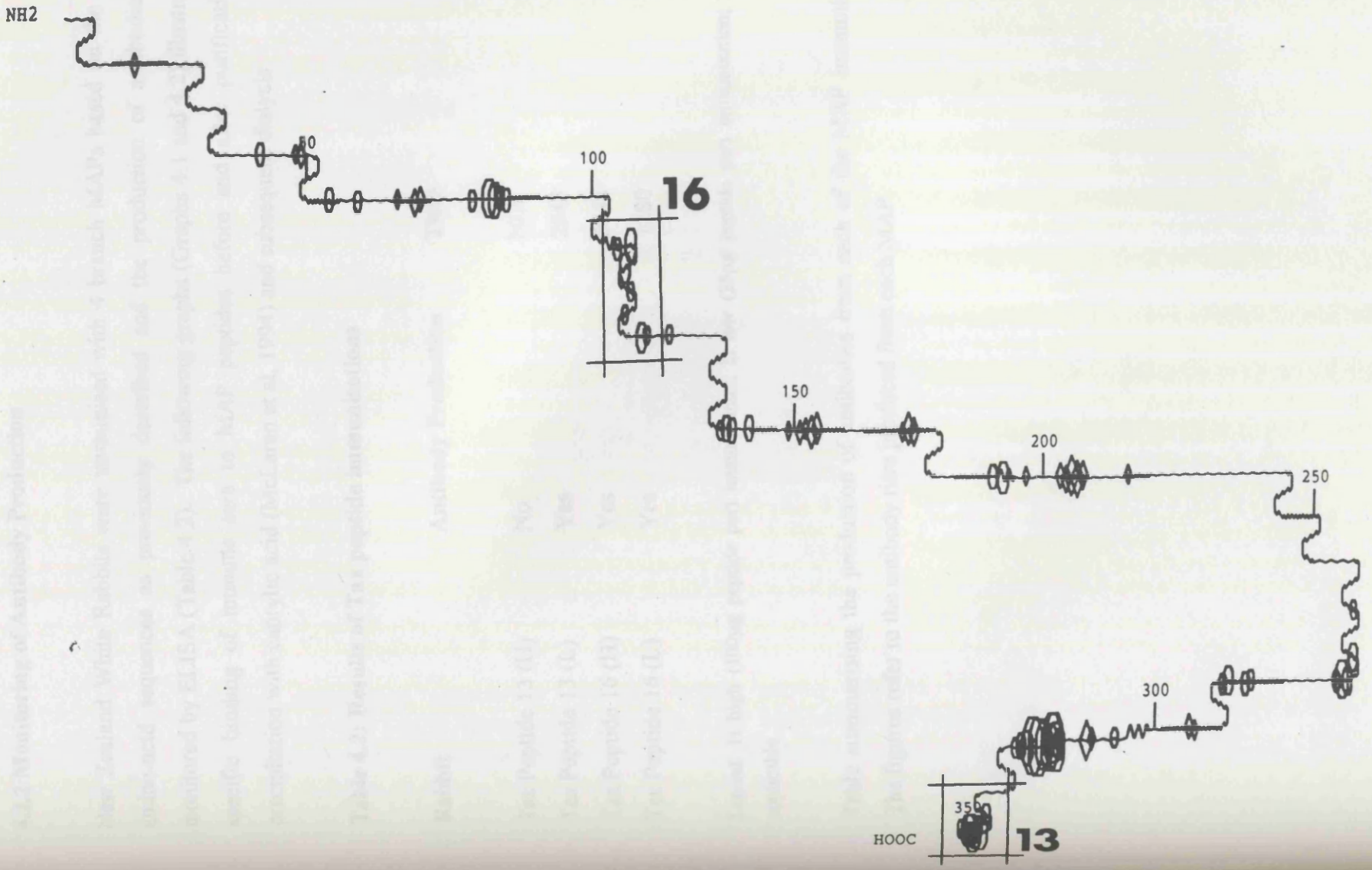

4.2.2 Monitoring of Antibody Production

New Zealand White Rabbits were immunised with 4 branch MAPs based on the above amino-acid sequences as previously described and the production of antibodies was monitored by ELISA (Table 4.2). The following graphs (Graphs 4.1 and 4.2) illustrate the specific binding of immune sera to MAP peptides before and after purification by precipitation with caprylic acid (McLaren et al, 1994) and subsequent dialysis.

Table 4.2: Results of Tax peptide immunisations

Rabbit	Antibody Production	Titre
Tax Peptide 13 (H)	No	N/A
Tax Peptide 13 (L)	Yes	2048
Tax Peptide 16 (H)	Yes	2048
Tax Peptide 16 (L)	Yes	1280

Legend: H high (100μg peptide per) immunisation; L low (25μg peptide per) immunisation; N/A not applicable.

Table summarising the production of antibodies from each of the MAP immunisations. The figures refer to the antibody titre produced from each MAP.

Graph 4.1: Graph illustrating relative absorbency versus serum dilution for rabbits immunised with Tax MAP 13

dilution	13H	13L	16L
0	0.085	0.075	0.077
2	0.3	0.391	0.274
4	0.238	0.716	0.248
8	0.184	1.279	0.179
16	0.149	1.481	0.14
32	0.127	1.203	0.115
64	0.098	0.889	0.133
128	0.106	0.619	0.1
256	0.097	0.398	0.092
512	0.089	0.251	0.084
1024	0.087	0.165	0.083
2048	0.085	0.121	0.102

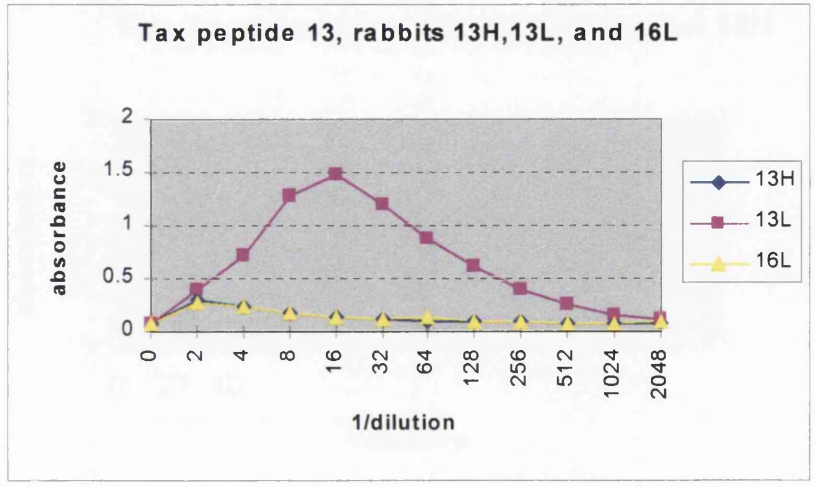

Graph illustrating absorbency (405nm) versus serum dilution of rabbits immunised with a high dose of MAP (H: 100μg per immunisation) or a low dose (L: 25μg per immunisation) of HTLV-I Tax MAP (MAP 13).

Graph 4.2: Graph illustrating relative absorbency versus serum dilution for rabbits immunised with Tax MAP 13 after purification

dilution	13H	13L	14H
0	0.079	0.081	0.089
20	0.111	1.503	0.184
40	0.091	1.248	0.172
80	0.089	0.892	0.146
160	0.081	0.708	0.123
320	0.076	0.476	0.107
640	0.083	0.319	0.108
1280	0.078	0.219	0.101
2560	0.076	0.151	0.092
5120	0.083	0.108	0.099
10240	0.075	0.111	0.09
20480	0.081	0.09	0.086

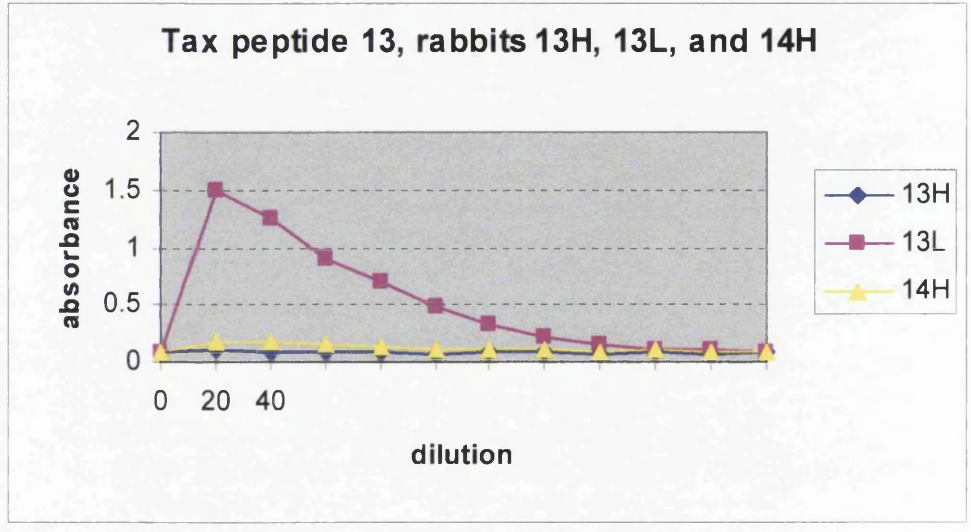

Graph illustrating absorbency (405nm) versus serum dilution of rabbits immunised with a high dose of MAP (H: 100μg per immunisation) or a low dose (L: 25μg per immunisation) of HTLV-I Tax 13 MAP (MAP 13) after caprylic acid/ammonium sulphate purification.

4.2.3 Determination of Antibody Specificity

Since we had no available source of Tax protein to directly determine specific recognition of the native protein by the anti-peptide antibodies we decided to test antibody specificity immunocytochemically. A paraffin embedded formalin fixed tumour (92/5259-3) derived from a founder HTLV-I *tax* transgenic mouse (Fo163) [which was known to express *tax* mRNA] was stained immunocytochemically for Tax protein expression using anti-Tax antibodies from rabbits 13L and 16H. Samples were pre-treated using three methods to unmask antigenic sites: microwave oven treatment, trypsin treatment, and untreated. In each case the pattern of staining was identical. Microwave oven and trypsin pre-treated slides stained slightly more intensely compared to untreated slides but also showed concomitant gains in background staining. Antibody 13L was judged to give the optimum staining diluted at 1:100 (Figure 4.4). Negative control tissues and non-tumour tissues showed no staining with Tax anti-serum.

4.2.4 Immunocytochemical analysis of Tax expression within the CD3-*tax* transgenic mouse tumours

Immunocytochemical analysis of tumours arising in CD3-*tax* mice demonstrated that Tax expression was detected in 9 of 9 mesenchymal tumours, 5 of 5 mammary adenomas, and 3 of 4 salivary adenomas (summarised in Table 4.3). No expression was detected in normal control samples. Northern blotting confirmed these results.

The pattern of Tax expression was characteristically diffuse occurring as individual as well as discrete clusters of immunopositive cells (Figure 4.4 and 4.5) distributed randomly throughout the substance of the tumours. Staining was predominantly nuclear although weaker cytoplasmic staining was also noted. Phagocytosis of apoptotic debris by the accompanying inflammatory infiltrate was frequently noted, indicated by weak cytoplasmic staining of those inflammatory cells closely juxtaposed to the immunopositive foci (Figure 4.4 inset). Interestingly, the overlying epithelium was hyperplastic and

frequently contained clusters of immunopositive cells predominantly localised to the terminally differentiating stratum spinosum/granulosum (Figure 4.4 photo (3)).

Mammary and salivary adenomas showed an identical pattern of Tax expression, which was broadly similar to that noted for the mesenchymal tumours. Immunopositive cells were distributed as individual or more often discrete clusters of expressing cells distributed diffusely throughout the substance of the tumour (Figure 4.5).

Table 4.3: Summary of Myc, Fos, Jun, and p53 protein expression in tumour samples

Table summarising the immunostaining of the mesenchymal tumours, mammary adenomas and salivary adenomas (plus appropriate control salivary gland, mammary gland, and pinna tissues) with Tax, Myc, Fos, Jun and p53 protein specific antibodies. The figures in the first column refer to the identity allocated to each tissue during histological processing. The scoring system is qualitative and scored either as positively stained, weakly staining or no staining. Where strong staining is present but is seen only in a few isolated foci the term occasional is used to denote this. The figures in the 'tumours' section of the table refers to the incidence of staining of each antibody for each type of tumour.

Key: + positive; - negative; occ occasional; n/t not tested

Table 4.3: Summary of Myc, Fos, Jun, and p53 protein expression in tumour samples

Tumour Type	Protein Immunostaining				
Mesenchymal	**Tax**	**Myc**	**Fos**	**Jun**	**p53**
93/63-4	occ +	-	occ. +	occ. +	occ. +
93/1239-2	+	+	+	+	+
93/1241-2	+	+	occ. +	+	+
93/1245-1	+	occ +	occ +	occ +	+
93/3627-1	occ +	occ +	+	occ +	occ +
93/3628-1	+	+	+	+	occ. +
92/4907-4	occ +	occ +	+	occ +	occ +
92/5259-3	+	+	+	n/t	n/t
92/5259-4	+	weak +	+	+	+
Mammary	**Tax**	**Myc**	**Fos**	**Jun**	**p53**
93/7599-1	+	weak +	+	+	+
93/7660-2	occ +	occ +	occ +	occ +	occ +
93/7662-4	+	occ +	+	occ +	+
93/7665-2	+	+	+	+	+
93/8068-1	+	+	+	+	+
Salivary	**Tax**	**Myc**	**Fos**	**Jun**	**p53**
93/1861-1	-	-	-	-	-
93/2412-3	occ +	+	+	+	weak +
93/3086-1	occ +	occ +	+	occ +	occ +
93/7600-4	+	+	+	+	+

Tumours	**Tax**	**Myc**	**Fos**	**Jun**	**p53**
Mesenchymal	9/9	8/9	9/9	8/8	8/8
Mammary	5/5	5/5	5/5	5/5	5/5
Salivary	3/4	3/4	3/4	3/4	3/4
All tumours	17/18 (94%)	16/18 (89%)	17/18 (94%)	16/17 (94%)	16/17 (94%)

Controls	**Tax**	**Myc**	**Fos**	**Jun**	**p53**	
96/1166-1	-	-	-	-	-	salivary gland
96/1166-2	-	-	-	-	-	salivary gland
96/1166-3	-	-	-	-	-	mammary gland
96/1166-4	-	-	-	-	-	mammary gland
96/1166-5	-	-	-	-	-	mammary gland
97/764-2	-	-	-	-	-	pinna
97/763-2	-	-	-	-	-	pinna
97/765-2	-	-	-	-	-	pinna

Figure 4.4: Photomicrographs demonstrating Tax protein expression in a mesenchymal tumour

Photographs of a mesenchymal tumour immunostained with a Tax specific antibody. Photograph 1 demonstrates Tax immunostaining throughout the substance of a mesenchymal tumour (original magnification x100). Photograph 2 is a higher power view of the same tumour (original magnification x1000). The inset reveals details of the predominantly cytoplasmic rather than nuclear immunostaining. Photograph 3 demonstrates Tax expression within the terminally differentiating epithelium (S spinosum/granulosum) surrounding the tumour (original magnification x1000). All slides counterstained with haematoxylin.

Figure 4.4: Photomicrographs demonstrating Tax protein expression in a mesenchymal tumour

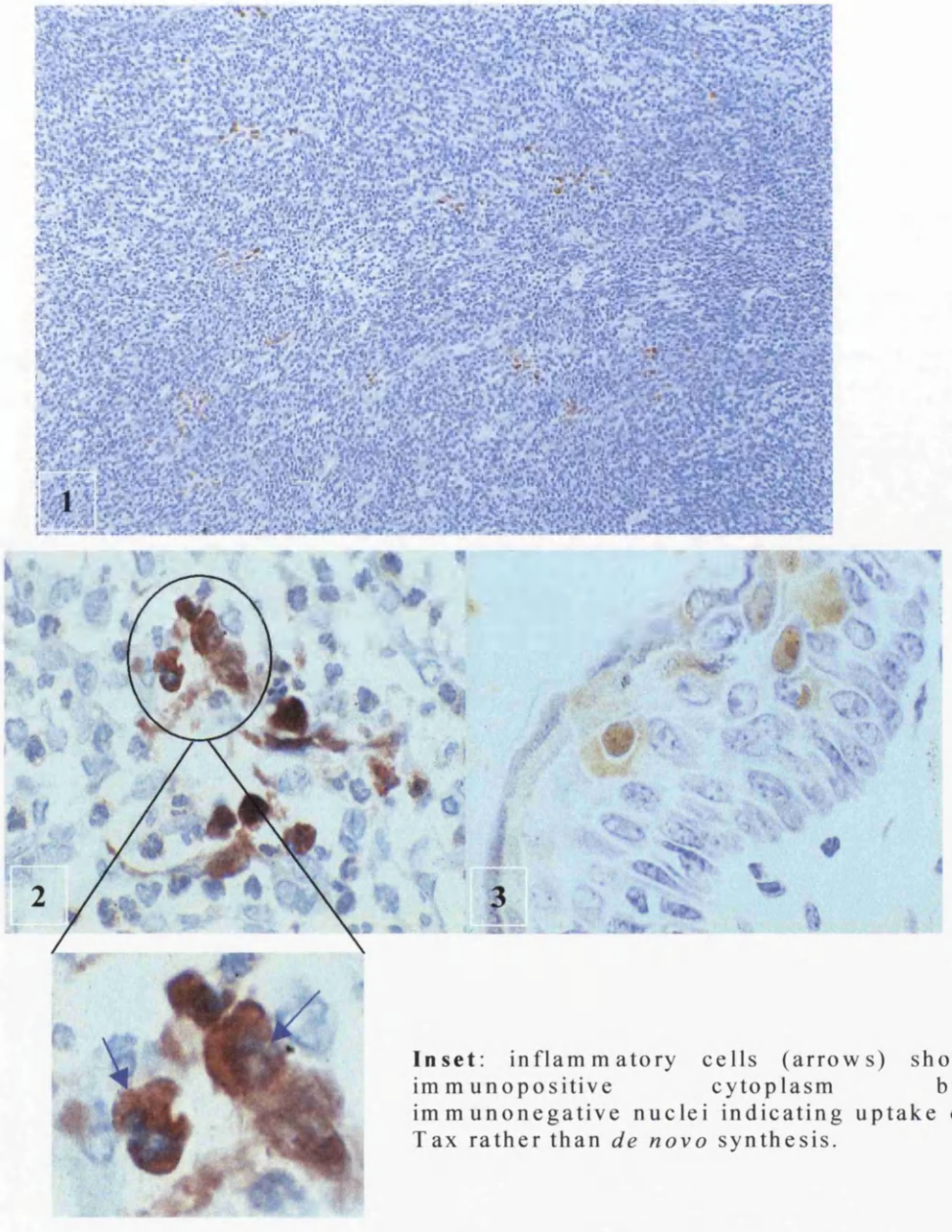

High power photomicrographs illustrating immunocytochemical detection of Tax expression using antibody 13L in a mesenchymal tumour (photo (1): original magnification x100; photo (2) oringinal magnification x1000 nickel enhanced) and the hyperplastic epithelium surrounding a mesenchymal tumour (photo (3): original magnification x1000).

Figure 4.5: Photomicrograph demonstrating Tax protein expression in a mammary adenoma

Photograph of a mammary adenoma immunostained with a Tax specific antibody (original magnification x1000). Immunopositive cells demonstrate strong, predominantly nuclear staining for the Tax protein. Slide counterstained with haematoxylin.

Figure 4.5: Photomicrograph demonstrating Tax protein expression in a mammary adenoma

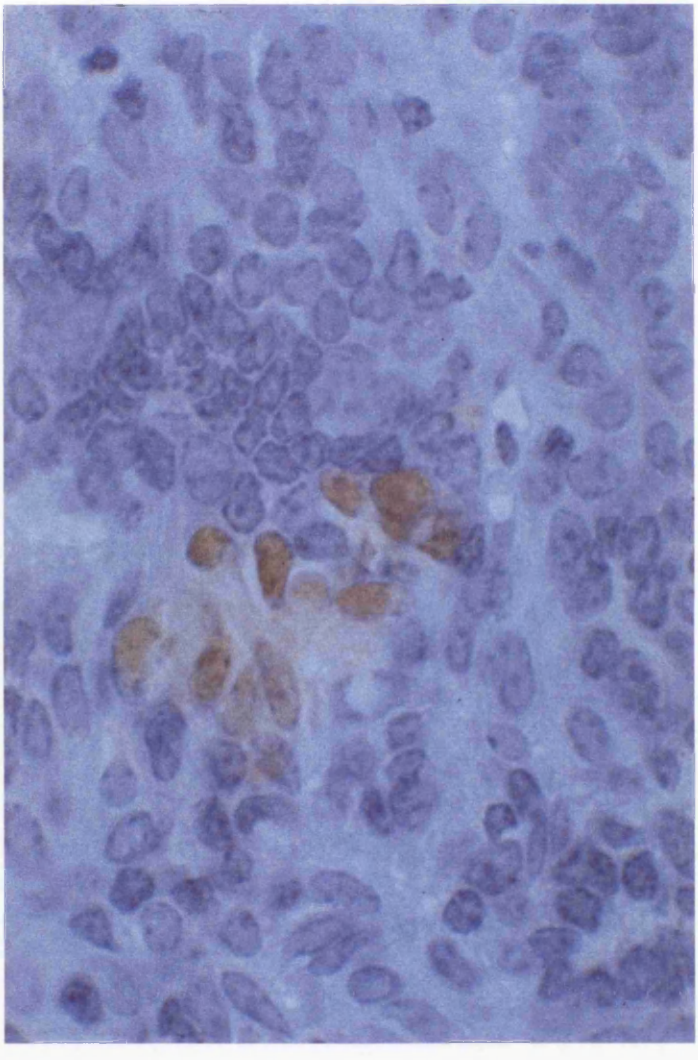

Expression of Tax protein within the mammary and salivary adenomas occurs as isolated foci of expressing cells randomly distributed throughout the substance of the tumour. This pattern was remarkably similar to that observed for Myc, Fos, Jun and p53 protein expression as well as the pattern of apoptosis.

4.2.5 Analysis of apoptosis in tumours

All the tumours in the cohort were assessed for apoptosis by DNA fragment labelling (Tdt-mediated dUTP Nick End labelling (TUNEL) technique) after the method of Gavrieli et al (1992). All tumours showed enhanced levels of apoptosis compared to normal control samples. The level and pattern of apoptosis within each tumour appeared to be highly correlated with the corresponding extent and distribution of Tax expression.

Mesenchymal tumours demonstrated apoptosis as individual cells and discrete clusters in a similar pattern to that observed for Tax expression (Figure 4.6 photo (1)). In addition they frequently exhibited apoptosis associated with phagocytic engulfment - a feature not unexpected given the high proportion of macrophages within these tumours. This served to restrict the pattern of apoptosis compared to the adenoma samples. We also noted apoptosis in the terminally differentiating layers (S. spinosum/granulosum) of the superficial epidermis (Figure 4.6 photo (3)) - again in a similar pattern to that observed for Tax expression.

Salivary adenomas and mammary adenomas demonstrated similar patterns of apoptosis. In these tumours apoptosis occurred as discrete clusters of cells and occasional individual cells which conformed very closely to the pattern seen for Tax expression (Figure 4.6 photo (2)).

Figure 4.6: Photomicrographs demonstrating apoptosis within mesenchymal tumours and mammary adenomas

Photographs of a mesenchymal tumour and mammary stained using the TUNEL technique. Photograph 1 demonstrates strong predominantly nuclear staining of a mesenchymal tumour (original magnification x400). Photograph 2 demonstrates strong nuclear staining of a mammary adenoma (original magnification x1000). Photograph 3 demonstrates strong nuclear staining of the terminally differentiating epithelium (stratum spinosum/granulosum surrounding a mesenchymal tumour(original magnification x1000). All slides counterstained with haematoxylin.

Figure 4.6: Photomicrographs demonstrating apoptosis within mesenchymal tumours and mammary adenomas

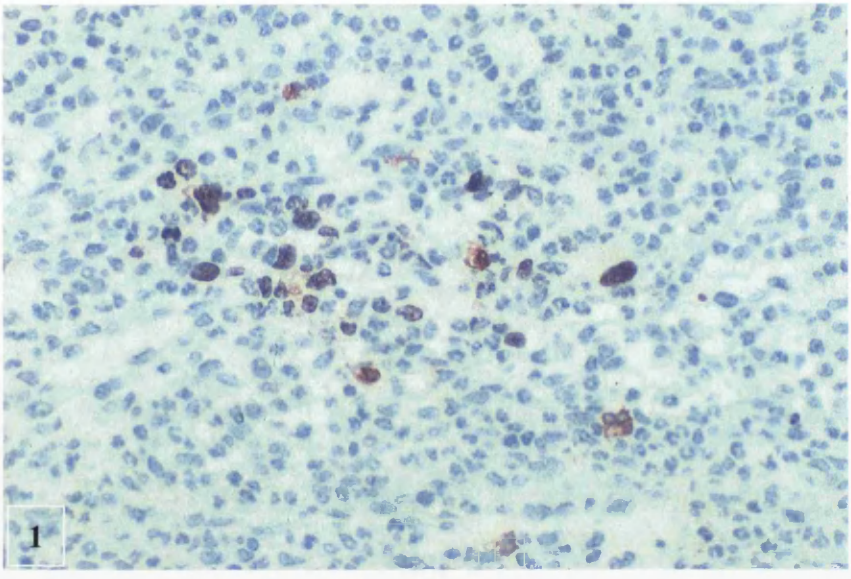

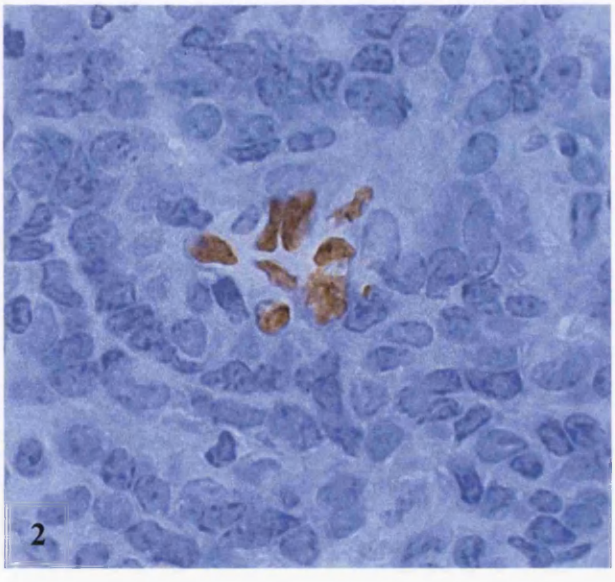

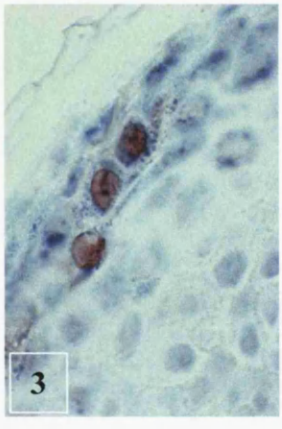

Photomicrographs of DNA fragment labelling using the TUNEL technique in mammary and mesenchymal tumours (DAB chromagen [brown] or AEC chromagen [red]). Photo (1) (original magnification x400) and photo (2) (original magnification x1000) demonstrate apoptosis occurs as discrete clusters of cells (as for Tax expression). Photo (3) (original magnification x1000) demonstrates apoptosis within the skin of the terminally differentiating epithelium of a mesenchymal tumour.

4.2.6 Immunofluorescent Co-localisation of Tax Expression and Apoptosis

The remarkable degree of overlap between Tax expression and apoptosis prompted us to investigate the spatial pattern and coincidence between these two processes. A mammary adenoma was chosen for double expression since this would be subject to the least distortion due to phagocytic clearance of apoptotic debris. Immunofluorescent co-localisation demonstrated that Tax expression was very highly associated with apoptotic induction (Figure 4.7 and 4.8). Indeed, only very rare cells exhibited spontaneous apoptosis without Tax expression (Figure 4.8 arrows). Control samples stained only for Tax expression or apoptosis showed no cross-reactivity.

4.2.7 Analysis of oncogene expression and p53 protein expression within tumours

Each tumour sample was also immunocytochemically analysed for Myc, Fos, Jun, and p53 protein expression (Figure 4.9). Myc expression was detected in 16/18 of tumours, Fos expression in 17/18 of tumours, Jun expression in 16/17 of tumours and p53 in 16/17 of samples (Summarised in Table 4.2). Normal control samples demonstrated no appreciable staining. Again, the pattern and extent of expression was very similar to that observed for Tax. Furthermore, positive staining was confined morphologically to the same cell types as seen for Tax expression. P53 expression although present in the majority of samples was generally weak, possibly indicative of low levels of protein expression. Expression was predominantly nuclear, with weak cytoplasmic staining. Control tissue taken from non-transgenic age-matched animals (pinna, mammary gland and salivary gland) demonstrated no staining for p53, Myc, Fos, or Jun protein expression.

Figure 4.7: Immunofluorescent photomicrographs demonstrating coincidence of Tax expression and apoptosis.

Photographs of a mammary adenoma fluorescently stained for Tax expression and apoptosis. The upper photograph demonstrates Tax immunofluoresence (original magnification x100) whereas the lower photograph demonstrates TUNEL staining (original magnification x100). Both photographs are taken from identical fields of view.

Figure 4.7: Immunofluorescent photomicrographs demonstrating coincidence of Tax expression and apoptosis.

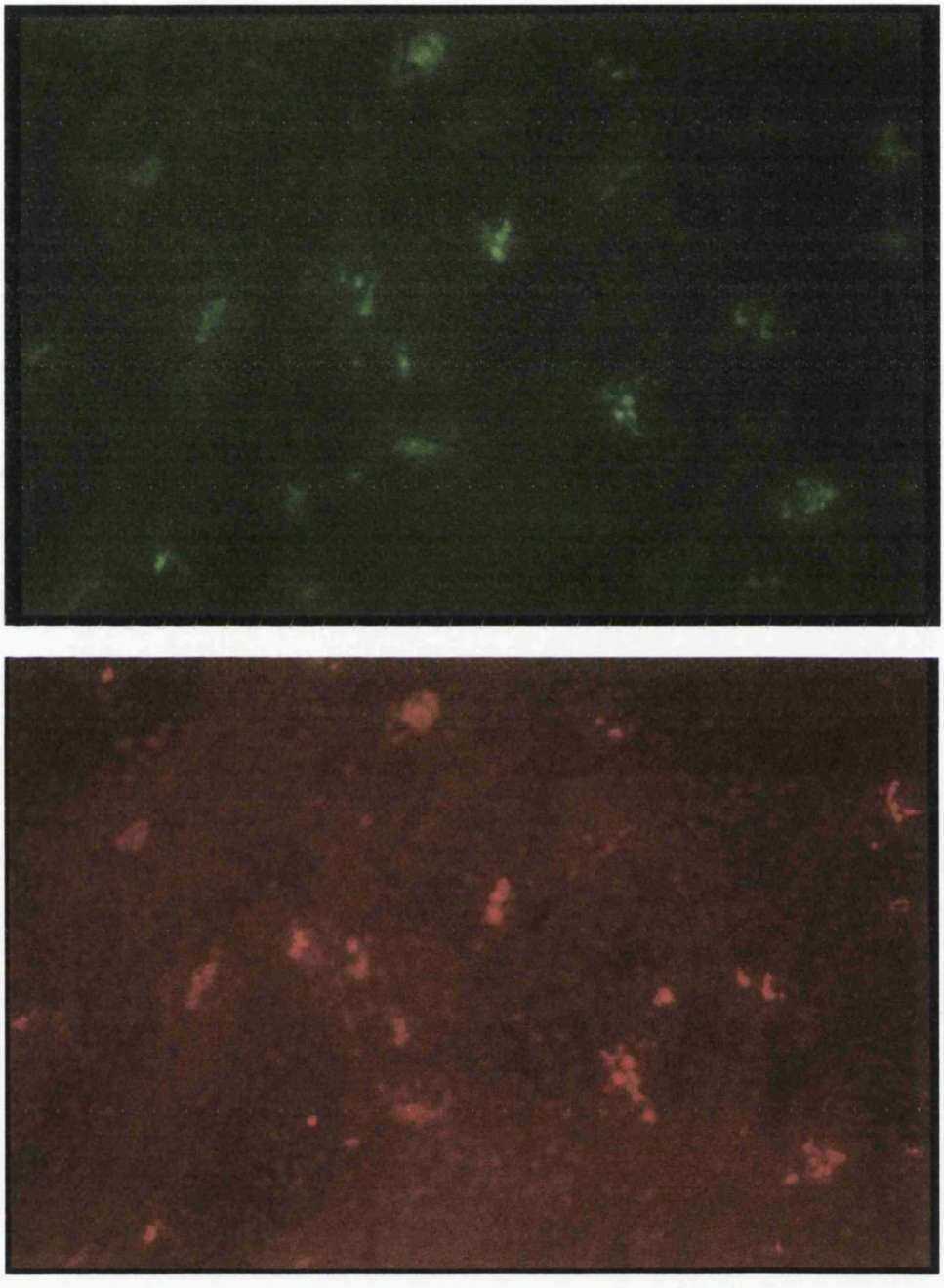

Upper photomicrograph (original magnification x10) illustrates Tax expression (FITC secondary conjugate) whereas lower photomicrograph (original magnification x10) illustrates apoptosis (Texas red secondary conjugate).

Figure 4.8: Immunofluorescent photomicrographs demonstrating coincidence of Tax expression and apoptosis.

Photographs of a mammary adenoma fluorescently stained for Tax expression and apoptosis. The upper photograph demonstrates Tax immunofluoresence (original magnification x1000) whereas the lower photograph demonstrates TUNEL staining (original magnification x1000). Both photographs are taken from identical fields of view. The arrows demonstrate TUNEL staining without Tax expression.

Figure 4.8: Immunofluorescent photomicrographs demonstrating coincidence of Tax expression and apoptosis.

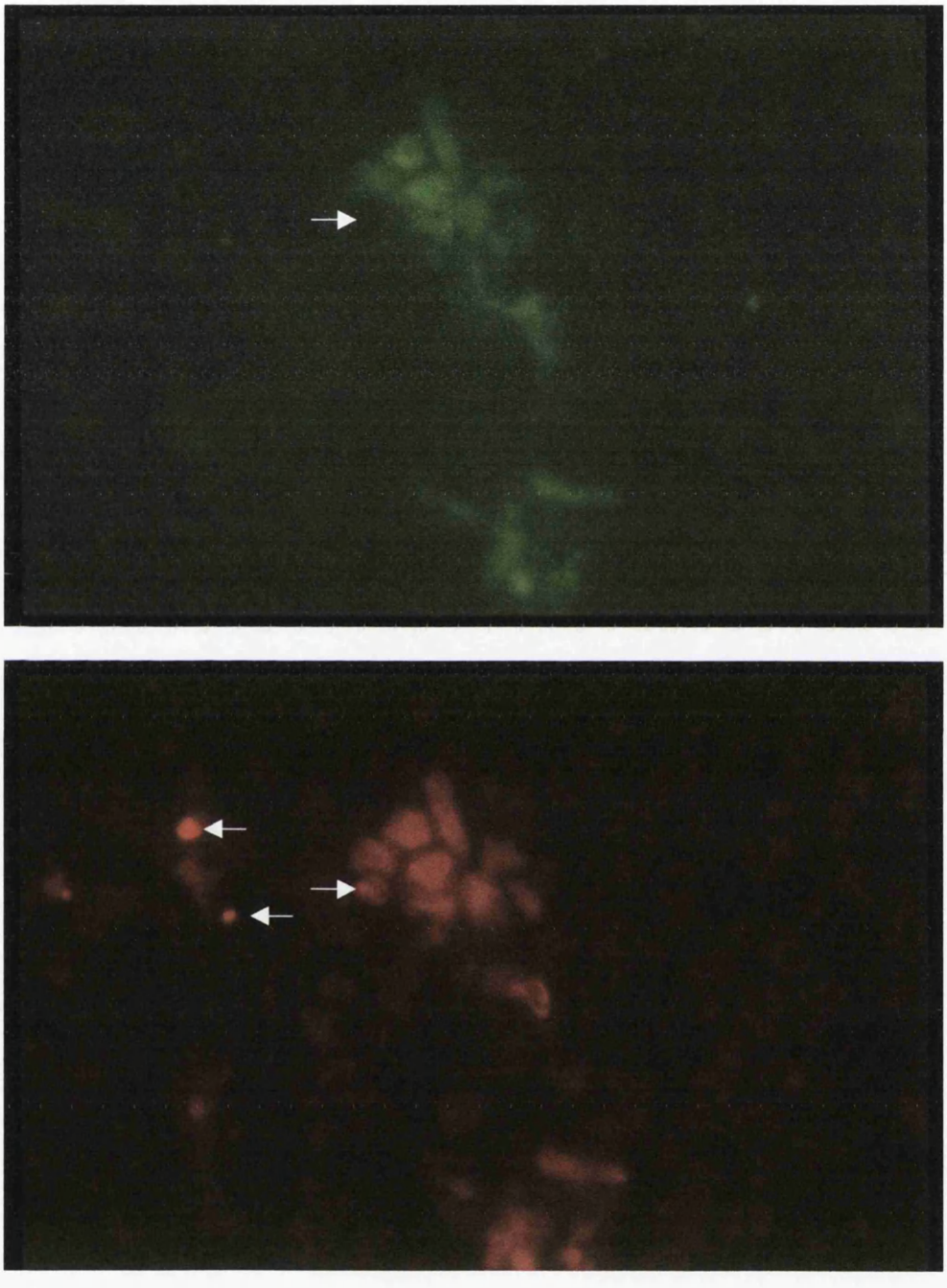

Upper photomicrograph (original magnification x1000) illustrates Tax expression (FITC secondary conjugate) whereas lower photomicrograph (original magnification x1000) illustrates apoptosis (Texas red secondary conjugate). Although the coincidence of these two processes is almost complete the arrows indicate that background apoptosis occurs without Tax expression.

Figure 4.9: Photomicrographs illustrating Myc, Fos, Jun and p53 protein expression in mammary adenomas

Photographs of a mammary adenoma immunostained with Myc, Fos, Jun and p53 specific antibodies. Photographs 1, 2, 3 and 4 demonstrate strong predominantly nuclear immunostaining with Fos, Myc, Jun and p53 specific antibodies respectively (original magnification x1000).

Figure 4.9: Photomicrographs illustrating Myc, Fos, Jun and p53 protein expression in mammary adenomas

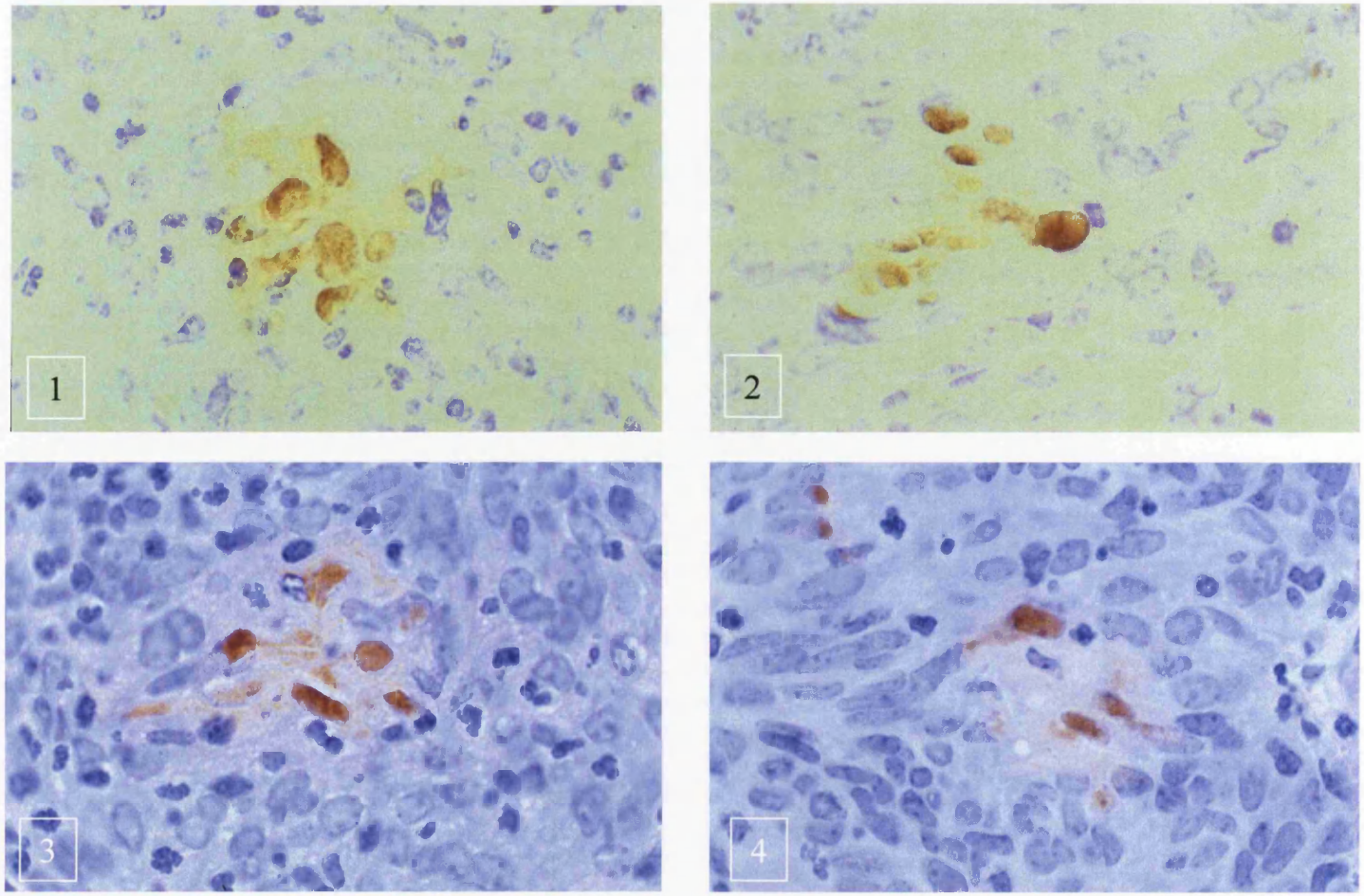

High power photomicrographs (original magnification x1000) demonstrating Fos (photo (1)) Myc (photo (2)) Jun (photo (3)) and p53 (photo (4)) protein expression in mammary adenomas.

4.3 Discussion

This report demonstrates that Tax induces a variety of phenotypes in CD3-*tax* transgenic mice that are characterised by enhanced levels of apoptosis. Tax expression and apoptosis show a remarkable degree of coincidence as evidenced by the pattern and distribution of expression and double immunofluorescence. These tumours also demonstrate enhanced levels of Myc, Fos, and Jun oncoprotein expression, as well as elevated levels of the p53 tumour suppressor gene product. An unexpected feature of these tumours was their common profile of gene expression. This occurred regardless of the derived lineage of tumour cell and raises the intriguing possibility that at least in the CD3-*tax* transgenic mouse system, *tax* induces a common phenotype which in susceptible cell types leads to transformation.

The Tax protein represents an immunodominant epitope (Kannagi et al, 1992; Pique et al, 1996) being subject to a vigorous immune response (Niewiesk et al, 1994; Parker et al, 1994) during the natural course of infection by HTLV-I. It was therefore not surprising that the MAP system generated high titre antibodies specific to the native protein allowing the immunocytochemical detection of the protein within the *tax* transgenic mouse tumours. Specific recognition of the Tax protein was concluded from several sources of data. The pattern of staining produced by both antibodies was identical despite the specificity of each antibody, which was directed towards different regions of the Tax protein. No staining was observed when parallel experiments were performed using no primary antibody or when non-transgenic tissues were stained with the Tax antibody. Furthermore the pattern of expression conformed to the expected pattern of Tax expression based on the known sub-cellular localisation of Tax i.e. intense nuclear staining with weaker cytoplasmic staining (Goh et al, 1985; Lee et al, 1989). Additionally, the pattern of staining generated by both anti-Tax sera was consistent with a previously published report demonstrating Tax expression immunocytochemically (within HTLV-I^{LTR}-*tax* transgenic mouse neurofibromas) (Green et al, 1992). Finally, immunostaining was specific to the tumour (ovoid-spindle) cell population. Infiltrating inflammatory cells adjacent to positive foci demonstrated weak cytoplasmic staining but never any nuclear staining which we

concluded was due to phagocytosis of immunopositive debris rather than evidence of gene expression *per se*.

In situ immunocytochemical detection of Tax expression not only confirmed the presence of Tax protein within tumour material (and conversely its absence from non-tumourous material) but also further defined the pattern and distribution of expression. Expression of Tax is confined to the background spindle cell population and is absent from the superimposed inflammatory cell influx. The peculiar heterogeneous pattern of Tax expression is consistent with other transgenic mouse tumour models in which transgene expression has been examined immunocytochemically (Schuch et al, 1990; Green et al, 1992).

Our results show that a very high proportion of *tax* induced tumours displayed increased Myc, Fos, and Jun oncoprotein expression, as well as elevated levels of the p53 tumour suppressor gene product. Accompanying this profile of gene expression were enhanced levels of apoptosis, which were coincident with Tax expression. It therefore appeared that a functional consequence of inappropriate Tax expression *in vivo* might be the enforced induction of apoptosis. Apoptosis has been described as a general feature of many spontaneously occurring tumours and more recently apoptotic induction has been attributed to a limited repertoire of oncogenes such as *c-myc* (Evan et al, 1992), *c-fos* (Preston et al, 1996), and Adenovirus *E1a* (Rao et al, 1992). Likewise *tax* has been linked with induction of apoptosis in immortalised rodent fibroblasts (Tanaka et al, 1990) and human T-cell lines (Grassman et al, 1989 and 1992). Our results demonstrate that Tax expression *in vivo* is associated with elevated levels of apoptosis. The high degree of coincidence between Tax expression and apoptosis suggests that these two processes are intimately linked and that like *c-myc* (Alarcon et al, 1996), *tax* is a potent inducer of apoptosis *in vivo*. However these observations also lead to an enigma concerning the role of *tax* in tumourigenesis. One possible explanation is that high levels of Tax may lead to cell death. Low levels of expression, which may occur within the background population, and which is undetectable by immunocytochemical analysis, may have a proliferative role

(Marriott et al, 1992) or even an anti-apoptotic role (Kishi et al, 1997; Brauweiler et al, 1997).

However, the mechanism by which Tax induces apoptosis is uncertain. Tax is known to upregulate a number of genes including *c-myc* (Duyao et al, 1992a and 1992b), *c-jun* (Iwakura et al, 1995; Hooper et al, 1991, Fujii et al, 1991) and *c-fos* (Fujii et al, 1988; Nagata et al, 1989; Alexandre et al, 1991; Iwakura et al, 1995) which have been shown to induce apoptosis. Our results demonstrate that a very high proportion of Tax induced tumours express elevated levels of these proteins which lends support to the notion that *tax* upregulates these genes *in vivo*. The similar deregulated expression of these oncogenes in pre-neoplastic lymphoproliferative conditions (Stone et al, 1996; Iwahashi et al, 1994; Kanaitsuka et al, 1989) and HTLV-I infected cell lines (Hooper et al, 1991) suggests that these oncogenes may be of wider significance than the *tax* transgenic system and may contribute to the induction of the neoplastic process. Conceivably these oncogenes could also act as transcriptional intermediates mediating the apoptotic response to *tax* expression. However it is unlikely that these genes alone are responsible for this effect since the sensitivity of rat 1 fibroblasts transformed by *tax* to the induction of apoptosis differed from cells transformed by either *c-myc* or *c-fos* (Fujita et al, 1995). An alternative hypothesis is that *tax* directly induces apoptosis in a manner analogous to that previously observed for *c-myc* (Evan et al, 1995) and *c-fos* (Preston et al, 1996) in which the activation of other genes is not required. In this system the induction of apoptosis by *c-myc*, and *E1a* has been intimately linked with the inappropriate entry into the cell cycle (Mymryk et al, 1994; Evan et al, 1992) which can be inhibited by the addition of specific cytokines (Harrington et al, 1994).

An additional feature noted within these tumours were enhanced levels of the p53 tumour suppressor gene product. Wild-type p53 protein is usually only detected at very low levels due to rapid turnover of newly synthesised protein (Rogel et al, 1985). Stabilisation of the p53 tumour suppressor gene (Reid et al, 1993) and impairment of its function (Ceresto et al, 1996) has been noted in cell lines transformed by HTLV-I infection as well as uncultured ATL cells. Since *tax* is not known either to transactivate (Reid et al, 1993;

Uittenbogaard et al, 1995) or bind the p53 protein (Reid et al, 1993) the mechanism by which this effect is achieved is unknown. The frequency with which these tumours express elevated levels of this protein indicates that this may be a direct consequence resulting from *tax* expression.

The observation of proliferation and concomitant apoptosis together with the characteristic latencies for each tumour phenotype in the CD3-*tax* transgenic mouse system provides a framework for tumourigenesis. The high degree of coincidence between Tax expression and apoptosis suggests that deregulated Tax expression induces apoptosis. The induction of tumours in CD3-*tax* transgenic mice favours a model whereby deregulated expression of *tax* results in apoptosis. In other cell types such as thymocytes and oxidative muscle cells, *tax* expression is non-permissive and results in thymic involution (our unpublished results and Furuta et al, 1989) or oxidative muscle fibre degeneration (Nerenberg et al, 1989). In the context of this model tumours emerge only if this pathway can be abrogated. Mesenchymal tumours only develop at sites of wounding, typically ear and tail tips. One possible mechanism is that a cocktail of growth promoting cytokines derived from inflammatory mediators released at wound sites provides a survival signal promoting tumour induction. To this point, the induction of fibrosarcomas in v-*jun* transgenic mice also requires wounding (Schuh et al, 1990) suggesting the need for epigenetic events to influence tumour genesis. The importance of this model in tumourigenesis and the role of survival factors in mitigating the effects of apoptosis is well established in cell culture (Harrington et al, 1994). In other systems of carcinogenesis, tumour promoters such as phorbol myristate acetate (PMA) and α-hexachlorocyclohexane (Thompson et al, 1995) have been shown to achieve their tumour promoting effects by acting as specific survival factors. The development of mammary and salivary adenomas in CD3-*tax* transgenic mice occurs after a latency of many months. This prolonged latency is compatible with the acquisition of a second complimenting genetic lesion, which allows the survival of Tax expressing cells. Clearly expression of Tax *in vivo* imposes a balance between life and death. In the absence of complimenting genetic lesions environmental factors such as survival cytokines may determine the fate of these cells and ultimately the emergence of the neoplastic phenotype.

Chapter 5

Investigation of the role of p53 in *tax* mediated tumourigenesis

Investigation of the role of p53 in *tax* mediated tumourigenesis

5.1 Introduction

The importance of the p53 tumour suppressor gene as the most frequently mutated gene in human cancer is firmly established (Nigro et al, 1989; Bartek et al, 1991; Hollstein et al, 1991). About half of all cancers have inactivating p53 mutations (Hollstein et al 1991) which appear to represent a critical late step (Vogelstein and Kinzler, 1993; Wynford-Thomas 1993; Kemp et al, 1993) in the evolution of malignant disease.

The generation of p53 knockout mice has allowed the assessment of p53 function *in vivo*. These mice develop normally but are prone to a variety of tumours at an early age (mainly lymphomas and sarcomas) (Donehower et al, 1992; Purdie et al, 1994). The importance of p53 loss of function is highlighted by its complementation with *c-myc* (Blyth et al, 1995; Hsu et al, 1995) in which there is dramatic acceleration of tumour development. This synergy mirrors that seen between over-expression of *bcl-2* and *c-myc* (Mcdonnell and Korsmeyer, 1991), and underlines the importance of this group of tumour suppressor genes in multi-stage tumourigenesis.

The role however that p53 plays in the development of ATL is still unclear since few naturally occurring p53 mutations have been found in ATL samples (Nagai et al, 1991). Tax has been shown to trans-repress the p53 promoter (Uittenbogaard et al, 1995) and inhibit its function (Akagi et al, 1997; Ceresto et al, 1996) as well as upregulating p21 waf1/cip1 (Ceresto et al, 1996). Furthermore *tax* may inhibit apoptosis (Kishi et al, 1997; Schwartz-Cornil et al, 1997) possibly through *tax* mediated trans-repression of *bax* (Brauweiler et al, 1997). The resulting phenotype of ATL cells is a marked resistance to chemotherapeutic intervention. Despite an intact p53 genotype, most patients with ATL die within 6-12 months of diagnosis (Taguchi et al, 1996; Uozomi et al, 1995). In contrast, tumours which have a functional p53 status, such as testicular carcinomas or childhood acute lymphoblastic leukaemias often respond favourably to chemotherapy (Lutzker and Levine, 1996; Lowe et al, 1993).

5.2 Aims of the experiments

We therefore decided to assess the role p53 plays in the development of mesenchymal tumours in CD3-*tax* transgenic mice. CD3-*tax* transgenic mice were crossed onto a p53 null background (Donehower et al, 1992) to generate an F1 $p53^{+/-}$/*tax* breeding cohort of mice (breeding experiments set up by Dr Blyth). The F1 generation was then backcrossed to generate an F2 experimental cohort containing *tax* transgenic mice on either a p53 wild type ($p53^{+/+}$), hemizygous ($p53^{+/-}$) or null ($p53^{-/-}$) background. The contribution that the p53 protein played in tumourigenesis could then be assessed by measuring tumour incidence, phenotype and latency as well as gene expression and apoptosis.

5.3 Results

5.3.1 p53 cross *tax* breeding experiments

The F1 breeding cohort produced 84 experimental F2 mice (Table 5.1). Mice not showing any pathology after 12-18 months were culled.

Table 5.1: Result of $p53^{+/-}$ x *tax* breeding experiment

Table summarising the results of the $p53^{+/-}$ cross *tax* transgenic mouse breeding experiments which generated the p53/tax (denoted as p/t) line of mice. The top pane summarises the phenotypes of the mice which carry either a $p53^{-/-}$ (null), $p53^{+/-}$ (heterozygous) or $p53^{+/+}$ (wild type) allele together with a *tax* allele. The middle panel summarises the phenotypes of the mice which carry either a $p53^{-/-}$ (null), $p53^{+/-}$ (heterozygous) of $p53^{+/+}$ (wild type) allele only. The bottom panel summarises the overall tumour incidence for each transgenic mouse cross. The p/t nomenclature refers to the identification number allocated to the offspring of the $p53^{+/-}$ cross tax mice.

Top panel: Summary of the phenotype of the $p53^{-/-}$/tax, $p53^{+/-}$/tax, $p53^{+/+}$/tax mice. The individual cause of death for each mouse is indicated by the symbols: * ear and/or tail (mesenchymal) tumours; • thymic lymphoma; ♣ sarcoma; ♠ hind leg paresis. Animals that do not have a symbol were culled after 12-18 months. The figures refer to the total number of animals in each group (grand total in brackets).

Middle panel: Summary of the phenotype of the $p53^{-/-}$, $p53^{+/-}$, $p53^{+/+}$ mice. The individual cause of death for each mouse is indicated by the symbols: * ear and/or tail (mesenchymal) tumours; • thymic lymphoma; ♣ sarcoma; ♠ hind leg paresis. Animals that do not have a symbol were culled after 12-18 months. The figures refer to the total number of animals in each group (grand total in brackets).

Lower panel: Summary of the overall tumour incidence and average latency (in days) for each of the p53/tax mice. Figures in brackets in the 'pathology' column refer to the total number of tumour for each mouse cross.

Key: * ear and/or tail (mesenchymal) tumours; • thymic lymphoma; ♣ sarcoma; ♠ hind leg paresis

Table 5.1: Result of $p53^{+/-}$ x *tax* breeding experiment

$p53^{-/-}$/*tax*	$p53^{+/-}$/*tax*	$p53^{+/+}$/*tax*	
•p/t 42; •p/t 77; p/t 121	*p/t 43; pt 66; p/t 97	p/t 58; *p/t 123	
♣p/t 49; •♣p/t 78; ♣p/t 124	*p/t 48; p/t 67; p/t 111	p/t 85;	
♣p/t 52; ♣p/t 90; p/t 126	*p/t 50; p/t 68; p/t 117	p/t 92	
p/t 56; •p/t 96;	*p/t 54; p/t 70; ♠p/t 120	p/t 93	
♣p/t 62; p/t 100;	*p/t 57; p/t 72; *p/t 125	*•p/t 99	
•p/t 63; •p/t 108	p/t 60; p/t 74; p/t 140	p/t 101	
•p/t 69; •p/t 114	p/t 61; p/t 79	p/t 115	
♣p/t 71; •♣p/t 116	p/t 64; p/t 80	p/t 122	
19	**22**	**9**	**Total (50)**

$p53^{-/-}$	$p53^{+/-}$	$p53^{+/+}$	
•p/t 53; p/t 143	p/t 44; p/t 84; p/t 105	p/t 59	
♣p/t 55	p/t 45; p/t 86; ♣p/t 106	p/t 89	
•p/t 65	♣p/t 51; p/t 87; p/t 112	p/t 118	
♣p/t 75	p/t 73; p/t 91; p/t 119		
•p/t 88	p/t 76; ♣p/t 94; p/t 141		
♣p/t 98	p/t 81; p/t 95; •♣p/t 142		
p/t107	p/t 82; p/t 103		
♣p/t 113	p/t 83; p/t 104		
9	**22**	**3**	**Total (34)**

Genotype	Pathology	Average Latency (days)	Tumour Incidence
$p53^{+/-}$/*tax*	mesenchymal tumours (6)	233	6/22 (27%)
$p53^{+/+}$/*tax*	mesenchymal tumours (2) thymic lymphoma (1)	156	2/9 (22%)
$p53^{+/-}$	thymic lymphoma (1) sarcomas (4)	249	4/22 (18%)
$p53^{-/-}$/*tax*	thymic lymphoma (9) sarcomas (8)	163	15/19 (79%)
$p53^{-/-}$	thymic lymphoma (3) sarcomas (4)	157	7/9 (78%)

5.3.2 Analysis of tumour incidence and latency

The p/t series of mice produced mesenchymal tumours at a reduced incidence rate compared to the original cohort of CD3-*tax* tumours but with no reduction in the tumour latency (Table 5.2). This indicates that a hemizygous or null p53 background did not accelerate tumour induction. p53 related pathology (chiefly thymic lymphoma and/or sarcomas) arose with high incidence, predominantly in the p53 null mice (approximately four fold more frequently compared to p53 hemizygous mice). Since these tumours emerged after only a short latency period and proved invariably fatal, this type of pathology may have pre-empted the emergence of the *tax* phenotype forestalling the development of *tax* related tumours in these mice.

Table 5.2: Comparison of tumour phenotypes emerging on a p53 homo- or hemizygous background compared to a p53 wild type background

Genotype	Average Latency	Tumour Incidence
$p53^{+/-}$/*tax*	233d (7.8 months)	6/22 (27%)
$p53^{+/+}$/*tax*	156d (5.2 months)	2/9 (22%)
1300 series	277d (9.2months)	2/4 (50%)
1400 series	128d (4.3 months)	16/27 (59%)

Table summarising the average latency in days (and months) and tumour incidence for the $p53^{+/-}$/tax, $p53^{+/+}$/tax, and 1300/1400 series *tax* mice.

5.3.3 Histological analysis of tumours

Analysis of the p/t series of mesenchymal tumours indicated that they were phenotypically and histologically similar to the original cohort of mesenchymal tumours. Tumours typically developed at wounding sites (ear and tail tips) in an identical fashion to the original cohort of 1300/1400 series of *tax* transgenic tumours. Histopathological examination revealed a spindle cell population together with a superimposed intense inflammatory cell infiltrate (polymorphs and macrophages) (Figure 5.1 and 5.2 - compare

to Figure 3.3). Again these tumours were locally aggressive infiltrating along tissue planes although no evidence of metastasis was noted. Frequently a large necrotic area within the centre of these tumours was observed (Figure 5.1) indicating rapid tumour growth - a feature not present within the original tumour cohort.

Figure 5.1: H+E photomicrographs of a mesenchymal tumour emerging in a p53 hemizygous background.

Photographs of a mesenchymal tumour which developed in a $p53^{+/-}$/*tax* mouse. Upper photograph (original magnification x10) and lower photograph (original magnification x400) showing the similarities and differences between the original 1300/1400 *tax* series of mesenchymal tumours and $p53^{+/-}$/tax tumours.

1 area of central necrosis; 2 cartilage plate; 3 spindle cell population

Figure 5.1: H+E photomicrographs of a mesenchymal tumour emerging in a p53 hemizygous background.

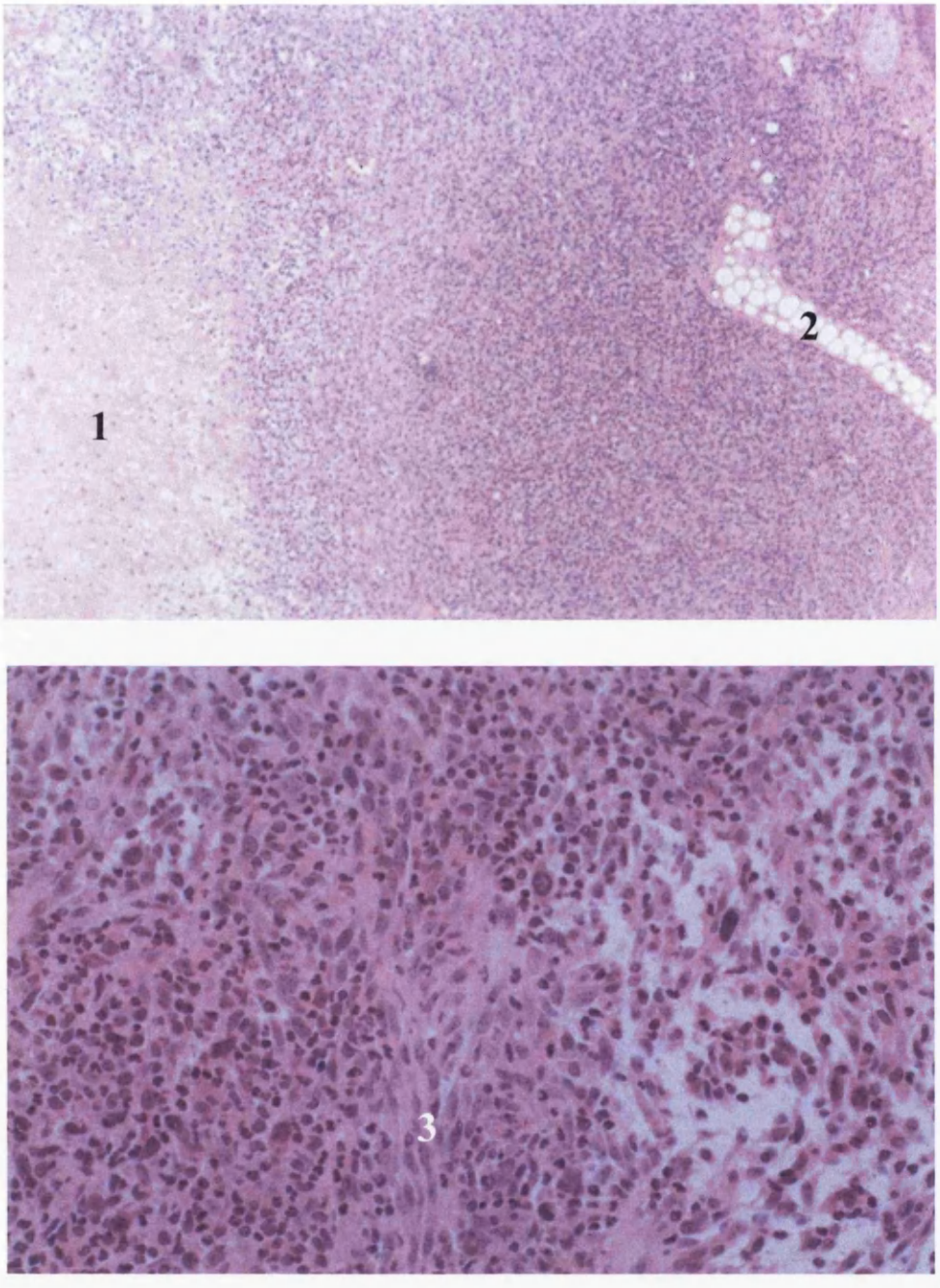

Low power (upper photo: original magnification x10) and high power photomicrograph (lower photo: original magnification x100) of a mesenchymal tumour arising in the p53x*tax* cohort of mice revealing a spindle cell background population of Tax expressing tumour cells accompanied by an intense inflammatory cell infiltrate.

1 area of central necrosis; 2 cartilage plate; 3 spindle cell population

5.3.4 Analysis of gene expression and apoptosis

TUNEL analysis of four tumours derived from the $p53^{+/-}$/*tax* cohort revealed that apoptosis occurred at a reduced rate and with an alternative pattern compared to the original cohort of mesenchymal tumours. Apoptotic cells were distributed as rare discrete cells scattered throughout the substance of the tumour (Figure 5.2). No foci of apoptotic cells were ever visible. Furthermore, Tax protein, oncoprotein (Myc, Fos, and Jun) as well as p53 protein expression could not be detected immunocytochemically indicating that localised high level expression of these proteins did not occur. However *tax* RNA expression could be detected by in situ hybridisation [Ms J. McMillan personal communication] and by Northern analysis from cell lines derived from these tumours.

5.3.5 Analysis of cell lines derived from $p53^{+/-}$/*tax* mesenchymal tumours

Two cell lines were derived from these tumours $p53^{+/-}$/*tax* 50 [p/t 50] and $p53^{+/-}$/*tax* 54 [p/t 54]. Morphological analysis of these cell lines together with a *tax* expressing cell line Tax 1 [T 1] derived from the original cohort of mesenchymal tumours revealed different patterns of growth. T 1 and p/t 54 grew as a contact inhibited monolayer being made up of an orderly array of ovoid or hexagonal cells. In contrast, p/t 50 grew as a disorderly array of smaller spindle shaped cells, which showed considerable cellular pleiomorphism, frequently piling up into foci of contact uninhibited independent cells (Figure 5.3). In cell culture, p/t 50 grew considerably more quickly and to a higher cellular density than either T 1 or p/t 54 (Graph 5.1).

PCR genotype analysis after 4 months in continuous culture revealed no loss of the wild-type allele (Figure 5.4). These results were confirmed using an alternative pair of primers directed to the same exon. Southern blot analysis (performed by Dr Campbell) confirmed the presence of an intact wild type p53 allele within the p/t series of tumours but loss of the wild type allele from the p/t 50 cell line and the nude tumours derived from that cell line (Figure 5.5).

Figure 5.2: Photomicrograph demonstrating apoptosis within a mesenchymal tumour emerging in a p53 hemizygous background .

Photograph of a mesenchymal tumour which developed in a $p53^{+/-}$/*tax* mouse demonstrating apoptosis staining using the TUNEL technique (original magnification x1000). Counter stained with haematoxylin.

Figure 5.2: Photomicrograph demonstrating apoptosis within a mesenchymal tumour emerging in a p53 hemizygous background

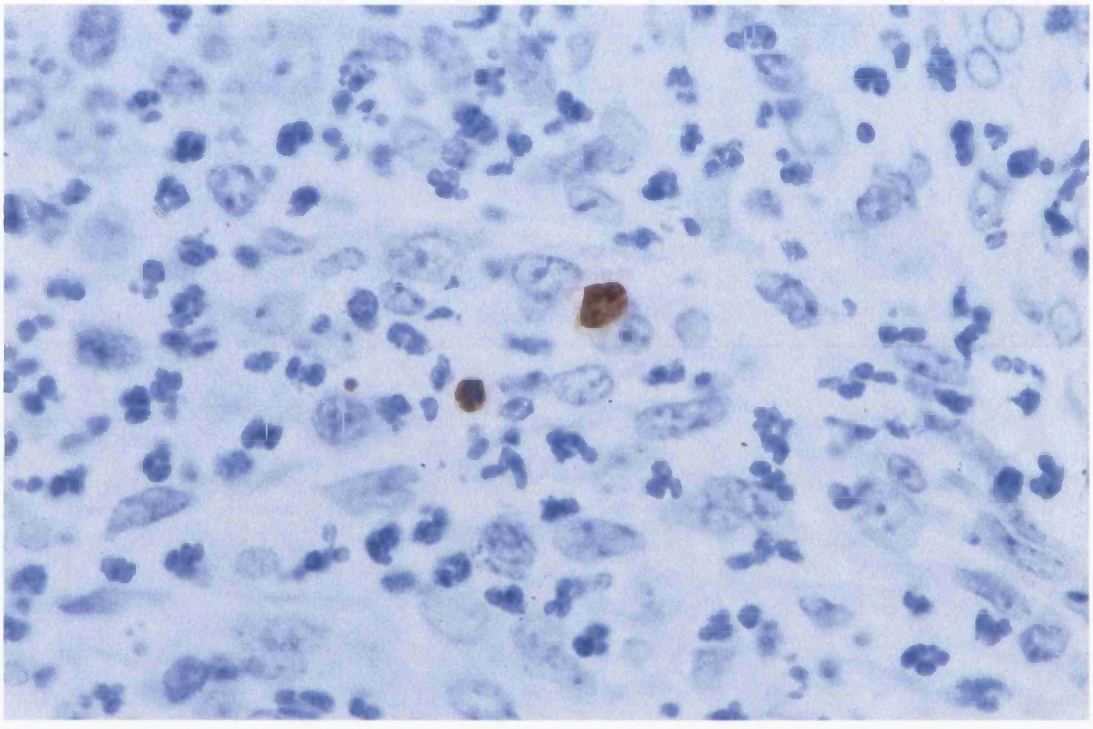

High power photomicrograph (original magnification x1000) of a TUNEL stained section demonstrating apoptosis in a mesenchymal tumour derived from the p53x*tax* cohort of mice. No foci of apoptotic cells were visible – apoptosis occurred only as occasional single cells.

Figure 5.3: Photomicrographs of p/t 50 and p/t 54 cell lines after 4 months of continuous cell culture

Photograph of the p/t 50 and p/t 54 cell lines after 4 months in continuous culture. The upper photograph (original magnification x100) of the p/t 50 cell line illustrates malignant behaviour whereas the lower photograph (original magnification x100) illustrates non-malignant behaviour.

Figure 5.3: Photomicrographs of p/t 50 and p/t 54 cell lines after 4 months of continuous cell culture

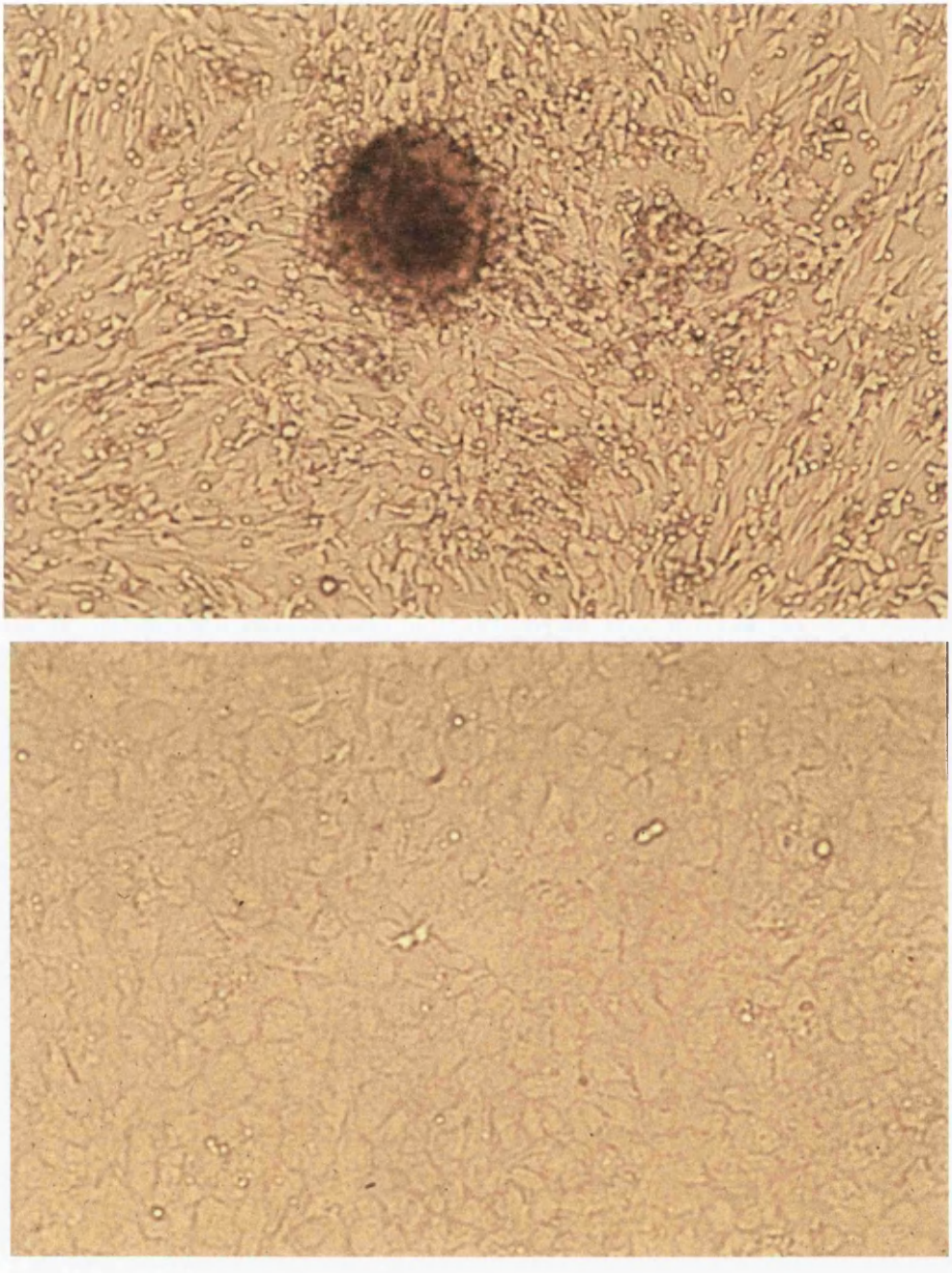

Comparison of p/t 50 cell line (upper photo: original magnification x100) and p/t 54 cell line (lower photo: original magnification x100) after 4 months of continuous cell culture. Cell line p/t 50 shows considerable variation in size and shape, and foci of contact uninhibited cells whereas p/t 54 maintains a uniform monolayer of hexagonal cells.

Graph 5.1: Graph illustrating number of cells versus time for cell lines p/t 50, p/t 54, T1 and Rat 1 cells

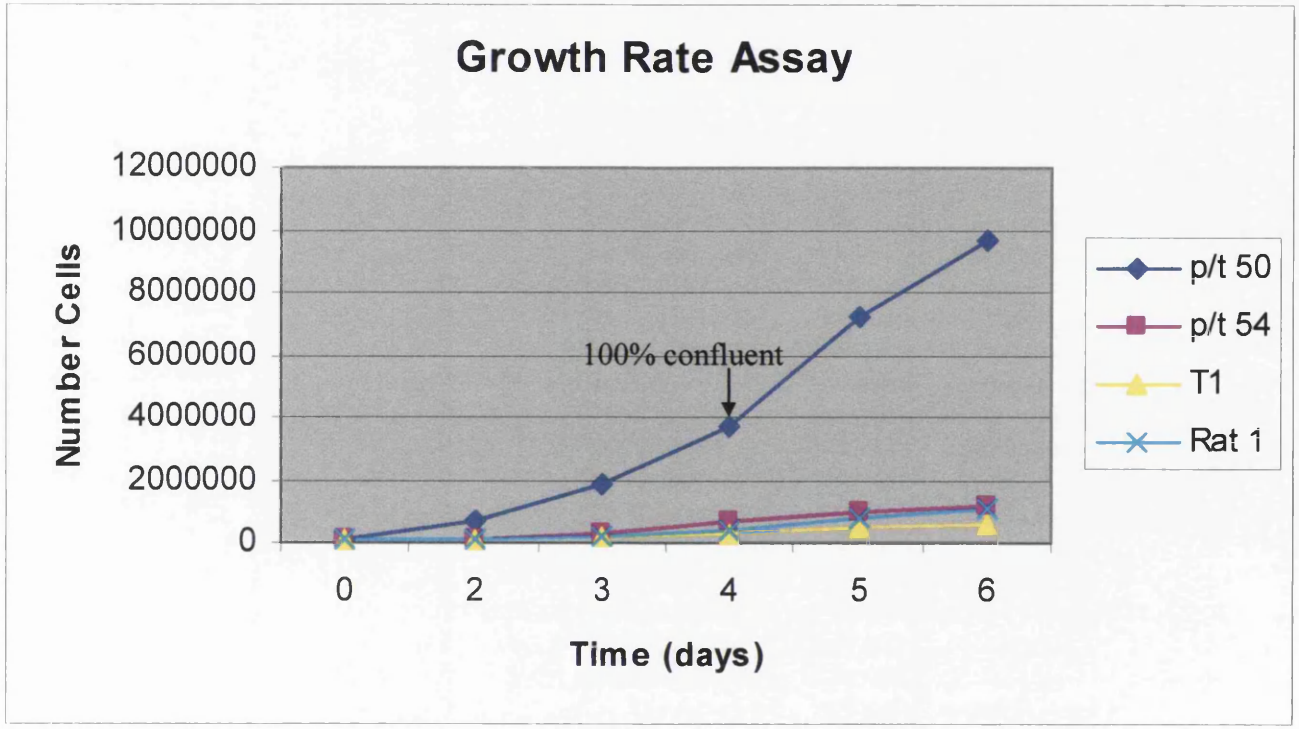

Graph 5.1 illustrating the growth rate of cell lines p/t 50, p/t 54, T1 and control rat 1 cells in 10% FCS at 37°C and 5% CO_2 over a period of 6 days. The point at which cell line p/t 50 reached 100% confluency (judged by light microscopy) is indicated by an arrow on day 4.

Figure 5.4: Photograph demonstrating p53 PCR genotyping of cell lines derived from $p53^{+/-}$/*tax* mesenchymal tumours (p/t 50 and p/t 54) and a $p53^{+/+}$/tax (T1) mesenchymal tumour after 4 months in culture.

Photograph of an ethidium bromide stained acrylamide gel demonstrating p53 allele genotyping of the *tax* and p53/tax derived cell lines. Lanes 1, 3, and 5 refer to cell lines T1, p/t 50, and p/t 54 respectively using PCR primers to detect the p53 knockout ($p53^-$) allele. Lanes 2, 4, and 6 refer to cell lines T1, p/t 50, and p/t 54 respectively using PCR primers to detect the p53 wild type ($p53^+$) allele. Lanes 7, 9, and 11 refer to $p53^{+/+}$, $p53^{+/-}$ and $p53^{-/-}$ control DNA respectively using PCR primers to detect the p53 knockout allele ($p53^-$). Lanes 8, 10, and 12 refer to $p53^{+/+}$, $p53^{+/-}$ and $p53^{-/-}$ control DNA respectively using PCR primers to detect the p53 wild type allele ($p53^+$) respectively. Lane 13 and 14 refer to negative control water using PCR primers to detect the p53 knockout ($p53^-$) and p53 wild type ($p53^+$) allele respectively. Lane 0 (not marked) refers to 5uL of Phi X molecular weight DNA ladder.

Figure 5.4: Photograph demonstrating p53 PCR genotyping of cell lines derived from $p53^{+/-}$/*tax* mesenchymal tumours (p/t 50 and p/t 54) and a $p53^{+/+}$/tax (T1) mesenchymal tumour after 4 months in culture.

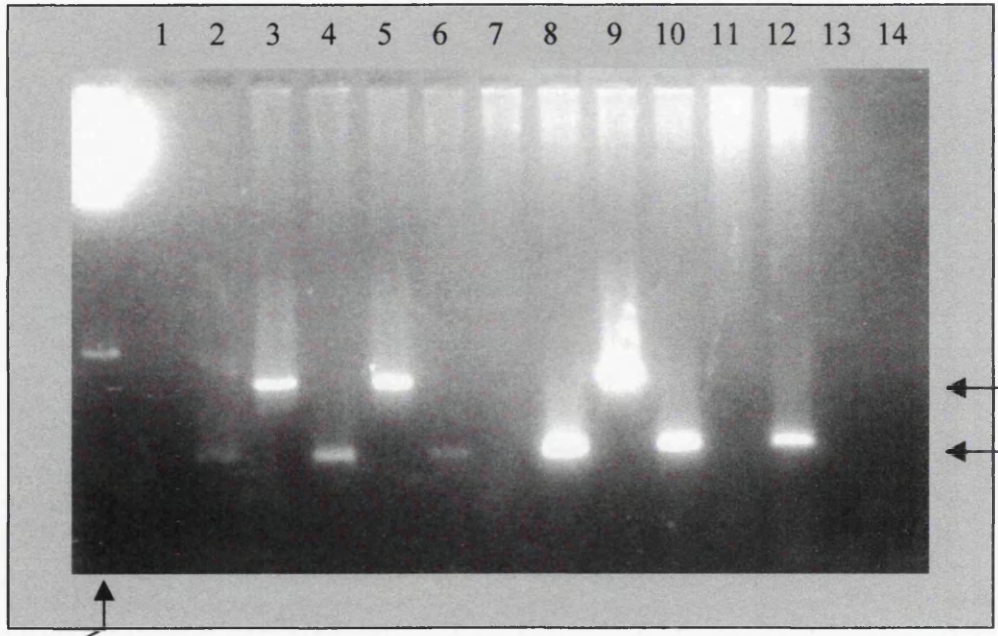

DNA	Knockout allele	Wildtype allele
T1	1	2
P/T50	3	4
P/T 54	5	6
*$p53^{+/+}$	7	8
*$p53^{+/-}$	9	10
*$p53^{-/-}$	11	12
*water	13	14
* controls		

Figure 5.5: p53 Southern blot of mesenchymal tumours (p/t 125, p/t 54, p/t 50) and p/t 50 cell line

Photograph of a Southern blot demonstrating p53 allele genotyping of the p53/tax mesenchymal tumours or p53/tax derived cell lines. Lane 1 refers to the PhiX molecular weight DNA ladder. Lanes 2, 3, and 4 refer to the p/t 125, p/t 54, and p/t 50 mesenchymal tumours respectively. Lanes 5 and 6 refer to the p/t 50 and p/t 50-2 cell lines respectively. The p53 pseudogene, p53 knock out allele and p53 wild type allele are marked.

Figure 5.5: p53 Southern blot of mesenchymal tumours (p/t 125, p/t 54, p/t 50) and p/t 50 cell line

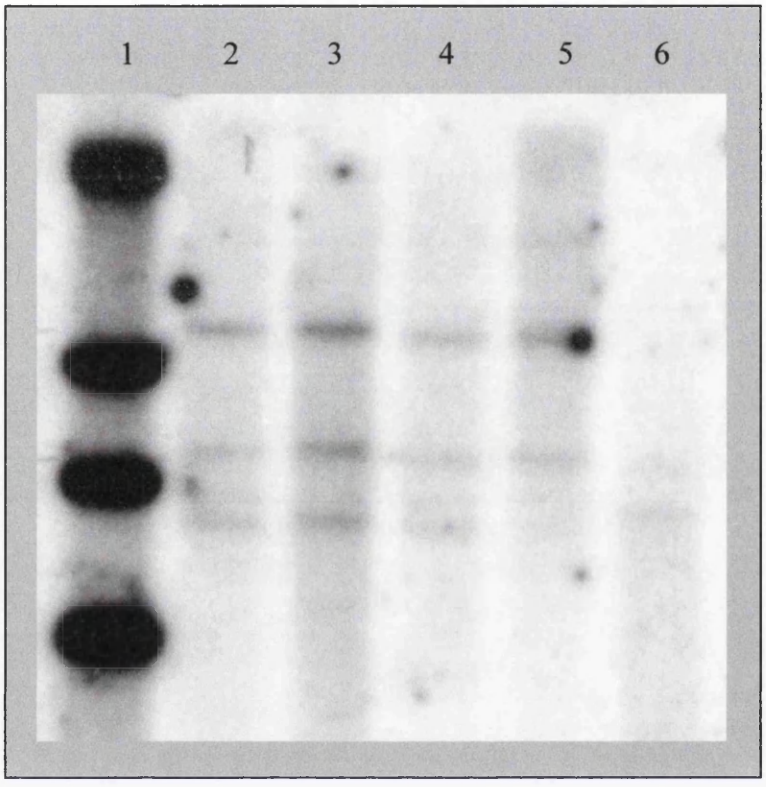

1	PhiX Molecular Weight Marker
2	p/t 125 tumour
3	p/t 54 tumour
4	p/t 50 tumour
5	p/t 50 cell line
6	nude p/t 50-2 cell line

Southern blot demonstrating the presence of both wild type and knockout p53 alleles retained within the p/t series of mesenchymal tumours (Lanes 2, 3, and 4). Cell line p/t 50 (Lane 5) has lost the wild type p53 allele but retains the knockout allele. Cell line nude p/t 50-2 (Lane 6) derived from cell line p/t 50 after transplantation into nude mice shows a weak p53 knockout allele and rearrangement to yield a weak band of similar size to the p53 wild type allele.

Transplantation of $5x10^6$ cells from each cell line (p/t 50, p/t 54 and T1) into nude mice resulted in the generation of tumours in only those mice which were injected with the p/t 50 cells (Table 5.3). These tumours grew rapidly to a diameter of 1-2cm (Figure 5.6) within 2-3 weeks of transplantation confirming that the p/t 50 cell line was fully transformed (whereas the failure of the other cell lines to establish in nude mice indicated that these cell lines are merely immortalised).

Table 5.3: Growth of transplanted cell lines in nude mice

Cell Line	Tumour Development	Latency
P/t 50	3/3	2-3 weeks
P/t 54	0/3	sacrificed after 3 months
T 1	0/3	sacrificed after 3 months

Table summarising the malignant potential (judged by the transplantability of tumour cell lines into nude mice) and latency of tumour production for cell lines P/t 50, P/t 54, and T1. The cell line reference P/t is taken from the parental P/t transgenic mouse from which the tumour cell line was derived.

5.3.6 Analysis of gene expression within the transplanted tumours

Histologically these tumours were unlike the original p/t 50 tumours being composed of a bland sheet of spindle cells unaccompanied by any inflammatory infiltrate (Figure 5.7). Mitoses and apoptotic bodies were frequently observed (Figure 5.7 and 5.8) scattered randomly as individual cells throughout the substance of the tumour (in a similar pattern to the original p/t 50 tumour). As for p/t 50, oncoprotein (Tax, Myc, Fos, and Jun) and p53 tumour suppressor protein expression could not be detected immunocytochemically (although again *tax* RNA was detected by Northern analysis from these tumours and cell lines derived from these tumours).

Figure 5.6: Photograph illustrating the growth of p/t 50 cells transplanted into a nude mouse.

Photograph of a nude mouse bearing a malignant tumour induced by transplantation of the p/t 50 cell line.

Figure 5.6: Photograph illustrating the growth of p/t 50 cells transplanted into a nude mouse.

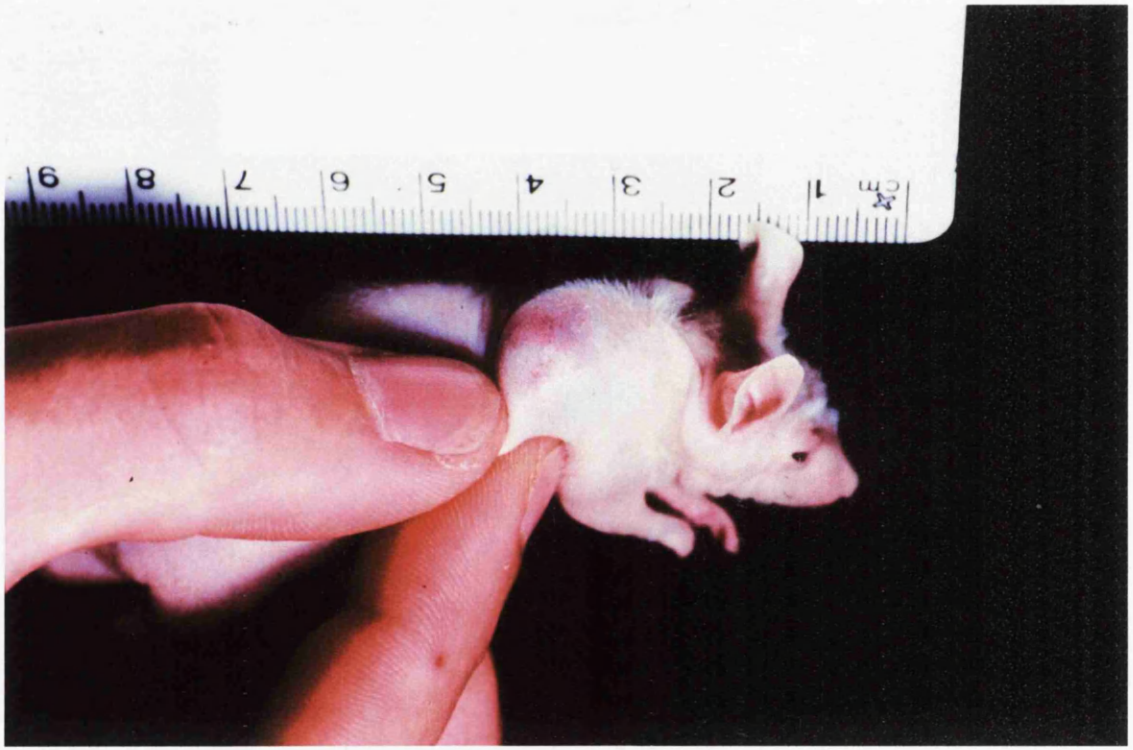

The photograph illustrates a ~1.5cm diameter mass derived from $5x10^6$ p/t 50 cells injected subcutaneously 2-3 weeks previously. Rapid growth was a feature of these tumours.

Figure 5.7: H+E photomicrographs of a transplanted tumour derived from the p/t 50 cell line.

Photograph of a tumour derived from transplantation of the p/t 50 cell line into nude mice. The upper photograph (original magnification x10) and lower photograph (original magnification x 400) illustrate the malignant nature of these tumours. Staining haematoxylin and eosin.

Figure 5.7: H+E photomicrographs of a transplanted tumour derived from the p/t 50 cell line

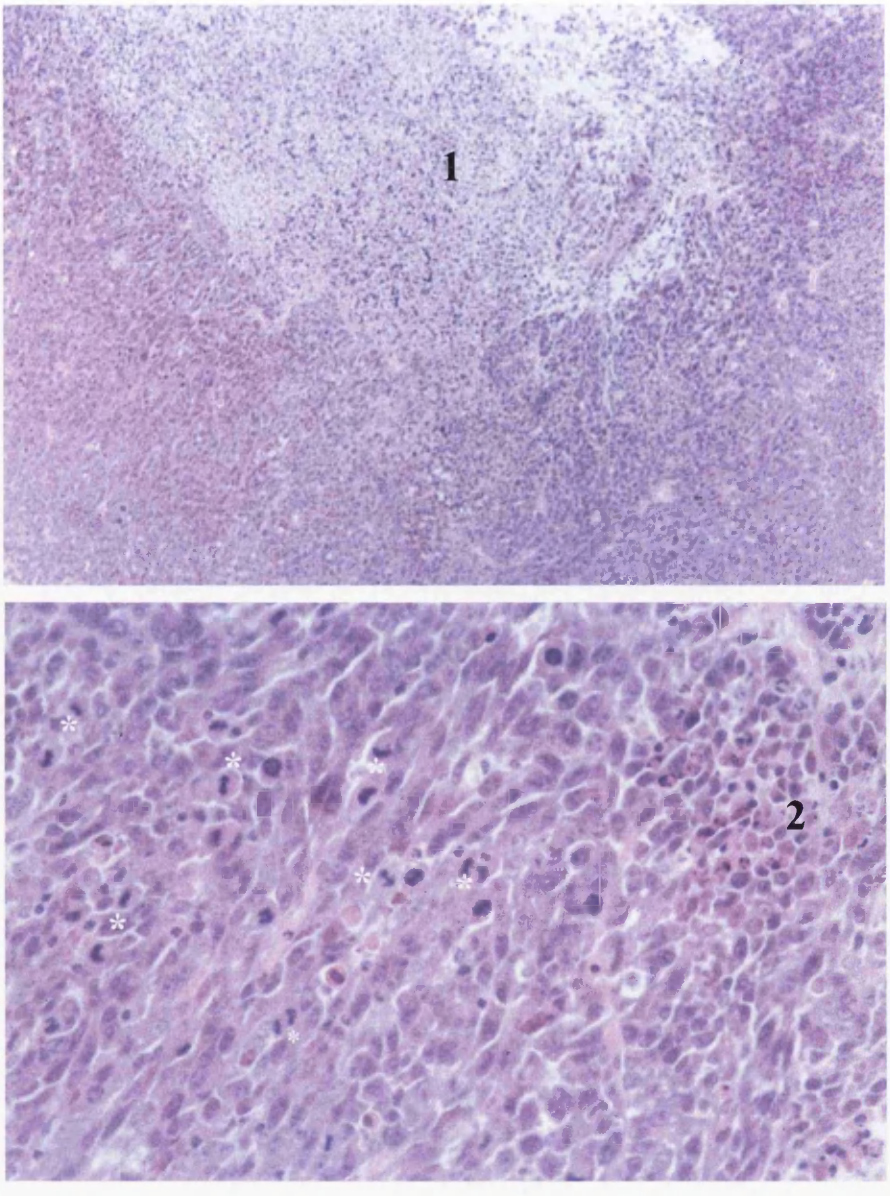

Low (upper photo: original magnification x10) and high (lower photo: original magnification x100) power photomicrographs of p/t 50 transplantable tumours growing in a nude mouse. The upper photo illustrates a large area of central necrosis whereas the lower photo illustrates the bland spindle cell population with numerous mitotic figures.

1 area of central necrosis; 2 area of apoptotic bodies * mitotic figures

Figure 5.8: Photomicrograph of apoptotic bodies stained with the TUNEL technique in the transplanted p/t 50 tumour.

Photograph of a tumour derived from transplantation of the p/t 50 cell line into nude mice. High power (original magnification x1000) demonstrating the high apoptotic rate. Stained by the TUNEL technique; counter stained with haematoxylin.

Figure 5.8: Photomicrograph of apoptotic bodies stained with the TUNEL technique in the transplanted p/t 50 tumour

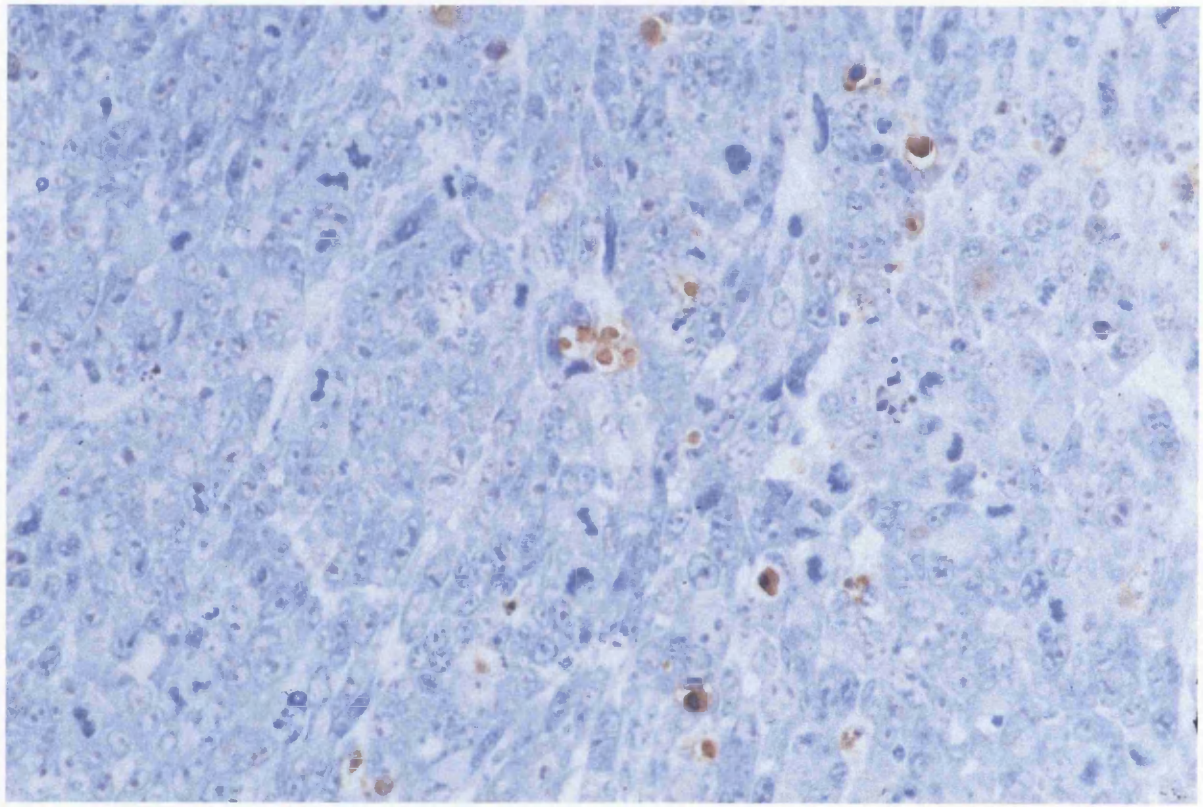

High power photomicrograph (original magnification x100) of the transplanted tumour derived from the p/t 50 cell line stained by the TUNEL technique highlighting numerous discrete apoptotic bodies. Apoptotic bodies occur in the same pattern as mitotic bodies.

5.3.7 Analysis of apoptotic and mitotic indices

In order to estimate the contribution to tumour growth imparted by the relative rates of apoptosis and mitosis we decided to estimate the numbers of mitotic figures and apoptotic bodies within TUNEL stained sections. Five random fields for each tumour were counted and averaged in order to derive the mitotic or apoptotic index. Analysis of apoptotic indices (AI) and mitotic indices (MI) revealed that although the rates of mitosis were similar between the original cohort of mesenchymal tumours/adenomas and the $p53^{+/-}$/*tax* tumours the rates of apoptosis were different (Table 5.4). The original cohort of mesenchymal tumours and adenomas had on average less than 1 mitotic figure per random high power view (indicative of a benign tumour). The p/t series of tumours also had on average less than 1 mitotic figure per random high power field view. In contrast the original group of mesenchymal tumours and adenomas had much higher levels of apoptosis compared to the p/t series of tumours. These figures indicate slower net tumour growth for the original 1300/1400 tumour series compared to the p/t series of tumours by virtue of their higher apoptotic indices consistent with the presence of large necrotic foci within the latter tumours. Finally, the transplantable tumours derived from the fully transformed p/t 50 cell line had very high mitotic and apoptotic indices indicating very rapid tumour growth with a correspondingly large area of central necrosis.

When this experiment was repeated for the original cohort of 1300/1400 series of tumours using PCNA immunocytochemical staining (performed by Ms J. McMillan) as a more accurate estimate of mitosis, the mitotic index was always greater than the apoptotic index (Table 5.5) indicating progressive tumour growth.

Table 5.4: Analysis of mitotic and apoptotic indices within each tumour type

Table summarising the mitotic index (MI) and apoptotic index (AI) for tax transgenic mouse tumours. The first column refers to the identification number assigned to the tumour at histological processing. P/T refers to tumours derived from the p53/tax transgenic mouse cross and Nu refers to tumours derived from p/t50. The mitotic index refers to the average number of mitotic cells (judged by light microscopy) at high power (x1000). The apoptotic index refers to the average number of apoptotic cells (judged by TUNEL technique) at high power (x1000).

Key: • original cohort of 1300/1400 series of mesenchymal or adenoma tumours with wild-type p53 status; ♣ $p53^{+/-}$/*tax* tumours; ♠ tumours derived from p/t 50 cell line transplanted into nude mice

Table 5.4: Analysis of mitotic and apoptotic indices within each tumour type

Tumour	Mitotic Index*(MI)	Apoptotic Index*(AI)
•93/8086-1	0.625	12.81
•93/7665-2	1.875	6.87
•93/7599-2	0	26.56
•93/1245-1	0	5.62
•93/1239-2	0.31	4.68
Average	0.940	11.308
♣P/T96/1441-4	0.31	1.875
♣P/T96/1440-5	0.31	2.18
♣P/T96/1440-4	0.31	4.68
Average	0.31	2.91
♠Nu96/4390-4	26.2	25.2
♠Nu96/4389-4	18.4	11.6
♠Nu96/4368-4	26	14.4
Average	23.53	17.06

Table 5.5: Analysis of mitotic and apoptotic index from the original cohort of 1300 and 1400 series of tumours

Tissue	Proliferation Index	Standard Deviation	Apoptotic Index	Standard Deviation
Healthy salivary and mammary tissue (4)	0	0	0.2	0.2
Mammary Adenocarcinoma (3)	118.3	21.4	8.8	0.6
Tax mammary and Salivary adenomas (8)	9.4	8.7	3.2	3.1
Tax ear and tail Tumours (5)	12.6	7.1	2.8	0.5

Table summarising the proliferation (mitotic) index (MI) and apoptotic index (AI) for *tax* transgenic mouse tumours. The numbers in brackets in the 'tissue' column refers to the total number of tumours examined. The figures in the proliferation and apoptotic index refer to the average number of cells stained with PCNA and the TUNEL technique respectively. The mammary adenocarcinomas were derived from spontaneously occurring tumours in outbred strains of mice.

5.4 Discussion

Analysis of the p53/*tax* breeding experiments revealed that the p/t series of mesenchymal tumours occurred at a reduced frequency but equivalent latency period compared to the original 1300/1400 series tumours. Macroscopically and microscopically the p/t tumours were identical to the original cohort of mesenchymal tumours. However further analysis revealed a reduced apoptotic index, which correlated with the presence of a variably sized centres within these tumours, indicating rapid tumour growth. Two cell lines (T 1 and p/t 54) derived from these tumours and propagated for 4 months in cell culture remained untransformed (non-malignant). One cell line (p/t 50) however was highly malignant and grew rapidly in tissue culture. Malignancy in the p/t 50 cell line correlated with loss of the remaining wild type allele by Southern blot analysis (although PCR analysis indicated the presence of a wild-type p53 allele in all three cell lines). The reason for the discrepancy between these results is unknown but may reflect the greater sensitivity of the PCR based assay detecting rare cells retaining the wild type allele or retention of part of the PCR exon with loss of other critical parts of the p53 gene.

The results of the p53 cross *tax* breeding experiment revealed that p53 null genotype did not co-operate with the *tax* transgene to accelerate mesenchymal or lymphoma tumour development. This is in contrast to the collaboration observed between the *c-myc* oncogene on a p53 null background (Blyth et al, 1995; Hsu et al, 1995) or bcl-2 background (McDonnell et al, 1991) which dramatically accelerated tumour development with rapid progression to high grade malignancy. Presumably the complete absence of mesenchymal tumours in this cohort resulted from the rapid development of p53 related pathology. In this scenario the latency period of *tax* related pathology is outside the life span of the p53 null mice.

Analysis of the $p53^{+/-}$/*tax* mice similarly indicated no synergy between p53 hemizygous genotype status and *tax* transgene status since the resultant mesenchymal tumours were phenotypically identical to the original cohort of tumours indicating no malignant progression. This agrees closely to that observed when CD2-*myc* mice are crossed onto a

$p53^{+/-}$ background (Dr Blyth PhD thesis) but is contrary to that observed when Eμ-*myc* or MMTV-*myc* mice are crossed onto a $p53^{+/-}$ background (Hsu et al, 1995). This may imply that for efficient co-operation, constitutive expression of the transgene is necessary since CD2-*myc* mice, like CD3-*tax* mice, only express the transgene in transformed cells. However failure of two of the three (T 1 and p/t 54) tumour derived cell lines to progress to a malignant phenotype in extended cell culture indicates that loss of the p53 wild type allele is not strongly selected for *in vitro*. In contrast, $p53^{+/-}$/CD2-*myc* cell lines rapidly lose their remaining wild type allele in cell culture (Dr Blyth PhD thesis).

Lack of p53 synergy and failure to lose the remaining wild type p53 allele in extended cell culture suggests that the loss of the p53 protein is not an important co-operating event in *tax* induced malignancy. Loss of the remaining wild type p53 allele is a common late event in human malignancy (Nigro et al, 1989; Baker et al, 1989) and tumours which develop in $p53^{+/-}$ mice (Harvey et al, 1993; Purdie et al, 1994) as well as $p53^{+/-}$/*myc* tumours (Hsu et al, 1995; Elson et al, 1995). However, retention of the wild type p53 allele in 2 of 3 $p53^{+/-}$/*tax* cell lines is consistent with other authors who failure to detect p53 mutations in naturally occurring cases of ATL (Nagai et al, 1991). Stabilisation (Reid et al, 1993) and functional inactivation of p53 (Ceresto et al, 1996; Gartenhaus et al, 1995) presumably substitute for p53 loss *in vivo*. Furthermore, inactivation of the cdki, $p16^{INK4A}$, probably serves to induce cell cycling (and inhibit senescence) - a function also served by p53 inactivation (Hsu et al, 1995).

The low frequency of tumours observed in the p/t series of mice (16% overall) most probably reflects increasing DNA methylation of the transgene over successive generations of mice (Allen et al, 1990) – an effect which is most apparent when multiple copies of the transgene are present within the genome (Garrick et al, 1998). This is consistent with the observed loss of the *tax* phenotype in later generations of 1200, 1300, and 1400 mice as well as the *tax* cross p53 mice..

Analysis of the p/t series of mesenchymal tumours clearly showed an alternative form of apoptosis compared to the original 1300/1400 tumours, as evidenced by the pattern (no

foci) and frequency of apoptosis, and the absence of concomitant oncogene expression. This alternative pattern was not associated with high level Tax expression *per se* since Tax could not be detected immunocytochemically within any of these tumours. It is more likely that this pattern represents background or spontaneous apoptosis associated with cycling cells, occurring in the absence of p53 or oncoprotein expression. This is consistent with *in vitro* models of tumourigenesis (Evan et al, 1992) in which conflicting environmental cues (typically growth factor deprivation for cultured cells; anoxia in *c-myc* induced transgenic mouse tumours [Alarcon et al, 1996]) readily induce apoptosis in cycling cells. Indeed the higher levels of apoptosis within the transplanted tumours, may be a direct consequence of the elevated mitotic rate seen in theses tumours [although the contribution of other apoptotic inducers activated by secondary mutations acquired during *in vitro* passage and *in vivo* selection cannot be determined].

Loss of a major (Tax associated) apoptotic pathway within the $p53^{+/-}$/*tax* tumours resulted in lower apoptotic indices compared to the original cohort of tumours. Consistent with this observation were the frequently noted areas of necrosis occurring within the centre of these tumours indicative of a rapidly growing neoplasm outstripping its blood supply. The 1200, 1300 and 1400 tumours never exhibited central necrosis consistent with a slower growth rate due to retention of both apoptotic pathways (i.e. background apoptosis upon which is superimposed the major Tax associated pattern of apoptosis). Background apoptosis within the original tumours was evident as rare cells undergoing apoptosis without concomitant Tax expression (Figure 4.8 arrows) in dual stained sections.

The reason for the absence of Tax associated apoptosis within the p/t tumours is unknown although progressive epigenetic down-regulation (methylation) of transgene expression may alter the tumour phenotype. In this model of tumourigenesis low level *tax* expression is sufficient to induce proliferation but not apoptosis i.e. the p/t cohort of tumours display the spontaneous background pattern of *tax* expression noted for the original 1300/1400 series of tumours. Clearly low-level expression of Tax must promote tumourigenesis as well as dissemination of virally infected lymphocytes in HTLV-I infected patients. Furthermore, evidence supporting the dual role of *tax* is just emerging. Low

concentrations of Tax (10pM [Marriott et al, 1991]) effectively induces proliferation in human lymphocytes whereas expression of *tax* under certain circumstances may repress apoptosis (Brauweiler et al, 1997; Kishi et al, 1997; Schwartz-Cornil et al, 1997). Thus the pharmacological effects of *tax* demonstrated and established *in vitro* may not necessarily reflect the consequences of normal *tax* expression from the HTLV-I viral promoter *in vivo*.

Chapter 6

Generation of a modified Tax expression system

Generation of an inducible *tax* expression system

6.1 Introduction

The HTLV-I *tax* oncogene transforms both rodent fibroblasts (Tanaka et al, 1990) and human T-cells (Grassman et al, 1989 and 1992) in culture as well as inducing tumours in HTLV-I *tax* transgenic mice (Ozden et al, 1996). The mechanism through which *tax* achieves this effect is still unclear although key functional domains have been implicated as likely oncogenic determinants. The most important of these domains are those which allow protein-protein interactions with the transcription factors NF-κB, CREB/ATF, and the SRF, as well as the cyclic dependent kinase inhibitor (cdki), $p16^{INK4a}$.

The NF-κB transcription factor has recently been implicated in the suppression of apoptosis in T-cells (Beg et al, 1996; Wang et al, 1996; Van Antwerp et al, 1996; and Liu et al, 1996) and appears essential to mediate the tumourigenic effects of *tax* (Kitajima et al, 1992; Yamaoka et al, 1996). However other authors have found that the CREB/ATF transcription factors, necessary for transcriptional transactivation of the HTLV-I LTR (Beimling et al, 1992; Zhao et al, 1992, Franklin et al, 1993), are also essential for transformation (Smith and Greene, 1991). This discrepancy highlights the equivocal role that each of these factors independently contribute towards the transformed phenotype. The generation of *tax* mutants, which segregate the CREB/ATF and NF-κB pathways, (Smith and Greene, 1991; Semmes and Jeang, 1992; Yamaoka et al, 1996) has demonstrated that the events leading to transformation are highly complex. In rodent fibroblasts, both the CREB/ATF and NF-κB domains have been shown to be independently necessary and sufficient for transformation (Smith and Greene, 1991; Yamaoka et al, 1996). Complementation by the alternative phenotype does not appear to be necessary since both *tax* mutants (CREB/ATF^+/NF-$κB^-$ [Smith and Greene, 1991] and NF-$κB^+$/CREB/ATF^- [Yamaoka et al, 1996]) transform rodent fibroblasts. Furthermore, the recent demonstration that a variant of *tax*, incapable of activating NF-κB can immortalise primary human T cells (Rosin et al, 1998) has further obscured the resolution to this paradox.

Additionally the SRF (Suzuki et al, 1993b; Fujii et al, 1995) and the cdki, $p16^{INK4a}$ (and other family members) (Low et al, 1997; Suzuki et al, 1996) have also been suggested to contribute to the oncogenic effects of *tax*. The role that $p16^{INK4a}$, and other family members play in the development of ATL is well-established (Hatta et al, 1995; Suzuki et al, 1997) suggesting that the importance of the Tax NF-κB binding domain may relate to the requirement of Tax to bind both IκB and $p16^{INK4a}$ through their common repeated ankrin motifs (Yoshida et al, 1997).

The generation of inducible vectors has provided a valuable tool to dissect gene function. Historically, a number of inducible systems have been developed in an attempt to generate high level expression with little background induction. Many of these relied upon induction by hormones (oestrogens), antibiotics (tetracycline) or heavy metal ions (metallothionin) and suffered from a number of drawbacks – most notably poorly regulated expression. The second generation of inducible vectors offered high level expression (Littlewood et al, 1995; Yoshida et al, 1997; Biebinger et al, 1997; Massie et al, 1998). The modified oestrogen receptor system offered an advantage in that the oestrogen analogue, 4-hydroxy tamoxifen, tightly regulated background induction, since the MER was unresponsive to natural oestrogens present *in vivo* and in tissue culture media (Littlewood et al, 1995). Fusion of the MER in frame with any gene, particularly transcription factors such as *c-myc*, *c-fos*, *tax* and p53 provided a simple switch (Littlewood et al, 1995; Preston et al, 1996; Vater et al, 1996; Chlichlia et al, 1995). The resulting fusion protein was constitutively expressed, but sequestered with heat shock proteins as an inactive complex within the cytoplasm. The addition of 100nm tamoxifen induced a conformational change in the fusion product allowing translocation of the active protein to the nucleus (Littlewood et al, 1995).

6.2 Aims of the experiment

In order to investigate the role that the various domains of Tax contributed towards the transformed phenotype *in vitro*, we decided to generate an inducible *tax* vector and mutants thereof (based on published data) which efficiently segregated the CREB/ATF and NF-κB

domains. The use of an inducible *tax* vector would not only provide a more refined way to investigate the importance of each functional domain, but would also allow more flexibility with other downstream experiments.

6.3 Results

6.3.1 Generation of the inducible *tax* retroviral vector

Three inducible *tax* constructs were generated by fusing *tax* in frame with either a 5' MER, a 3' MER or a 5'/3' double MER (as described in chapter 2: *Materials and methods* and Figure 6.1). Restriction enzyme digests were performed to validate the orientation and fidelity of the sub-cloning steps (Figure 6.2). Additionally, each construct was sequenced to ensure accuracy of the PCR-cloning step using the 'in house' licor automated gene sequencer.

Figure 6.1: Schematic diagram summarising the cloning steps involved in the generation of the Tax-MER fusion construct.

Step 1: The 5' portion of tax was pcr amplified with primers which maintained the Bam HI/Sma I restriction site. The pcr product was then ligated into the TA cloning vector, 'pcr II'.

Step 2: The 3' portion of tax was pcr amplified with primers which removed the stop codon (tga→tgg), shifted the open reading frame to that of the MER, and introduced appropriate restriction sites (Sma I/ Bam HI). The pcr product was then ligated into the TA cloning vector for subsequent fusion with the MER.

Step 3: The 5' and 3' portions were ligated to generate the full-length *tax* molecule and subcloned into the pBabe retroviral vector.

Step 4: the MER molecule was then ligated in frame with the tax molecule.

Figure 6.1: Schematic diagram summarising the cloning steps involved in the generation of the Tax-MER fusion construct

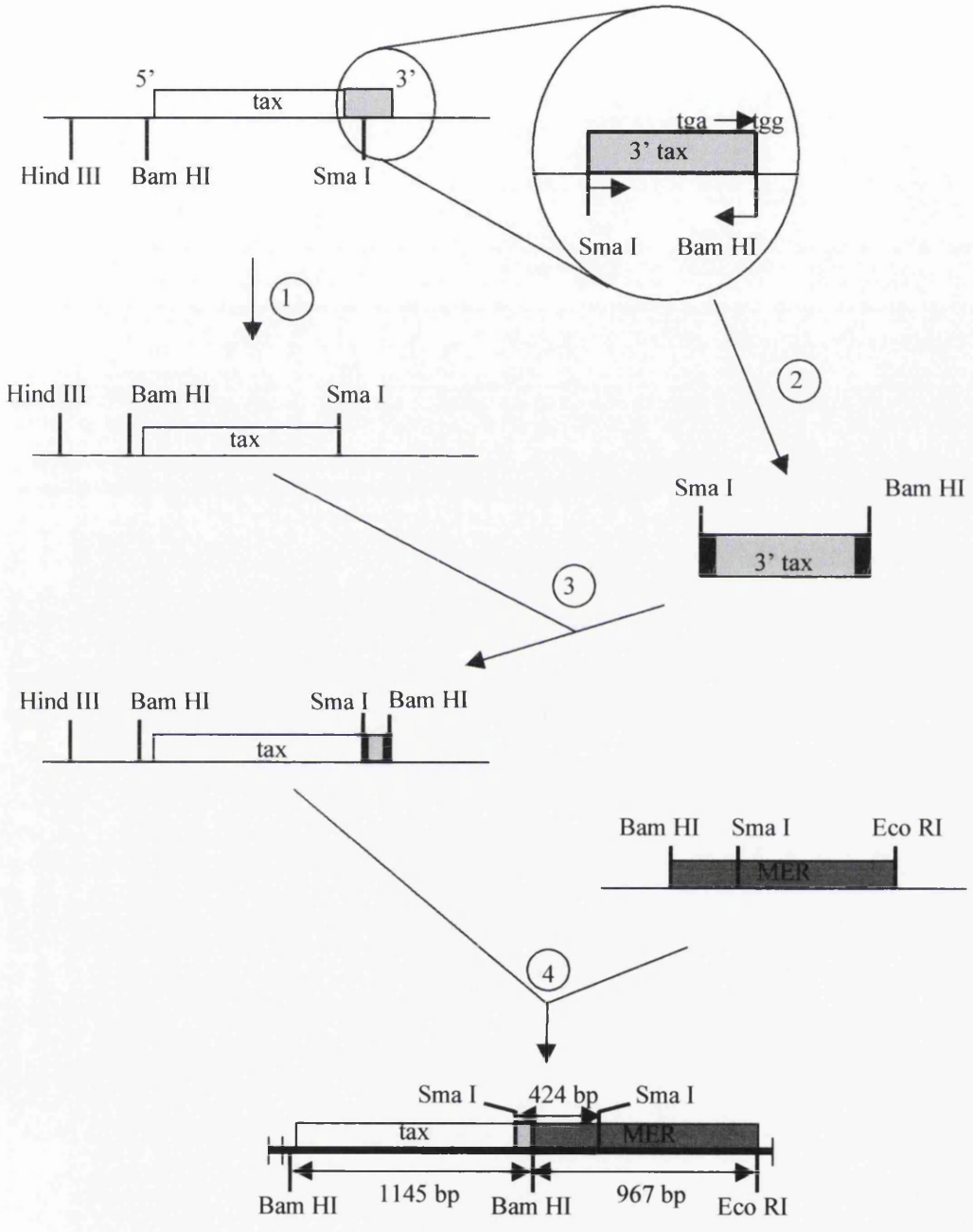

Figure 6.2: Diagnostic digests of Tax-MER fusion construct

The top figure represents the predicted restriction fragments based on the DNA sequence of the pBabe-Tax-MER construct.

The bottom figure is a photograph of the restriction fragments produced by digestion of the pBabe-Tax-MER plasmid with Sma I (lane 1), Bam HI (lane 2), Bsp EI (lane3). Lane 4 is the parental undigested pBabe-Tax-MER plasmid. The fragment sizes were calculated relative to the reference 1kb DNA molecular weight ladder as indicated on the photograph. Correct sized fragments at 424bp (Lane 1) and 1145bp and 967bp (Lane 2) were generated indicating fidelity of the subcloning steps. The wild type tax molecule does not contain a Bsp EI restriction site (Lane 3).

Figure 6.2: Diagnostic digests of Tax-MER fusion construct

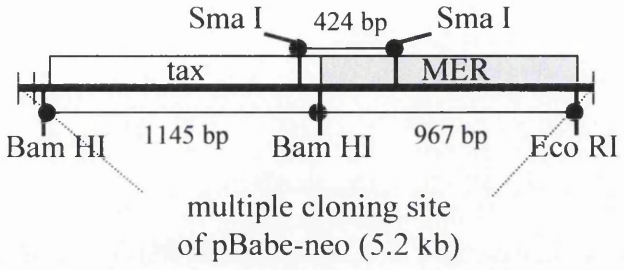

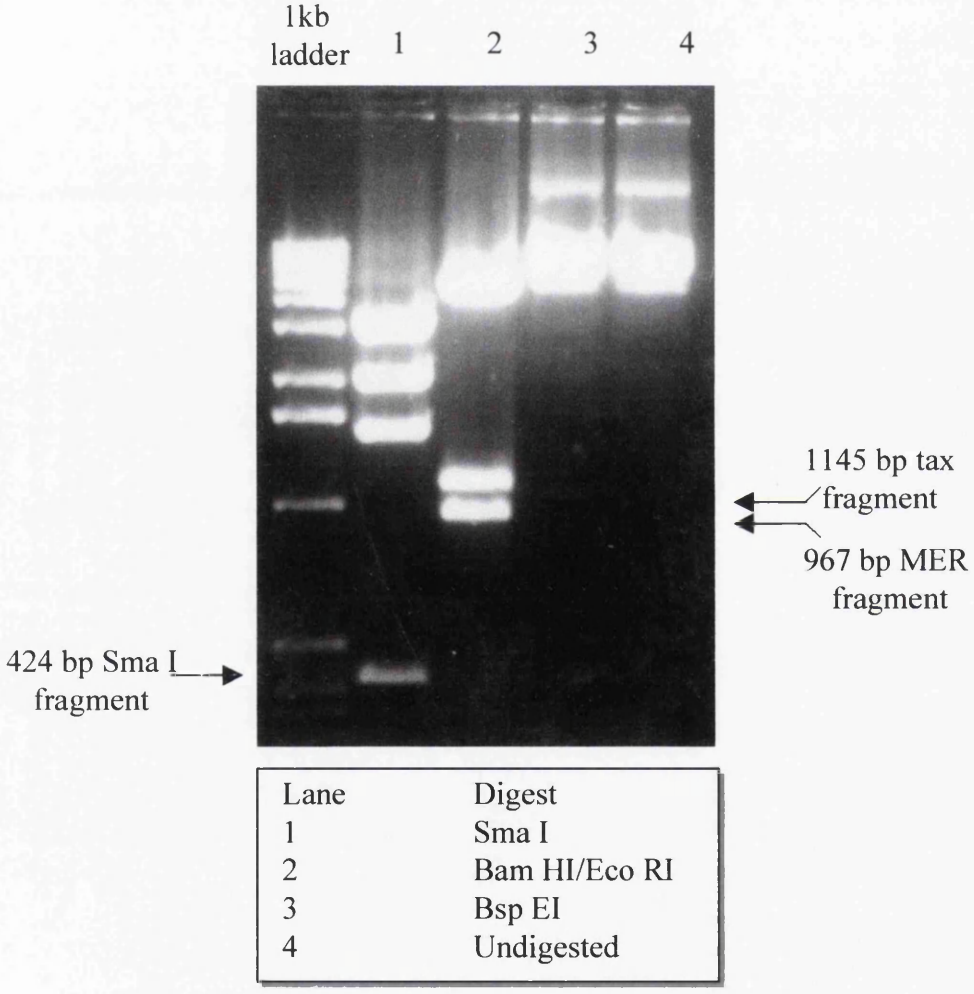

Lane	Digest
1	Sma I
2	Bam HI/Eco RI
3	Bsp EI
4	Undigested

6.3.2 Demonstration of expression and inducibility of the Tax-MER/tamoxifen system

6.3.2.1 Optimisation of transient CAT assays

A transient CAT assay was chosen as the method of choice to measure functional protein expression from each of the inducible *tax* constructs. This was achieved using reporter gene plasmids which were upregulated through each of the functional domains of Tax (i.e. CREB/ATF responsive (HTLV-I LTR), NF-κB responsive (HIV-I LTR), and SRE responsive (c-fos upstream element) CAT constructs). Initially a transient transfection assay system using BHK cells and a β-gal/*tax* reporter assay system was optimised. Our results indicated that 5μg of *tax* DNA with 2.5μg of carrier DNA (ratio 2:1), 8% modified bovine foetal serum, and 80,000 cells per 35mm dish (lane 4 Figure 6.3) provided optimal transfection conditions. The use of a fluorescent substrate (1-deoxy-CAM) with only one acetylation site was chosen as this produced only one reaction product with greater reaction linearity.

Figure 6.3: Photographs illustrating optimisation of transient transfections

Optimisation of the transient transfection system. Lanes 1 and 2 represent 10μg of *tax* DNA with 5μg of $LTR^{HTLV\text{-}1\text{-}CAT}$ DNA and 55,000 or 80,000 cells per petri dish respectively. Lanes 3 and 4 represent 5μg of *tax* DNA with 2.5μg of $LTR^{HTLV\text{-}1\text{-}CAT}$ DNA and 55,000 or 80,000 cells per petri dish respectively. Lanes 5 and 6 represent 2.5μg of *tax* DNA with 1.25μg of $LTR^{HTLV\text{-}1\text{-}CAT}$ DNA and 55,000 or 80,000 cells per petri dish respectively. Lane 7 represents acetylation of 1-deoxy-CAM with 0.5μL of CAT enzyme control. Lane 8 represents 5μL of acetylated reference standard.

Optimal transfection efficiency with BHK cells occurred using 5μm of *tax* DNA, 2.5μg of reporter plasmid (2:1 ratio) DNA. Signal detection was maximised using 80,000 BHK cells per culture dish (30μg of protein). The use of a non-radioactive substrate (1-deoxy-CAM) with only a single acetylation site produced only one reaction product with greater reaction linearity.

Figure 6.3: Photographs illustrating optimisation of transient transfections

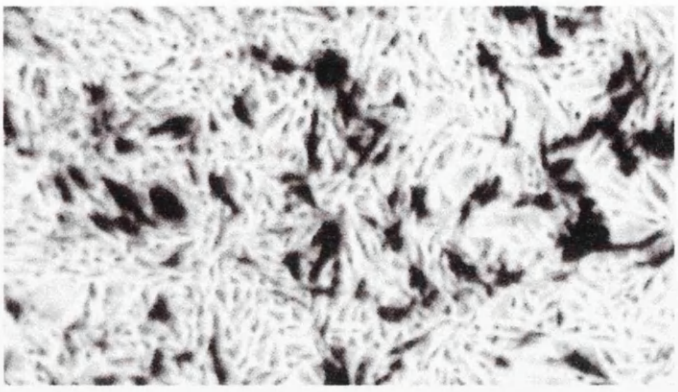

Transient transfection of a beta-gal reporter construct into BHK cells followed by histochemical staining 24 hours after transfection.

1 2 3 4 5 6 7 8

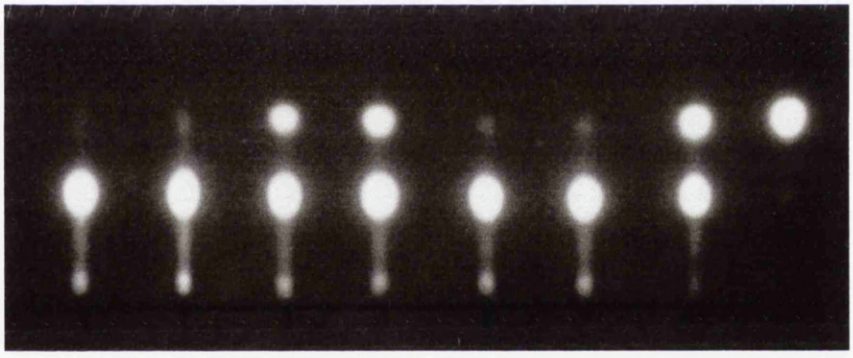

Lane	Transfection	
1	10ug tax; 5ug LTR-cat;	55,000 cells per dish
2	10ug tax; 5ug LTR-cat;	80,000 cells per dish
3	5ug tax; 2.5ug LTR-cat;	55,000 cells per dish
4	5ug tax; 2.5ug LTR-cat;	80,000 cells per dish
5	2.5ug tax; 1.25ug LTR-cat;	55,000 cells per dish
6	2.5ug tax; 1.25ug LTR-cat;	80,000 cells per dish
7	0.5uL cat enzyme positive control	
8	5uL acetylated reference standard	

6.3.2.2 Functional transactivation of reporter plasmids

Functional activity of the inducible fusion constructs was investigated using this system by measuring transactivation of the LTR^{HTLV-I}-CAT (CREB/ATF responsive) and LTR^{HIV-I}-CAT (NF-κB responsive) reporter plasmids relative to wild type *tax* (Tax^{GlaWT}). Our results (Table 6.1) indicated that transactivation of the LTR^{HTLV-I}-CAT (CREB/ATF) reporter plasmid by *tax* is efficient. However transactivation of the LTR^{HIV-I}-CAT (NF-κB) using this system was inefficient. Background induction matched that induced by *tax*. These results were similarly repeated using the adenovirus major late promoter-CAT reporter construct which contains three repeated NF-κB responsive motifs. These results were also confirmed later using the inducible mutants of *tax* (M47, M1 and C23S) and also an external wild type *tax* (IEX-Tax) [a gift from Dr KT Jeang, NIAID Bethseda, USA] [described later].

Table 6.1: Transactivation of the LTR^{HTLV-I}-CAT (CREB/ATF) and LTR^{HIV-I}–CAT (NF-κB) reporter plasmids by wild type *tax* (Tax^{GlaWT})

	CREB/ATF % acetylation	ST Dev	Fold Induction
$Tax^{Gla\ WT}$	37.4	11.1	2.4
LTR^{HTLV-I}/pBabe	15.31	6.3	*1
	NF-κB		
	% acetylation	**ST Dev**	**Fold Induction**
$Tax^{Gla\ WT}$	12.59	6.9	0.93
LTR^{HIV-I} /pBabe	13.51	7.66	*1

The % acetylation and all subsequent results were the average of at least 3 separate experiments performed on different days.
*Results normalised to 1

Table summarising percentage acetylation of CREB/ATF or NF-κB CAT reporter constructs with Tax^{GlaWT} and LTR-pBabe plasmids. The figures refer to percentage acetylation of 1-deoxy-CAM, standard deviation, and fold induction relative to the LTR-pBabe construct.

6.3.2.3 Transactivation of the SRE

In order to assess transcriptional upregulation of the SRE through the third critical domain of *tax* we decided to measure CAT activity from a number of *c-fos* promoter mutants (a gift from Dr G. Birrie, Beatson Institute, Glasgow, UK) which segregated the important upstream regulatory elements governing *c-fos* transcription (Figure 6.4). The results indicated (Table 6.2 and Figure 6.5) that *tax* transactivated c-fos-1, c-fos-2 and c-fos-5-CAT reporter constructs most efficiently (~1.6-1.7 fold). These constructs each contained the minimal promoter elements (DRE and CRE the latter containing a CREB responsive element). Presence of the SRE and or the ATF element did not further upregulate CAT activity. Tax transactivated the c-fos-3 and c-fos-7 construct least efficiently (~1.2-1.3 fold). Since these constructs contain both the minimal promoter element plus the SRE element, reduced CAT activity indicated inhibition through the SRE. The presence of additional elements such as the SIE and ATF served only to increase transactivation by *tax* with a concomitant proportional increase in background transactivation.

Figure 6.4: Schematic diagram illustrating the various *c-fos* promoter mutant constructs.

The c-fos upstream promoter region contains at least 5 regulatory promoter elements (Alexandre and Verrier, 1991): v-sis conditioned medium inducible element (SIE), the serum response element (SRE), the activating transcription factor/activating protein element (ATF/AP1), the octanucleotide direct repeat element (DRE), and the cyclic AMP response element (CRE). Tax is able to transactivate the c-fos promoter through each of these elements (Alexandre and Verrier, 1991). Five promoter mutant reporter constructs were used to dissect the c-fos promoter: c-fos-2 (the minimal promoter region), c-fos-7 (the full upstream region), and c-fos-3 and c-fos-5 which segregate the SRE and ATF1/AP1 sites.

Figure 6.4: Schematic diagram illustrating the various *c-fos* promoter mutant constructs.

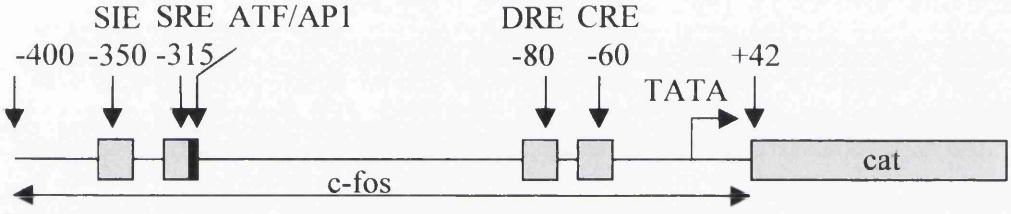

SIE	v-sis conditioned medium inducible element
SRE	serum response element
DRE	direct repeat element
ATF/AP1	activating transcription factor/activating protein
CRE	cyclic AMP response element

c-fos-1	DRE+CRE+SRE+ATF/AP1
c-fos-2	DRE+CRE
c-fos-3	DRE+CRE+SRE
c-fos-5	DRE+CRE+ATF/AP1
c-fos-7	DRE+CRE+SRE+ATF/AP1+SIE

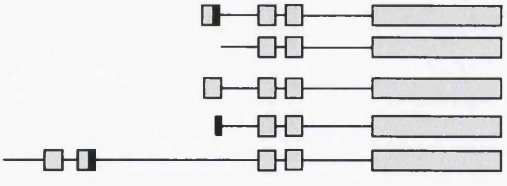

Table 6.2: Transactivation of the c-fos-CAT reporter plasmids by wild type *tax* (Tax^{GlaWT})

	$Tax^{Gla\ WT}$ % acetylation	ST Dev	Background % acetylation	ST Dev	Fold Induction
Fos-1	18.2	6.8	10.6	2.4	1.7
Fos-2	30.0	9.1	19.3	9.4	1.6
Fos-3	20.3	2.4	16.7	7.4	1.2
Fos-5	25.5	6.7	15.9	5.5	1.6
Fos-7	30.2	10.5	22.7	9.7	1.3

Table summarising the percentage acetylation of the various c-fos-CAT reporter plasmids by wild type tax (Tax^{GlaWT}) with and without tamoxifen induction. The figures refer to percentage acetylation of 1-deoxy-Cam, standard deviation, and fold induction relative to background induction normalised to 1.

Figure 6.5: Transactivation of the various c-fos promoter mutant reporter plasmids by the pBabe-*tax* construct.

Photograph of transactivation of the various *c-fos* promoter regions by wild type Tax. Lanes 1, 3, 5, 7, and 9 represent induction of *c-fos* 1, 2, 3, 5 and 7 plasmids by wild type Tax respectively with the addition of tamoxifen. Lanes 2, 4, 6, 8, and 10 represent induction of c-fos 1, 2, 3, 5 and 7 plasmids by wild type Tax respectively without the addition of tamoxifen. Lane 11 represents 5μL of acetylated 1-deoxy-CAM reference standard.

Figure 6.5: Transactivation of the various c-fos promoter mutant reporter plasmids by the pBabe-*tax* construct.

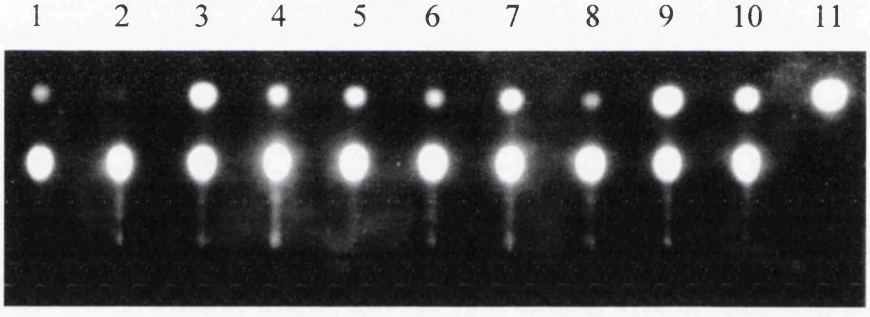

Lane	Construct	Lane	Construct
1	pBabe-Tax c-fos-1	2	pBabe-ER c-fos-1
3	pBabe-Tax c-fos-2	4	pBabe-ER c-fos-2
5	pBabe-Tax c-fos-3	6	pBabe-ER c-fos-3
7	pBabe-Tax c-fos-5	8	pBabe-ER c-fos-5
9	pBabe-Tax c-fos-7	10	pBabe-ER c-fos-7

Transient transactivation of the c-fos promoter mutant reporter plasmids by Tax. Maximal expression occurs with c-fos-7 (full upstream regulatory region) although background induction is also high. Constructs c-fos-2, -3, and 5 give greatest induction relative to background. The principal elements upregulated by tax are the CRE and ATF/AP1 sites (c-fos-5). However tax can also upregulate expression through the SRE and the minimal DRE/CRE elements.

6.3.2.4 Tamoxifen induction of Tax activity

Functional inducibility of the Tax-MER construct was then assayed using LTR^{HTLV-I}-CAT reporter plasmid in a transient transfection assay together with (and without) induction by 4-hydroxy-tamoxifen (Figure 6.6). These results indicated that Tax-MER upregulated transcription from the LTR^{HTLV-I}-CAT construct demonstrating the synthesis of a functional fusion protein, which was actively sequestered in the cytoplasm. Induction by tamoxifen over a range of concentrations (100-1000nm) [optimal 4-hydoxy-tamoxifen concentration of 500nm] demonstrated functional activation of the Tax protein and translocation to the nucleus.

Figure 6.6: Tamoxifen induction of the LTR^{HTLV-I}-CAT (CREB/ATF) and LTR^{HIV-I}-CAT (NF-κB) reporter constructs by the tax-MER fusion construct.

Photograph of transactivation of the LTR^{HTLV-I}-CAT and LTR^{HIV-I}-CAT reporter plasmids by the wild type tax-ER fusion construct. Lanes 1-6 represent transactivation of LTR^{HTLV-I}-cat by the wild type tax-MER fusion construct with 0, 100, 500, 1000, 2500, and 10000nm tamoxifen. Lanes 7 and 8 represent transactivation of LTR^{HIV-I}-CAT by the wild type tax-MER fusion construct with 0 and 500nm tamoxifen. Lanes 9 and 10 represent transactivation of the LTR^{HTLV-I}-CAT and LTR^{HIV-I}-CAT reporter plasmids by PIC (negative control) with no tamoxifen. Lane 12 represents 5uL acetylated reference standard.

Figure 6.6: Tamoxifen induction of the LTR^{HTLV-I}-CAT (CREB/ATF) and LTR^{HIV-I}-CAT (NF-κB) reporter constructs by the tax-ER fusion construct.

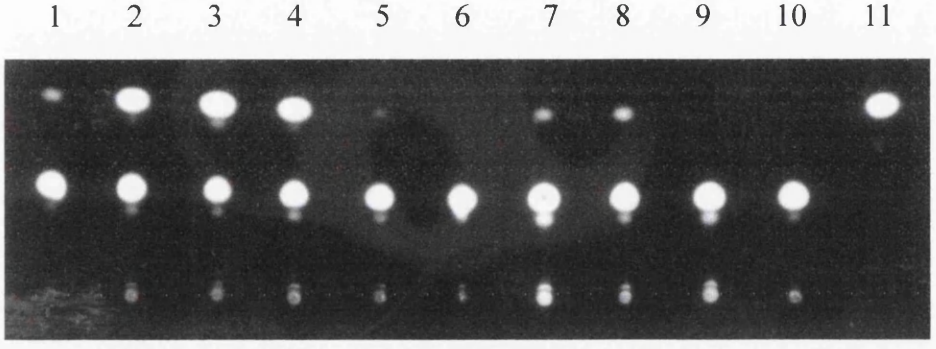

Lane	Transfection	
1	pBabe-Tax-MER LTR^{HTLV-I}-cat	no tamoxifen
2	pBabe-Tax-MER LTR^{HTLV-I}-cat	100nm tamoxifen
3	pBabe-Tax-MER LTR^{HTLV-I}-cat	500nm tamoxifen
4	pBabe-Tax-MER LTR^{HTLV-I}-cat,	1000nm tamoxifen
5	pBabe-Tax-MER LTR^{HTLV-I}-cat	2500nm tamoxifen
6	pBabe-Tax-MER LTR^{HTLV-I}-cat	10,000nm tamoxifen
7	pBabe-Tax-MER LTR^{HIV-I}-cat	no tamoxifen
8	pBabe-Tax-MER LTR^{HIV-I}-cat	500nm tamoxifen
9	PIC LTR^{HTLV-I}-cat	no tamoxifen
10	PIC LTR^{HIV-I}-cat	no tamoxifen
11	5uL acetylated reference standard	

Tamoxifen induction of the Tax-MER fusion construct: lane 1 and 7 illustrate background induction without tamoxifen; lanes 2-4 demonstrate strong induction of the using the LTR^{HTLV-I}-cat (CREB/ATF) reporter construct; lane 8 demonstrates weak induction of the LTR $^{HIV-I}$-cat construct; lanes 9 and 10 demonstrate low cat activity in the absence of *tax*.

6.3.2.5 Analysis of each of the inducible pBabe-Tax-MER fusion constructs

Comparative analysis of each of the Tax-MER fusion constructs [Tax-MER, MER-Tax and MER-Tax-MER] with the LTR^{HTLV-I}-CAT reporter plasmid demonstrated that maximal expression occurred from the 3' Tax-MER construct [2.6 fold induction] (Figure 6.7 and Table 6.3). This figure compared favourably to that obtained from experiments using a constitutively expressed pBabe-Tax construct [2.4 fold]. Both the 5' MER-tax and the 5'3' double MER-Tax-MER constructs showed reduced activity compared to the 3' Tax-MER construct (1.3 and 1.4 fold induction respectively).

Background induction of the fusion constructs was tightly controlled. Those constructs with a 5' MER demonstrated no appreciable CAT activity (relative to background) without tamoxifen induction (1 fold [MER-Tax] and 0.8 fold [MER-tax-MER] induction). The Tax-MER construct demonstrated some unregulated activity (relative to [pBabe-MER] background) without tamoxifen induction (1.5 fold induction).

Figure 6.7: Tamoxifen induction of the LTR^{HTLV-I}-CAT reporter construct using the Tax-MER, MER-Tax, and MER-Tax-MER fusion constructs.

Tamoxifen induction of the LTR^{HTLV-I}-CAT reporter plasmid with the various inducible pBabe-Tax fusion constructs. Lanes 1, 2, 3, 5 and 7 represent induction of the LTR^{HTLV-I}-CAT reporter construct with the addition of 500nm tamoxifen by pBabe-MER, pBabe-Tax, pBabe-MER-Tax, pBabe-Tax-MER, and pBabe-MER-Tax-MER respectively. Lanes 4, 6, and 8 represent induction of the LTR^{HTLV-I}-CAT reporter construct without tamoxifen addition by pBabe-MER-Tax, pBabe-Tax-MER and pBabe-MER-Tax-MER respectively. Lane 9 represents 5μL of acetylated reference standard.

Figure 6.7: Tamoxifen induction of the LTR^{HTLV-I}-CAT reporter construct using the Tax-MER, MER-Tax, and MER-Tax-MER fusion constructs.

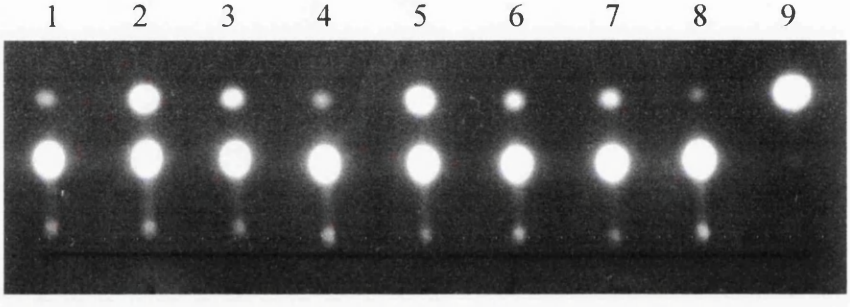

Lane	Transfection		
1	pBabe-MER	LTR^{HTLV-I}-cat	500uM tamoxifen
2	pBabe-Tax	LTR^{HTLV-I}-cat	500uM tamoxifen
3	pBabe-MER-Tax	LTR^{HTLV-I}-cat	500uM tamoxifen
4	pBabe-MER-Tax	LTR^{HTLV-I}-cat	No tamoxifen
5	pBabe-Tax-MER	LTR^{HTLV-I}-cat	500uM tamoxifen
6	pBabe-Tax-MER	LTR^{HTLV-I}-cat	No tamoxifen
7	pBabe-MER-Tax-MER	LTR^{HTLV-I}-cat	500uM tamoxifen
8	pBabe-MER-Tax-MER	LTR^{HTLV-I}-cat	No tamoxifen
9	5uL acetylated reference standard		

Tamoxifen induction of the various inducible pBabe-Tax fusion constructs demonstrates that most efficient induction occurs with the 3' Tax-MER construct. Reduced levels of expression from the other constructs is likely due to steric hindrance of the active tax domain by the fusion MER molecule. Note inhibition is strongest in the double MER construct. Little inhibition is noted for the 5' Tax-MER construct (which approaches wild type activity) presumably due to the redundancy of the terminal 5' 20-30 amino-acids.

Table 6.3: Tamoxifen induction of each of the Tax/MER fusion constructs with the LTR^{HTLV-I} CAT constructs

	†Tamoxifen % acetylation	ST Dev	Fold Induction
$Tax^{Gla\ WT}$-MER	37.4	11.1	2.4
Tax-MER	39.05	4.1	2.6
MER-Tax	20.4	8.2	1.3
MER-Tax-MER	22.0	6.6	1.4
LTR^{HTLV-I}/pBabe-MER	15.31	6.3	*1

	No Tamoxifen % acetylation	ST Dev	Fold Induction
Tax-MER	22.6	4.1	1.5
MER-Tax	16	3.7	1.0
MER-Tax-MER	12.7	4.3	0.8

†Tamoxifen used at optimal concentration (500nm) in this and all subsequent experiments; * normalised to 1

Table demonstrating the percentage acetylation of the various tax/MER fusion constructs with and without tamoxifen induction. The figures refer to the percentage acetylation of 1-deoxy-Cam, standard deviation, and fold induction relative to background induction normalised to 1.

The results of these experiments indicated that the fusion constructs synthesised functional proteins whose activity could be regulated by the modified oestrogen receptor analogue, 4-hydroxy-tamoxifen, and that the fusion construct efficiently upregulated CREB/ATF responsive promoters with little background induction but poorly upregulated the NF-κB or SRE promoter constructs.

6.3.3 Analysis of the functional domains of Tax

6.3.3.1 Segregation of trans-activating domains of Tax

Having demonstrated that the MER fusion constructs produced functional proteins, we decided to make mutants of *tax* based upon previously published data. This data had demonstrated that single or double amino acid mutations in the primary amino acid sequence of Tax generated discrete functional mutations in the domains of the Tax protein (Smith and Greene, 1991; Semmes and Jeang, 1992) [Figure 6.8] effectively segregating the key functional NF-κB and CREB/ATF activating domains (Table 6.4).

Table 6.4: Phenotypes of M1, M47 and C23S relative to wild type *tax*

	LTR^{HTLV-I}	LTR^{HIV-I}	Reference
M1	<5%	55%	Smith and Greene (1990)
M47	<5%	>120%	Smith and Greene (1990)
C23S	100%	<10%	Semmes and Jeang (1992)

Table summarising the relative induction of LTR^{HTLV-I} and LTR^{HIV-I} CAT reporter gene constructs by mutants M1, M47 and C23S.

Our laboratory reproduced these mutations using the wild type Tax protein (Figure 6.8) as the parent backbone (itself a gift from Dr Franchini, NIH, Bethseda, USA). These mutants were cloned into the pBabe retroviral vector as previously described to generate three inducible mutants of *tax*, designated M1-MER, M47-MER, and C23S-MER.

Figure 6.8: Schematic diagram illustrating the position in the primary amino acid sequence of Tax in which mutations have been introduced to generate the HTLV-I tax mutants M1, C23S and M47.

Schematic diagram illustrating the primary amino acid sequence position of the engineered mutations (M1, M47 and C23S) of wild type Tax together with the key functional domains.

Figure 6.8: Schematic diagram illustrating the position in the primary amino acid sequence of Tax in which mutations have been introduced to generate the HTLV-I tax mutants M1, C23S and M47.

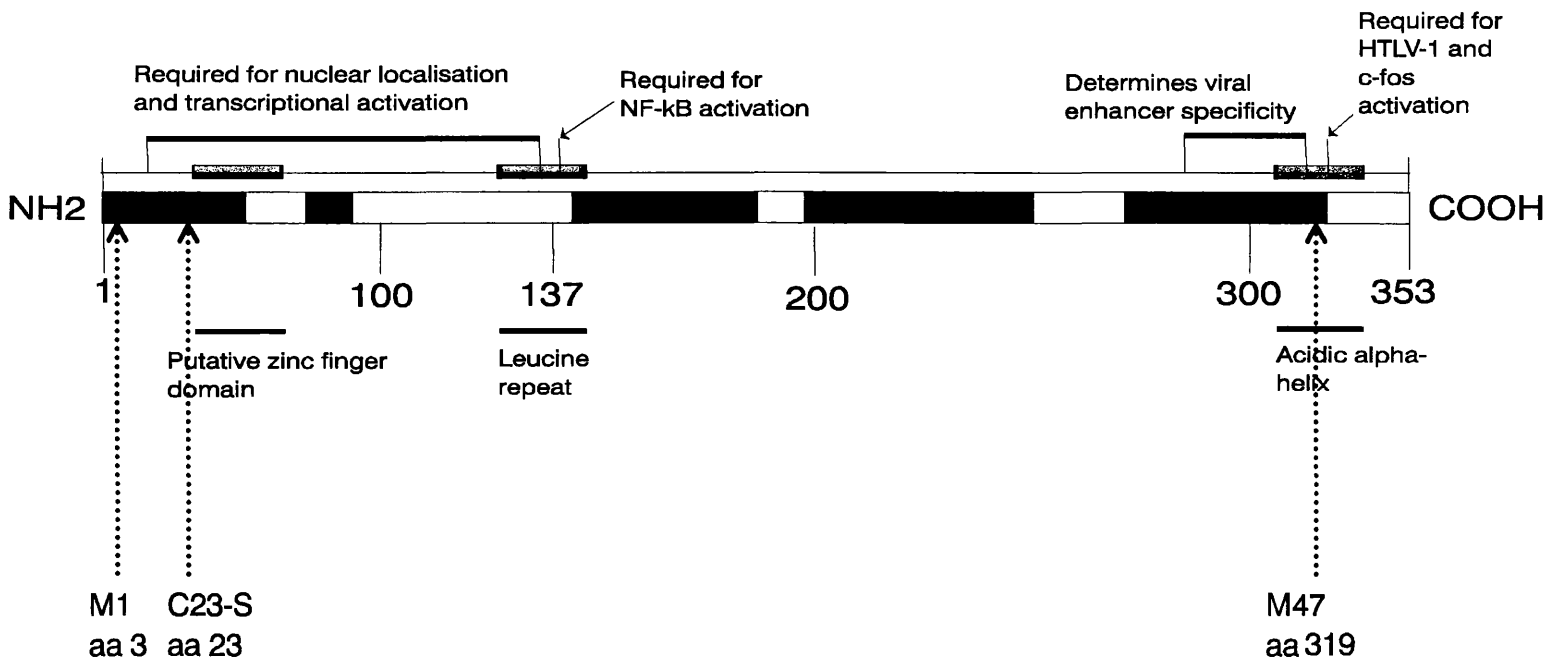

6.3.3.2 M1, M47 and C23S transactivation of the LTR^{HTLV-I}-CAT (CREB/ATF) reporter plasmid

As before, each mutant was analysed for functional transactivation of the CREB/ATF, and NF-κB reporter plasmids. These results indicated (Figure 6.9 and Table 6.5) that mutant C23S and wild type Tax most efficiently upregulated the CREB/ATF reporter construct (4.8 fold and 4.2 fold induction respectively) relative to the other mutants. Mutant M1 and wild type inducible Tax demonstrated intermediary amounts of CAT activity (2.7 fold induction each) whereas mutant M47 demonstrated minimal CREB/ATF activity (0.72 fold induction). CAT activity was also assessed without tamoxifen induction and as before was tightly regulated. Background activity ranked in the same order as before, with C23S showing most activity (1.6 fold activity) and M47 showing least activity (0.56 fold induction).

Table 6.5: Transactivation of the LTR^{HTLV-I}-CAT (CREB/ATF) reporter plasmid by mutants C23S, M47, and M1

	Tamoxifen % acetylation	ST Dev	Fold Induction
$Tax^{Gla\ WT}$-MER	19.2	1.6	2.7
M1-MER	19.31	1.2	2.7
M47-MER	5.11	3.94	0.72
C23S-MER	33.99	2.5	4.81
$Tax^{Gla\ WT}$	33.0	1.6	4.22
LTR^{HTLV-I} pBabe-MER	7.06	2.95	1.0
	No Tamoxifen % acetylation	**ST Dev**	**Fold Induction**
$Tax^{Gla\ WT}$-MER	5.98	4.5	0.85
M1-MER	8.16	3.98	1.2
M47-MER	3.94	1.32	0.56
C23S-MER	11.12	2.06	1.6

Table summarising the percentage acetylation of the LTR^{HTLV-I}-CAT (CREB/ATF) reporter gene plasmid with and without tamoxifen induction by $Tax^{Gla\ WT}$-MER, M1-MER, M47-MER, C23S-MER, $Tax^{Gla\ WT}$, and LTR^{HTLV-I} pBabe-MER. The figures refer to the percentage acetylation of 1-deoxy-Cam, standard deviation, and fold induction relative to background induction normalised to 1.

Figure 6.9: Tamoxifen induction of the LTR HTLV-I-CAT (CREB/ATF) reporter construct by wild type tax-MER, M1-MER, M47-MER, and C23S-MER fusion constructs.

Photograph summarising transient transfection of the LTR HTLV-I-CAT (CREB/ATF) reporter gene construct by the various inducible Tax mutants. Lanes 1, 3, 5, and 7 refer to pBabe-Tax-MER, pBabe-M1-MER, pBabe-M47-MER, and pBabe-C23S-MER with 500μM tamoxifen induction respectively. Lanes 2, 4, 6, 8 refer to pBabe-Tax-MER, pBabe-M1-MER, pBabe-M47-MER, and pBabe-C23S-MER without tamoxifen induction respectively. Lanes 9 and 10 refer to wild type Tax (pBabe-Tax) and pBabe-MER respectively. Lane 10 represents 5μL of acetylated reference standard.

Figure 6.9: Tamoxifen induction of the LTR HTLV-I-CAT (CREB/ATF) reporter construct by wild type tax-MER, M1-MER, M47-MER, and C23S-MER fusion constructs.

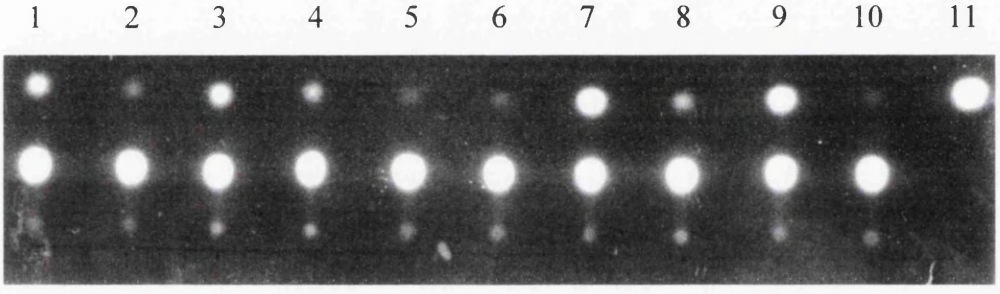

Lane	Construct		
1	pBabe-Tax-MER	LTR^{HTLV-I}-cat	500uM Tamoxifen
2	pBabe-Tax-MER	LTR^{HTLV-I}-cat	No Tamoxifen
3	pBabe-M1-MER	LTR^{HTLV-I}-cat	500uM Tamoxifen
4	pBabe-M1-MER	LTR^{HTLV-I}-cat	No Tamoxifen
5	pBabe-M47-MER	LTR^{HTLV-I}-cat	500uM Tamoxifen
6	pBabe-M47-MER	LTR^{HTLV-I}-cat	No Tamoxifen
7	pBabe-C23S-MER	LTR^{HTLV-I}-cat	500uM Tamoxifen
8	pBabe-C23S-MER	LTR^{HTLV-I}-cat	No Tamoxifen
9	pBabe-Tax	LTR^{HTLV-I}-cat	500uL Tamoxifen
10	pBabe-MER	LTR^{HTLV-I}-cat	500uM Tamoxifen
11	5uL acetylated reference standard		

Transient transfection of the various inducible tax mutants demonstrates that M47 is unable to transactivate the CREB/ATF pathway whereas mutant C23S hyper-transactivates the CREB/ATF (compared to wild type fusion Tax-MER) and is comparable to the activity of wild type Tax without the fusion MER molecule. M1 shows intermediate levels of CREB/ATF transactivation similar to wild type Tax-MER.

6.3.3.3 Transactivation of the LTR^{HIV-I}-CAT (NF-κB) reporter plasmid

Analysis with the NF-κB reporter construct (Figure 6.10 and Table 6.6) with tamoxifen induction indicated that M1 and C23S demonstrated most CAT activity (1.4 fold induction each) compared to M47 which displayed intermediary levels of CAT activity (1.0 fold induction respectively). Both versions of the wild type Tax (constitutively expressed and inducible) displayed least activity (0.93 and 0.61 fold induction respectively). CAT activity without tamoxifen induction demonstrated the same relative order of activity. Mutant C23S and M1 displayed most activity (1.1 and 1.4 fold induction respectively) whereas wild type Tax displayed least activity (0.59 fold induction). M47 displayed intermediary levels of activity (0.85 fold induction).

Table 6.6: Transactivation of the LTR^{HIV-I}-CAT (NF-κB) reporter plasmid by mutants C23S, M47, and M1

	Tamoxifen % acetylation	**ST Dev**	**Fold Induction**
$Tax^{Gla\ WT}$-MER	8.33	3.03	0.61
M1-MER	18.8	4.21	1.4
M47-MER	13.7	3.8	1.0
C23S-MER	19.2	4.2	1.4
$Tax^{Gla\ WT}$	12.59	6.87	0.93
LTR^{HTLV-I}/ pBabe-MER	13.51	7:66	1.0
	No Tamoxifen % acetylation	**ST Dev**	**Fold Induction**
$Tax^{Gla\ WT}$-MER	7.95	3.03	0.59
M1-MER	18.8	3.14	1.4
M47-MER	11.6	4.44	0.85
C23S-MER	15.07	2.16	1.11
$Tax^{Gla\ WT}$	n/d	n/d	n/d

Table summarising the percentage acetylation of the LTR^{HIV-I}-CAT (NF-κB) reporter gene plasmid with and without tamoxifen induction by $Tax^{Gla\ WT}$-MER, M1-MER, M47-MER, C23S-MER, $Tax^{Gla\ WT}$, and LTR^{HIV-I} pBabe-MER. The figures refer to the percentage acetylation of 1-deoxy-Cam, standard deviation, and fold induction relative to background induction normalised to 1.

Figure 6.10: Tamoxifen induction of the LTR HIV-I-CAT (NF-kB) reporter construct by wild type tax-MER, M1-MER, M47-MER, and C23S-MER fusion constructs

Photograph of transient transfection of the LTR HIV-I-CAT (NF-κB) reporter gene construct by the various inducible Tax mutants. Lanes 1, 3, 5, and 7 refer to pBabe-Tax-MER, pBabe-M1-MER, pBabe-M47-MER, and pBabe-C23S-MER with 500μM tamoxifen induction respectively. Lanes 2, 4, 6, 8 refer to pBabe-Tax-MER, pBabe-M1-MER, pBabe-M47-MER, and pBabe-C23S-MER without tamoxifen induction respectively. Lanes 9 and 10 refer to wild type Tax (pBabe-Tax) and pBabe-MER respectively. Lane 10 represents 5μL of acetylated reference standard.

Figure 6.10: Tamoxifen induction of the LTR HIV-I-CAT (NF-kB) reporter construct by wild type tax-MER, M1-MER, M47-MER, and C23S-MER fusion constructs

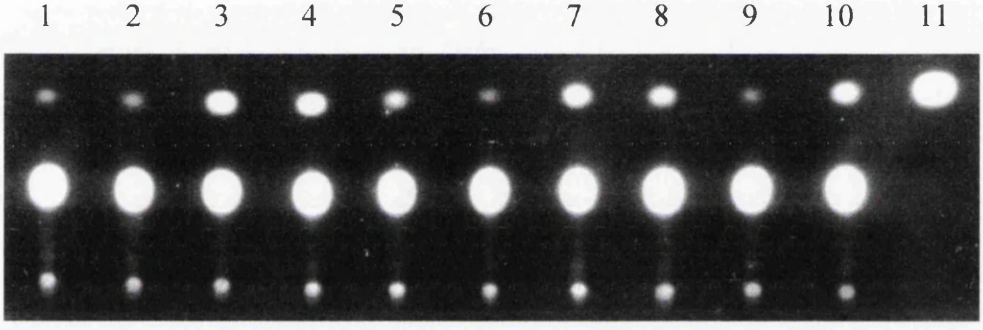

Lane	Construct
1	pBabe-Tax-MER LTR^{HIV-I}-cat 500uM Tamoxifen
2	pBabe-Tax-MER LTR^{HIV-I}-cat No Tamoxifen
3	pBabe-M1-MER LTR^{HIV-I}-cat 500uM Tamoxifen
4	pBabe-M1-MER LTR^{HIV-I}-cat No Tamoxifen
5	pBabe-M47-MER LTR^{HIV-I}-cat 500uM Tamoxifen
6	pBabe-M47-MER LTR^{HIV-I}-cat No Tamoxifen
7	pBabe-C23S-MER LTR^{HIV-I}-cat 500uM Tamoxifen
8	pBabe-C23S-MER LTR^{HIV-I}-cat No Tamoxifen
9	pBabe-Tax LTR^{HIV-I}-cat 500uM Tamoxifen
10	pBabe-MER LTR^{HIV-I}-cat 500uM Tamoxifen
11	5uL acetylated reference standard

Tamoxifen induction of the LTR^{HIV-I}-cat (NF-kB) reporter construct. Again weak induction of the NF-kB pathway with high background levels. As before mutant C23S shows hyper-transactivation of the NF-kB pathway relative to wild type Tax. M47 shows good induction whereas M1 is inactive in this pathway.

Table 6.7: Summary of CAT activity with tamoxifen induction of mutants M1-MER, M47-MER, and C23S-MER relative to wild type Tax-MER

	LTR $^{HTLV-I}$	LTR $^{HIV-I}$
C23S-MER	178%	229%
M1-MER	100%	229%
M47-MER	26%	164%
Tax$^{Gla\ WT}$-MER	*100%	*100%

*Wild type Tax normalised to 100%

Table summarising the relative percentage acetylation of the LTR^{HTLV-I}-CAT (CREB/ATF) and the LTR^{HIV-I}-CAT (NF-κB) reporter gene plasmid with and without tamoxifen induction by C23S-MER, M1-MER, M47-MER, and Tax$^{Gla\ WT}$-MER. The figures refer to the percentage acetylation of 1-deoxy-Cam relative to induction by wild type Tax (Tax$^{Gla\ WT}$-MER) normalised to 100%.

These results indicated that C23S demonstrated the most relative activity with both reporter plasmids whereas M47 showed the least activity. These results suggest that within this system, the engineered mutations do not have the same discrete effects as predicted from published data (Table 6.4).

6.3.3.4 Comparison of different clones of *tax*

The results generated with the NF-κB reporter plasmid were unexpected. We therefore decided to test the validity of the BHK transient transfection system by comparing the activity of our wild type *tax* clone relative to a clone of *tax* (Tax^{Tumour}) derived from a transgenic mouse mesenchymal tumour and a second external clone of wild type *tax* (IEX-Tax). These experiments would also help us to assess the importance of each of the functional domains of Tax with regard to tumour induction in the transgenic mouse experiments.

Repeating the same analysis as before, our results indicated (Table 6.8) that the parental wild type *tax* clone (Tax $^{WT\ Gla}$) strongly upregulated the CREB/ATF pathway (5.2 fold induction). The clone of *tax* derived from the mesenchymal tumour (Tax^{Tumour}) displayed intermediate levels of CREB/ATF CAT activity (3.8 fold induction) compared to external wild type *tax* clone (IEX-Tax) (2.6 fold induction).

Induction of NF-κB CAT activity with wild type *tax* ($Tax^{WT\ Gla}$), the tumour derived *tax* clone (Tax^{Tumour}) and the external *tax* clone (IEX-Tax) produced similar levels of CAT activity.

Table 6.8: Transactivation of the LTR^{HTLV-I} (CREB/ATF) and LTR^{HIV-I}-CAT (NF-κB) reporter plasmid by $Tax^{WT\ Gla}$, Tax^{Tumour}, and IEX-Tax

	CREB/ATF % acetylation	ST Dev % acetylation	Fold Induction
$Tax^{WT\ Gla}$	27.82	4.91	5.2
Tax^{Tumour}	20.66	6.95	3.8
IEX-Tax	14.02	6.58	2.6
LTR^{HTLV-I}/ pBabe-MER	7.63	5.38	1.0

	NF-κB % acetylation	ST Dev % acetylation	Fold Induction
$Tax^{WT\ Gla}$	11.20	4.49	1.0
Tax^{Tumour}	12.42	6.40	0.81
IEX-Tax	13.96	6.24	0.90
LTR^{HIV-I}/ pBabe-MER	13.76	8.70	1.0

Table summarising the percentage acetylation of the LTR^{HTLV-I}-CAT (CREB/ATF) and the LTR^{HIV-I}-CAT (NF-κB) reporter gene plasmid with tamoxifen induction by $Tax^{Gla\ WT}$, Tax^{tumour}, IEX-Tax, and LTR^{HTLV-I} pBabe-MER. The figures refer to the percentage acetylation of 1-deoxy-Cam, standard deviation, and fold induction relative to background induction normalised to 1.

6.4 Discussion

The tamoxifen-modified oestrogen receptor system was created as an improved switch to regulate inducible gene activity (Littlewood et al, 1995). This system had significant advantages over other oestrogen receptor based systems since it did not suffer from endogenous activation from naturally circulating oestrogens found in serum and did not require phenol-red free tissue culture medium (Littlewood et al, 1995). Furthermore, the modified oestrogen binding domain was not thought to be transcriptionally active (Littlewood et al, 1995) – a confounding factor to the interpretation of experiments using unmodified oestrogen receptor binding domains.

Analysis of the Tax-MER fusion proteins using the various reporter plasmids indicated the potential of this system. Good induction of the CREB/ATF reporter plasmid with relatively little background was achieved. Fusion of the MER at either the 3' or 5' terminus of *tax* did not significantly reduce activity apart from that expected from steric hindrance. The redundancy of the terminal 22 amino acids of Tax (Smith and Greene, 1990) may account for the slighter greater activity of the 3' terminal Tax-MER fusion protein. The flexibility of this system was further underscored by the use of a retroviral-based strategy, which allowed the downstream option to infect primary cells via an amphotropic or ecotrophic packaging cell. However this system had significant drawbacks, not least the inefficiency of NF-κB and SRF induction using BHK cells. A second potential drawback was the small but significant amount of background CAT activity observed in the absence of tamoxifen induction. CREB/ATF activity appeared to be tightly regulated whereas NF-κB activity, although more difficult to assess, appeared to be less well regulated (discussed further in Chapter 7). This may be due to the ability of this system to more tightly regulate nuclear transcription factors (Littlewood et al, 1995; Preston et al, 1996; Vater et al, 1996; Chlichlia et al, 1995) [i.e. CREB/ATF versus NF-κB] as the modified oestrogen receptor sequesters the fusion complex within the cytoplasm. Therefore, since Tax binds the ankrin repeat motifs of the cytoplasmic NF-κB inhibitor protein, IκB, residual activity may be

expected resulting in the sequestered complex exhibiting more cytoplasmic NF-κB activity than nuclear CREB/ATF activity.

The low activity of *tax* with the LTR^{HIV-I}–CAT reporter construct suggested that in our hands *tax* did not efficiently upregulate the HIV LTR. Although this could formally be due to mutation of the *tax* molecule or one of the two consensus NF-κB binding sites found in the HIV-I viral LTR (or flanking sequences thereof) we favoured a more simple explanation based on low endogenous levels of NF-κB activity in BHK cells. Other authors have commented upon this phenomenon in certain cell types (Semmes and Jeang, 1992) which further serves to underline the importance of developing relevant models to study human disease and the possibility of idiosyncratic effects between different species. Similarly, cooperation of Tax with the SRF may require HeLa cells for optimal induction (Fujii et al, 1988).

The three mutants of Tax - M1, C23S, and M47 - were developed in our laboratory according to published data which introduced specific functional deficits into the protein binding domains of Tax (Table 6.4) designed to segregate the NF-κB and CREB/ATF binding domains. Analysis of our mutants revealed a departure from the predicted phenotypes suggesting that mutations within the primary amino acid structure of Tax imparted subtle and unpredictable effects on the overall conformation of the protein. Reproductions of these mutations in other laboratories have also highlighted similar effects. In two similar systems, M22 developed by Smith and Greene (1990) was able to induce NF-κB activity whereas the same mutant (named M137) developed by Semmes and Jeang (1992) was unable to induce NF-κB activity. Presumably introduction of identical mutations into clones of wild type Tax which differ slightly in primary amino acid structure imparts unique overall patterns of folding of the native protein and therefore different functional effects.

Comparison of different clones of wild type Tax revealed differences in the overall activity of these proteins. All three clones were able to activate the CREB/ATF transcription

factors, although $Tax^{WT\ Gla}$ was two fold more efficient than IEX-Tax. Induction of the NF-κB transcription factor was uniformly weak with little difference between the clone of Tax derived from our laboratory and IEX-Tax donated by Dr Jeang. These differences may reflect point mutations in the Tax open reading frame occurring during the course of natural infection in humans which presumably similarly impart functional differences in the native protein responsible for variance in the immune response to the protein. These effects may be important not only in the persistence of Tax expression and TSP induction (previously discussed in Chapter 1) but may also be important for the selection of more pathogenic clones of Tax in ATL patients. This therefore raises the intriguing possibility that the search for functional phenotypes associated with pathogenicity may not be straightforward since introduction of specific point mutations into Tax imparts functional properties dependent upon the overall amino acid sequence of the parental clone.

Chapter 7

Functional effects of the inducible Tax mutants *in vitro*

Functional effects of the inducible Tax mutants *in vitro*

7.1 Introduction

The precise mechanism by which HTLV-I transforms naturally infected human lymphocytes *in vivo* is unknown. The requirement of tax_I or tax_{II} in the transformation process, although absolutely necessary for immortalisation (Tanaka et al, 1990; Ross et al, 1996), is still largely unknown. Full transformation of human lymphocytes requires infection by the complete virus (HTLV-I or –II) (Popovic et al, 1983; Chen et al, 1983) and presumably secondary events in addition to *tax* expression. To this effect the role of p12 and other minor pX gene products is still largely unknown (Mulloy et al, 1996; Franchini et al, 1993; Koralnik et al, 1993). Secondary events such as transrepression of the β polymerase gene (Jeang et al, 1990) and inactivation of the p53 tumour suppressor gene by *tax* (Cereseto et al, 1996; Akagi et al, 1997) although important, are more likely to play late events in the progression of ATL by promoting karyotypic instability (Kamada et al, 1992).

HTLV-I *tax* however can induce tumours in transgenic mice (Nerenberg et al, 1987), and acts as a dominantly acting oncogene *in vitro*. Indeed, *tax* transforms rodent fibroblasts (Tanaka et al, 1990), and co-operates with the *ras* oncogene to transform primary rat embryo fibroblasts (Pozzati et al, 1990) [which ordinarily it immortalises (Pozzati et al, 1990)]. Depending upon the context of expression, *tax* like *c-myc* (Evan et al, 1992) and *c-fos* (Preston et al, 1996) can also serve to induce apoptosis (Yamada et al, 1994) or possibly inhibit it (Brauweiler et al, 1997; Kishi et al, 1997; Schwartz-Cornil et al, 1997).

Previous analysis of the Tax-tamoxifen system (Chapter 6) had already demonstrated the functional induction of Tax expression *in vitro* by tamoxifen. However this system was not without certain restrictions since it was known that tamoxifen clinically induced apoptosis in certain forms of human cancer (Burroughs et al, 1997; Cameron et al, 1997; Ellis et al, 1997). Induction of apoptosis was not restricted to hormone dependent tumours since tamoxifen reliably induced liver tumours in rats due to promotion through reactive

hyperplasia secondary to chronic cell loss by apoptosis (Carthew et al, 1996). Furthermore, these effects were attributed, at least in part, to the induction of *c-myc*, *bcl-2* and p53 genes (Kellen et al, 1996) which are known to modify the apoptotic response.

7.2 Aims of the experiment

In light of the plethora of functional attributes imbued upon *tax* we decided to test which of the functional domains of *tax* were necessary for transformation and apoptosis using the inducible Tax-MER system. Due to the low level of NF-κB activity in the BHK cells we switched to a well characterised Rat 1 model system which had been previously characterised in other apoptosis assays (Evan et al, 1992).

7.3 Results

7.3.1 Generation of stable cell lines

Rat 1 cells were transfected with each vector (Tax-MER, M1-MER, M47-MER and C23S-MER) and selected in G418 to generate stable cell lines (Chapter 2: Materials and methods). This procedure produced in excess of 20 to 30 colonies per transfection experiment indicating that *tax* expression *per se* was not associated with a toxic phenotype in Rat 1 cells.

7.3.2 Analysis of cell lines

In order to determine the effects of *tax* expression *in vitro*, we decided to initially assess the growth rate of the *tax* expressing cell lines in 10% bovine foetal calf serum together with and without tamoxifen induction. The results of these experiments (Graph 7.1) indicated that although growth rates were similar between each cell line, by day six, each cell line grew to a higher cell density with tamoxifen induction compared to its counterpart grown without tamoxifen addition. These experiments indicated that tamoxifen induction had not markedly altered mitotic rate but may have reduced contact inhibition - a classical feature usually associated with transformation of immortalised cell lines by dominantly acting oncogenes.

Graph 7.1: Growth of stable cell lines in 10% bovine foetal calf serum expressing Tax-MER, C23S-MER, M1-MER, and M47-MER

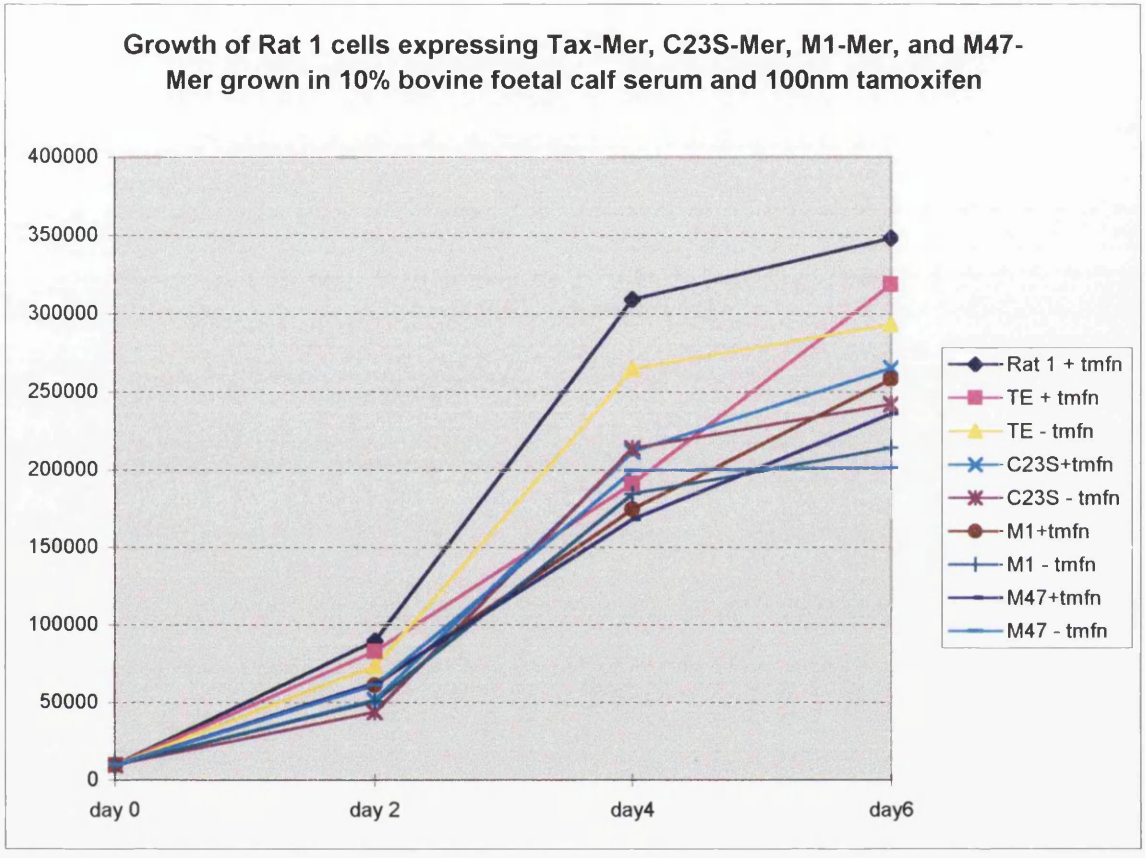

Each data point (and all subsequent experiments) represents the average of four separate cell counts performed on at least two separate occasions.

Graph illustrating the growth of Rat 1 cells, Tax-MER, C23S-MER, M1-MER, and M47-MER expressing cell lines in 10% bovine foetal calf serum with the addition of 100nm tamoxifen. Cell lines grown in tamoxifen reach a higher cell density by day 6 compared to the same cell lines grown without tamoxifen.

7.3.3 Analysis of apoptosis

7.3.3.1 Optimisation of apoptosis assay

In order to assess the effect of *tax* expression upon apoptosis we decided to measure viable cell numbers (live adherent cells) in each of the cell lines after 2 days and 4 days growth in 0.1% FCS. Cells grown in 0.1% (or less) FCS normally undergo growth arrest – however cells expressing oncogenes which induce inappropriate entry into the cell cycle die by apoptosis (Evan et al, 1992 and 1995). We therefore decided to characterise this system using control Rat 1 cells grown in either 100nm or 250nm tamoxifen. Our results (Graph 7.2) indicated that Rat 1 cells grown in 100nm tamoxifen were unable to proliferate in 0.2-0.5% bovine foetal calf serum. However, Rat 1 cells grown in 250nm tamoxifen were able to proliferate (conforming to the pattern of Rat 1 cell growth when no tamoxifen is added). The presence of dead cells within the supernatant indicated that a proportion of cells were detaching and dying both at 100 and 250nm tamoxifen. These results indicated that 250nm tamoxifen was the optimum concentration to assay apoptosis using Rat 1 cells in 0.1% FCS.

Graph 7.2: Growth of Rat 1 cells in 100nm and 250nm tamoxifen.

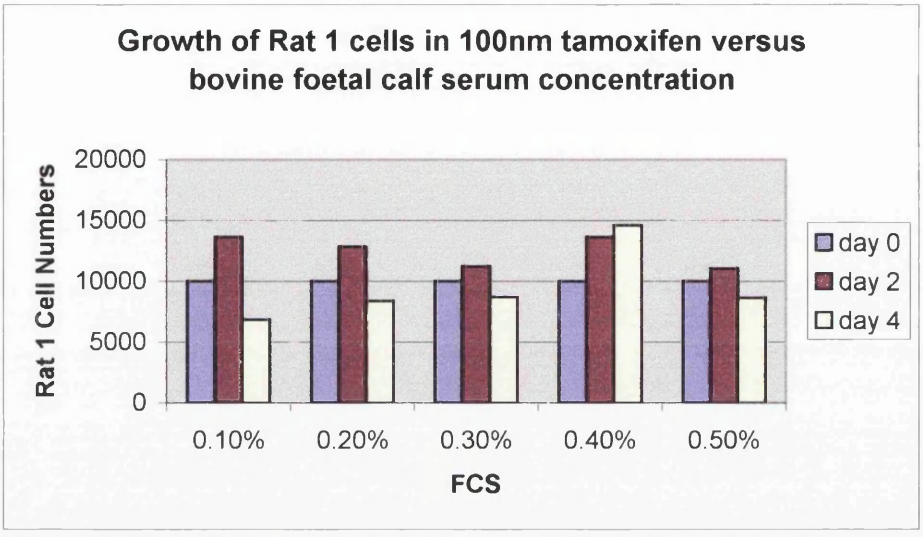

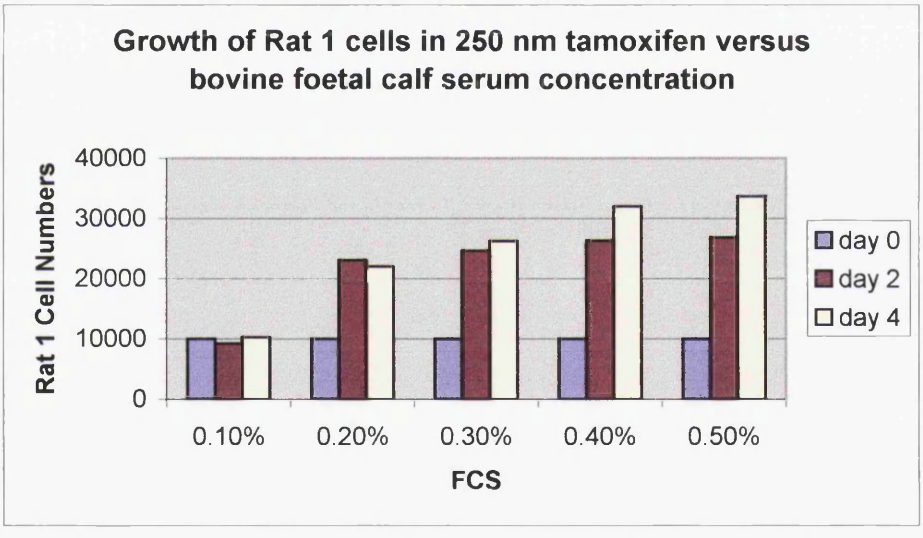

Graph illustrating the growth of Rat 1 cells in 100nm or 250nm concentration of tamoxifen at 0.1 – 0.5% bovine foetal calf serum over a 4 day time period. At 100nm concentration of tamoxifen Rat 1 cell numbers remain stable from day 0 to day 4 whereas at 250nm concentration of tamoxifen Rat 1 cell numbers increase.

7.3.3.2 Analysis of apoptosis in cell lines

In order to assay the effect that *tax* expression (and the various engineered mutants thereof) contributed to apoptosis we repeated the previous apoptosis assay using the stable *tax* expressing Rat 1 cell lines. The results of these experiments (Graph 7.3) indicated that each of the stable cell lines exhibited enhanced apoptosis and consequently reduced viable cell numbers compared to the parental Rat 1 control cells. Most cell death occurred in cell lines expressing wild type Tax, mutant C23S and M1, whereas M47 exhibited least cell death. Treatment with 250nm tamoxifen appeared to reduce the amount of apoptosis. Indeed, background induction of Tax activity without tamoxifen addition appeared sufficient to efficiently induce apoptosis. Although the contribution through transactivation of the NF-κB pathway was difficult to determine in the BHK cell lines, these results indicate that induction of apoptosis was weakest in the M47 cell line. This cell line least efficiently transactivated the CREB/ATF pathway, and may indicate the general importance of this pathway for apoptotic induction *in vitro*.

Graph 7.3: Growth of stable cell lines expressing Tax-MER, C23S-MER, M1-MER and M47-MER in 0.1% FCS and 250nm tamoxifen.

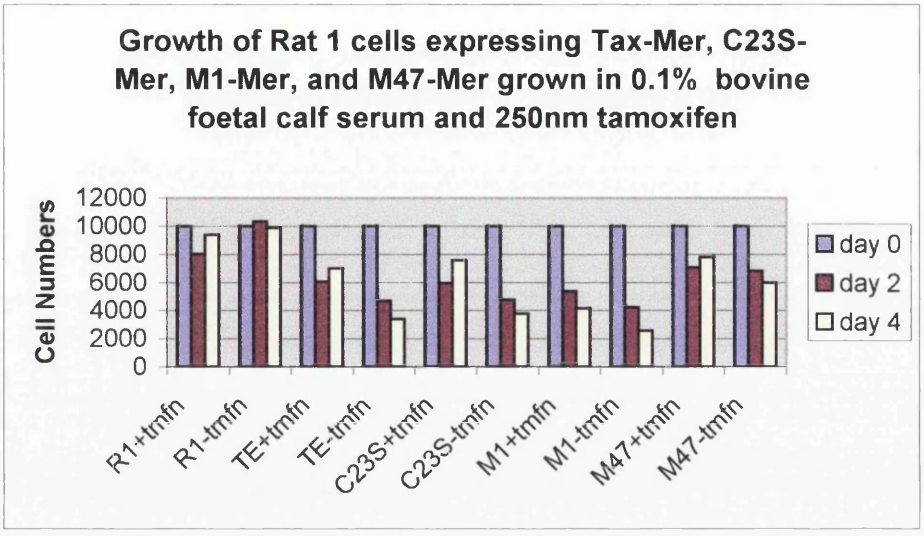

Graph illustrating growth of Rat 1 cells and Tax-MER, C23S-MER, M1-MER, and M47-MER cell lines in 0.1% bovine foetal calf serum, with and without 250nm concentration of tamoxifen over a 4 day time period. Cell lines expressing the inducible *tax* vector show reduced cell numbers compared to the parental Rat 1 cell line. The addition of tamoxifen increased the number of viable cells for each *tax* expressing cell line compared to the same cell line grown without tamoxifen.

7.4 Discussion

The results of these experiments indicate that expression of *tax* is associated with a stochastic risk of apoptosis. Expression of *tax in vivo* resulted in apoptosis in a sub-population of 'high expressing cells' in CD3-*tax* transgenic mice. Expression of *tax in vitro* also resulted in apoptosis. Since environmental effects *in vitro* should be similar if not identical, and since all cells were clonally derived, apoptosis *in vitro* must also be stochastic. Presumably a complex biochemical network in which the balance between inducers and repressors determines the overall outcome governing apoptosis. In this scenario, the level of *tax* expression would be one factor contributing to the apoptotic decision. Low level expression presumably would be consistent with cell survival. To this effect, low level expression of *tax* from the pBabe promoter may have contributed to the apparent ease of generating a large number of *tax* expressing stable cell lines – in apparent contrast to other authors using more efficient promoters (Chlichlia et al, 1995; Furuta et al, 1989). This is also consistent with the expression of *tax* in the naturally infected host in which evolution has likely resulted in the selection of those viral clones, which express *tax* at sufficiently low levels to escape immune surveillance and apoptotic induction.

Growth of Rat 1 cells in low FCS conditions resulted in reduced viable cell numbers when grown at 100nm tamoxifen compared to 250nm tamoxifen. Tamoxifen therefore appears to have opposing effects at different concentrations. The results of the apoptosis experiments in the *tax* expressing cell lines suggests that 250nm tamoxifen may inhibit or rescue from apoptosis since viable cell numbers are increased in those cells which receive tamoxifen. [Similar results have been observed in *c-myc*-MER transgenic mice (Dr Cameron personal communication)]. This is consistent with the observation that control Rat 1 cells (already committed to mitosis from prior culture in 10% FCS) proliferate at 0.2-0.5% FCS compared to the same cells grown in 100nm tamoxifen which detach, presumably due to apoptosis. The differential effects of tamoxifen may be related to a concentration dependent induction of gene activity that serves to modify the apoptotic response.

Background activity of the Tax-MER system, although apparently negligible, is sufficient to exert potent biological effects. *In vitro* this resulted in efficient apoptotic induction, whereas *in vivo* this resulted in tumour formation in *c-myc*-MER transgenic mice (Dr Cameron personal communication). This serves to illustrate that a mild biochemical perturbation can markedly shift the overall biological response of the cell suggesting that the outcome between life and death is finely balanced.

Our results indicated that induction of apoptosis was least efficient in the M47 cell line. Although the contribution of the NF-κB pathway could not be established for the BHK cell lines, the M47 cell line least efficiently transactivated the CREB/ATF pathway. These results may therefore indicate the general importance of the CREB/ATF pathway for apoptotic induction *in vitro* (Smith and Greene, 1991; Rosin et al, 1998). These results are also consistent with the notion that the decision to engage apoptosis is dependent upon the level of *tax* expression. Results from the transgenic mouse experiments in which only those cells expressing high levels of Tax protein enter into apoptosis support this notion, whereas the background population expressing lower amounts of Tax protein proliferate (Hall et al, 1998).

Recent work has now shed light on other biochemical interactions between *tax* and cell cycle control proteins – most notably $p16^{INK4a}$ (Suzuki et al, 1996) and the mitotic checkpoint protein, MAD1 (Jin et al, 1998). The importance of these interactions and the contribution that they make towards the transformed phenotype and induction of apoptosis remain to be seen, but most likely will reveal yet more functional attributes to the already considerable repertoire of this most enigmatic of proteins.

Future Work

The results presented here concur with the observations made by other authors that *tax* expression results in the induction of a variety of tumours as well as certain degenerative conditions. Expression using the CD3-ε enhancer-promoter regulatory elements resulted in mesenchymal tumours at ear and tail tips, salivary and mammary adenomas, and histiocytic tumours. We also observed thymic atrophy, immunosuppression, and hindleg paralysis. Analysis of the mesenchymal tumours and salivary and mammary adenomas using an *in situ* technique demonstrated that although all tumours were presumalby clonally derived, their patterns of gene expression were not uniform. Expression of large amounts of Tax protein as well as Myc, Fos, Jun and p53 proteins occurred as isolated foci of cells distributed randomly throughout the substance of the tumours. Coincident with Tax expression we also observed similar patterns of apoptosis indicating that the processes of apoptosis and Tax protein expression were intimately linked *in vivo*. In addition to these studies we also demonstrated that induction of apoptosis by *tax* was dependent upon the CREB/ATF activating domain.

Expression of *tax* within the lymphoid compartment has not resulted in T-cell lymphoma, but rather in severe immunosuppresion due to thymic atrophy. This phenotype may result form the expression of the Tax protein using very efficient promoter-enhancer elements inducing apoptosis rather than neoplasia. Expression from less efficient regulatory elements may prove more permissive. Regulation of *tax* expression using inducible promoters or activation of sequestered proteins may therefore allow targeted expression within the lymphoid compartment. To this effect the tamoxifen-modified oestrogen receptor may prove useful although our experience indicates that background induction probably would be sufficient to allow penetrance of the transgene phenotype.

The generation of mutants that segregate the various activating domains of Tax has already generated discordant results. The introduction of Tax into a complex biochemical network of proteins clearly has subtle effects dependent upon the assay system employed. The

importance of individual protein-protein interactions may therefore vary depending upon the context of expression - hence the relevance of Tax expression in rodent fibroblasts *in vitro* may be questionable since species and cell specific effects cannot be easily assessed. It therefore appears pertinent to generate an improved transgenic model, possibly using species other than rats and mice (due to their propensity to develop tumours). The development of this model system would then allow the elucidation of oncogenic collaborators and mechanisms of apoptosis in *tax* transformed T-cells.

Bibliography

1. Adya N, Giam CZ: Distinct regions in human T-cell lymphotropic virus type I tax mediate interactions with activator protein CREB and basal transcription factors. J Virol 1995, 69:1834-41.

2. Agarwal ML, Agarwal A, Taylor WR, Stark GR: p53 controls both the G2/M and the G1 cell cycle checkpoints and mediates reversible growth arrest in human fibroblasts. Proc Natl Acad Sci U S A 1995, 92:8493-7.

3. Ahmed YF, Gilmartin GM, Hanly SM, Nevins JR, Greene WC: The HTLV-I Rex response element mediates a novel form of mRNA polyadenylation. Cell 1991, 64:727-37.

4. Akagi T, Ono H, Tsuchida N, Shimotohno K: Aberrant expression and function of p53 in T-cells immortalized by HTLV- I Tax1. FEBS Lett 1997, 406:263-6.

5. Akagi T, Ono H, Shimotohno K: Characterization of T cells immortalized by Tax1 of human T-cell leukemia virus type 1. Blood 1995, 86:4243-9.

6. Akiyama T, Ohuchi T, Sumuda S, Matsumoto K, Toyoshima K: Phosphorylation of the retinoblastoma protein by cdk2. Proc Natl Acad Sci U S A 1992, 89:7900-4.

7. Akizuki S, Nakazato O, Higuchi Y, Tanabe K, Setoguchi M, Yoshida S, Miyazaki Y, Yamamoto S, Sudou S, Sannomiya K, et al. Necropsy findings in HTLV-I associated myelopathy [letter]. Lancet 1987, 1:156-7.

8. Alarcon RM, Rupnow BA, Graeber TG, Knox SJ, Giaccia AJ: Modulation of c-Myc activity and apoptosis in vivo. Cancer Res 1996, 56:4315-9.

9. Albrecht H, Shakov AN, Jongeneel CV: trans Activation of the Tumor Necrosis Factor Alpha Promoter by the Human T-Cell Leukaemia Virus Type I Tax1 Protein. J Virol 1992, 66:6191-3.

10. Alexandre C, Charnay P, Verrier B: Transactivation of Krox-20 and Krox-24 promoters by the HTLV-1 Tax protein through common regulatory elements. Oncogene 1991, 6:1851-7.

11. Alexandre C, Verrier B: Four regulatory elements in the human c-fos promoter mediate transactivation by HTLV-1 Tax protein. Oncogene 1991, 6:543-51.

12. Allen ND, Norris ML, Surani MA: Epigenetic control of transgene expression and imprinting by genotype- specific modifiers. Cell 1990, 61:853-61.

13. Arai N, Nomura D, Villaret D, DeWaal Malefijt R, Seiki M, Yoshida M, Minoshima S, Fukuyama R, Maekawa M, Kudoh J, et al. Complete nucleotide sequence of the chromosomal gene for human IL-4 and its expression. J Immunol 1989, 142:274-82.

14. Arends M, Wyllie A: Apoptosis: mechanisms and role in pathology. Int Rev Exp Path 1991, 32:254

15. Arima N, Molitor JA, Smith MR, Kim JH, Daitoku Y, Greene WC: Human T-cell leukemia virus type I Tax induces expression of the Rel-related family of kappa B enhancer-binding proteins: evidence for a pretranslational component of regulation. J Virol 1991, 65:6892-9.

16. Arya SK, Wong Staal F, Gallo RC: T-cell growth factor gene: lack of expression in human T-cell leukemia-lymphoma virus-infected cells. Science 1984, 223:1086-7.

17. Baeuerle PA, Baltimore D: Actication of DNA binding activity in an apparently cytoplasmic precursor of the NF-*k*B transcription factor. Cell 1988, 53:211-7.

18. Bagchi S, Weinmann R, Raychaudhuri P: The retinoblastoma protein copurifies with E2F-I, an E1A-regulated inhibitor of the transcription factor E2F. Cell 1991, 65:1063-72.

19. Baker SJ, Fearon ER, Nigro JM, Hamilton SR, Preisinger AC, Jessup JM, vanTuinen P, Ledbetter DH, Barker DF, Nakamura Y: Chromosome 17 deletions and p53 gene mutations in colorectal carcinomas. Science 1989, 244:217-21.

20. Bakker A, Li X, Ruland CT, Stephens DW, Black AC, Rosenblatt JD: Human T-cell leukemia virus type 2 Rex inhibits pre-mRNA splicing in vitro at an early stage of spliceosome formation. Journal of Virology 1996, 70:5511-8.

21. Ballester R, Marchuk D, Boguski M, Saülino A, Letcher R, Wigler M, Collins F: The NF1 locus encodes a protein functionally related to mammalian GAP and yeast IRA proteins. Cell 1990, 63:851-9.

22. Baranger AM, Palmer CR, Hamm MK, Giebler HA, Brauweiler A, Nyborg JK, Schepartz A: Mechanism of DNA-binding enhancement by the human T-cell leukaemia virus transactivator Tax. Nature 1995, 376:606-8.

23. Bartek J, Bartkova J, Vojtesek B, Staskova Z, Lukas J, Rejthar A, Kovarik J, Midgley CA, Gannon JV, Lane DP: Aberrant expression of the p53 oncoprotein is a common feature of a wide spectrum of human malignancies. Oncogene 1991, 6:1699-703.

24. Baskerville S, Zapp M, Ellington AD: High-resolution mapping of the human T-cell leukemia virus type 1 Rex-binding element by in vitro selection. J Virol 1995, 69:7559-69.

25. Beg AA, Baltimore D: An essential role for NF-kappaB in preventing TNF-alpha-induced cell death. Science 1996, 274:782-4.

26. Beimling P, Moelling K: Direct interaction of CREB protein with 21 bp Tax-response elements of HTLV-ILTR. Oncogene 1992, 7:257-62.

27. Beimling P, Moelling K: Isolation and characterization of the tax protein of HTLV-I. Oncogene 1989, 4:511-6.

28. Belliveau MJ, Lutchman M, Claudio JO, Marineau C, Rouleau GA: Schwannomin: new insights into this member of the band 4.1 superfamily. Biochem Cell Biol 1995, 73:733-7.

29. Benacerraf B, McDevitt HO. Histocompatibility-linked immune response genes. Science 1972, 175:273-9.

30. Benvenisty N, Ornitz DM, Bennett GL, Sahagan BG, Kuo A, Cardiff RD, Leder P: Brain tumours and lymphomas in transgenic mice that carry HTLV-I LTR/c-myc and Ig/tax genes. Oncogene 1992, 7:2399-405.

31. Beraud C, Greene WC: Interaction of HTLV-I tax with the human proteasome: Implications for NF-kappaB induction. Journal of Acquired Immune Deficiency Syndromes and Human Retrovirology 1996, 13:S76-84.

32. Beraud C, Sun SC, Ganchi P, Ballard DW, Greene WC: Human T-cell leukemia virus type I Tax associates with and is negatively regulated by the NF-kappa B2 p100 gene product: implications for viral latency. Mol Cell Biol 1994, 14:1374-82.

33. Berneman ZN, Gartenhaus RB, Reitz MS, Jr., Klotman ME, Gallo RC: cDNA sequencing confirms HTLV-I expression in adult T-cell leukemia/lymphoma and different sequence variations in vivo and in vitro. Leukemia 1992, 6 Suppl 3:67S-71S.

34. Berneman ZN, Gartenhaus RB, Reitz MS, Jr., Blattner WA, Manns A, Hanchard B, Ikehara O, Gallo RC, Klotman ME: Expression of alternatively spliced human T-lymphotropic virus type I pX mRNA in infected cell lines and in primary uncultured cells from patients with adult T-cell leukemia/lymphoma and healthy carriers. Proc Natl Acad Sci U S A 1992, 89:3005-9.

35. Bianchi AB, Mitsunaga SI, Cheng JQ, Klein WM, Jhanwar SC, Seizinger B, Kley N, Klein-Szanto AJ, Testa JR: High frequency of inactivating mutations in the neurofibromatosis type 2 gene (NF2) in primary malignant mesotheliomas [see comments]. Proc Natl Acad Sci U S A 1995, 92:10854-8.

36. Biebinger S, Wirtz LE, Lorenz P, Clayton C: Vectors for inducible expression of toxic gene products in bloodstream and procyclic Trypanosoma brucei. Mol Biochem Parasitol 1997, 85:99-112.

37. Black AC, Luo J, Watanabe C, Chun S, Bakker A, Fraser JK, Morgan JP, Rosenblatt JD: Polypyrimidine tract-binding protein and heterogeneous nuclear ribonucleoprotein A1 bind to human T-cell leukemia virus type 2 RNA regulatory elements. J Virol 1995, 69:6852-8.

38. Black AC, Ruland CT, Luo J, Bakker A, Fraser JK, Rosenblatt JD: Binding of nuclear proteins to HTLV-II cis-acting repressive sequence (CRS) RNA correlates with CRS function. Virology 1994, 200:29-41.

39. Black AC, Ruland CT, Yip MT, Luo J, Tran B, Kalsi A, Quan E, Aboud M, Chen IS, Rosenblatt JD: Human T-cell leukemia virus type II Rex binding and activity require an

intact splice donor site and a specific RNA secondary structure. J Virol 1991, 65:6645-53.

40. Black AC, Chen IS, Arrigo S, Ruland CT, Allogiamento T, Chin E, Rosenblatt JD: Regulation of HTLV-II gene expression by Rex involves positive and negative cis-acting elements in the 5'long terminal repeat. Virology 1991, 181:433-44.

41. Blyth K, Terry A, O'Hara M, Baxter EW, Campbell M, Stewart M, Donehower LA, Onions DE, Neil JC, Cameron ER: Synergy between a c-myc transgene and p53 null genotype in murine thymic lymphomas: contrasting effects of homozygous and heterzygous p53 loss. Oncogene 1995, 10:1717-23.

42. Bogerd HP, Tiley LS, Cullen BR: Specific binding of the human T-cell leukemia virus type I Rex protein to a short RNA sequence located within the Rex-response element. J Virol 1992, 66:7572-5.

43. Bosselut R, Lim F, Romond PC, Frampton J, Brady J, Ghysdael J: Myb protein binds to multiple sites in the human T cell lymphotropic virus type 1 long terminal repeat and transactivates LTR-mediated expression. Virology 1992, 186:764-9.

44. Bosselut R, Duvall JF, Gegonne A, Bailly M, Hemar A, Brady J, Ghysdael J: The product of the c-ets-1 proto-oncogene and the related Ets2 protein act as transcriptional activators of the long terminal repeat of human T cell leukemia virus HTLV-1. EMBO J 1990, 9:3137-44.

45. Brady JN: "Extracellular Tax1 protein stimulates NF-kB and expression of NF-kB-responsive Ig kappa and TNF beta genes in lymphoid cells". AIDS Res Hum Retroviruses 1992, 8:724-7.

46. Brauweiler A, Garrus JE, Reed JC, Nyborg JK: Repression of bax gene expression by the HTLV-1 Tax protein: implications for suppression of apoptosis in virally infected cells. Virology 1997, 231:135-40.

47. Brauweiler A, Garl P, Franklin AA, Giebler HA, Nyborg JK: A molecular mechanism for human T-cell leukemia virus latency and Tax transactivation. J Biol Chem 1995, 270:12814-22.

48. Broder S: T cell proliferation and ablation. A biologic spectrum of abnormalities induced by the human T cell lymphotropic virus group. Prog Allergy 1986, 37:224-43.

49. Buchkovich K, Duffy LA, Harlow E: The retinoblastoma protein is phosphorylated during specific phases of the cell cycle. Cell 1989, 58:1097-105.

50. Burroughs KD, Kiguchi K, Howe SR, Fuchs-Young R, Trono D, Barrett JC, Walker C: Regulation of apoptosis in uterine leiomyomata. Endocrinology 1997, 138:3056-64.

51. Butcher EC, Picker LJ: Lymphocyte homing and homeostasis. Science 1996, 272:60-6.

52. Cameron DA, Ritchie AA, Langdon S, Anderson TJ, Miller WR: Tamoxifen induced apoptosis in ZR-75 breast cancer xenografts antedates tumour regression [In Process Citation]. Breast Cancer Res Treat 1997, 45:99-107.

53. Cann AJ, Rosenblatt JD, Wachsman W, Shah NP, Chen IS: Identification of the gene responsible for human T-cell leukaemia virus transcriptional regulation. Nature 1985, 318:571-4.

54. Capesius C, Saal F, Maero E, Bazarbachi A, Lasneret J, Laroche L, Gessain A, Hojman F, Peries J: No evidence for HTLV-I infection in 24 cases of French and

Portuguese mycosis fungoides and Sezary syndrome (as seen in France). Leukemia 1991, 5:416-9.

55. Caron C, Rousset R, Beraud C, Moncollin V, Egly JM, Jalinot P: Functional and biochemical interaction of the HTLV-I Tax1 transactivator with TBP. EMBO J 1993, 12:4269-78.

56. Carthew P, Nolan BM, Edwards RE, Smith LL: The role of cell death and cell proliferation in the promotion of rat liver tumours by tamoxifen. Cancer Lett 1996, 106:163-9.

57. Cassens S, Ulrich U, Beimling P, Simon D: Inhibition of human T cell leukaemia virus type I long terminal repeat expression by DNA methylation: implications for latency. J Gen Virol 1994, 75:3255-9.

58. Cawthon RM, Weiss R, Xu GF, Viskochil D, Culver M, Stevens J, Robertson M, Dunn D, Gesteland R, O'Connell P: A major segment of the neurofibromatosis type 1 gene: cDNA sequence, genomic structure, and point mutations [published erratum appears in Cell 1990 Aug 10;62(3):following 608]. Cell 1990, 62:193-201.

59. Cereseto A, Diella F, Mulloy JC, Cara A, Michieli P, Grassmann R, Franchini G, Klotman ME: p53 functional impairment and high p21waf1/cip1 expression in human T-cell lymphotropic/leukemia virus type I-transformed T cells. Blood 1996, 88:1551-60.

60. Cesarman E, Chadburn A, Inghirami G, Gaidano G, Knowles DM: Structural and functional analysis of oncogenes and tumor suppressor genes in adult T-cell leukemia/lymphoma shows frequent p53 mutations. Blood 1992, 80:3205-16.

61. Chan WC, Hooper C, Wickert R, Benson JM, Vardiman J, Hinrichs S, Weisenburger D: HTLV-I sequence in lymphoproliferative disorders. Diagn Mol Pathol 1993, 2:192-9.

62. Chang Y, Cesarman E, Pessin MS: Identification of herpesvirus-like DNA sequences in AIDS- associated Karposi's sarcoma. Science 1994, 266:1865-9.

63. Chellappan S, Kraus VB, Kroger B, Munger K, Howley PM, Phelps WC, Nevins JR: Adenovirus E1A, simian virus 40 tumor antigen, and human papillomavirus E7 protein share the capacity to disrupt the interaction between transcription factor E2F and the retinoblastoma gene product. Proc Natl Acad Sci U S A 1992, 89:4549-53.

64. Chellappan SP, Hiebert S, Mudryj M, Horowitz JM, Nevins JR: The E2F transcription factor is a cellular target for the RB protein. Cell 1991, 65:1053-61.

65. Chen IS, Quan SG, Golde DW: Human T-cell leukemia virus type II transforms normal human lymphocytes. Proc Natl Acad Sci U S A 1983, 80:7006-9.

66. Chen PL, Scully P, Shew J, Wang JY, Lee WH: Phosphorylation of the retinoblastoma gene product is modulated during the cell cyle and cellular differentiation. Cell 1989, 58:1193-8.

67. Chiou SK, Tseng CC, Rao L, White E: Functional complementation of the adenovirus E1B 19-kilodalton protein with Bcl-2 in the inhibition of apoptosis in infected cells. J Virol 1994, 68:6553-66.

68. Chlichlia K, Moldenhauer G, Daniel PT, Busslinger M, Gazzolo L, Schirrmacher V, Khazaie K: Immediate effects of reversible HTLV-1 tax function: T-cell activation and apoptosis. Oncogene 1995, 10:269-77.

69. Chou KS, Okayama A, Tachibana N, Lee TH, Essex M: Nucleotide sequence analysis of a full-length human T-cell leukemia virus type I from adult T-cell leukemia cells: a prematurely terminated PX open reading frame II. Int J Cancer 1995, 60:701-6.

70. Chou PY, Fasman GD: Prediction of the secondary struture of proteins from their amino acid sequence. Adv Enzymol Relat Areas Mol Biol 1978, 47:45-148.

71. Chou PY, Fasman GD: Empiracal predictions of protein conformation. Annu Rev Biochem 1978, 47:251-76.

72. Chresta CM, Arriola EL, Hickman JA: Apoptosis and cancer chemotherapy. Behring Inst Mitt 1996,232-40.

73. Ciminale V, Pavlakis GN, Derse D, Cunningham CP, Felber BK: Complex splicing in the human T-cell leukemia virus (HTLV) family of retroviruses: novel mRNAs and proteins produced by HTLV type I. J Virol 1992, 66:1737-45.

74. Clark NM, Smith MJ, Hilfinger JM, Markovitz DM: Activation of the human T-cell leukemia virus type I enhancer is mediated by binding sites for Elf-1 and the pets factor. J Virol 1993, 67:5522-8.

75. Clemens KE, Piras G, Radonovich MF, Choi KS, Duvall JF, DeJong J, Roeder R, Brady JN: Interaction of the human T-cell lymphotropic virus type 1 tax transactivator with transcription factor IIA. Mol Cell Biol 1996, 16:4656-64.

76. Clevers H, Lonberg N, Dunlap S, Lacy E, Terhorst C: An enhancer located in a CpG-island 3' to the TCR-CD3-epsilon gene confers T lymphocyte-specificity to its promoter. EMBO Journal 1989, 8:2527-35.

77. Croce CM, Isobe M, Palumbo A, Puck J, Ming J, Tweardy T: Gene for alpha-chain of human T-cell receptor: Location on chromosome 14 region involved in T-cell neoplasms. Science 1985, 227:1044-7.

78. Daenke S, Kermode AG, Hall SE, Taylor G, Weber J, Nightingale S, Bangham CR: High activated and memory cytotoxic T-cell responses to HTLV-1 in healthy carriers and patients with tropical spastic paraparesis. Virology 1996, 217:139-46.

79. Daenke S, Bangham CR: Do T cells cause HTLV-1-associated disease?: a taxing problem [editorial]. Clin Exp Immunol 1994, 96:179-81.

80. DAgostino DM, Ciminale V, Zotti L, Rosato A, ChiecoBianchi L: The human T-cell lymphotropic virus type 1 Tof protein contains a bipartite nuclear localization signal that is able to functionally replace the amino-terminal domain of Rex. Journal of Virology 1997, 71:75-83.

81. Dasgupta P, Reddy CD, Saikumar P, Reddy EP: The cellular proto-oncogene product Myb acts as transcriptional activator of the long terminal repeat of human T-lymphotropic virus type I. J Virol 1992, 66:270-6.

82. Dawson M: Pathogenesis of maedi-visna. Vet Rec 1987, 120:451-4.

83. Dawson M, Jeffrey M, Chasey D, Venables C, Sharp JM: Isolation of a syncytium-forming virus from a goat with polyarthritis. Vet Rec 1983, 112:319-21.

84. de Waal Malefyt R, Yssel H, Spits H, de Vries JE, Sancho J, Terhorst C, Alarcon B: Human T cell leukemia virus type I prevents cell surface expression of the T cell receptor through down-regulation of the CD3-gamma, -delta, -epsilon, and -zeta genes. J Immunol 1990, 145:2297-303.

85. Debbas M, White E: Wild-type p53 mediates apoptosis by E1A, which is inhibited by E1B. Genes Dev 1993, 7:546-54.

86. DeCaprio JA, Ludlow JW, Lynch D, Furukawa Y, Griffin J, Piwnica-Worms H, Huang CM, Livingston DM: The product of the retinoblastoma susceptibility gene has properties of a cell cylce regulatory element. Cell 1989, 58:1085-95.

87. DeCaprio JA, Ludlow JW, Figgle J, Shew JY, Huang CM, Lee WH, Marsilio E, Paucha E, Livingston DM: SV40 large tumor antigen forms a specific complex with the product of the retinoblastoma susceptibility gene. Cell 1988, 54:275-83.

88. Detmar M, Pauli G, Anagnostopoulos I, Wunderlich U, Herbst H, Garbe C, Stein H, Orfanos CE: A case of classical mycosis fungoides associated with human T-cell lymphotropic virus type I. Br J Dermatol 1991, 124:198-202.

89. Di Leonardo A, Linke SP, Clarkin K, Wahl GM: DNA damage triggers a prolonged p53-dependent G1 arrest and long-term induction of Cip1 in normal human fibroblasts. Genes Dev 1994, 8:2540-51.

90. Dittmer J, Gitlin SD, Reid RL, Brady JN: Transactivation of the P2 promoter of parathyroid hormone-related protein by human T-cell lymphotropic virus type I Tax1: evidence for the involvement of transcription factor Ets1. J Virol 1993, 67:6087-95.

91. Donehower LA, Harvey M, Slagle BL, McArthur MJ, Montgomery CA, Jr., Butel JS, Bradley A: Mice deficient for p53 are developmentally normal but susceptible to spontaneous tumours. Nature 1992, 356:215-21.

92. Dowdy SF, Hinds PW, Louie K, Reed SI, Arnold A, Weinberg RA: Physical interaction of the retinoblastoma protein with human D cyclins. Cell 1993, 73:499-511.

93. Dube DK, Sherman MP, Saksena NK, Bryz Gornia V, Mendelson J, Love J, Arnold CB, Spicer T, Dube S, Glaser JB, et al. Genetic heterogeneity in human T-cell leukemia/lymphoma virus type II. J Virol 1993, 67:1175-84.

94. Duvall JF, Kashanchi F, Cvekl A, Radonovich MF, Piras G, Brady JN: Transactivation of the human T-cell lymphotropic virus type 1 Tax1-responsive 21-base-pair repeats requires Holo-TFIID and TFIIA. J Virol 1995, 69:5077-86.

95. Duyao MP, Kessler DJ, Spicer DB, Sonenshein GE: Transactivation of the c-myc gene by HTLV-1 tax is mediated by NFkB. Curr Top Microbiol Immunol 1992, 182:421-4.

96. Duyao MP, Kessler DJ, Spicer DB, Sonenshein GE: Transactivation of the murine c-myc gene by HTLV-1 tax is mediated by NFkB. AIDS Res Hum Retroviruses 1992, 8:752-4.

97. Dyson H, Howley PM, Munger K, Harlow E: The human papilloma virus type-16 E7 oncoprotein is able to bind to the retinoblastoma gene product. Science 1989, 243:934-7.

98. Eguchi K, Origuchi T, Takashima H, Iwata K, Katamine S, Nagataki S: High seroprevalence of anti-HTLV-I antibody in rheumatoid arthritis. Arthritis Rheum 1996, 39:463-6.

99. Eguchi K, Mizokami A, Katamine S: [HTLV-I infection in primary Sjogren's syndrome--epidemiological, clinical and virological studies]. Nippon Rinsho 1995, 53:2467-72.

100. Ellis PA, Saccani-Jotti G, Clarke R, Johnston SR, Anderson E, Howell A, A'Hern R, Salter J, Detre S, Nicholson R, et al. Induction of apoptosis by tamoxifen and ICI 182780 in primary breast cancer. Int J Cancer 1997, 72:608-13.

101. Emini EA, Hughes JV, Perlow DS, Boger J: Induction of hepatitis A virus-neutralizing antibody by a virus-specific synthetic peptide. Journal of Virology 1985, 55:836-9.

102. Erlandson RA: The enigmatic perineurial cell and its participation in tumors and in tumorlike entities. Ultrastruct Pathol 1991, 15:335-51.

103. Erlandson RA: Peripheral nerve sheath tumors. Ultrastruct Pathol 1985, 9:113-22.

104. Erlandson RA, Woodruff JM: Peripheral nerve sheath tumors: an electron microscopic study of 43 cases. Cancer 1982, 49:273-87.

105. Evan G, Wyllie A, Gilbert C, Littlewood T, Land H, Brooks M, Waters C, Penn L, Hancock D: Induction of apoptosis in fibroblasts by c-myc protein. Cell 1992, 69:119

106. Evan GI, Brown L, Whyte M, Harrington E: Apoptosis and the cell cycle. Current Opinion in Cell Biology 1995, 7:825-34.

107. Ewen ME, Sluss HK, Sherr CJ, Matsushime H, Kato JY, Livingston DM: Functional interactions of the retinoblastoma protein with mammalian D- type cyclins. Cell 1993, 73:487-97.

108. Feigenbaum L, Fujita K, Collins FS, Jay G: Repression of the NF1 gene by Tax may expain the development of neurofibromas in human T-lymphotropic virus type 1 transgenic mice. J Virol 1996, 70:3280-5.

109. Felber BK, Paskalis H, Kleinman Ewing C, Wong Staal F, Pavlakis GN: The pX protein of HTLV-I is a transcriptional activator of its long terminal repeats. Science 1985, 229:675-9.

110. Fox HB, Gutman PD, Dave HP, Cao SX, Mittelman M, Berg PE, Schechter AN: Trans-activation of human globin genes by HTLV-I tax1. Blood 1989, 74:2749-54.

111. Franchini G, Mulloy JC, Koralnik IJ, Lo Monico A, Sparkowski JJ, Andresson T, Goldstein DJ, Schlegel R: The human T-cell leukemia/lymphotropic virus type I p12I protein cooperates with the E5 oncoprotein of bovine papillomavirus in cell transformation and binds the 16-kilodalton subunit of the vacuolar H+ ATPase. J Virol 1993, 67:7701-4.

112. Franchini G, Wong Staal F, Gallo RC: Molecular studies of human T-cell leukemia virus and adult T-cell leukemia. J Invest Dermatol 1984, 83:63s-6s.

113. Franklin AA, Kubik MF, Uittenbogaard MN, Brauweiler A, Utaisincharoen P, Matthews MA, Dynan WS, Hoeffler JP, Nyborg JK: Transactivation by the human T-cell leukemia virus Tax protein is mediated through enhanced binding of activating transcription factor-2 (ATF-2) ATF-2 response and cAMP element-binding protein (CREB). J Biol Chem 1993, 268:21225-31.

114. Fujihara K, Goldman B, Oseroff AR, Glenister N, Jaffe ES, Bisaccia E, Pincus S, Greenberg SJ: HTLV-associated diseases: Human retroviral infection and cutaneous T-cell lymphomas. Immunological Investigations 1997, 26:231-42.

115. Fujii M, Chuhjo T, Minamino T, Masaaki N, Miyamoto K, Seiki M: Identification of the Tax interaction region of serum response factor that mediates the aberrant induction of immediate early genes through CArG boxes by HTLV-I Tax. Oncogene 1995, 11:7-14.

116. Fujii M, Tsuchiya H, Meng XB, Seiki M: c-Jun, c-Fos and their family members activate the transcription mediated by three 21-bp repetitive sequences in the HTLV-I long terminal repeat. Intervirology 1995, 38:221-8.

117. Fujii M, Tsuchiya H, Chuhjo T, Minamino T, Miyamoto K, Seiki M: Serum response factor has functional roles both in indirect binding to the CArG box and in the transcriptional activation function of human T-cell leukemia virus type I Tax. J Virol 1994, 68:7275-83.

118. Fujii M, Tsuchiya H, Chuhjo T, Akizawa T, Seiki M: Interaction of HTLV-1 Tax1 with p67SRF causes the aberrant induction of cellular immediate early genes through CArG boxes. Genes Dev 1992, 6:2066-76.

119. Fujii M, Niki T, Mori T, Matsuda T, Matsui M, Nomura N, Seiki M: HTLV-1 Tax induces expression of various immediate early serum responsive genes. Oncogene 1991, 6:1023-9.

120. Fujii M, Sassone Corsi P, Verma IM: c-fos promoter trans-activation by the tax1 protein of human T-cell leukemia virus type I. Proc Natl Acad Sci U S A 1988, 85:8526-30.

121. Fujisawa J, Toita M, Yoshimura T, Yoshida M: The indirect association of human T-cell leukemia virus tax protein with DNA results in transcriptional activation. J Virol 1991, 65:4525-8.

122. Furuta Y, Aizawa S, Suda Y, Ikawa Y, Kishimoto H, Asano Y, Tada T, Hikikoshi A, Yoshida M, Seiki M: Thymic atrophy characteristic in transgenic mice that harbor pX genes of human T-cell leukemia virus type I. J Virol 1989, 63:3185-9.

123. Garnier J, Osguthorpe DJ, Robson B: Analysis of the accuracy and implications of simple methods for predicting the secondary structure of globular proteins. J Mol Biol 1978, 120:97-120.

124. Garrick D, Fiering S, Martin DI, Whitelaw E: Repeat-induced gene silencing in mammals [In Process Citation]. Nat Genet 1998, 18:56-9.

125. Gegonne A, Bosselut R, Bailly RA, Ghysdael J: Synergistic activation of the HTLV1 LTR Ets-responsive region by transcription factors Ets1 and Sp1. EMBO J 1993, 12:1169-78.

126. Gessain A, Saal F, Gout O, Daniel MT, Flandrin G, de The G, Peries J, Sigaux F: High human T-cell lymphotropic virus type I proviral DNA load with polyclonal integration in peripheral blood mononuclear cells of French West Indian, Guianese, and African patients with tropical spastic paraparesis. Blood 1990, 75:428-33.

127. Ghosh S, Baltimore D: Activation *in vitro* of NF-*k*B by phosphorylation of its inhibitor I*k*B. Nature 1990, 344:678-82.

128. Giri JG, Ahdieh M, Eisenman J, Shaneback K, Grabstein K, Kumaki S, Namen D, Anderson D: Utilization of the □ and *g* chains of the IL-2 receptor by the novel cytokine IL-15. EMBO J 1994, 13:2822-30.

129. Gitlin SD, Dittmer J, Reid RL, et al. Cullen BR, editors.Human Retroviruses. Oxford, New York, Tokyo: IRL Press at Oxford University Press, 1993; 7, The molecular Biology of human T-cell Leukaemia viruses. p. 159-92.

130. Gitlin SD, Dittmer J, Shin RC, Brady JN: Transcriptional activation of the human T-lymphotropic virus type I long terminal repeat by functional interaction of Tax1 and Ets1. J Virol 1993, 67:7307-16.

131. Gitlin SD, Bosselut R, Gegonne A, Ghysdael J, Brady JN: Sequence-specific interaction of the Ets1 protein with the long terminal repeat of the human T-lymphotropic virus type I. J Virol 1991, 65:5513-23.

132. Gitlin SD, Lindholm PF, Marriott SJ, Brady JN: Transdominant human T-cell lymphotropic virus type I TAX1 mutant that fails to localize to the nucleus. J Virol 1991, 65:2612-21.

133. Goh WC, Sodroski J, Rosen C, Essex M, Haseltine WA: Subcellular localization of the product of the long open reading frame of human T-cell leukemia virus type I. Science 1985, 227:1227-8.

134. Goldstein DJ, Li W, Wang L, Heidaran MA, Aaronson SA, Shinn R, Schlegel R, Pierce JH: The bovine papillomavirus type 1 E5 transforming protein specifically binds and activates the □-type receptor for the platelet derived growth factor but not other related tyrosine kinase-containing receptors to induce cellular transformation. J Virol 1994, 68:4432-41.

135. Gonzalez Dunia D, Grimber G, Briand P, Brahic M, Ozden S: Tissue expression pattern directed in transgenic mice by the LTR of an HTLV-I provirus isolated from a case of tropical spastic paraparesis. Virology 1992, 187:705-10.

136. Goren I, Semmes OJ, Jeang KT, Moelling K: The amino terminus of Tax is required for interaction with the cyclic AMP response element binding protein. J Virol 1995, 69:5806-11.

137. Gout O, Baulac M, Gessain A, Semah F, Saal F, Peries J, Cabrol C, Foucault Fretz C, Laplane D, Sigaux F, et al. Rapid development of myelopathy after HTLV-I infection acquired by transfusion during cardiac transplantation. N Engl J Med 1990, 322:383-8.

138. Grana X, Reddy EP: Cell cycle control in mammalian cells: Role of cyclins, cyclin dependent kinases (CDKs), growth suppressor genes and cyclin-dependent kinase inhibitors (CKIs). Oncogene 1995, 11:211-9.

139. Grassmann R, Berchtold S, Radant I, Alt M, Fleckenstein B, Sodroski JG, Haseltine WA, Ramstedt U: Role of human T-cell leukemia virus type 1 X region proteins in immortalization of primary human lymphocytes in culture. J Virol 1992, 66:4570-5.

140. Grassmann R, Dengler C, Muller Fleckenstein I, Fleckenstein B, McGuire K, Dokhelar MC, Sodroski JG, Haseltine WA: Transformation to continuous growth of primary human T lymphocytes by human T-cell leukemia virus type I X-region genes transduced by a Herpesvirus saimiri vector. Proc Natl Acad Sci U S A 1989, 86:3351-5.

141. Green JE, Baird AM, Hinrichs SH, Klintworth GK, Jay G: Adrenal medullary tumors and iris proliferation in a transgenic mouse model of neurofibromatosis. Am J Pathol 1992, 140:1401-10.

142. Green JE: trans activation of nerve growth factor in transgenic mice containing the human T-cell lymphotropic virus type I tax gene. Mol Cell Biol 1991, 11:4635-41.

143. Green JE, Hinrichs SH, Vogel J, Jay G: Exocrinopathy resembling Sjogren's syndrome in HTLV-1 tax transgenic mice. Nature 1989, 341:72-4.

144. Griffiths DJ, Venables PJ, Weiss RA, Boyd MT: A novel exogenous retrovirus sequence identified in humans. J Virol 1997, 71:2866-72.

145. Grone M, Koch C, Grassmann R: The HTLV-1 Rex protein induces nuclear accumulation of unspliced viral RNA by avoiding intron excision and degradation. Virology 1996, 218:316-25.

146. Grone M, Hoffmann E, Berchtold S, Cullen BR, Grassmann R: A single stem-loop structure within the HTLV-1 Rex response element is sufficient to mediate Rex activity in vivo. Virology 1994, 204:144-52.

147. Grossman WJ, Ratner L: Transgenic mouse models for HTLV-I infection. Journal of Acquired Immune Deficiency Syndromes and Human Retrovirology 1996, 13:S162-9.

148. Grossman WJ, Kimata JT, Wong FH, Zutter M, Ley TJ, Ratner L: Development of leukemia in mice transgenic for the tax gene of human T-cell leukemia virus type I. Proc Natl Acad Sci U S A 1995, 92:1057-61.

149. Haas-Kogan DA, Kogan SC, Levi D, Dazin P, T'Ang A, Fung YT, Israel MA: Inhibition of apoptosis by the retinoblastoma gene product. EMBO J 1996, 14:461-72.

150. Hall AP, Irvine J, Blyth K, Cameron ER, Onions DE, Campbell ME: Tumours derived from HTLV-I tax transgenic mice are characterized by enhanced levels of apoptosis and oncogene expression. J Pathol 1998, 186:209-14.

151. Hall WW, Liu CR, Schneewind O, Takahashi H, Kaplan MH, Roupe G, Vahlne A: Deleted HTLV-I provirus in blood and cutaneous lesions of patients with mycosis fungoides [see comments]. Science 1991, 253:317-20.

152. Harkin JC: Pathology of nerve sheath tumors. Ann N Y Acad Sci 1986, 486:147-54:147-54.

153. Harrington EA, Bennett MR, Fanidi A, Evan GI: c-Myc-induced apoptosis in fibroblasts is inhibited by specific cytokines. EMBO J 1994, 13:3286-95.

154. Harvey M, McArthur MJ, Montgomery CA, Jr., Butel JS, Bradley A, Donehower LA: Spontaneous and carcinogen-induced tumorigenesis in p53-deficient mice [see comments]. Nat Genet 1993, 5:225-9.

155. Hatakeyama M, Kono T, Kobayashi N, Kawahara A, Levin SD, Perlmutter RM, Taniguchi T: Interaction of the IL-2 receptor with the src-family kinase $p56^{lck}$: identification of novel intermolecular association. Science 1991, 252:1523-8.

156. Hatta Y, Hirama T, Miller CW, Yamada Y, Tomonaga M, Koeffler HP: Homozygous deletions of the p15 (MTS2) and p16 (CDKN2/MTS1) genes in adult T-cell leukemia. Blood 1995, 85:2699-704.

157. Haupt Y, Rowan S, Oren M: p53-mediated apoptosis in Hela cells can be overcome by excess pRB. Oncogene 1995, 10:1563-71.

158. Hayward GS. Immediate-early gene regulation in herpes simplex virus. [Abstract] Semin virol 1993;4:15-23.

159. Hayward WS, Neel BG, Astrin SM: Activation of a cellular onc gene by promoter insertion in ALV-induced lymphoid leukosis. Nature 1981, 290:475-80.

160. Hidaka M, Inoue J, Yoshida M, Seiki M: Post-transcriptional regulator (rex) of HTLV-1 initiates expression of viral structural proteins but suppresses expression of regulatory proteins. EMBO J 1988, 7:519-23.

161. Himes SR, Coles LS, Katsikeros R, Lang RK, Shannon MF: HTLV-1 tax activation of the GM-CSF and G-CSF promoters requires the interaction of NF-kB with other transcription factor families. Oncogene 1993, 8:3189-97.

162. Hinds PW, Mittnacht S, Dulic V, Arnold A, Reed SI, Weinberg RA: Regulation of retinoblastoma proteins functions by ectopic expression of human cyclins. Cell 1996, 70:993-1006.

163. Hino S, Katamine S, Kawase K, Miyamoto T, Doi H, Tsuji Y, Yamabe T: Intervention of maternal transmission of HTLV-1 in Nagasaki, Japan. Leukemia 1994, 8 Suppl 1:S68-70.

164. Hino S: Milk-borne transmission of HTLV-I as a major route in the endemic cycle. Acta Paediatr Jpn 1989, 31:428-35.

165. Hinrichs SH, Nerenberg M, Reynolds RK, Khoury G, Jay G: A transgenic mouse model for human neurofibromatosis. Science 1987, 237:1340-3.

166. Hinuma Y, Nagata K, Hanaoka M: Adult T-cell Leukaemia: antigen in an ATL cell line and detection of antibodies to the antigen in human sera. Proc Natl Acad Sci U S A 1981, 78:6467-80.

167. Hirai H, Suzuki T, Fujisawa J, Inoue J, Yoshida M: Tax protein of human T-cell leukemia virus type I binds to the ankyrin motifs of inhibitory factor kappa B and induces nuclear translocation of transcription factor NF-kappa B proteins for transcriptional activation. Proc Natl Acad Sci U S A 1994, 91:3584-8.

168. Hirai H, Fujisawa J, Suzuki T, Ueda K, Muramatsu M, Tsuboi A, Arai N, Yoshida M: Transcriptional activator Tax of HTLV-1 binds to the NF-kappa B precursor p105. Oncogene 1992, 7:1737-42.

169. Hirama T, Koeffler HP: Role of the cyclin-dependent kinase inhibitors in the development of cancer. Blood 1995, 86:841-54.

170. Hirano Y, Yamato K, Tsuchida N: A temperature sensitive mutant of the human p53, Val138, arrests rat cell growth without induced expression of cip1/waf1/sdi1 after temperature shift-down. Oncogene 1995, 10:1879-85.

171. Hiscott J, Petropoulos L, Lacoste J: Molecular interactions between HTLV-1 Tax protein and the NF-kappa B/kappa B transcription complex. Virology 1995, 214:3-11.

172. Hjelle B: Chronic neurodegenerative disease associated with HTLV-II infection. Lancet 1992, 339:645-6.

173. Hjelle B, Mills R, Swenson S, Mertz G, Key C, Allen S: Incidence of hairy cell leukemia, mycosis fungoides, and chronic lymphocytic leukemia in first known HTLV-II-endemic population. J Infect Dis 1991, 163:435-40.

174. Hoffman PM, Cimino EF, Robbins DS, Broadwell RD, Powers JM, Ruscetti SK: Cellular tropism and localization in the rodent nervous system of a neuropathogenic variant of Friend murine leukemia virus. Lab Invest 1992, 67:314-21.

175. Hollstein M, Rice K, Greenblatt MS, Soussi T, Fuchs R, Sorlie T, Hovig E, SmithSorensen B, Montesano R, Harris CC: Database of p53 gene somatic mutations in human tumors and cell lines. Nucleic Acids Research 1994, 22:3551-5.

176. Hollstein M, Sidransky D, Vogelstein B, Harris CC: p53 Mutations in human cancers. Science 1991, 253:49-53.

177. Hooper WC, Rudolph DL, Lairmore MD, Lal RB: Constitutive expression of c-jun and jun-B in cell lines infected with human T-lymphotropic virus types I and II. Biochem Biophys Res Commun 1991, 181:976-80.

178. Hope IA, Mahadevan S, Struhl K: Structural and functional characterization of the short acidic transcriptional activation region of yeast GCN4 protein. Nature 1988, 333:635-40.

179. Hopp TP, Woods KR: Prediction of protein antigenic determinants from amino acid sequences. Proceedings of the National Academy of Sciences of the United States of America 1981, 78:3824-8.

180. Hoyos B, Ballard DW, Bohnlein E, Siekevitz M, Greene WC: Kappa B-specific DNA binding proteins: role in the regulation of human interleukin-2 gene expression. Science 1989, 244:457-60.

181. Hsu B, Marin MC, el-Naggar AK, Stephens LC, Brisbay S, McDonnell TJ: Evidence that c-myc mediated apoptosis does not require wild-type p53 during lymphomagenesis. Oncogene 1995, 11:175-9.

182. Hunter T, Pines J: Cyclins and cancer II: Cyclin D and CDK inhibitors come of age. Cell 1994, 79:573-82.

183. Ichimaru M, Ikeda S, Kinoshita K, Hino S, Tsuji Y: Mother-to-child transmission of HTLV-1. Cancer Detect Prev 1991, 15:177-81.

184. Ihle JN. Cytokine receptor signalling. [Abstract] Nature 1995;377:(19 Oct.)591-4.

185. Ina Y, Gojobori T: Molecular evolution of human T-cell leukemia virus. J Mol Evol 1990, 31:493-9.

186. Inoue J, Seiki M, Taniguchi T, Tsuru S, Yoshida M: Induction of interleukin 2 receptor gene expression by p40x encoded by human T-cell leukemia virus type 1. EMBO J 1986, 5:2883-8.

187. Iwakura Y, Tosu M, Yoshida E, Saijo S, Nakayama Yamada J, Itagaki K, Asano M, Siomi H, Hatanaka M, Takeda T, et al. Augmentation of c-fos and c-jun expression in transgenic mice carrying the human T-cell leukemia virus type-I tax gene. Virus Genes 1995, 9:161-70.

188. Iwakura Y, Tosu M, Yoshida E, Takiguchi M, Sato K, Kitajima I, Nishioka K, Yamamoto K, Takeda T, Hatanaka M, et al. Induction of inflammatory arthropathy resembling rheumatoid arthritis in mice transgenic for HTLV-I. Science 1991, 253:1026-8.

189. Iwasaki Y, Ohara Y, Kobayashi I, Akizuki S: Infiltration of helper/inducer T lymphocytes heralds central nervous system damage in human T-cell leukemia virus infection. Am J Pathol 1992, 140:1003-8.

190. Iwasaki Y: Pathology of chronic myelopathy associated with HTLV-I infection (HAM/TSP). J Neurol Sci 1990, 96:103-23.

191. Izumo S, Umehara F, Kashio N, Kubota R, Sato E, Osame M: Neuropathology of HTLV-1-associated myelopathy (HAM/TSP) [In Process Citation]. Leukemia 1997, 11 Suppl 3:82-4:82-4.

192. Jackwood MW, Hilt DA: Production and immunogenicity of multiple antigenic peptide (MAP) constructs derived from the S1 glycoprotein of infectious bronchitis virus (IBV). Advances in Experimental Medicine and Biology 1995, 380:213-9.

193. Jacobson S, Lehky T, Nishimura M, Robinson S, McFarlin DE, Dhib Jalbut S: Isolation of HTLV-II from a patient with chronic, progressive neurological disease clinically indistinguishable from HTLV-I-associated myelopathy/tropical spastic paraparesis. Ann Neurol 1993, 33:392-6.

194. Jacobson S, Shida H, McFarlin DE, Fauci AS, Koenig S: Circulating CD8+ cytotoxic T lymphocytes specific for HTLV-I pX in patients with HTLV-I associated neurological disease. Nature 1990, 348:245-8.

195. Jacobson S, Raine CS, Mingioli ES, McFarlin DE: Isolation of an HTLV-1-like retrovirus from patients with tropical spastic paraparesis. Nature 1988, 331:540-3.

196. Jameson BA, Wolf H: The antigenic index: A novel algorithm for predicting antigenic determinants. Computer Applications in the Biosciences 1988, 4:181-6.

197. Jeang KT, Chiu R, Santos E, Kim SJ: Induction of the HTLV-I LTR by Jun occurs through the Tax-responsive 21-bp elements. Virology 1991, 181:218-27.

198. Jeang KT, Widen SG, Semmes OJ, 4th, Wilson SH: HTLV-I trans-activator protein, tax, is a trans-repressor of the human beta-polymerase gene. Science 1990, 247:1082-4.

199. Jin DY, Spencer F, Jeang KT: Human T cell leukemia virus type 1 oncoprotein Tax targets the human mitotic checkpoint protein MAD1 [In Process Citation]. Cell 1998, 93:81-91.

200. Jin DY, Jeang KT: HTLV-I Tax self-association in optimal trans-activation function. Nucleic Acids Res 1997, 25:379-87.

201. Jones CLA, Kane MA: Oncogenic signalling. Curr Opin Oncol 1996, 8:54-9.

202. Josephs SF, Wong Staal F, Manzari V, Gallo RC, Sodroski JG, Trus MD, Perkins D, Patarca R, Haseltine WA: Long terminal repeat structure of an American isolate of type I human T-cell leukemia virus. Virology 1984, 139:340-5.

203. Joshi JB, Dave HP: Transactivation of the proenkephalin gene promoter by the Tax1 protein of human T-cell lymphotropic virus type I. Proc Natl Acad Sci U S A 1992, 89:1006-10.

204. Jurecka W: Neurogenic tumors of the skin. Wien Klin Wochenschr Suppl 1987, 176:3-16:3-16.

205. Kamada N, Sakurai M, Miyamoto K, Sanada I, Sadamori N, Fukuhara S, Abe S, Shiraishi Y, Abe T, Kaneko Y, et al. Chromosome abnormalities in adult T-cell leukemia/lymphoma: a karyotype review committee report. Cancer Res 1992, 52:1481-93.

206. Kamb A: Sun protection factor p53. Nature 1994, 372:730-1.

207. Kamihira S, Sohda H, Atogami S, Toriya K, Yamada Y, Tsukazaki K, Momita S, Ikeda S, Kusano M, Amagasaki T, et al. Phenotypic diversity and prognosis of adult T-cell leukemia. Leuk Res 1992, 16:435-41.

208. Kanamori H, Suzuki N, Siomi H, Nosaka T, Sato A, Sabe H, Hatanaka M, Honjo T: HTLV-1 p27rex stabilizes human interleukin-2 receptor alpha chain mRNA. EMBO J 1990, 9:4161-6.

209. Kang Y, Cortina R, Perry RR: Role of c-myc in tamoxifen-induced apoptosis estrogen-independent breast cancer cells [see comments]. J Natl Cancer Inst 1996, 88:279-84.

210. Kannagi M, Shida H, Igarashi H, Kuruma K, Murai H, Aono Y, Maruyama I, Osame M, Hattori T, Inoko H, et al. Target epitope in the Tax protein of human T-cell leukemia virus type I recognized by class I major histocompatibility complex-restricted cytotoxic T cells. J Virol 1992, 66:2928-33.

211. Kanno T, Franzoso G, Siebenlist U: Human T-cell leukemia virus type I Tax-protein-mediated activation of NF-kappa B from p100 (NF-kappa B2)-inhibited cytoplasmic reservoirs. Proc Natl Acad Sci U S A 1994, 91:12634-8.

212. Karplus PA, Schulz GE: Prediction of chain flexibility in proteins. A tool for the selection of peptide antigens. Naturwissenschaften 1985, 72:212-3.

213. Kashanchi F, Duvall JF, Dittmer J, Mireskandari A, Reid RL, Gitlin SD, Brady JN: Involvement of transcription factor YB-1 in human T-cell lymphotropic virus type I basal gene expression. J Virol 1994, 68:561-5.

214. Kastan MB, Onkyekwere O, Sidransky D, Vogelstein B, Craig RW: Participation of the p53 protein in the cellular response to DNA damage. Cancer Res 1991, 51:6304-11.

215. Kawano F, Yamaguchi K, Nishimura H, Tsuda H, Takatsuki K: Variation in the clinical course of Adult T-cell Leukaemia. Cancer 1985, 55:851-6.

216. Kellen JA: Genomic effects of tamoxifen. Anticancer Res 1996, 16:3537-41.

217. Kelly K, Davis P, Mitsuya H, Irving S, Wright J, Grassmann R, Fleckenstein B, Wano Y, Greene W, Siebenlist U: A high proportion of early response genes are constitutively activated in T cells by HTLV-I. Oncogene 1992, 7:1463-70.

218. Kemp CJ, Donehower LA, Bradley A, Balmain A: Reduction of p53 gene dosage does not increase initiation or promotion but enhances malignant progression of chemically induced skin tumors. Cell 1993, 74:813-22.

219. Kharbanda K, Dinda AK, Sarkar C, Karak AK, Mathur M, Roy S: Cell culture studies on human nerve sheath tumors. Pathology 1994, 26:29-32.

220. Kim SJ, Winokur TS, Lee HD, Danielpour D, Kim KY, Geiser AG, Chen LS, Sporn MB, Roberts AB, Jay G: Overexpression of transforming growth factor-beta in transgenic mice carrying the human T-cell lymphotropic virus type I tax gene. Mol Cell Biol 1991, 11:5222-8.

221. King RW, Jackson PK, Kirschner MW: Mitosis in transition. Cell 1994, 79:563-71.

222. Kira J, Itoyama Y, Koyanagi Y, Tateishi J, Kishikawa M, Akizuki S, Kobayashi I, Toki N, Sueishi K, Sato H, et al. Presence of HTLV-I proviral DNA in central nervous system of patients with HTLV-I-associated myelopathy. Ann Neurol 1992, 31:39-45.

223. Kira J, Koyanagi Y, Yamada T, Itoyama Y, Goto I, Yamamoto N, Sasaki H, Sakaki Y: Increased HTLV-I proviral DNA in HTLV-I-associated myelopathy: a quantitative polymerase chain reaction study [published erratum appears in Ann Neurol 1991 Apr;29(4):363]. Ann Neurol 1991, 29:194-201.

224. Kishi S, Saijyo S, Arai M, Karasawa S, Ueda S, Kannagi M, Iwakura Y, Fujii M, Yonehara S: Resistance to fas-mediated apoptosis of peripheral T cells in human T lymphocyte virus type I (HTLV-I) transgenic mice with autoimmune arthropathy [In Process Citation]. J Exp Med 1997, 186:57-64.

225. Kitajima I, Shinohara T, Bilakovics J, Brown DA, Xu X, Nerenberg M: Ablation of transplanted HTLV-I Tax-transformed tumors in mice by antisense inhibition of NF-kappa B [published erratum appears in Science 1993 Mar 12;259(5101):1523]. Science 1992, 258:1792-5.

226. Kitajima I, Yamamoto K, Sato K, Nakajima Y, Nakajima T, Maruyama I, Osame M, Nishioka K: Detection of human T cell lymphotropic virus type I proviral DNA and its gene expression in synovial cells in chronic inflammatory arthropathy. J Clin Invest 1991, 88:1315-22.

227. Kiyokawa T, Seiki M, Iwashita S, Imagawa K, Shimizu F, Yoshida M: p27x-III and p21x-III, proteins encoded by the pX sequence of human T-cell leukemia virus type I. Proc Natl Acad Sci U S A 1985, 82:8359-63.

228. Kiyokawa T, Seiki M, Imagawa K, Shimizu F, Yoshida M: Identification of a protein (p40x) encoded by a unique sequence pX of human T-cell leukemia virus type I. Gann 1984, 75:747-51.

229. Komurian F, Pelloquin F, de The G: In vivo genomic variability of human T-cell leukemia virus type I depends more upon geography than upon pathologies. J Virol 1991, 65:3770-8.

230. Koralnik IJ, Mulloy JC, Andresson T, Fullen J, Franchini G: Mapping of the intermolecular association of human T cell leukaemia/lymphotropic virus type I p12I and the vacuolar H+-ATPase 16 kDa subunit protein. J Gen Virol 1995, 76:1909-16.

231. Koralnik IJ, Fullen J, Franchini G: The p12I, p13II, and p30II proteins encoded by human T-cell leukemia/lymphotropic virus type I open reading frames I and II are localized in three different cellular compartments. J Virol 1993, 67:2360-6.

232. Koralnik IJ, Gessain A, Klotman ME, Lo Monico A, Berneman ZN, Franchini G: Protein isoforms encoded by the pX region of human T-cell leukemia/lymphotropic virus type I. Proc Natl Acad Sci U S A 1992, 89:8813-7.

233. Korber B, Okayama A, Donnelly R, Tachibana N, Essex M: Polymerase chain reaction analysis of defective human T-cell leukemia virus type I proviral genomes in leukemic cells of patients with adult T-cell leukemia. J Virol 1991, 65:5471-6.

234. Kramer A, Maloney EM, Morgan OS, Rodgers Johnson P, Manns A, Murphy EL, Larsen S, Cranston B, Murphy J, Benichou J, et al. Risk factors and cofactors for human T-cell lymphotropic virus type I (HTLV-I)-associated myelopathy/tropical spastic paraparesis (HAM/TSP) in Jamaica. Am J Epidemiol 1995, 142:1212-20.

235. Kubota S, Hatanaka M, Pomerantz RJ: Nucleo-cytoplasmic redistribution of the HTLV-I Rex protein: alterations by coexpression of the HTLV-I p21x protein. Virology 1996, 220:502-7.

236. Kuerbitz SJ, Plunkett BS, Walsh WV, Katan MB: Wild-type p53 is a cell cycle checkpoint determinant following irradiation. Proc Natl Acad Sci U S A 1992, 89:7491-5.

237. Kung H, Boerkoel C, Carter TH: Retroviral mutagenesis of cellular oncogenes: a review with insights into the mechanisms of insertional activation. Curr Top Microbiol Immunol 1991, 171:1-25.

238. Kwok RP, Laurance ME, Lundblad JR, Goldman PS, Shih H, Connor LM, Marriott SJ, Goodman RH: Control of cAMP-regulated enhancers by the viral transactivator Tax through CREB and the co-activator CBP. Nature 1996, 380:642-6.

239. Lacoste J, Petropoulos L, Pepin N, Hiscott J: Constitutive phosphorylation and turnover of I kappa B alpha in human T-cell leukemia virus type I-infected and Tax-expressing T cells. J Virol 1995, 69:564-9.

240. LaGrenade L, Sonoda S, Miller W, Pate E, Rodgers Johnson P, Hanchard B, Cranston B, Fujiyoshi T, Yashiki S, Blank M, et al. HLA DRB1*DQB1* haplotype in HTLV-I-associated familial infective dermatitis may predict development of HTLV-I-associated myelopathy/tropical spastic paraparesis. Am J Med Genet 1996, 61:37-41.

241. LaGrenade L, Hanchard B, Fletcher V, Cranston B, Blattner W: Infective dermatitis of Jamaican children: a marker for HTLV-I infection [see comments]. Lancet 1990, 336:1345-7.

242. Lal RB, Rudolph DL: Constitutive production of interleukin-6 and tumor necrosis factor-alpha from spontaneously proliferating T cells in patients with human T-cell lymphotropic virus type-I/II. Blood 1991, 78:571-4.

243. Lanoix J, Lacoste J, Pepin N, Rice N, Hiscott J: Overproduction of NFKB2 (lyt-10) and c-Rel: a mechanism for HTLV-I Tax-mediated trans-activation via the NF-kappa B signalling pathway. Oncogene 1994, 9:841-52.

244. Lassmann H, Jurecka W, Lassmann G, Gebhart W, Matras H, Watzek G: Different types of benign nerve sheath tumors. Light microscopy, electron microscopy and autoradiography. Virchows Arch A Pathol Pathol Anat 1977, 375:197-210.

245. Lazarides E: Intermediate filaments as mechanical integrators of cellular space. Nature 1980, 283:249-56.

246. Lee B, Tanaka Y, Tozawa H: Monoclonal antibody defining tax protein of human T-cell leukemia virus type-I. Tohoku J Exp Med 1989, 157:1-11.

247. Lee SY, Mastushita K, Machida J, Tajiri M, Yamaguchi K, Takatsuki K: Human T-cell leukemia virus type I infection in hemodialysis patients. Cancer 1987, 60:1474-8.

248. Lehky TJ, Fox CH, Koenig S, Levin MC, Flerlage N, Izumo S, Sato E, Raine CS, Osame M, Jacobson S: Detection of human T-lymphotropic virus type I (HTLV-I) tax RNA in the central nervous system of HTLV-I-associated myelopathy/tropical spastic paraparesis patients by in situ hybridization [see comments]. Ann Neurol 1995, 37:167-75.

249. Lemasson I, Robert-Hebmann V, Hamaia S, Duc Dodon M, Gazzolo L, Devaux C: Transrepression of lck gene expression by human T-cell leukemia virus type 1-encoded p40tax. J Virol 1997, 71:1975-83.

250. Leung K, Nabel GJ: HTLV-1 transactivator induces interleukin-2 receptor expression through an NF-kappa B-like factor. Nature 1988, 333:776-8.

251. Li CC, Ruscetti FW, Rice NR, Chen E, Yang NS, Mikovits J, Longo DL: Differential expression of Rel family members in human T-cell leukemia virus type I-infected cells: transcriptional activation of c-rel by Tax protein. J Virol 1993, 67:4205-13.

252. Lilienbaum A, Duc Dodon M, Alexandre C, Gazzolo L, Paulin D: Effect of human T-cell leukemia virus type I tax protein on activation of the human vimentin gene. J Virol 1990, 64:256-63.

253. Lindholm PF, Tamami M, Makowski J, Brady JN: Human T-cell lymphotropic virus type 1 Tax1 activation of NF-kappaB: involvement of the protein kinase C pathway. J Virol 1996, 70:2525-32.

254. Lindholm PF, Reid RL, Brady JN: Extracellular Tax1 protein stimulates tumor necrosis factor-beta and immunoglobulin kappa light chain expression in lymphoid cells. J Virol 1992, 66:1294-302.

255. Lindholm PF, Marriott SJ, Gitlin SD, Bohan CA, Brady JN: Induction of nuclear NF-kappa B DNA binding activity after exposure of lymphoid cells to soluble tax1 protein. New Biol 1990, 2:1034-43.

256. Linzer DI, Levine AJ: Characterisation of 54K dalton cellular SV40 tumour antigen present in SV40-transformed cells and uninfected embryonal carcinoma cells. Cell 1979, 17:43-52.

257. Lion T, Razvi N, Golomb HM, Brownstein RH: B-lymphocytic hairy cells contain no HTLV-II DNA sequences. Blood 1988, 72:1428-30.

258. Lisby G, Reitz MS, Jr., Vejlsgaard GL: No detection of HTLV-I DNA in punch skin biopsies from patients with cutaneous T-cell lymphoma by the polymerase chain reaction [see comments]. J Invest Dermatol 1992, 98:417-20.

259. Littlewood TD, Hancock DC, Danielian PS, Parker MG, Evan GI: A modified oestrogen receptor ligand-binding domain as an improved switch for the regulation of heterologous proteins. Nucleic Acids Research 1995, 23:1686-90.

260. Liu X, Zachar V, Hager H, Koppelhus U, Ebbesen P: Transfer of human T cell lymphotropic virus type I to human term trophoblast cells in vitro. J Gen Virol 1996, 77:369-74.

261. Liu ZG, Hsu H, Goeddel DV, Karin M: Dissection of TNF receptor 1 effector functions: JNK activation is not linked to apoptosis while NF-kappaB activation prevents cell death. Cell 1996, 87:565-76.

262. Livingstone LR, White A, Sprouse J, Livanos E, Jacks T, Tisty TD: Altered cell cycle arrest and gene amplification potential accompany loss of wild-type p53. Cell 1992, 70:923-35.

263. Loughran TP, Jr., Sherman MP, Ruscetti FW, Frey S, Coyle T, Montagna RA, Jones B, Starkebaum G, Poiesz BJ: Prototypical HTLV-I/II infection is rare in LGL leukemia. Leuk Res 1994, 18:423-9.

264. Loughran TP, Jr., Coyle T, Sherman MP, Starkebaum G, Ehrlich GD, Ruscetti FW, Poiesz BJ: Detection of human T-cell leukemia/lymphoma virus, type II, in a patient with large granular lymphocyte leukemia. Blood 1992, 80:1116-9.

265. Low KG, Dorner LF, Fernando DB, Grossman J, Jeang KT, Comb MJ: Human T-cell leukemia virus type 1 Tax releases cell cycle arrest induced by p16INK4a. J Virol 1997, 71:1956-62.

266. Lowe SW, Ruley HE, Jacks T, Housman DE: p53-dependent apoptosis modulates the cytotoxicity of anticancer agents. Cell 1993, 74:957-67.

267. Lowe SW, Schmitt EM, Smith SW, Osborne BA, Jacks T: p53 is required for radiation-induced apoptosis in mouse thymocytes. Nature 1993, 362:847-9.

268. Lutchman M, Rouleau GA: The neurofibromatosis type 2 gene product, schwannomin, suppresses growth of NIH 3T3 cells. Cancer Res 1995, 55:2270-4.

269. Lutzker SG, Levine AJ: A functionally inactive p53 protein in teratocarcinoma cells is activated by either DNA damage or cellular differentiation. Nat Med 1996, 2:804-10.

270. Maggirwar SB, Harhaj E, Sun SC: Activation of NF-kappa B/Rel by Tax involves degradation of I kappa B alpha and is blocked by a proteasome inhibitor. Oncogene 1995, 11:993-8.

271. Mahieux R, Ibrahim F, Mauclere P, Herve V, Michel P, Tekaia F, Chappey C, Garin B, van der Ryst E, Guillemain B, et al. Molecular epidemiology of 58 new African human T-cell leukemia virus type 1 (HTLV-1) strains: identification of a new and distinct HTLV-1 molecular subtype in Central Africa and in Pygmies. J Virol 1997, 71:1317-33.

272. Mahieux R, de The G, Gessain A: The tax mutation at nucleotide 7959 of human T-cell leukemia virus type 1 (HTLV-1) is not associated with tropical spastic paraparesis/HTLV-1-associated myelopathy but is linked to the cosmopolitan molecular genotype [letter]. J Virol 1995, 69:5925-7.

273. Malik KT, Even J, Karpas A: Molecular cloning and complete nucleotide sequence of an adult T cell leukaemia virus/human T cell leukaemia virus type I (ATLV/HTLV-I) isolate of Caribbean origin: relationship to other members of the ATLV/HTLV-I subgroup. J Gen Virol 1988, 69:1695-710.

274. Manns A, Wilks RJ, Murphy EL, Haynes G, Figueroa JP, Barnett M, Hanchard B, Blattner WA: A prospective study of transmission by transfusion of HTLV-I and risk factors associated with seroconversion. Int J Cancer 1992, 51:886-91.

275. Manzari V, Gismondi A, Barillari G, Morrone S, Modesti A, Albonici L, De Marchis L, Fazio V, Gradilone A, Zani M, et al. HTLV-V: a new human retrovirus isolated in a Tac-negative T cell lymphoma/leukemia. Science 1987, 238:1581-3.

276. Mariette X, Cherot P, Cazals D, Brocheriou C, Brouet JC, Agbalika F, Belec L, Georges MC, Pillot J, Georges A, et al. Antibodies to HTLV-I in Sjogren's syndrome (23). Lancet 1995, 345:71-2.

277. Mariette X, Agbalika F, Daniel MT, Bisson M, Lagrange P, Brouet JC, Morinet F: Detection of human T lymphotropic virus type I tax gene in salivary gland epithelium from two patients with Sjogren's syndrome. Arthritis Rheum 1993, 36:1423-8.

278. Marriott SJ, Trinh D, Brady JN: Activation of interleukin-2 receptor alpha expression by extracellular HTLV-I Tax1 protein: a potential role in HTLV-I pathogenesis. Oncogene 1992, 7:1749-55.

279. Marriott SJ, Lindholm PF, Reid RL, Brady JN: Soluble HTLV-I Tax1 protein stimulates proliferation of human peripheral blood lymphocytes. New Biol 1991, 3:678-86.

280. Marriott SJ, Boros I, Duvall JF, Brady JN: Indirect binding of human T-cell leukemia virus type I tax1 to a responsive element in the viral long terminal repeat. Mol Cell Biol 1989, 9:4152-60.

281. Martin GA, Viskochil D, Bollag G, McCabe PC, Crosier WJ, Haubruck H, Conroy L, Clark R, O'Connell P, Cawthon RM: The GAP-related domain of the neurofibromatosis type 1 gene product interacts with ras p21. Cell 1990, 63:843-9.

282. Maruyama M, Shibuya H, Harada H, Hatakeyama M, Seiki M, Fujita T, Inoue J, Yoshida M, Taniguchi T: Evidence for aberrant activation of the interleukin-2 autocrine loop by HTLV-1-encoded p40x and T3/Ti complex triggering. Cell 1987, 48:343-50.

283. Massie B, Couture F, Lamoureux L, Mosser DD, Guilbault C, Jolicoeur P, Belanger F, Langelier Y: Inducible overexpression of a toxic protein by an adenovirus vector with a tetracycline-regulatable expression cassette. J Virol 1998, 72:2289-96.

284. Mathieu Mahul D, Caubet JF, Bernheim A, Mauchauffle M, Palmer E, Berger E: Molecular cloning of a DNA fragment from human chromosome 14(14q11) involved in T-cell malignancies. EMBO J 1985, 4:3427-33.

285. Matsumoto K, Akashi K, Shibata H, Yutsudo M, Hakura A: Single amino acid substitution (58Pro-->Ser) in HTLV-I tax results in loss of ras cooperative focus formation in rat embryo fibroblasts. Virology 1994, 200:813-5.

286. Matsuzaki H, Yamaguchi K, Kagimoto Te: Monoclonal gammopathies in adult T-cell leukaemia. Cancer 1985, 56:1380-3.

287. McDonnell TJ, Korsmeyer SJ: Progression from lymphoid hyperplasia to high-grade malignant lymphoma in mice transgenic for the t(14; 18). Nature 1991, 349:254-6.

288. McGee JO, Isaacson PG, Wright NA. AnonymousOxford Textbook of Pathology. Oxford: Oxford University Press, 1992;p. 1885-2124.

289. Mckeithan TW, Shima EA, Le Beau MM, Minowada J, Rowley JD, Diaz MO: Molecular cloning of the breakpoint junction of a human chromosomal 8;14 translocation involving the T-cell receptor alpha-chain and sequences on the 3' side of MYC. Proc Natl Acad Sci U S A 1986, 83:6636-40.

290. McLaren RD, Prosser CG, Grieve RC, Borissenko M: The use of caprylic acid for the extraction of the immunoglobulin fraction from egg yolk of chickens immunised with ovine alpha- lactalbumin. J Immunol Methods 1994, 177:175-84.

291. Michalovitz D, Halevy O, Oren M: Conditional inhibtion of Transformation and of Cell Proliferation by a Temperature-sensitive mutant of p53. Cell 1990, 62:671-80.

292. Migone TS, Lin JX, Cereseto A, Mulloy JC, O'Shea JJ, Franchini G, Leonard WJ: Constitutively activated Jak-STAT pathway in T cells transformed with HTLV-I. Science 1995, 269:79-81.

293. Mita S, Sugimoto M, Nakamura M, Murakami T, Tokunaga M, Uyama E, Araki S: Increased human T lymphotropic virus type-1 (HTLV-1) proviral DNA in peripheral blood mononuclear cells and bronchoalveolar lavage cells from Japanese patients with HTLV-1-associated myelopathy. Am J Trop Med Hyg 1993, 48:170-7.

294. Mitchison NA: The carrier effect in the secondary immune response to hapten-protein conjugates. V. Use of antilymphocyte serum to deplete animals of helper cells. Eur J Immunol 1971, 1:68-75.

295. Miura S, Ohtani K, Numata N, Niki M, Ohbo K, Ina Y, Gojobori T, Tanaka Y, Tozawa H, Nakamura M, et al. Molecular cloning and characterization of a novel glycoprotein, gp34, that is specifically induced by the human T-cell leukemia virus type I transactivator p40tax. Mol Cell Biol 1991, 11:1313-25.

296. Miura T, Fukunaga T, Igarashi T, Yamashita M, Ido E, Funahashi S, Ishida T, Washio K, Ueda S, Hashimoto K, et al. Phylogenetic subtypes of human T-lymphotropic virus type I and their relations to the anthropological background. Proc Natl Acad Sci U S A 1994, 91:1124-7.

297. Miwa M, Shimotohno K, Hoshino H, Fujino M, Sugimura T: Detection of pX proteins in human T-cell leukemia virus (HTLV)-infected cells by using antibody against peptide deduced from sequences of X-IV DNA of HTLV-I and Xc DNA of HTLV-II proviruses. Gann 1984, 75:752-5.

298. Miyatake S, Seiki M, Malefijt RD, Heike T, Fujisawa J, Takebe Y, Nishida J, Shlomai J, Yokota T, Yoshida M, et al. Activation of T cell-derived lymphokine genes in T cells

and fibroblasts: effects of human T cell leukemia virus type I p40x protein and bovine papilloma virus encoded E2 protein. Nucleic Acids Res 1988, 16:6547-66.

299. Miyatake S, Seiki M, Yoshida M, Arai K: T-cell activation signals and human T-cell leukemia virus type I-encoded p40x protein activate the mouse granulocyte-macrophage colony-stimulating factor gene through a common DNA element. Mol Cell Biol 1988, 8:5581-7.

300. Moch H, Lang D, Stamminger T: Strong trans activation of the human cytomegalovirus major immediate-early enhancer by p40tax of human T-cell leukemia virus type I via two repetitive tax-responsive sequence elements. J Virol 1992, 66:7346-54.

301. Mochizuki M, Yamaguchi K, Takatsuki K, Watanabe T, Mori S, Tajima K: HTLV-I and uveitis [letter; comment]. Lancet 1992, 339:1110

302. Mochizuki M, Watanabe T, Yamaguchi K, Takatsuki K, Yoshimura K, Shirao M, Nakashima S, Mori S, Araki S, Miyata N: HTLV-I uveitis: a distinct clinical entity caused by HTLV-I. Jpn J Cancer Res 1992, 83:236-9.

303. Montagne J, Beraud C, Crenon I, Lombard Platet G, Gazzolo L, Sergeant A, Jalinot P: Tax1 induction of the HTLV-I 21 bp enhancer requires cooperation between two cellular DNA-binding proteins. EMBO J 1990, 9:957-64.

304. Moore GR, Traugott U, Scheinberg LC, Raine CS: Tropical spastic paraparesis: a model of virus-induced, cytotoxic T-cell-mediated demyelination? Ann Neurol 1989, 26:523-30.

305. Morgan D, Ruscetti FW, Gallo RC: Science 1976, 193:1007-8.

306. Mori N, Shirakawa F, Murakami S, Oda S, Eto S: Lack of interleukin-4 mRNA expression in adult T-cell leukemia cells [letter]. Eur J Haematol 1994, 52:191-2.

307. Motokawa S, Hasunuma T, Tajima K, Krieg AM, Ito S, Iwasaki K, Nishioka K: High prevalence of arthropathy in HTLV-I carriers on a Japanese island. Ann Rheum Dis 1996, 55:193-5.

308. Mulloy JC, Crownley RW, Fullen J, Leonard WJ, Franchini G: The human T-cell leukemia/lymphotropic virus type 1 p12I proteins bind the interleukin-2 receptor beta and gammac chains and affects their expression on the cell surface. J Virol 1996, 70:3599-605.

309. Munoz E, Israel A: Activation of NF-kappa B by the Tax protein of HTLV-1. Immunobiology 1995, 193:128-36.

310. Murakami T, Hirai H, Suzuki T, Fujisawa J, Yoshida M: HTLV-1 Tax enhances NF-kappa B2 expression and binds to the products p52 and p100, but does not suppress the inhibitory function of p100. Virology 1995, 206:1066-74.

311. Muraoka O, Kaisho T, Tanabe M, Hirano T: Transcriptional activation of the interleukin-6 gene by HTLV-1 p40tax through an NF-kappa B-like binding site. Immunol Lett 1993, 37:159-65.

312. Murphy EL, Figueroa JP, Gibbs WN, Brathwaite A, Holding Cobham M, Waters D, Cranston B, Hanchard B, Blattner WA: Sexual transmission of human T-lymphotropic virus type I (HTLV-I). Ann Intern Med 1989, 111:555-60.

313. Murphy EL, Hanchard B, Figueroa JP, Gibbs WN, Lofters WS, Campbell M, Goedert JJ, Blattner WA: Modelling the risk of adult T-cell leukemia/lymphoma in persons infected with human T-lymphotropic virus type I. Int J Cancer 1989, 43:250-3.

314. Nagai H, Kinoshita T, Imamura J, Murakami Y, Hayashi K, Mukai K, Ikeda S, Tobinai K, Saito H, Shimoyama M, et al. Genetic alteration of p53 in some patients with adult T-cell leukemia. Jpn J Cancer Res 1991, 82:1421-7.

315. Nagata K, Ohtani K, Nakamura M, Sugamura K: Activation of endogenous c-fos proto-oncogene expression by human T-cell leukemia virus type I-encoded p40tax protein in the human T-cell line, Jurkat. J Virol 1989, 63:3220-6.

316. Nakada K, Yamaguchi K, Furugen S, Nakasone T, Nakasone K, Oshiro Y, Kohakura M, Hinuma Y, Seiki M, Yoshida M, et al. Monoclonal integration of HTLV-I proviral DNA in patients with strongyloidiasis. Int J Cancer 1987, 40:145-8.

317. Nakamura H, Eguchi K, Nakamura T, Mizokami A, Shirabe S, Kawakami A, Matsuoka N, Migita K, Kawabe Y, Nagataki S: High prevalence of Sjogren's syndrome in patients with HTLV-I associated myelopathy. Ann Rheum Dis 1997, 56:167-72.

318. Napolitano M, Modi WS, Cevario SJ, Gnarra JR, Seuanez HN, Leonard WJ: The gene encoding the Act-2 cytokine. Genomic structure, HTLV-I/Tax responsiveness of 5' upstream sequences, and chromosomal localization. J Biol Chem 1991, 266:17531-6.

319. Nei M, Gojobori T: Simple methods for estimating the numbers of synonymous and nonsynonymous nucleotide susbstitutions. Mol Biol Evol 1986, 3:418-26.

320. Neil JC, Hughes D, McFarlane R, et al: Transduction and rearrangement of the myc gene by feline leukaemic virus in naturally occurring T-cell leukaemias. Nature 1984, 308:814-20.

321. Nelson PN, Lever AM, Bruckner FE, Isenberg DA, Kessaris N, Hay FC: Polymerase chain reaction fails to incriminate exogenous retroviruses HTLV-I and HIV-1 in

rheumatological diseases although a minority of sera cross react with retroviral antigens. Ann Rheum Dis 1994, 53:749-54.

322. Nerenberg M, Hinrichs SH, Reynolds RK, Khoury G, Jay G: The tat gene of human T-lymphotropic virus type 1 induces mesenchymal tumors in transgenic mice. Science 1987, 237:1324-9.

323. Nerenberg MI, Minor T, Nagashima K, Takebayashi K, Akai K, Wiley CA, Riccardi VM: Absence of association of HTLV-I infection with type 1 neurofibromatosis in the United States or Japan. Neurology 1991, 41:1687-9.

324. Nerenberg MI, Minor T, Price J, Ernst DN, Shinohara T, Schwarz H: Transgenic thymocytes are refractory to transformation by the human T-cell leukemia virus type I tax gene. J Virol 1991, 65:3349-53.

325. Nerenberg MI, Wiley CA: Degeneration of oxidative muscle fibers in HTLV-1 tax transgenic mice. Am J Pathol 1989, 135:1025-33.

326. Nevins JR. Transcripitonal activation by the adenovirus E1A proteins. [Abstract] Semin virol 1993;4:25-31.

327. Nevins JR: E2F: A link between the Rb tumor suppressor protein and viral oncoproteins. Science 1992, 258:424-9.

328. Newbold RF, Overell RW: Fibroblast immortality is a prerequisite for transformation by EJ c-Ha- ras oncogene. Nature 1983, 304:648-51.

329. Niewiesk S, Bangham CR: Evolution in a chronic RNA virus infection: selection on HTLV-I tax protein differs between healthy carriers and patients with tropical spastic paraparesis. J Mol Evol 1996, 42:452-8.

330. Niewiesk S, Daenke S, Parker CE, Taylor G, Weber J, Nightingale S, Bangham CR: Naturally occurring variants of human T-cell leukemia virus type I Tax protein impair its recognition by cytotoxic T lymphocytes and the transactivation function of Tax. J Virol 1995, 69:2649-53.

331. Niewiesk S, Daenke S, Parker CE, Taylor G, Weber J, Nightingale S, Bangham CR: The transactivator gene of human T-cell leukemia virus type I is more variable within and between healthy carriers than patients with tropical spastic paraparesis. J Virol 1994, 68:6778-81.

332. Nigro JM, Baker SJ, Preisinger AC, Jessup JM, Hostetter R, Cleary K, Bigner SH, Davidson N, Baylin S, Devilee P: Mutations in the p53 gene occur in diverse human tumour types. Nature 1989, 342:705-8.

333. Nishida J, Yoshida M, Arai K, Yokota T: Definition of a GC-rich motif as regulatory sequence of the human IL-3 gene: coordinate regulation of the IL-3 gene by CLE2/GC box of the GM-CSF gene in T cell activation. Int Immunol 1991, 3:245-54.

334. Nishioka K, Nakajima T, Hasunuma T, Sato K: Rheumatic manifestation of human leukemia virus infection. Rheum Dis Clin North Am 1993, 19:489-503.

335. Nishioka K, Maruyama I, Sato K, Kitajima I, Nakajima Y, Osame M: Chronic inflammatory arthropathy associated with HTLV-I [letter]. Lancet 1989, 1:441

336. Nobori T, Miura K, Wu DJ, Lois A, Takabayashi K, Carson DA: Deletions of the cyclin-dependent kinase-4 inhibitor gene in multiple human cancers. Nature 1994, 368:753-6.

337. Nosaka T, Siomi H, Adachi Y, Ishibashi M, Kubota S, Maki M, Hatanaka M: Nucleolar targeting signal of human T-cell leukemia virus type I rex-encoded protein is essential for cytoplasmic accumulation of unspliced viral mRNA. Proc Natl Acad Sci U S A 1989, 86:9798-802.

338. Nowak MA, Bangham CR: Population dynamics of immune responses to persistent viruses. Science 1996, 272:74-9.

339. Nurse P: Ordering S phase and M phase in the cell cycle. Cell 1994, 79:547-50.

340. Nyborg JK, Matthews MA, Yucel J, Walls L, Golde WT, Dynan WS, Wachsman W: Interaction of host cell proteins with the human T-cell leukemia virus type I transcriptional control region. II. A comprehensive map of protein-binding sites facilitates construction of a simple chimeric promoter responsive to the viral tax2 gene product. J Biol Chem 1990, 265:8237-42.

341. Ohshima K, Kikuchi M, Masuda Y, Sumiyoshi Y, Eguchi F, Mohtai H, Takeshita M, Kimura N: Human T-cell leukemia virus type I associated lymphadenitis. Cancer 1992, 69:239-48.

342. Okamoto T. [Multi-stop carcinogenesis model for adult T-cell leukemia]. [Abstract] Rinsho Ketsueki (abstract only) 1990;31:(5)569-71.

343. Orita S, Takagi S, Saiga A, Minoura N, Araki K, Kinoshita K, Kondo T, Hinuma Y, Igarashi H: Human T cell leukaemia virus type 1 p21X mRNA: constitutive expression in peripheral blood mononuclear cells of patients with adult T cell leukaemia. J Gen Virol 1992, 73:2283-9.

344. Osame M, Janssen R, Kubota H, Nishitani H, Igata A, Nagataki S, Mori M, Goto I, Shimabukuro H, Khabbaz R, et al. Nationwide survey of HTLV-I-associated myelopathy in Japan: association with blood transfusion. Ann Neurol 1990, 28:50-6.

345. Ozden S, Coscoy L, GonzalezDunia D: HTLV-I transgenic models: An overview. Journal of Acquired Immune Deficiency Syndromes and Human Retrovirology 1996, 13:S154-61.

346. Ozer J, Moore PA, Bolden AH, Lee A, Rosen CA, Lieberman PM: Molecular cloning of the small (gamma) subunit of human TFIIA reveals functions critical for activated transcription. Genes Dev 1994, 8:2324-35.

347. Palmiter RD, Brinster RL, Hammer RE, Trumbauer ME, Rosenfeld MG, Birnberg NC, Evans RM: Dramatic growth of mice that develop from eggs microinjected with metallothionein-growth hormone fusion genes. Nature 1982, 300:611-5.

348. Palombella VJ, Rando OJ, Goldberg AL, Maniatis T: The ubiquitin-proteasome pathway is required for processing the NF- kappaB1 precursor protein and the activation of NF-kappaB. Cell 1994, 78:773-85.

349. Pancake BA, Zucker Franklin D, Coutavas EE: The cutaneous T cell lymphoma, mycosis fungoides, is a human T cell lymphotropic virus-associated disease. A study of 50 patients. J Clin Invest 1995, 95:547-54.

350. Pandolfi F, Zambello R, Cafaro A, Semenzato G: Biology of disease: Biologic and clinical heterogeneity of lymphoproliferative diseases of peripheral mature T lymphocytes. Lab Invest 1992, 67:274-302.

351. Pantazis P, Sariban E, Bohan CA, Antoniades HN, Kalyanaraman VS: Synthesis of PDGF by cultured human T cells transformed with HTLV-I and II. Oncogene 1987, 1:285-9.

352. Parker CE, Nightingale S, Taylor GP, Weber J, Bangham CR: Circulating anti-Tax cytotoxic T lymphocytes from human T-cell leukemia virus type I-infected people, with and without tropical spastic paraparesis, recognize multiple epitopes simultaneously. J Virol 1994, 68:2860-8.

353. Parker CE, Daenke S, Nightingale S, Bangham CR: Activated, HTLV-1-specific cytotoxic T-lymphocytes are found in healthy seropositives as well as in patients with tropical spastic paraparesis. Virology 1992, 188:628-36.

354. Parker SB, Eichele G, Zhang P, Rawls A, Sands AT, Bradley A, Olson EN, Harper JW, Elledge SJ: p53-independent expression of p21Cip1 in muscle and other terminally differentiating cells. Science 1995, 267:1024-7.

355. Paskalis H, Felber BK, Pavlakis GN: Cis-acting sequences responsible for the transcriptional activation of human T-cell leukemia virus type I constitute a conditional enhancer. Proc Natl Acad Sci U S A 1986, 83:6558-62.

356. Peebles RS, Maliszewski CR, Sato TA, Hanley Hyde J, Maroulakou IG, Hunziker R, Schneck JP, Green JE: Abnormal B-cell function in HTLV-I-tax transgenic mice. Oncogene 1995, 10:1045-51.

357. Perini G, Wagner S, Green MR: Recognition of bZIP proteins by the human T-cell leukaemia virus transactivator Tax. Nature 1995, 376:602-5.

358. Pinheiro SR, Lana-Peixoto MA, Proietti AB, Orefice F, Lima-Martins MV, Proietti FA: HTLV-I associated uveitis, myelopathy, rheumatoid arthritis and Sjogren's syndrome. Arq Neuropsiquiatr 1995, 53:777-81.

359. Pique C, Connan F, Levilain JP, Choppin J, Dokhelar MC: Among all human T-cell leukemia virus type 1 proteins, tax, polymerase, and envelope proteins are predicted as preferential targets for the HLA-A2-restricted cytotoxic T-cell response. J Virol 1996, 70:4919-26.

360. Poiesz BJ, Ruscetti FW, Reitz MS, Kalyanaraman VS, Gallo RC: Isolation of a new type C retrovirus (HTLV) in primary uncultured cells of a patient with Sezary T-cell leukaemia. Nature 1981, 294:268-71.

361. Poiesz BJ, Ruscetti FW, Gazdar AF, Bunn PA, Minna JD, Gallo RC: Detection and isolation of type C retrovirus particles from fresh and cultures lymphocytes of a patient with cutaneous T-cell lymphoma. Proc Natl Acad Sci U S A 1980, 77:7415

362. Popovic M, Lange Wantzin G, Sarin PS, Mann D, Gallo RC: Transformation of human umbilical cord blood T cells by human T-cell leukemia/lymphoma virus. Proc Natl Acad Sci U S A 1983, 80:5402-6.

363. Popovic M, Sarin PS, Robert Gurroff M, Kalyanaraman VS, Mann D, Minowada J, Gallo RC: Isolation and transmission of human retrovirus (human t-cell leukemia virus). Science 1983, 219:856-9.

364. Posnett DN, McGrath H, Tam JP: A novel method for producing anti-peptide antibodies. Production of site-specific antibodies to the T cell antigen receptor beta-chain. Journal of Biological Chemistry 1988, 263:1719-25.

365. Pozzatti R, Vogel J, Jay G: The human T-lymphotropic virus type I tax gene can cooperate with the ras oncogene to induce neoplastic transformation of cells. Mol Cell Biol 1990, 10:413-7.

366. Preston GA, Lyon TT, Yin Y, Lang JE, Solomon G, Annab L, Srinivasan DG, Alcorta DA, and Barrett JC. Induction of apoptosis by the c-fos protein. Mol Cell Biol 1996;16(1):211-8.

367. Purdie CA, Harrison DJ, Peter A, Dobbie L, White S, Howie SE, Salter DM, Bird CC, Wyllie AH, Hooper ML: Tumour incidence, spectrum and ploidy in mice with a large deletion in the p53 gene. Oncogene 1994, 9:603-9.

368. Rao L, Debbas M, Sabbatini P, Hockenbery D, Korsmeyer S, White E: The adenovirus E1A proteins induce apoptosis, which is inhibited by the E1B 19-kDa and Bcl-2 proteins [published erratum appears in Proc Natl Acad Sci U S A 1992 Oct 15;89(20):9974]. Proc Natl Acad Sci U S A 1992, 89:7742-6.

369. Ratner L: Regulation of expression of the c-sis proto-oncogene. Nucleic Acids Res 1989, 17:4101-15.

370. Reddy EP, Mettus RV, DeFreitas E, Wroblewska Z, Cisco M, Koprowski H: Molecular cloning of human T-cell lymphotrophic virus type I-like proviral genome from the peripheral lymphocyte DNA of a patient with chronic neurologic disorders. Proc Natl Acad Sci U S A 1988, 85:3599-603.

371. Reid RL, Lindholm PF, Mireskandari A, Dittmer J, Brady JN: Stabilization of wild-type p53 in human T-lymphocytes transformed by HTLV-I. Oncogene 1993, 8:3029-36.

372. Reik W, Collick A, Norris ML, Barton SC, Surani MA: Genomic imprinting determines methylation of parental alleles in transgenic mice. Nature 1987, 328:248-51.

373. Renjifo B, Borrero I, Essex M: Tax mutation associated with tropical spastic paraparesis/human T-cell leukemia virus type I-associated myelopathy. J Virol 1995, 69:2611-6.

374. Riccardi VM: Von Recklinghausen neurofibromatosis. N Engl J Med 1981, 305:1617-27.

375. Rigby SP, Cooke SP, Weerasinghe D, Venables PJ: Absence of HTLV-1 tax in Sjogren's syndrome [letter]. Arthritis Rheum 1996, 39:1609-11.

376. Rosenblatt JD, Giorgi JV, Golde DW, Ezra JB, Wu A, Winberg CD, Glaspy J, Wachsman W, Chen IS: Integrated human T-cell leukemia virus II genome in CD8 + T cells from a patient with "atypical" hairy cell leukemia: evidence for distinct T and B cell lymphoproliferative disorders. Blood 1988, 71:363-9.

377. Rosenblatt JD, Gasson JC, Glaspy J, Bhuta S, Aboud M, Chen IS, Golde DW: Relationship between human T cell leukemia virus-II and atypical hairy cell leukemia: a serologic study of hairy cell leukemia patients. Leukemia 1987, 1:397-401.

378. Rosenblatt JD, Golde DW, Wachsman W, Giorgi JV, Jacobs A, Schmidt GM, Quan S, Gasson JC, Chen IS: A second isolate of HTLV-II associated with atypical hairy-cell leukemia. N Engl J Med 1986, 315:372-7.

379. Rosin O, Koch C, Schmitt I, Semmes OJ, Jeang KT, Grassmann R: A human T-cell leukemia virus Tax variant incapable of activating NF- kappaB retains its immortalizing potential for primary T-lymphocytes. J Biol Chem 1998, 273:6698-703.

380. Ross TM, Pettiford SM, Green PL: The tax gene of human T-cell leukemia virus type 2 is essential for transformation of human T lymphocytes. J Virol 1996, 70:5194-202.

381. Rouleau GA, Merel P, Lutchman M, Sanson M, Zucman J, Marineau C, Hoang-Xuan K, Demczuk S, Desmaze C, Plougastel B: Alteration in a new gene encoding a putative membrane-organizing protein causes neuro-fibromatosis type 2 [see comments]. Nature 1993, 363:515-21.

382. Ruben S, Poteat H, Tan TH, Kawakami K, Roeder R, Haseltine W, Rosen CA: Cellular transcription factors and regulation of IL-2 receptor gene expression by HTLV-I tax gene product. Science 1988, 241:89-92.

383. Sadamori N, Nishino K, Kusano M, Tomonaga Y, Tagawa M, Yao E, Sasagawa I, Nakamura H, Ichimaru M: Significance of chromosome 14 anomaly at band 14q11 in Japanese patients with adult T-cell leukemia. Cancer 1986, 58:2244-50.

384. Saggioro D, Rosato A, Esposito G, Rosenberg MP, Harrison J, Felber BK, Pavlakis GN, Chieco-Bianchi L: Inflammatory polyarthropathy and bone remodeling in HTLV-I Tax-transgenic mice. J Acquir Immune Defic Syndr Hum Retrovirol 1997, 14:272-80.

385. Saggioro D, Majone F, Forino M, Turchetto L, Leszl A, Chieco Bianchi L: Tax protein of human T-lymphotropic virus type I triggers DNA damage. Leuk Lymphoma 1994, 12:281-6.

386. Saggioro D, Forino M, Chieco Bianchi L: Transcriptional block of HTLV-I LTR by sequence-specific methylation. Virology 1991, 182:68-75.

387. Saggioro D, Panozzo M, Chieco Bianchi L: Human T-lymphotropic virus type I transcriptional regulation by methylation. Cancer Res 1990, 50:4968-73.

388. Saida K, Saida T, Kai K, Iwamura K: Central nervous system lesions in rats infected with Friend murine leukemia virus-related PVC441: ultrastructural and immunohistochemical studies. Acta Neuropathol (Berl) 1997, 93:369-78.

389. Salvetti A, Lilienbaum A, Li Z, Paulin D, Gazzolo L: Identification of a negative element in the human vimentin promoter: modulation by the human T-cell leukemia virus type I Tax protein. Mol Cell Biol 1993, 13:89-97.

390. Sanada I, Yamaguchi K, Yoshida M, Ishii T, Tsukamoto A, Sato M, Obata S, Shido T: Adult T-cell leukemia in spouses [see comments]. Jpn J Cancer Res 1989, 80:401-4.

391. Sands AT, Suraokar MB, Sanchez A, Marth JE, Donehower LA, Bradley A: p53 deficiency does not affect the accumulation of point mutations in a transgene target. Proc Natl Acad Sci U S A 1995, 92:8517-21.

392. Sapienza C, Peterson AC, Rossant J, Balling R: Degree of methylation of transgenes is dependent on gamete of origin. Nature 1987, 328:251-4.

393. Sarnow P, Ho YS, Williams J, Levine AJ: Adenovirus E1b-58kd tumor antigen and SV40 large tumor antigen are physically associated with the same 54 kd cellular protein in transformed cells. Cell 1982, 28:387-94.

394. Sato K, Maruyama I, Maruyama Y, Kitajima I, Nakajima Y, Higaki M, Yamamoto K, Miyasaka N, Osame M, Nishioka K: Arthritis in patients infected with human T lymphotropic virus type I. Clinical and immunopathologic features. Arthritis Rheum 1991, 34:714-21.

395. Sawada M, Suzumura A, Yoshida M, Marunouchi T: Human T-cell leukemia virus type I trans activator induces class I major histocompatibility complex antigen expression in glial cells. J Virol 1990, 64:4002-6.

396. Scheffner M, Werness B, Huibregtse J, Levine A, Howley P: The E6 oncoprotien encoded by human papillomavirus types 16 and 18 promotes the degradation of p53. Cell 1990, 63:1129-36.

397. Schwartz-Cornil I, Chevallier N, Belloc C, Le Rhun D, Laine V, Berthelemy M, Mateo A, Levy D: Bovine leukaemia virus-induced lymphocytosis in sheep is associated with reduction of spontaneous B cell apoptosis. J Gen Virol 1997, 78:153-62.

398. Seiki M, Eddy R, Shows TB, Yoshida M: Nonspecific integration of the HTLV provirus genome into adult T-cell leukaemia cells. Nature 1984, 309:640-2.

399. Seizinger BR, Martuza RL, Gusella JF: Loss of genes on chromosome 22 in tumorigenesis of human acoustic neuroma. Nature 1986, 322:644-7.

400. Semmes OJ, Jeang KT: Definition of a minimal activation domain in human T-cell leukemia virus type I Tax. J Virol 1995, 69:1827-33.

401. Semmes OJ, Jeang KT: HTLV-I Tax is a zinc-binding protein: role of zinc in Tax structure and function. Virology 1992, 188:754-64.

402. Serrano M: The tumor suppressor protein p16INK4a. Exp Cell Res 1997, 237:7-13.

403. Setoyama M, Fujiyoshi T, Mizoguchi S, Katahira Y, Yashiki S, Tara M, Kanzaki T, Sonoda S: HTLV-I messenger RNA is expressed in vivo in adult T-cell leukemia/lymphoma patients: an in situ hybridization study. Int J Cancer 1994, 57:760-4.

404. Sharma S, Sarkar C, Mathur M, Dinda AK, Roy S: Benign nerve sheath tumors: a light microscopic, electron microscopic and immunohistochemical study of 102 cases. Pathology 1990, 22:191-5.

405. Sherr CJ, Roberts JM: Inhibitors of mammalian G1 cyclin-dependent kinases. Genes and Development 1995, 9:1149-63.

406. Sherr CJ: G1 phase progression: cycling on cue. Cell 1994, 79:551-5.

407. Shimotohno K, Takano M, Teruuchi T, Miwa M: Requirement of multiple copies of a 21-nucleotide sequence in the U3 regions of human T-cell leukemia virus type I and type II long terminal repeats for trans-acting activation of transcription. Proc Natl Acad Sci U S A 1986, 83:8112-6.

408. Shimotohno K, Takahashi Y, Shimizu N, Gojobori T, Golde DW, Chen IS, Miwa M, Sugimura T: Complete nucleotide sequence of an infectious clone of human T-cell leukemia virus type II: an open reading frame for the protease gene. Proc Natl Acad Sci U S A 1985, 82:3101-5.

409. Shinzato O, Kamihira S, Ikeda S, Kondo H, Kanda T, Nagata Y, Nakayama E, Shiku H: Relationship between the anti-HTLV-1 antibody level, the number of abnormal lymphocytes and the viral-genome dose in HTLV-1-infected individuals. Int J Cancer 1993, 54:208-12.

410. Shirabe S, Nakamura T, Tsujihata M, Nagataki S, Seiki M, Yoshida M: Retrovirus from human T-cell leukemia virus type I-associated myelopathy is the same strain as a prototype human T-cell leukemia virus type I. Arch Neurol 1990, 47:1258-60.

411. Shirodkar S, Ewen M, DeCaprio JA, Morgan J, Livingston DM, Chittenden T: The transciption factor E2F interacts with the retinoblastoma product and a p107-cyclin A complex in a cell regulated manner. Cell 1992, 68:157-66.

412. Shnyreva M, Munder T: The oncoprotein Tax of the human T-cell leukemia virus type 1 activates transcription via interaction with cellular ATF-1/CREB factors in Saccharomyces cerevisiae. Journal of Virology 1996, 70:7478-84.

413. Siekevitz M, Josephs SF, Dukovich M, Peffer N, Wong Staal F, Greene WC: Activation of the HIV-1 LTR by T cell mitogens and the trans-activator protein of HTLV-I [published erratum appears in Science 1988 Jan 29;239(4839):451]. Science 1987, 238:1575-8.

414. Sinn E, Muller W, Pattengale P, Tepler I, Wallace R, Leder P: Coexpression of MMTV/v-Ha-res and MMTV/c-myc genes in transgenic mice: synergistic action of oncogens in vivo. Cell 1987, 49:465-75.

415. Siomi H, Shida H, Nam SH, Nosaka T, Maki M, Hatanaka M: Sequence requirements for nucleolar localization of human T cell leukemia virus type I pX protein, which regulates viral RNA processing. Cell 1988, 55:197-209.

416. Smith CA, Farrah T, Goodwin RG: The TNF receptor superfamily of cellular and viral proteins: activation, costimulation, and death. Cell 1994, 76:959-62.

417. Smith MR, Greene WC: Characterization of a novel nuclear localization signal in the HTLV-I tax transactivator protein. Virology 1992, 187:316-20.

418. Smith MR, Greene WC: Type I human T cell leukemia virus tax protein transforms rat fibroblasts through the cyclic adenosine monophosphate response element binding protein/activating transcription factor pathway. J Clin Invest 1991, 88:1038-42.

419. Smith MR, Greene WC: Identification of HTLV-I tax trans-activator mutants exhibiting novel transcriptional phenotypes [published erratum appears in Genes Dev 1991 Jan;5(1):150]. Genes Dev 1990, 4:1875-85.

420. Sodroski J, Trus M, Perkins D, Patarca R, Wong Staal F, Gelmann E, Gallo R, Haseltine WA: Repetitive structure in the long-terminal-repeat element of a type II human T-cell leukemia virus. Proc Natl Acad Sci U S A 1984, 81:4617-21.

421. Starkebaum G, Shasteen NM, Fleming Jones RM, Loughran TP, Jr., Mannik M: Sera of patients with rheumatoid arthritis contain antibodies to recombinant human T-lymphotrophic virus type I/II envelope glycoprotein p21. Clin Immunol Immunopathol 1996, 79:182-8.

422. Stehelin D, Varmus HE, Bishop JM, Vogt PK: DNA related to the transforming gene(s) of avian sarcoma viruses is present in normal avian DNA. Nature 1976, 260:170-3.

423. Stewart N, Hicks GG, Paraskevas F, Mowat M: Evidence for a second cell cycle block at G2/M by p53. Oncogene 1995, 10:109-15.

424. Stoica G, Illanes O, Tasca SI, Wong PK: Temporal central and peripheral nervous system changes induced by a paralytogenic mutant of Moloney murine leukemia virus TB. Lab Invest 1993, 69:724-35.

425. Strickler HD, Rattray C, Escoffery C, Manns A, Schiffman MH, Brown C, Cranston B, Hanchard B, Palefsky JM, Blattner WA: Human T-cell lymphotropic virus type I and severe neoplasia of the cervix in Jamaica. Int J Cancer 1995, 61:23-6.

426. Sugimoto M, Mita S, Tokunaga M, Yamaguchi K, Cho I, Matsumoto M, Mochizuki M, Araki S, Takatsuki K, Ando M: Pulmonary involvement in human T-cell lymphotropic virus type-I uveitis: T-lymphocytosis and high proviral DNA load in bronchoalveolar lavage fluid [see comments]. Eur Respir J 1993, 6:938-43.

427. Sun SC, Elwood J, Beraud C, Greene WC: Human T-cell leukemia virus type I Tax activation of NF-kappa B/Rel involves phosphorylation and degradation of I kappa B alpha and RelA (p65)-mediated induction of the c-rel gene. Mol Cell Biol 1994, 14:7377-84.

428. Suzuki T, Yoshida M: HTLV-1 Tax protein interacts with cyclin-dependent kinase inhibitor p16Ink4a and counteracts its inhibitory activity to CDK4. Leukemia 1997, 11 Suppl 3:14-6:14-6.

429. Suzuki T, Kitao S, Matsushime H, Yoshida M: HTLV-1 Tax protein interacts with cyclin-dependent kinase inhibitor p16(INK4A) and counteracts its inhibitory activity towards CDK4. EMBO Journal 1996, 15:1607-14.

430. Suzuki T, Hirai H, Murakami T, Yoshida M: Tax protein of HTLV-1 destabilizes the complexes of NF-kappa B and I kappa B-alpha and induces nuclear translocation of NF-kappa B for transcriptional activation. Oncogene 1995, 10:1199-207.

431. Suzuki T, Hirai H, Yoshida M: Tax protein of HTLV-1 interacts with the Rel homology domain of NF-kappa B p65 and c-Rel proteins bound to the NF-kappa B binding site and activates transcription. Oncogene 1994, 9:3099-105.

432. Suzuki T, Fujisawa JI, Toita M, Yoshida M: The trans-activator tax of human T-cell leukemia virus type 1 (HTLV-1) interacts with cAMP-responsive element (CRE) binding and CRE modulator proteins that bind to the 21-base-pair enhancer of HTLV-1. Proc Natl Acad Sci U S A 1993, 90:610-4.

433. Suzuki T, Hirai H, Fujisawa J, Fujita T, Yoshida M: A trans-activator Tax of human T-cell leukemia virus type 1 binds to NF-kappa B p50 and serum response factor (SRF) and associates with enhancer DNAs of the NF-kappa B site and CArG box. Oncogene 1993, 8:2391-7.

434. Swain JL, Stewart TA, Leder P: Parental legacy determines methylation and expression of an autosomal transgene: a molecular mechanism for parental imprinting. Cell 1987, 50:719-27.

435. Taguchi H, Kinoshita KI, Takatsuki K, Tomonaga M, Araki K, Arima N, Ikeda S, Uozumi K, Kohno H, Kawano F, et al. An intensive chemotherapy of adult T-cell leukemia/lymphoma: CHOP followed by etoposide, vindesine, ranimustine, and mitoxantrone with granulocyte colony-stimulating factor support. J Acquir Immune Defic Syndr Hum Retrovirol 1996, 12:182-6.

436. Taguchi H, Sawada T, Fukushima A, Iwata J, Ohtsuki Y, Ueno H, Miyoshi I: Bilateral uveitis in a rabbit experimentally infected with human T-lymphotropic virus type I. Lab Invest 1993, 69:336-9.

437. Takatsuki K, Yamaguchi K, Kawano F, Hattori T, Nishimura H, Tsuda H, Sanada I, Nakada K, Itai Y: Clinical diversity in adult T-cell leukemia-lymphoma. Cancer Res 1985, 45:4644s-5s.

438. Tam JP, Lu Y: Vaccine engineering: Enhancement of immunogenicity of synthetic peptide vaccines related to hepatitis in chemicaly defined models consisting of T- and B- cell epitopes. Proc Natl Acad Sci U S A 1989, 86:9084-8.

439. Tam JP: Synthetic peptide vaccine design: Synthesis and properties of a high- density multiple antigenic peptide system. Proceedings of the National Academy of Sciences of the United States of America 1988, 85:5409-13.

440. Tamiya S, Matsuoka M, Etoh K, Watanabe T, Kamihira S, Yamaguchi K, Takasuki K: Two types of defective human T-lymphotropic virus type I provirus in adult T-cell leukemia. Blood 1996, 88:3065-73.

441. Tanaka A, Takahashi C, Yamaoka S, Nosaka T, Maki M, Hatanaka M: Oncogenic transformation by the tax gene of human T-cell leukemia virus type I in vitro. Proc Natl Acad Sci U S A 1990, 87:1071-5.

442. Tendler CL, Greenberg SJ, Blattner WA, Manns A, Murphy E, Fleisher T, Hanchard B, Morgan O, Burton JD, Nelson DL, et al. Transactivation of interleukin 2 and its receptor induces immune activation in human T-cell lymphotropic virus type I-associated myelopathy: pathogenic implications and a rationale for immunotherapy. Proc Natl Acad Sci U S A 1990, 87:5218-22.

443. Theze J, Alzari PM, Bertoglio J: Interleukin 2 and its receptors: recent advances and new immunological functions. Immunol Today 1996, 17:481-6.

444. Tie F, Adya N, Greene WC, Giam CZ: Interaction of the human T-lymphotropic virus type 1 Tax dimer with CREB and the viral 21-base-pair repeat. J Virol 1996, 70:8368-74.

445. Toyoshima H, Itoh M, Inoue J, Seiki M, Takaku F, Yoshida M: Secondary structure of the human T-cell leukemia virus type 1 rex-responsive element is essential for rex regulation of RNA processing and transport of unspliced RNAs. J Virol 1990, 64:2825-32.

446. Trofatter JA, MacCollin MM, Rutter JL, Murrell JR, Duyao MP, Parry DM, Eldridge R, Kley N, Menon AG, Pulaski K: A novel moesin-, ezrin-, radixin-like gene is a candidate for the neurofibromatosis 2 tumor suppressor. Cell 1993, 75:826

447. Tschachler E, Bohnlein E, Felzmann S, Reitz MS, Jr. Human T-lymphotropic virus type I tax regulates the expression of the human lymphotoxin gene. Blood 1993, 81:95-100.

448. Tsuchiya H, Fujii M, Tanaka Y, Tozawa H, Seiki M: Two distinct regions form a functional activation domain of the HTLV-1 trans-activator Tax1. Oncogene 1994, 9:337-40.

449. Turker MS, Bestor TH: Formation of methylation patterns in the mammalian genome [see comments]. Mutat Res 1997, 386:119-30.

450. Uchijima M, Sato H, Fujii M, Seiki M: Tax proteins of human T-cell leukemia virus type 1 and 2 induce expression of the gene encoding erythroid-potentiating activity (tissue inhibitor of metalloproteinases-1, TIMP-1). J Biol Chem 1994, 269:14946-50.

451. Uchiyama T, Yodoi J, Sagawa K, Takatsuki K, Uchino H: Adult T-cell Leukaemia: clinical and haematological features of 16 cases. Blood 1977, 50:481-92.

452. Ucker DS: Death by suicide: one way to go in mammalian cellular development? New Biol 1991, 3:103-9.

453. Uittenbogaard MN, Giebler HA, Reisman D, Nyborg JK: Transcriptional repression of p53 by Human T-cell Leukaemia Virus Type I Protein. J Biol Chem 1995, 270:28503-6.

454. Umehara F, Nakamura A, Izumo S, Kubota R, Ijichi S, Kashio N, Hashimoto K, Usuku K, Sato E, Osame M: Apoptosis of T lymphocytes in the spinal cord lesions in HTLV-I-associated myelopathy: a possible mechanism to control viral infection in the central nervous system. J Neuropathol Exp Neurol 1994, 53:617-24.

455. Uozumi K, Hanada S, Ohno N, Ishitsuka K, Shimotakahara S, Otsuka M, Chyuman Y, Nakahara K, Takeshita T, Kuwazuru Y, et al. Combination chemotherapy (RCM protocol: response-oriented cyclic multidrug protocol) for the acute or lymphoma type adult T-cell leukemia. Leuk Lymphoma 1995, 18:317-23.

456. Urnovitz HB, Murphy WH: Human endogenous retroviruses: nature, occurrence, and clinical implications in human disease. Clin Microbiol Rev 1996, 9:72-99.

457. Usuku K, Nishizawa M, Matsuki K, Tokunaga K, Takahashi K, Eiraku N, Suehara M, Juji T, Osame M, Tabira T: Association of a particular amino acid sequence of the HLA-DR beta 1 chain with HTLV-I-associated myelopathy. Eur J Immunol 1990, 20:1603-6.

458. Usuku K, Nishizawa M, Eiraku N, Osame M, Tabira T: Autoproliferative and self-reactive T-cell lines from patients with HTLV-I-associated myelopathy. Tohoku J Exp Med 1990, 162:243-53.

459. Usuku K, Sonoda S, Osame M, Yashiki S, Takahashi K, Matsumoto M, Sawada T, Tsuji K, Tara M, Igata A: HLA haplotype-linked high immune responsiveness against HTLV-I in HTLV-I-associated myelopathy: comparison with adult T-cell leukemia/lymphoma. Ann Neurol 1988, 23 Suppl:S143-50.

460. Van Antwerp DJ, Martin SJ, Kafri T, Green DR, Verma IM: Suppression of TNF-alpha-induced apoptosis by NF-kappaB. Science 1996, 274:787-9.

461. Varmus H, Weinberg RA. ; Scientific American Library, editors.Genes and the biology of cancer. 1st ed. Scientific American Library, 1993; 3, Clues to the origin of cancer. p. 45-66.

462. Vater CA, Bartle LM, Dionne CA, Littlewood TD, Goldmacher VS: Induction of apoptosis by tamoxifen-activation of a p53-estrogen receptor fusion protein expressed in E1A and T24 H-ras transformed p53- /- mouse embryo fibroblasts. Oncogene 1996, 13:739-48.

463. Viale G, Gambacorta M, Coggi G, Dell'Orto P, Milani M, Doglioni C: Glial fibrillary acidic protein immunoreactivity in normal and diseased human breast. Virchows Arch A Pathol Anat Histopathol 1991, 418:339-48.

464. Vidal AU, Gessain A, Yoshida M, Tekaia F, Garin B, Guillemain B, Schulz T, Farid R, de The G: Phylogenetic classification of human T cell leukaemia/lymphoma virus type I genotypes in five major molecular and geographical subtypes. J Gen Virol 1994, 75:3655-66.

465. Viskochil D, Buchberg AM, Xu G, Cawthon RM, Stevens J, Wolff RK, Culver M, Carey JC, Copeland NG, Jenkins NA: Deletions and a translocation interrupt a cloned gene at the neurofibromatosis type 1 locus. Cell 1990, 62:187-92.

466. Vogelstein B, Kinzler KW: The multistep nature of cancer. Trends Genet 1993, 9:138-41.

467. Wagner S, Green MR: HTLV-I Tax protein stimulation of DNA binding of bZIP proteins by enhancing dimerization. Science 1993, 262:395-9.

468. Wallace MR, Marchuk DA, Andersen LB, Letcher R, Odeh HM, Saulino AM, Fountain JW, Brereton A, Nicholson J, Mitchell AL: Type 1 neurofibromatosis gene:

identification of a large transcript disrupted in three NF1 patients [published erratum appears in Science 1990 Dec 21;250(4988):1749]. Science 1990, 249:181-6.

469. Wang CY, Mayo MW, Baldwin AS Jr: TNF- and cancer therapy-induced apoptosis: Potentiation by inhibition of NF-kappaB. Science 1996, 274:784-7.

470. Wang CY, Looney DJ, Li ML, Walfield AM, Ye J, Hosein B, Tam JP, WongStaal F: Long-term high-titer neutralizing activity induced by octameric synthetic HIV-1 antigen. Science 1991, 254:285-8.

471. Wantzin GL, Thomsen K, Nissen NI, Saxinger C, Gallo RC: Occurrence of human T cell lymphotropic virus (type I) antibodies in cutaneous T cell lymphoma. J Am Acad Dermatol 1986, 15:598-602.

472. Watanabe M, Muramatsu M, Tsuboi A, Arai K: Differential response of NF-kappa B1 p105 and NF-kappa B2 p100 to HTLV-I encoded Tax. FEBS Lett 1994, 342:115-8.

473. Watanabe T, Yamaguchi K, Takatsuki K, Osame M, Yoshida M: Constitutive expression of parathyroid hormone-related protein gene in human T cell leukemia virus type 1 (HTLV-1) carriers and adult T cell leukemia patients that can be trans-activated by HTLV-1 tax gene. J Exp Med 1990, 172:759-65.

474. Watson JD, Gilman M, Witkowski J, et al. W.H.Freeman and Co. editors.Recombinant DNA. 2nd ed. New York: Scientific American Books, 1992; 9, p. 153-74.

475. Weinberg R: The retinoblastoma gene and gene product. Cancer Surv 1992, 12:43-57.

476. Weinberg RA: The cat and mouse games that genes, viruses, and cells play. Cell 1997, 88:573-5.

477. Weinberg RA: Tumor suppressor genes. Science 1991, 254:1138-46.

478. Weinberg RA: The action of oncogenes in the cytoplasm and nucleus. Science 1985, 230:770-6.

479. Werness BA, Levine AJ, Howley PM: Association of human papillomavirus types 16 and 18 E6 proteins with p53. Science 1990, 248:76-9.

480. White E, Cipriani R, Sabbatini P, Denton A: Adenovirus E1B 19-kilodalton protiein overcomes the cytotoxicity of E1A proteins. J Virol 1991, 65:2968-78.

481. Whyte P, Buchkovich KJ, Horowitz JM, Friend SH, Raybuck M, Weinberg RA, Harlow E: Association between an oncogene and an anti-oncogene: the adenovirus E1A proteins bind to the retinoblastoma gene product. Nature 1988, 334:124-9.

482. Wiley CA, Nerenberg M, Cros D, Soto Aguilar MC: HTLV-I polymyositis in a patient also infected with the human immunodeficiency virus. N Engl J Med 1989, 320:992-5.

483. Wolf H, Modrow S, Motz M, Jameson BA, Hermann G, Fortsch B: An integrated family of amino acid sequence analysis programs. Computer Applications in the Biosciences 1988, 4:187-91.

484. Wong Staal F, Hahn B, Manzari V, Colombini S, Franchini G, Gelmann EP, Gallo RC: A survey of human leukaemias for sequences of a human retrovirus. Nature 1983, 302:626-8.

485. Wood GS, Schaffer JM, Boni R, Dummer R, Burg G, Takeshita M, Kikuchi M: No evidence of HTLV-I proviral integration in lymphoproliferative disorders associated with cutaneous T-cell lymphoma. American Journal of Pathology 1997, 150:667-73.

486. Woodard JC, Gaskin JM, Poulos PW, MacKay RJ, Burridge MJ: Caprine arthritis-encephalitis: clinicopathologic study. Am J Vet Res 1982, 43:2085-96.

487. Wright JJ, Gunter KC, Mitsuya H, Irving SG, Kelly K, Siebenlist U: Expression of a zinc finger gene in HTLV-I- and HTLV-II-transformed cells. Science 1990, 248:588-91.

488. Wynford-Thomas D: p53: Guardian of cellular senescence. J Pathol 1996, 180:118-21.

489. Wynford-Thomas D: Molecular basis of epithelial tumorigenesis: the thyroid model. Crit Rev Oncog 1993, 4:1-23.

490. Xu G, OConnell P, Viskochil D, Cawthon R, Robertson M, Culver M, Dunn D, Stevens J, Gesteland R, White R, et al. The neurofibromatosis type 1 gene encodes a protein related to GAP. Cell 1990, 62:599-608.

491. Xu X, Kang SH, Heidenreich O, Brown DA, Nerenberg MI: Sequence requirements of ATF2 and CREB binding to the human T-cell leukemia virus type 1 LTR R region. Virology 1996, 218:362-71.

492. Xu X, Brown DA, Kitajima I, Bilakovics J, Fey LW, Nerenberg MI: Transcriptional suppression of the human T-cell leukemia virus type I long terminal repeat occurs by an unconventional interaction of a CREB factor with the R region. Mol Cell Biol 1994, 14:5371-83.

493. Xu YL, Adya N, Siores E, Gao QS, Giam CZ: Cellular factors involved in transcription and Tax-mediated trans-activation directed by the TGACGT motifs in human T-cell leukemia virus type I promoter. J Biol Chem 1990, 265:20285-92.

494. Yamada T, Yamaoka S, Goto T, Nakai M, Tsujimoto Y, Hatanaka M: The human T-cell leukemia virus type I Tax protein induces apoptosis which is blocked by the Bcl-2 protein. J Virol 1994, 68:3374-9.

495. Yamaguchi K, Mochizuki M, Watanabe T, Miyata N, Tajima K, Mori S, Takatsuki K: Human T-lymphotropic virus type I uveitis. Leukemia 1994, 8 Suppl 1:S88-90.

496. Yamaguchi K, Takatsuki K: Adult T cell leukaemia-lymphoma. Baillieres Clin Haematol 1993, 6:899-915.

497. Yamaguchi K, Kiyokawa T, Nakada K, Yul LS, Asou N, Ishii T, Sanada I, Seiki M, Yoshida M, Matutes E, et al. Polyclonal integration of HTLV-I proviral DNA in lymphocytes from HTLV-I seropositive individuals: an intermediate state between the healthy carrier state and smouldering ATL. Br J Haematol 1988, 68:169-74.

498. Yamamoto H, Sekiguchi T, Itagaki K, Saijo S, Iwakura Y: Inflammatory polyarthritis in mice transgenic for human T cell leukemia virus type I. Arthritis Rheum 1993, 36:1612-20.

499. Yamanashi Y, Mori S, Yoshida M, Kishimoto T, Inoue K, Yamamoto T, Toyoshima K: Selective expression of a protein-tyrosine kinase, p56lyn, in hematopoietic cells and association with production of human T-cell lymphotropic virus type I. Proc Natl Acad Sci U S A 1989, 86:6538-42.

500. Yamaoka S, Inoue H, Sakurai M, Sugiyama T, Hazama M, Yamada T, Hatanaka M: Constitutive activation of NF-kappa B is essential for transformation of rat fibroblasts by the human T-cell leukemia virus type I Tax protein. EMBO J 1996, 15:873-87.

501. Yamaoka S, Tobe T, Hatanaka M: Tax protein of human T-cell leukemia virus type I is required for maintenance of the transformed phenotype. Oncogene 1992, 7:433-7.

502. Yamashita I, Katamine S, Moriuchi R, Nakamura Y, Miyamoto T, Eguchi K, Nagataki S: Transactivation of the human interleukin-6 gene by human T-lymphotropic virus type 1 Tax protein. Blood 1994, 84:1573-8.

503. Yamato K, Oka T, Hiroi M, Iwahara Y, Sugito S, Tsuchida N, Miyoshi I: Aberrant expression of the p53 tumor suppressor gene in adult T-cell leukemia and HTLV-I-infected cells. Jpn J Cancer Res 1993, 84:4-8.

504. Yin MJ, Paulssen EJ, Seeler JS, Gaynor RB: Protein domains involved in both in vivo and in vitro interactions between human T-cell leukemia virus type I tax and CREB. J Virol 1995, 69:3420-32.

505. Yonaha Nagato F, Sumida T: [Expression of sequences homologous to HTLV-I pXIV gene in the labial salivary glands of Japanese patients with Sjogren's syndrome and pathogenesis]. Nippon Rinsho 1995, 53:2473-8.

506. Yoshida M: Howard Temin Memorial Lectureship. Molecular biology of HTLV-1: deregulation of host cell gene expression and cell cycle [In Process Citation]. Leukemia 1997, 11 Suppl 3:1-2:1-2.

507. Yoshida M, Osame M, Kawai H, Toita M, Kuwasaki N, Nishida Y, Hiraki Y, Takahashi K, Nomura K, Sonoda S, et al. Increased replication of HTLV-I in HTLV-I-associated myelopathy. Ann Neurol 1989, 26:331-5.

508. Yoshida M, Osame M, Usuku K, Matsumoto M, Igata A: Viruses detected in HTLV-I-associated myelopathy and adult T-cell leukaemia are identical on DNA blotting [letter]. Lancet 1987, 1:1085-6.

509. Yoshida M, Miyoshi I, Hinuma Y: Isolation and characterisation of retrovirus from cell lines of human adult T-cell leukemia and its implication in the disease. Proc Natl Acad Sci U S A 1982, 79:2031

510. Yoshida Y, Hamada H: Adenovirus-mediated inducible gene expression through tetracycline- controllable transactivator with nuclear localization signal. Biochem Biophys Res Commun 1997, 230:426-30.

511. Yoshimura T, Fujisawa J, Yoshida M: Multiple cDNA clones encoding nuclear proteins that bind to the tax-dependent enhancer of HTLV-1: all contain a leucine zipper structure and basic amino acid domain. EMBO J 1990, 9:2537-42.

512. Zech L, Gahrton G, Hammarstrom L, Juliusson G, Mellstedt H, Robert L: Inversion of chromosome 14 marks human T-cell chronic lymphocytic leukeamia. Nature 1984, 308:858-60.

513. Zhao LJ, Giam CZ: Human T-cell lymphotropic virus type I (HTLV-I) transcriptional activator, Tax, enhances CREB binding to HTLV-I 21-base-pair repeats by protein-protein interaction. Proc Natl Acad Sci U S A 1992, 89:7070-4.

514. Zimmermann K, Dobrovnik M, Ballaun C, Bevec D, Hauber J, Bohnlein E: trans-activation of the HIV-1 LTR by the HIV-1 Tat and HTLV-I Tax proteins is mediated by different cis-acting sequences. Virology 1991, 182:874-8.

515. Zucker Franklin D, Hooper WC, Evatt BL: Human lymphotropic retroviruses associated with mycosis fungoides: evidence that human T-cell lymphotropic virus type II (HTLV-II) as well as HTLV-I may play a role in the disease. Blood 1992, 80:1537-45.

516. Zucker Franklin D, Coutavas EE, Rush MG, Zouzias DC: Detection of human T-lymphotropic virus-like particles in cultures of peripheral blood lymphocytes from patients with mycosis fungoides. Proc Natl Acad Sci U S A 1991, 88:7630-4.